Office of Environmental Management – Grand Junction

MOAB UMTRA UTAH

UMTRA Project

Remedial Action Plan and Site Design for Stabilization of Moab Title I Uranium Mill Tailings at the Crescent Junction, Utah, Disposal Site

Attachment 2: Geology

August 2006

U.S. Department of Energy

Office of Environmental Management

Work Performed Under DOE Contract No. DE–AC01–02GJ79491
for the U.S. Department of Energy Office of Environmental Management.
Approved for public release; distribution is unlimited.

Remedial Action Plan and Site Design for Stabilization of Moab Title I Uranium Mill Tailings at the Crescent Junction, Utah , Disposal Site

Attachment 2: Geology

Work performed under DOE Contract No. DE–AC01–02GJ79491
for the U.S. Department of Energy Office of Environmental Management.

Calculation Cross-Reference Guide

Location	Calculation Number	Calculation Title
Attachment 1: Disposal Cell Design Specifications		
Appendix A	MOA-02-05-2006-5-19-01	Freeze/Thaw Layer Design
Appendix B	MOA-02-05-2006-5-13-01	Radon Barrier Design Remedial Action Plan Calculation
Appendix C	MOA-02-05-2006-5-17-01	Slope Stability of Crescent Junction Disposal Cell
Appendix D	MOA-02-05-2006-3-16-00	Settlement, Cracking, and Liquefaction Analysis
Appendix E	MOA-02-08-2005-2-05-01	Site Drainage—Hydrology Parameters
Appendix F	MOA-02-05-2006-5-08-00	Crescent Junction Site Hydrology Report
Appendix G	MOA-02-05-2006-5-25-01	Diversion Channel Design, North Side Disposal Cell
Appendix H	MOA-02-05-2006-5-01-00	Erosional Protection of Disposal Cell Cover
Appendix I	MOA-01-05-2006-5-02-01	Volume Calculation for the Moab Tailings Pile
Appendix J	MOA-01-05-2006-5-03-00	Weight/Volume Calculation for the Moab Tailings Pile
Appendix K	MOA-01-08-2006-5-14-00	Average Radium-226 Concentrations for the Moab Tailings Pile
Attachment 2: Geology		
Appendix A	MOA-02-08-2005-1-05-00	Site and Regional Geology—Results of Literature Research
Appendix B	MOA-02-03-2006-1-01-00	Geologic and Geophysical Properties—Surficial and Bedrock Geology of the Crescent Junction Disposal Site
Appendix C	MOA-02-08-2005-1-06-00	Site and Regional Geomorphology—Results of Literature Research
Appendix D	MOA-02-08-2005-1-08-00	Site and Regional Geomorphology—Results of Site Investigations
Appendix E	MOA-02-08-2005-7-01-00	Site and Regional Seismicity—Results of Literature Research
Appendix F	MOA-02-09-2005-1-09-01	Site and Regional Seismicity—Results of Maximum Credible Earthquake Estimation and Peak Horizontal Acceleration
Appendix G	MOA-02-11-2005-1-02-00	Photogeologic Interpretation
Attachment 3: Ground Water Hydrology		
Appendix A	MOA-02-02-2006-2-07-00	Saturated Hydraulic Conductivity Determination of Weathered Mancos Shale
Appendix B	MOA-02-03-2006-2-10-00	Field Permeability "Bail" Testing
Appendix C	MOA-02-02-2006-2-06-00	Field Permeability "Packer" Testing
Appendix D	MOA-02-03-2006-2-03-00	Hydrologic Characterization—Ground Water Pumping Records
Appendix E	MOA-02-05-2006-2-13-00	Hydrologic Characterization—Vertical Travel Time to Uppermost (Dakota) Aquifer Calculation
Attachment 4: Water Resources Protection		
Appendix A	MOA-02-05-2006-5-24-00	Material Placement in the Disposal Cell
Appendix B	MOA-02-05-2006-3-05-00	Geochemical Attenuation and Performance Assessment Modeling
Attachment 5: Field and Laboratory Results Volume 1		
Appendix A	MOA-02-02-2006-1-03-00	Corehole Logs
Appendix B	MOA-02-02-2006-1-11-00	Borehole Logs
Appendix C	MOA-02-02-2006-1-04-00	Geophysical Logs
Appendix D	MOA-02-02-2006-1-10-00	Test Pit Logs
Appendix E	MOA-02-03-2006-4-01-00	Geotechnical Properties of Native Materials
Appendix F	MOA-01-05-2006-5-22-00	Cone Penetration Tests
Appendix G	MOA-02-03-2006-4-07-00	Seismic Rippability Investigation
Appendix H	MOA-02-03-2006-3-04-00	Background Ground Water Quality
Appendix I	MOA-01-07-2006-4-08-00	Boring and Test Pit Logs
Appendix J	MOA-01-07-2006-4-09-00	Geotechnical Laboratory Testing Results for the Moab Processing Site
Appendix K	MOA-02-07-2006-4-03-00	Supplemental Geotechnical Properties of Native Materials
Attachment 5: Field and Laboratory Results Volume 2		
Appendix L	MOA-02-07-2006-1-06-00	Compilation of Geologic and Geophysical Logs
Appendix M	N/A	Radiological Assessment for Non-Pile Areas of the Moab Project Site

Attachment 2
Table of Contents

Appendix A

U.S. Department of Energy—Grand Junction, Colorado

Calculation Cover Sheet

Calc. No.: MOA-02-08-2005-1-05-00 **Discipline:** Geologic and Geophysical Properties **No. of Sheets:** 7

Project: Moab Project

Site: Crescent Junction Disposal Site

Feature: Site and Regional Geology – Results of Literature Research

Sources of Data:

Published reports and maps – see list of references at end of calculation set.

Sources of Formulae and References:

See list of references at end of calculation set.

Preliminary Calc. ☐ **Final Calc.** ☑ **Supersedes Calc. No.**

Author: Mark Kautsky for CSG 8-30-05 (Name / Date)

Checked by: (Name / Date)

Mark Kautsky 30 Aug '05 (Name / Date)

Joseph L. Rael 30 Aug 05 (Name / Date)

Joel Berwick 8/14/06 (Name / Date)

Approved by: Kenneth Kopp 8-30-05 (Name / Date)

Problem Statement:

Determination of the suitability of the Crescent Junction disposal site as the repository for the Moab uranium mill tailings material, and development of the site and regional geology sections of the Remedial Action Plan (RAP) require a thorough review of available literature that applies to the Crescent Junction site. The compiled list of references is presented at the end of this calculation set and relevant information is summarized below.

This is Calculation Set No. 3 as defined in the Moab Project Task Order ST05-203 Modification P, to be completed by 31 August 2005. This information will be incorporated into the RAP for the Moab site.

Method of Solution:

Literature sources were identified using a combination of published reports and maps that were developed during the Crescent Junction site-selection process, on-line (internet-based) resources, and relevant literature citations from the other UMTRCA sites.

Assumptions:

It is assumed that the literature sources are reliable and representative of the current understanding of the geology of the region.

Calculation:

None required.

Discussion:

A general summary of geologic conditions based on the literature research is provided in this calculation set. This summary is preliminary and will be expanded as a result of future, detailed geologic studies. Additional information will be presented in the RAP.

Physiographic Setting

Crescent Junction is located approximately 19 miles east of the town of Green River, Utah, and approximately 30 miles north of Moab, Utah (Figure 1). The physiographic location of the Crescent Junction disposal site is on a broad, nearly level, plain at the base of the Book Cliffs. The elevation of Crescent Flat ranges from approximately 4,900 feet above mean sea level (ft amsl) at the southwest corner of the withdrawn area to approximately 5,120, ft amsl at the northeast corner of the withdrawn area. Crescent Flat is bounded to the north by the steep slopes of the Book Cliffs whose elevation rises to approximately 5,900 ft amsl.

General Geology

The Crescent Junction disposal site is on the Crescent Junction 7.5-minute topographic quadrangle in Section 27, T21S, R9E, approximately 1 mile north-northeast of Crescent Junction, Utah. Geologic maps for the area include the Salt Valley area geologic map (Woodward-Clyde Consultants 1984) at a scale of 1:62,500, and the Moab and eastern part of the San Rafael Desert 30' x 60' quadrangles at a scale of 1:100,000 (Doelling 2001 and 2002). Larger scale 1:24,000 geologic maps are available for 7.5-minute quadrangles Hatch Mesa (Chitwood 1994) and Valley City (Doelling 1997), west and south, respectively, of the Crescent Junction quadrangle.

Stratigraphic Setting

A general geologic map of the Crescent Junction site is presented in Figure 2. Bedrock exposed in several places at the Crescent Junction site is the Mancos Shale of Late Cretaceous age. Most of the Mancos Shale was deposited in an open marine environment of the Late Cretaceous western interior seaway. The upper part of the Mancos Shale underlies the site and is approximately 3,000 ft thick in this

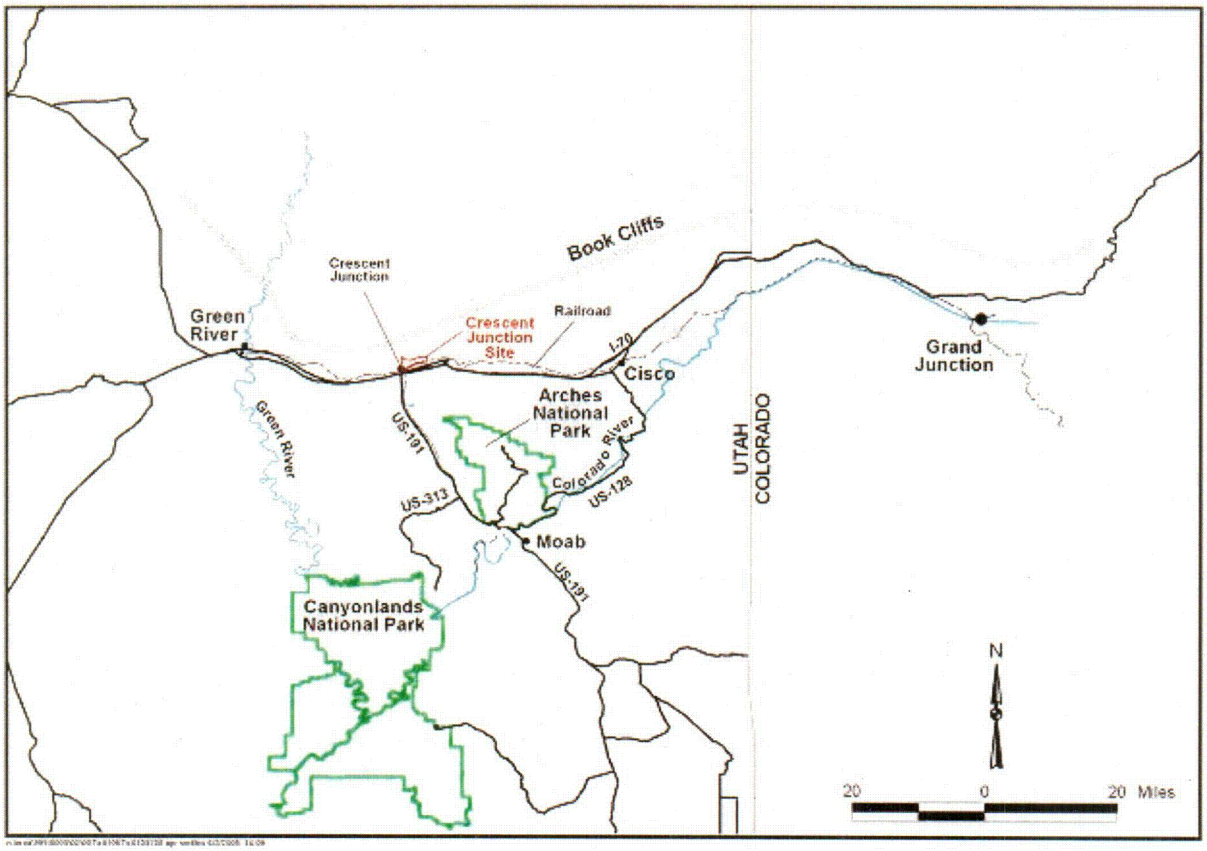

Figure 1. Site Location map for the Crescent Junction Site

area. Approximately 1,000 ft of the upper part of the formation have been removed by erosion. Mancos Shale exposed in the site area is best described as a thickly bedded, calcareous mudstone (Chitwood 1994), with thinly-bedded siltstone, fine-grained sandstone, and bentonite interbeds widely spaced within the mudstone. The Ferron Sandstone Member of the Mancos Shale is approximately 60 ft thick and occurs in the lower 300 to 350 ft of the Mancos Shale. This member contains two sandstone beds with fine- to medium-gained sand. Below the Ferron Sandstone Member is the lowermost member of the Mancos Shale, the Tununk Shale Member.

The Dakota Sandstone of Early Cretaceous age underlies the Mancos Shale and consists of sandstone, conglomeratic sandstone, and shale. This formation is less than 100 ft thick in the site area and is likely the shallowest bedrock unit containing ground water. The Cedar Mountain Formation, also of Early Cretaceous age, underlies the Dakota Sandstone and consists of several sandstone and conglomeratic sandstone beds interbedded with thickly-bedded mudstone. Ground water is also present in the sandstone and conglomeratic sandstone beds of the Cedar Mountain Formation. Ground water in the Dakota Sandstone and Cedar Mountain Formation may be under slight artesian head from recharge to the north along the north edge of the Uinta Basin.

Exposures of the Mancos Shale bedrock are covered over much of the site by alluvial mud of Quaternary age (Doelling 2001). This unconsolidated gray material, less than 20 ft thick, fills swales in the Mancos Shale and consists of silt, clay, sand, and minor fragments of sandstone. Along the west side of the site area, Quaternary stream alluvium up to 20 ft thick from Crescent Wash covers Mancos Shale (Doelling 2001). This material consists of sand, silt, clay, pebbles, and sparse cobbles derived from the Book Cliffs, some 10 miles to the north.

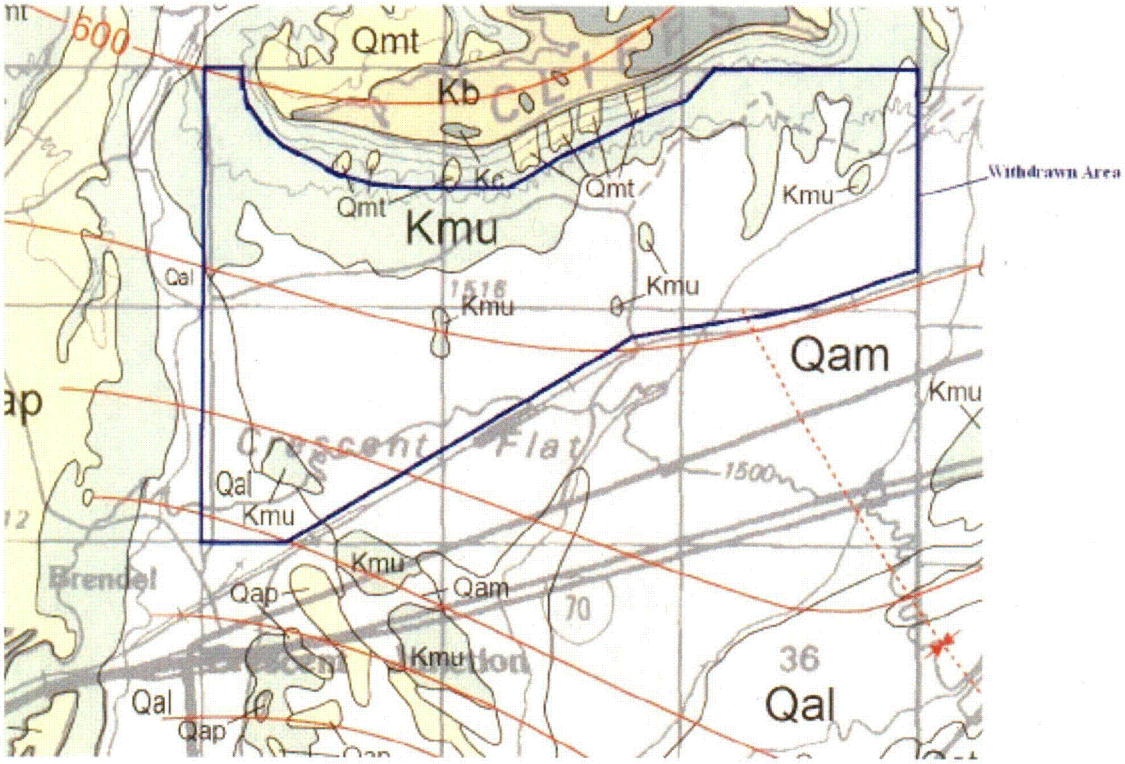

EXPLANATION OF GEOLOGIC UNITS

Quaternary Deposits

Qal	Stream alluvium -- Sand, silt, clay, granules, pebbles, and sparse cobbles
Qam	Alluvial mud -- Light- to medium-gray silt, clay, sand, and minor fragments of sandstone, mostly derived from members of the Cretaceous Mancos Shale
Qap	Pediment-mantle deposits -- Poorly to moderately sorted, rounded to angular boulders, cobbles, pebbles, granules, sand, silt, and clay.
Qmt	Talus and colluvium -- Rock-fall blocks, boulders, smaller angular gravel, sand, and silt

Cretaceous Rocks

Kc	Castlegate Sandstone -- Pale yellow-orange and light-gray, cross-bedded sandstone interbedded with minor mudstone, carbonaceous shale, and coal
Kb	Blackhawk Formation -- Pale yellow-orange to light-brown sandstone interbedded with mudstone, carbonaceous shale, and coal.
Kmu Kms	Upper shale (Blue Gate) member of Mancos Shale -- Mostly light-to dark- gray, marine, thinly laminated to thinly bedded, slope-forming shale, mudstone, and siltstone interbedded with calcareous sandstone

Figure 2. Geologic Map of the Crescent Junction Site (Modified after Doelling 2001 and 2002)

Structural Setting

The Crescent Junction disposal site is located in the southern edge of the Uinta Basin and overlies the northwestern part of the ancestral Paradox Basin (in the Paradox fold and fault belt). The Book Cliffs, less than 1 mile north of the site, are the erosional escarpment on the south flank of the Uinta Basin. Mancos Shale bedrock at the site dips gently (less than 10 degrees) to the north-northeast toward the axis of the subtle, northwest-trending Whipsaw Flat Syncline. Northwest-striking normal faults defining a graben of the northwest extension of the Salt Valley salt-cored anticline are approximately 1 to 2 miles to the southwest of the site. These faults are not exposed at the surface, but reportedly have as much as 1,000 ft of displacement (Fisher 1936) as determined by oil test wells drilled in the area in the 1920s and 1930s.

A northeast-striking normal fault extends into the southwest quarter of Section 27 in the site area. This fault was mapped in 1924 as part of oil exploration in the Crescent area (Harrison 1927, Figure 9). Fisher (1936) described the fault as a "minor dip fault with 100 ft of downthrow on the south". It is unlikely that this fault has a surface expression—it is not shown on geologic maps by Woodward-Clyde Consultants (1984) or Doelling (2001). Fisher (1936) noted that an oil test well (McCarthy No. 1) was being drilled in the NW 1/4 of Section 34 by Western States Development Company. Drilling had started in December 1924 and after several shut downs, the well was at a depth of 2,200 ft in March 1930. Later maps and references (Dane 1935 and Baker and others 1954) refer to this well as being drilled by the Crescent Oil Syndicate and show its location in the extreme southwest corner of Section 27. A possible log of this well was found on the Utah State Water Resources Well–Log Search webpage; a follow–on telephone conversation with the Oil and Gas Division revealed that this well is given the API reference No. 4301911525. The mapping of the minor fault seems to predate the drilling of the Crescent Oil Syndicate (McCarthy No. 1) well; therefore, it is unclear what subsurface evidence was used to justify the existence of the fault. Surface field work and an additional search for well data in the area will be undertaken to confirm or deny the existence of the fault. No other lineaments or geologic structures were noted by Friedman and Simpson (1980) in the site area during mapping of the northern Paradox Basin.

Resource Development

No significant oil and gas resources are known in the Cretaceous Rocks in the site area. The Crescent Oil Syndicate well described above encountered a natural gas pocket that "blew rocks over the top of the mast"; however, this appears to have been a shallow, isolated show. The nearest known petroleum accumulation is in the Morrison Formation of Jurassic age in the small and abandoned Crescent Junction field approximately 3 miles south-southwest of the site in the extension of the Salt Valley structure. Exploratory drilling for natural gas was completed recently at one location (MSC 26-1) just south of the withdrawn area ((API No. 43-019-31407-00-00) (http://utstnrogmsql3.state.ut.us/UtahRBDMSWeb/well_data_lookup.cfm)). Data concerning the targeted gas horizons and the actual results of this exploration are not currently available.

Potash resources are known in the Paradox Formation of Pennsylvanian age in the northwest extension of the Salt Valley structure approximately 3 miles south of the site. The site area, however, is northeast of the Salt Valley salt-cored anticline and thick saline deposits are not present.

Uranium and vanadium deposits are known in scattered locations in the region in the Morrison Formation of Jurassic age and the Chinle Formation of Triassic age. At the site, these formations are 3,000 to 4,000 ft below the surface, making exploration for such deposits very uneconomical. Copper and silver mineralization also is known to occur in a few locations in the region in fault-related deposits in the Morrison Formation (Woodward-Clyde Consultants 1984). Exploration for such deposits in the site area also would be uneconomical because of their great depth. Coal resources occur in the Book Cliffs several miles north of the site, but they are in stratigraphically younger rocks (Mesaverde Group of Late Cretaceous age) than are present at the site.

Black shales, such as the Mancos Shale, are naturally enriched to above background concentrations in metals such as uranium, copper, silver, vanadium, mercury, arsenic, and gold. These metals likely originated in volcanic ash material (since altered to bentonite) that was deposited during deposition of the Mancos Shale. In a study by Marlatt (1991), sampling of Mancos Shale generally in the area between Salt

Valley and the Book Cliffs found that gold content ranged from 30 to 100 parts per billion (ppb). These values are about ten times the background levels, but are much too low for economic extraction.

No sand and gravel deposits are present in the site area. Potential deposits of such material are present just south of the site in Section 34 and west of Crescent Wash approximately 0.5 mile west of the site (McDonald 1999). This material occurs as pediment-mantle deposits that cover Mancos Shale bedrock surfaces.

Geologic Hazards

Swelling clay (montmorillonite) in the Mancos Shale underlying the site area creates a potential geologic hazard (Mulvey 1992). Change in water content will cause shrinking and swelling leading to subsidence or heave of concrete slab structures, as evidenced by the constant maintenance required for Interstate Highway 70 crossing Mancos Shale just south of the site.

The site area has a moderate to high radon-hazard potential for occurrence of indoor radon based on the geologic factors of uranium concentration, soil permeability, and ground water depth (Black 1993). The moderate to high rating is created by the relatively high concentration of uranium in the Mancos Shale, the relatively high soil permeability caused by shrinking and swelling of the Mancos Shale-derived soil, and the relatively deep groundwater depths (shallow ground water retards radon migration).

Conclusion and Recommendations:

Based on preliminary evaluation of the results of the literature research effort, the Crescent Junction site appears to be suitable for disposal of the Moab uranium mill tailings and contaminated material. Potential geologic hazards appear to be limited to the presence of swelling clays. Although numerous geologic faults occur in the area, none appear to have a surface expression, suggesting any significant offset of the faults occurred prior to Quaternary deposition. Also, use of the area as a disposal site will not impede any potential mineral development. Additional information will be collected and reported in the RAP.

Computer Source:

Not applicable.

References:

Baker, A.A., Dane, C.H., and McKnight, E.T., 1954. *Preliminary Map Showing Geologic Structure of Parts of Grand and San Juan Counties*, Utah: U.S. Geological Survey Oil and Gas Investigations Map OM- 169, scale 1:125,000.

Black, B.D., 1993. *The Radon-Hazard-Potential Map of Utah*: Utah Geological Survey Map 149, 12 p., scale 1:1,000,000.

Chitwood, J.P., 1994. *Provisional Geologic Map of the Hatch Mesa Quadrangle*, Grand County, Utah: Utah Geological Survey Map 152, 16 p., scale 1:24,000.

Dane, C.H., 1935. *Geology of the Salt Valley Anticline and Adjacent Areas, Grand County, Utah*: U.S. Geological Survey Bulletin 863, 184 p., scale 1:62,500.

Doelling, H.H., 1997. *Interim Geologic Map of the Valley City Quadrangle, Grand County, Utah*: Utah Geological Survey Open-File Report 351, 55 p., scale 1:24,000.

Doelling, H.H., 2001. *Geologic Map of the Moab and Eastern Part of the San Rafael Desert 30' x60' Quadrangles, Grand and Emery Counties, Utah, and Mesa County, Colorado*: Utah Geological Survey Map 180, scale 1:100,000.

Doelling, H.H., 2002. *Geologic Map of the Moab and Eastern Part of the San Rafael Desert 30' x60' Quadrangles, Grand and Emery Counties, Utah, and Mesa County, Colorado*: Utah Geological Survey Map 180M, scale 1:100,000.

Fisher, D.J., 1936. *Book Cliffs Coal Field in Emery and Grand Counties, Utah*: U.S. Geological Survey Bulletin 852, 104 p., scale 1:62,500.

Friedman, J.D., and Simpson, S.L., 1980. *Lineaments and Geologic Structure of the Northern Paradox Basin, Colorado and Utah*: U.S. Geological Survey Miscellaneous Field Studies Map MF-1221, scale 1:250,000.

Harrison, T.S., 1927. *Colorado-Utah Salt Domes*: American Association of Petroleum Geologists Bulletin, vol. 11, no. 2, p. 111-133.

Marlatt, Gordon, 1991. *Gold Occurrence in the Cretaceous Mancos Shale, Eastern Utah*: Utah Geological and Mineral Survey Contract Report 91-5, 21 p.

McDonald, G.N., 1999. *Known and Potential Sand, Gravel, and Crushed Stone Resources in Grand County, Utah*: Utah Geological Survey Open-File Report 369, 21 p.

Mulvey, W.E., 1992. *Soil and Rock Causing Engineering Geologic Problems in Utah*: Utah Geological Survey Special Study 80, 23 p., scale 1:500,000.

Woodward-Clyde Consultants, 1984. *Geologic Characterization Report for the Paradox Basin Study Region, Utah Study Areas, Volume VI, Salt Valley*: Walnut Creek, California, unpublished Consultant's Report for Battelle Memorial Institute, Office of Nuclear Waste Isolation, ONWI-290, 190 p., scale 1:62,500.

Appendix B

U.S. Department of Energy—Grand Junction, Colorado

Calculation Cover Sheet

Calc. No.: MOA-02-03-2006-1-01-00 XE 8-21-06 **Discipline:** Geology **No. of Sheets:** 15

Project: Moab UMTRA Project

Site: Crescent Junction Disposal Site

Feature:

Geologic and Geophysical Properties – Surficial and Bedrock Geology of the Crescent Junction Disposal Site

Sources of Data:

Geologic mapping of the Crescent Junction disposal site area. Geologic literature research for a 30-mile radius of the disposal site area. Lithologic logs for boreholes and test pits emplaced at the disposal site area from August to December 2005.

Sources of Formulae and References:

See list of references at end of calculation set.

Preliminary Calc. ☐ **Final Calc.** ☑ **Supersedes Calc. No.**

Author: Craig Goodknight 3/9/06 (Name / Date)

Checked by: D E. Cummins 3/9/06 (Name / Date)

Mark Kautsky 3-9-06 (Name K. K. for / Date)

R. Hagedenhuvg 3-9-06 (Name / Date)

Joel Berwick 3-9-06 (Name / Date)

Approved by: Kent. Kung 3-9-06 (Name / Date)

Problem Statement:

Preliminary site selection performed jointly by the U.S. Department of Energy (DOE) and the Contractor has identified a 2,300 acre withdrawal area in the Crescent Flat area just northeast of Crescent Junction, Utah, as a possible site for a final disposal cell for the Moab uranium mill tailings. The proposed disposal cell would cover approximately 300 acres. Based on the preliminary site-selection process, the suitability of the Crescent Junction disposal site is being evaluated from several technical aspects, including geomorphic, geologic, hydrologic, seismic, geochemical, and geotechnical. The objective of this calculation set is to discuss the surface and bedrock geology of the site and provide the geologic map, cross sections, and bedrock contour map that were generated during the investigation.

This calculation will be incorporated into Attachment 2 (Geology) of the Remedial Action Plan (RAP) and Site Design for Stabilization of Moab Title I Uranium Mill Tailings at the Crescent Junction, Utah, Site, and summarized in the appropriate sections of the Remedial Action Selection (RAS) report for the Moab site.

Method of Solution:

Surface geologic features were identified by aerial photography and field observation mapping. A geologic map of the site area (Plate 1) was prepared that shows these features. Subsurface features of the Quaternary material and bedrock were identified from lithologic logging at test pits and from core retrieved from coreholes and geotechnical boreholes (RAP, Attachment 5). Cross sections across the site area (Plate 2) were prepared from the borehole lithologic logs that show bedrock features. A bedrock (top of weathered Mancos Shale) contour map for the site area (Plate 3) was prepared from the borehole lithologic logs and mapped surface outcrops. Review of geologic literature for the region provided the stratigraphic framework for the surface and subsurface features identified in the site area.

Assumptions:

Not applicable

Calculation:

Not applicable – see discussion of information in next section.

Discussion:

1.0 Maps of Site Area

A geologic map (Plate 1) and bedrock contour map (Plate 3) were prepared for the Crescent Junction site area, which covers about 2 square miles (mi). For this calculation, the site area is synonymous with the (geologically) mapped area.

1.1 Geologic Map

The geologic map of the site area was prepared during field work in September and October 2005. The approximately 2 square mi mapped area includes the proposed disposal cell footprint and the larger area covered by characterization boreholes (coreholes and geotechnical boreholes) and test pits. Mapping was done on a base map with a 2-foot topographic contour interval at a scale of 1:4,800 (1 inch = 400 feet [ft]). Contacts of the few and scattered bedrock outcrops of Mancos Shale of Late Cretaceous age in the area are shown on the map. At these bedrock outcrops, a Brunton compass was used to measure strike and dip of bedding and strike of vertical joints in the few places these features could be observed. Contacts between several types of unconsolidated surficial material of Quaternary age are shown on the map; these contacts are subtle and gradational and are not as evident or as sharp as the contacts between bedrock units. Descriptions of the mapped units of Quaternary age and the mapped units in the Mancos Shale are in the following subsections. Also shown on the geologic map are lines for five cross sections (Plate 2) connecting the coreholes and geotechnical boreholes included in each section.

1.2 Bedrock Contour Map

A contour map of the top of bedrock topography is shown in Plate 3 at the same scale as the geologic map. The bedrock topography shows two subtle ridges that tend north-northwest. One ridge extends through the west part of the proposed disposal cell and one is through the east-central part. Both bedrock ridges coincide with subtle surface ridges in the proposed disposal cell area. In addition, the east-central bedrock ridge appears to be a southward continuation of the surface ridge north of the 3 ponds area. Local relief of as much as 20 ft occurs on the bedrock surface, as shown in the east end of the mapped area where bedrock in test pit 0156 is 20 ft lower than exposed bedrock on a nearby ridge to the southwest. Similar occurrences of high local bedrock relief are likely present in the proposed disposal cell area. These occurrences would be evident with closer spaced boreholes with depth to bedrock data.

2.0 Surficial Geology - Quaternary Material

Unconsolidated Quaternary material covers approximately 98 percent of the mapped area. This material covers Mancos Shale bedrock and reaches a thickness of nearly 25 ft. Five types of Quaternary material were mapped – the most significant from areal and volume perspectives are alluvial-mud (mixed silt and clay) deposits. Material along active sheet wash flow paths and litter from the Book Cliffs that mantles the alluvial mud are two other mapped units that are related to the alluvial mud. The two other Quaternary units mapped are sandy alluvium and pediment-mantling litter. Both of these are in the southwest and west parts of the mapped area and represent alluvial deposits from the Crescent Wash drainage system, which has transported sandy material southward from the Book and Roan Cliffs.

2.1 Alluvial-Mud Deposits

Gray mud, silt, and clay cover most of the surface of the site area at distances of more than 0.5 mi south of the base of the Book Cliffs. This material is mostly of alluvial origin, derived from sheet wash erosion from the lower slopes of the Book Cliffs where Mancos Shale is exposed. Some of the material is residual and forms from weathering of muddy outcrops of Mancos Shale. Alluvial-mud deposits covering Mancos Shale are mapped by Doelling (2001) who described these deposits in the site area and to the south in the Valley City quadrangle (Doelling 1997).

Surface expression of the alluvial mud is mostly in the form of silt to clayey silt and was described in the field as ML, in the Unified Soil Classification System (USCS). This fine-grained material is typically light brownish gray (10YR 6/2), highly calcareous, and represents successive sheet wash deposits. Laboratory test results of this material sampled from geotechnical boreholes indicates a high clay (CL in the USCS) content.

Below the surface, most of the alluvial mud is fine grained, but discontinuous layers of coarser grained material of eolian and channel-fill origin are also present around the site area. Material of eolian origin was found in several boreholes and test pits (see lithologic logs of test pits 0151 and 0153 in RAP, Attachment 5). Eolian material is typically sandy silt (ML in the USCS), light brown (7.5YR 6/4), 1 to 3 ft thick, and at depths of 6 to 12 ft. The brown eolian material exposed in test pit 0151 is shown in Figure 1. The sporadic occurrence of this material, not in a continuous layer, indicates it was removed by erosion and reworked after its deposition – probably in a dry period during mid-Holocene time.

Coarser grained, sand to gravel and small boulder-sized, material occurs also in sporadic, discontinuous layers and lenses in the alluvium. Several of the coreholes and geotechnical boreholes around the site area penetrated gravelly sand (SW in the USCS) layers that contained shale and sandstone fragments. Some of this deeper material has been calcareously cemented. The gravelly sand material represents alluvial detritus deposited in small channels similar to the litter deposits on the surface in the north part of the site area closer to the base of the Book Cliffs. Material up to small boulder in size also is present in a few locations – notably exposed in test pit 0156. Here, small boulders up to 2 ft in diameter are present that fill an alluvial channel cut into Mancos Shale bedrock at a depth of approximately 20 ft. Mancos Shale is exposed in the bottom of test pit 0156 in Figure 2. Sandstone bedrock is exposed at the surface (Plate 1) only about 200 ft to the southwest of this coarse bouldery material. This relief of at least 20 ft on the bedrock surface in a short distance and the coarse bouldery deposits indicates the presence of a high-energy paleochannel where coarse material was transported southward from the ancestral Book Cliffs (Plate 2, cross section E-E', and Plate 3). No indication of ground water was found in this

paleochannel. Other paleochannels similar to this one exposed at test pit 0156 likely occur westward across the site area.

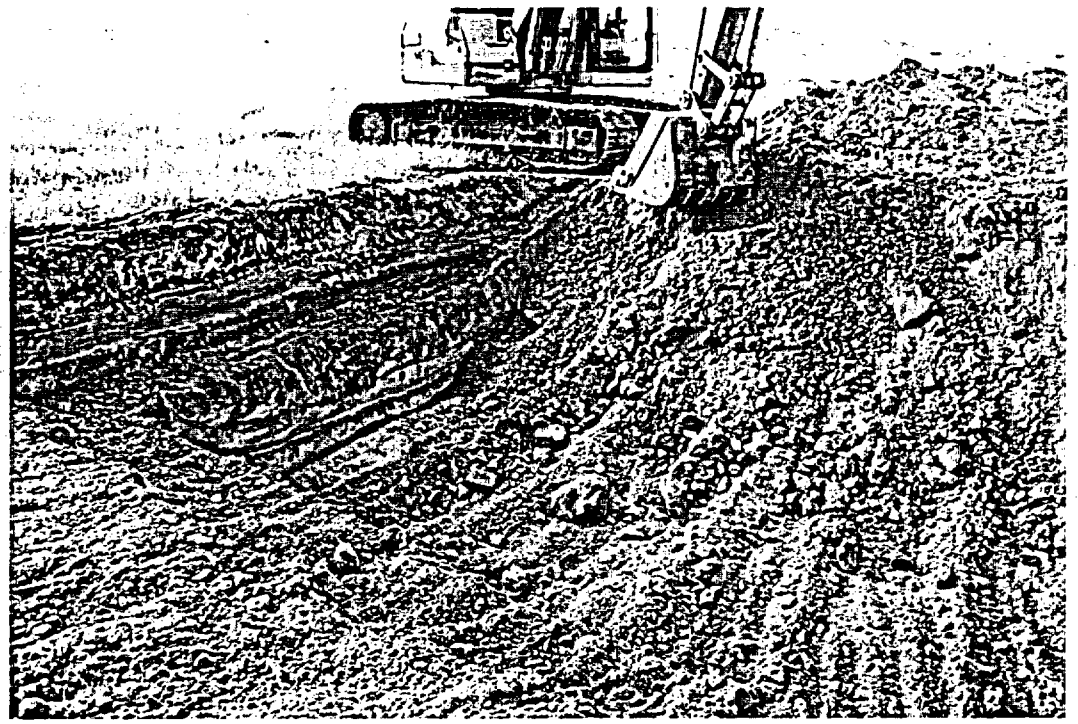

Figure 1. View of brown eolian material exposed at a depth of 7 ft in test pit 0151.

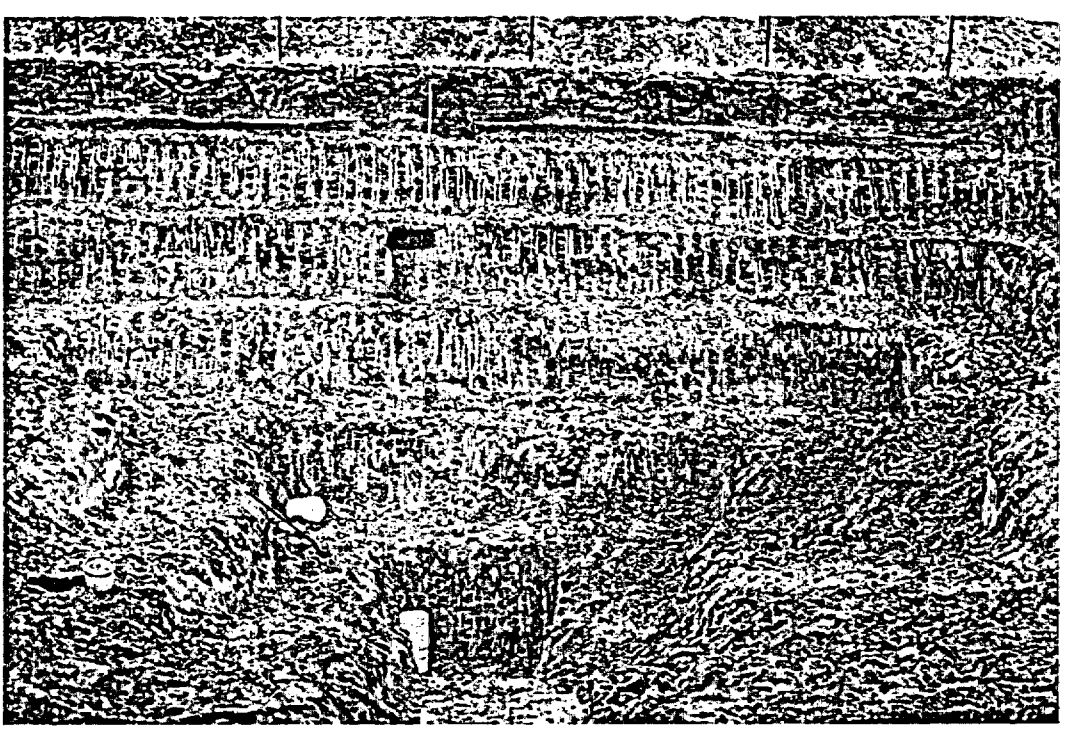

Figure 2. Test pit 0156–Alluvial-mud deposits are approximately 20 ft thick, and Mancos Shale is at bottom of pit. White 5-gallon buckets and shovel provide scale.

Alluvial mud in the site area has been deposited over Mancos Shale bedrock in a long-term process of successive sheet wash episodes during much of Quaternary time. The thickest accumulation of alluvial mud is in subtle bedrock lows between several north-northwest trending bedrock ridges that cross the site area (Plate 3). The thickest alluvial mud accumulations of about 23 ft were found in geotechnical boreholes 0014 and 0025, just north of the west part of the proposed disposal cell. A thick accumulation is also present along the east edge of the proposed disposal cell where 22 ft of alluvial mud was found in coreholes 0208 and 0209. The average thickness of alluvial mud at the proposed disposal cell is approximately 10 to 12 ft. Alluvial mud thickness overlying the two bedrock ridges in the west and east-central parts of the proposed disposal cell is less than 10 ft. Between these ridges, the thickness is from 10 to 20 ft, and along the east side of the eastern ridge, the thickness is from 10 to 22 ft.

2.2 Material Along Active Sheet Wash Flow Paths

Several paths along which the sheet wash process is presently active are shown on the geologic map (Plate 1). These paths are visible in the high-altitude vertical aerial photos by their drab-gray color and are shown in Plate 1 of the Photogeologic Interpretation calculation set. Vegetation is generally absent from the paths, and recently-deposited gray mud covers most of the surface. Some small fragments of sandstone transported from the flanks and base of the Book Cliffs may be scattered on the surface of the paths.

The active sheet wash paths are generally in the north part of the site area within about 0.5 mi of the base of the Book Cliffs. The north ends of these paths usually merge into gullies that drain away from the base of the Book Cliffs (Plate 1). Only two paths enter or cross the proposed disposal cell area. Of these, the most prominent is the north-northwest trending path that crosses the east part of the proposed cell area. This path extends southward from the drainage just west of the three ponds area (Plate 1 and Figure 3). Material transported down this drainage is deposited to the south along the path as the gradient decreases across the proposed cell area. The path extends south-southeastward to the Union Pacific Railroad.

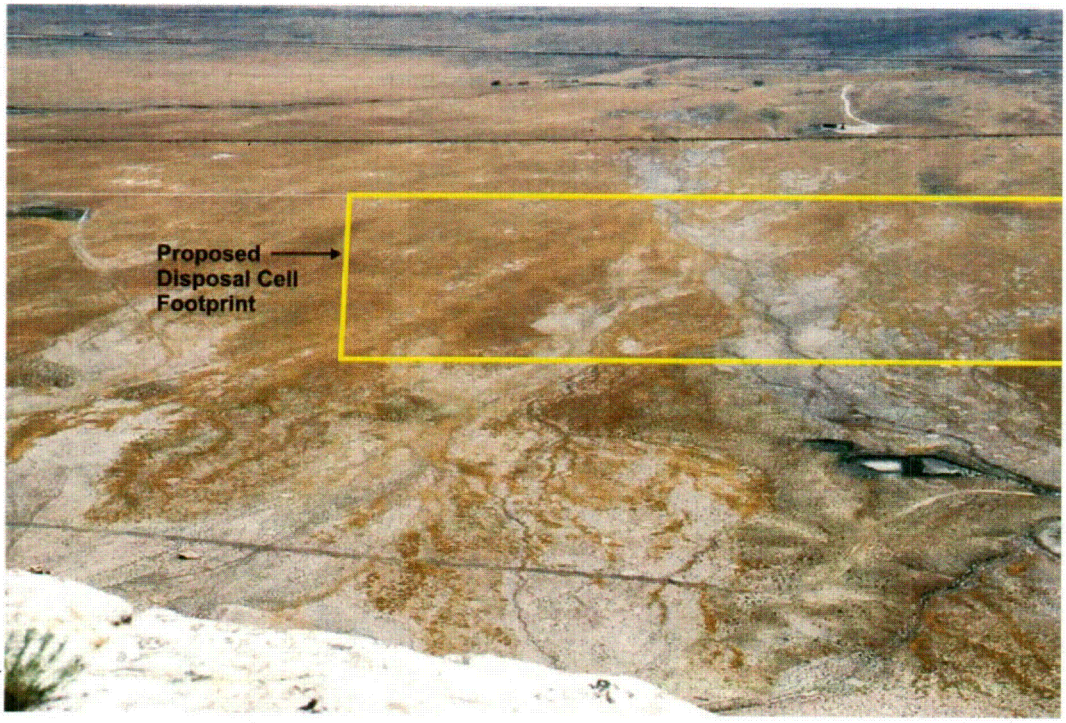

Figure 3. View south from top of Book Cliffs toward sheet wash path extending south-southeast from the three ponds across the eastern quarter of the proposed disposal cell area.

Flows along the sheet wash paths are infrequent, but represents the main process by which alluvial mud has been slowly deposited over bedrock at the site area. One episode of active sheet wash flow was witnessed in late September 2005 during site characterization drilling. Flows occurred in several sheet wash paths (Figure 4) immediately following a high-intensity rain and hail event during which at least 0.5 inch of precipitation fell in less than one-half hour. It is estimated that events of this magnitude typically occur once per year or less.

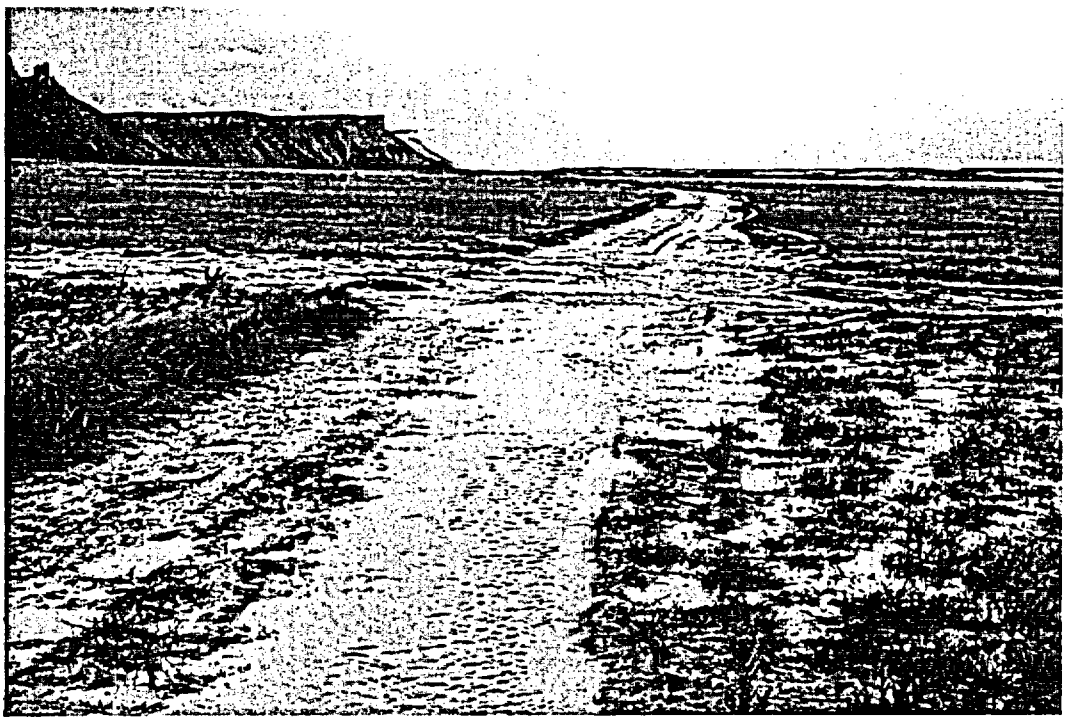

Figure 4. View east of active sheet wash flowing over site access road just north of geotechnical borehole 0025, September 21, 2005.

2.3 Litter from Book Cliffs that Mantles Alluvial Mud and Mancos Shale

Mancos Shale and alluvial mud are increasingly covered from south to north across the mapped area by what is referred to as litter that is composed mainly of sandstone fragments ranging from one inch to as much as 3 ft in diameter. North of the mapped area and closer to the base of the Book Cliffs, sandstone boulders are as large as several tens of ft in diameter. The smaller sandstone fragments in the mapped area are derived from the top of the Book Cliffs and consist of tan, friable, subrounded fragments and chunks of fine-grained sandstone of the Blackhawk Formation and slabs of rusty-colored, brittle, well-cemented, fine-grained dolomitic sandstone of the Castlegate Sandstone. The surface areas covered by the litter are also characterized by dark cryptogamic soil that supports scattered prickly pear cactus.

Northward from the proposed disposal cell to the base of the Book Cliffs (nearer to the source of the sandstone), the sandstone litter covers most of the surface. Southward through the proposed disposal cell, the litter is present only in narrow strips that generally correspond to subtle, north-northwest trending ridges (Plate 1). The litter-covered low ridges also correspond, in most places in the proposed disposal cell area, to subtle bedrock ridges, as shown in Plate 3. The litter in the proposed disposal cell area represents residual sandstone material that was deposited along the base of the Book Cliffs as rock falls during erosion of the supporting Mancos Shale that has not yet been eroded away or has not been covered by sheet wash material during the accumulation of the alluvial-mud deposits.

2.4 Sandy Alluvium

Alluvium from the Crescent Wash drainage system occurs in low ridges along the southwest edge of the mapped area. This material consists mainly of silty sand, and the sand is mostly fine- to very fine-grained. The sandy character of this alluvium is different from the Mancos Shale-derived alluvial mud and reflects the dominantly sandstone lithology present in the Book and Roan Cliffs area that the Crescent Wash system drains. A few sandstone chunks (rarely as large as boulders) and chert pebbles occur in the alluvium; these are representative of the Mesaverde Group sandstones and early Tertiary sandstones with chert that are present in the Crescent Wash drainage. The sandy alluvial ridges also support more vegetation than the alluvial mud flats.

Evidence of ancestral courses of Crescent Wash is expressed in the sandy alluvium as arcuate topographic lows in the west-central edge of Section 27 (Plate 1). These former stream courses were as much as 1,000 ft east of the present wash. Sandy alluvium is not present immediately east of the large incised meander of Crescent Wash near the northwest corner of Section 27. This indicates that no ancestral Crescent Wash has been present east of the present wash course at the large meander.

2.5 Pediment-Mantling Litter

Several small areas along the west and southwest edges of the mapped area are covered by a distinctive, resistant, gravelly material that veneers alluvial mud, sandy alluvium, or Mancos Shale outcrops. Pebbles in this gravelly material consist of brown sandstone and resistant white quartzite and distinctive, exotic, black chert (up to 2 inches in diameter). The pebbles are loose and scattered and "litter" the surface.

These deposits represent the erosion-resistant lag material from former pediment-mantling deposits laid down by the ancestral Crescent Wash drainage system. The pediment-mantling deposits are no longer preserved in place in the mapped area. These deposits are preserved in place about 0.5 mi west of the mapped area where they cap a low mesa about 100 ft above Crescent Wash and are mapped as pediment-mantle deposits by Doelling (2001). These in-place deposits contain the same type of resistant pebbles found as lag (or litter) in the mapped area. The distinctive, exotic, black chert and vari-colored quartzite pebbles in the pediment-mantle deposits are a constituent of a conglomerate in the Dark Canyon Sequence of the Wasatch Formation of early Paleocene age that crops out in the Roan Cliffs about 6 to 8 mi north up the Crescent Wash drainage (Franczyk and others 1990). The occurrence of this pediment-mantling deposit whose matrix contains Stage II carbonate development about 100 ft above present drainages probably correlates to similar cemented deposits on Mancos Shale pediments mapped by Willis (1994) in the Harley Dome area about 35 mi to the east-northeast. Those deposits were estimated by Willis (1994) to be 100,000 to 200,000 years old based on their height (50-110 ft) above present drainages and their carbonate development (Stage II).

At the southwest end of the mapped area, several areas of pediment-mantling litter lie on the sides of a low hill where weathered Mancos Shale is poorly exposed (Plate 1). This hill is likely an erosional remnant of a Mancos Shale pediment surface east of the present Crescent Wash that was capped by the pediment-mantle deposits about 100,000 to 200,000 years ago (late to middle Pleistocene age) emplaced by the ancestral Crescent Wash system. The other scattered small deposits of pediment-mantling litter (mainly in the area near corehole 0202) are evidence of the former extent of this pediment.

3.0 Bedrock Geology – Cretaceous Mancos Shale

The mapped site area is underlain by the Mancos Shale of Late Cretaceous age that dips gently northward. The shale forms a broad, east-trending belt immediately south of the Book Cliffs. Topographically, the shale forms the lower or buttressing part of the Book Cliffs and the wide expanse of lowlands, or "flats", extending several miles to the south (Fisher and others 1960).

Total thickness of the Mancos Shale, which generally represents the open-marine mudstones deposited in the Cretaceous Western Interior Seaway, is approximately 3,500 ft if measured from the top of the Book Cliffs just north of the site area. Most of the Mancos is a monotonously uniform, drab or bluish gray shale; however, in the site area, which is in the upper third of the formation, an anomalously sandy interval is present that represents some nearshore deposition. This sandy interval was earlier recognized

as the "Mancos B" (zone or horizon) because of its natural gas-producing characteristics on the Douglas Creek arch near the Utah-Colorado border (Kellogg 1977). More recent stratigraphic studies have identified the nearshore facies of this sandy interval and formalized this unit and renamed it the Prairie Canyon Member (Cole and others 1997). Some facies of the Prairie Canyon Member, as identified by Hampson and others (1999) as fluvial-dominated delta front deposits, occur in the north part of the mapped area. These delta-front deposits, therefore, are mapped as representing the Prairie Canyon Member in the site area. From the sandy (generally very fine grained) nature of this member as exposed in a few outcrops, seen in several coreholes and test pits, and expressed as a marked reduction in the gamma ray geophysical log response from coreholes, the thickness of the Prairie Canyon Member in the mapped area is approximately 150 to 200 ft. Up to approximately 100 ft of the lower part of the Prairie Canyon Member is present along the north edge of the proposed disposal cell.

Underlying and overlying the sandy interval of the Prairie Canyon is the Blue Gate Member of the Mancos Shale. The Blue Gate consists mainly of open-marine mudstone and shale, with a few thin siltstone layers. In the site area, the Blue Gate is divided into lower and upper parts to accommodate the Prairie Canyon Member. Outcrops of both lower and upper parts of the Blue Gate are rare – only one of each was found in the mapped area (Plate 1). A thickness of approximately 2,000 ft of lower Blue Gate is present in the site area. Below the Blue Gate are the lowermost members of the Mancos Shale, the Ferron Sandstone underlain by the Tununk Shale, that combine for an approximate 300 to 400 ft thickness. It is therefore estimated that approximately 2,400 ft of Mancos Shale underlies the center of the proposed disposal cell; this includes all of the lower Blue Gate, the Ferron Sandstone, and the Tununk Shale.

The upper Blue Gate, above the Prairie Canyon, is approximately 700 to 800 ft thick. It is overlain by the Blackhawk Formation, the lowermost unit of the Mesaverde Group, that forms the sandstone crest of the Book Cliffs immediately north of the site area.

A generalized stratigraphic section of the mapped site area is shown in Figure 5. Characteristics of each member of Mancos Shale as seen in outcrops and in borehole core are discussed in the following subsections, in chronologic order from oldest to youngest. Detailed lithologic descriptions of bedrock from the ten deep (300 ft) coreholes are in Attachment 5 of the RAP. Five cross sections (Plate 2) across the site show the lithologic position of the Prairie Canyon Member in the subsurface. The bedrock contour map (Plate 3) shows subtle ridges and other variations in the bedrock topography.

3.1 Lower Blue Gate Member

The lower part of the Blue Gate Member does not crop out on or immediately around the proposed disposal cell; however, the unit is present in the subsurface and all of the ten coreholes penetrated part of the unit. The unit crops out in poor exposures in one place in the southwest edge of the mapped area on a low hill that is an eroded remnant of a pediment surface (Plate 1). Here, the exposures are mainly gray shale and minor, thin, lenticular beds of light gray to brown-orange (limonitic) siltstone that contains small tracks and other trace fossils.

Bedrock penetrated by four of the coreholes (0202, 0205, 0207, and 0209) consisted of the lower Blue Gate. Also, one packer test hole (0212) was cored solely in the lower Blue Gate, and the bottom of test pit 0154 was in the lower Blue Gate. The other coreholes passed through part of the Prairie Canyon Member before reaching total depth in the lower Blue Gate.

The lower Blue Gate penetrated by the coreholes is mostly medium gray (N5), calcareous, silty claystone, and is fissile in some places. Several thin zones occur that have a small percentage (less than 20%) of bioturbated bedding of siltstone or very fine grained sandstone that is lighter colored, very light gray (N8). Fine, black carbonaceous material and framboidal pyrite (plated on fossils in places) occur in trace amounts. Large fossils that were found in the core consist mainly of coiled and flattened cephalopods and pelecypods. Curious dense masses up to 2 inches in diameter of white, highly calcareous (porcelaneous-appearing) material occur rarely in the deeper part of the lower Blue Gate (more than 150 ft below the upper contact). Small beads (up to 0.05 inch diameter) of amber or resin occur in trace amounts in

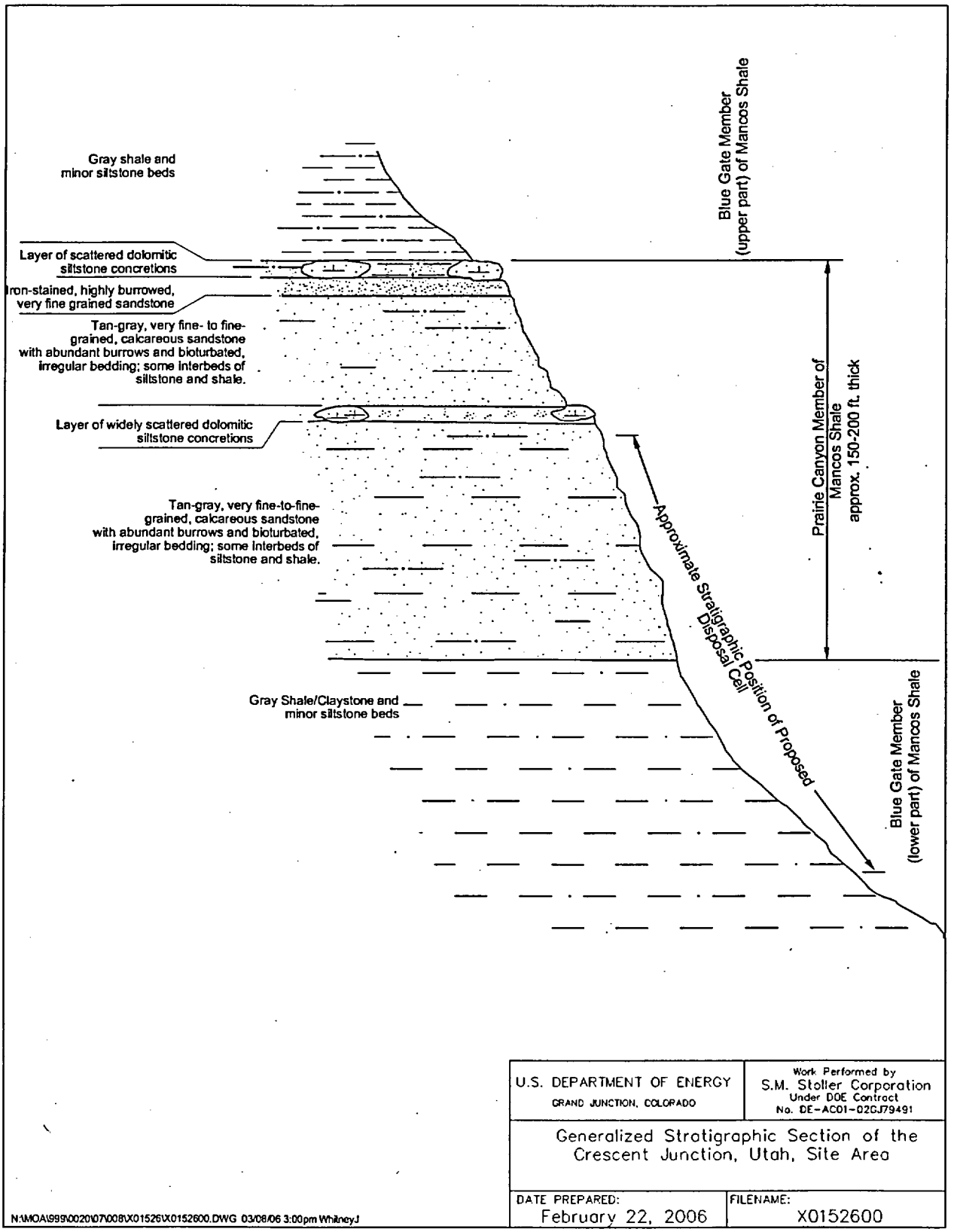

Figure 5. Generalized Stratigraphic Section of the Crescent Junction, Utah, Site Area

various depths in most coreholes into the lower Blue Gate. Below a depth of 100 ft into this bedrock, no natural fractures were noted and no evidence was seen of water movement (interior of broken core was dry).

The top of the lower Blue Gate occurs generally in the space of several ft where bioturbated bedding and associated very fine-grained sandstone increases to about 30 percent. This change is best seen in the geophysical logs as a marked reduction in gamma ray response. In the five coreholes that were geophysically logged, the depth of the contact of the lower Blue Gate and Prairie Canyon is picked as follows: 0203 – 117 ft, 0204 – 52 ft, 0206 – 107 ft, 0208 – 117 ft, and 0210 – 139 ft. In corehole 0201, which was not geophysically logged, the contact is placed where the amount of bioturbation increases very rapidly at approximately 157 ft. The Prairie Canyon – top of lower Blue Gate contact is shown in the north-south cross sections A-A', B-B', and C-C', and more along strike in the west-east cross section D-D' (Plate 2).

3.2 Prairie Canyon Member

Several outcrops of very fine-grained sandstone of the Prairie Canyon Member occur in the proposed disposal cell area (Plate 1). Additional small outcrop areas of sandstone occur east and north of the proposed disposal cell. A band of scattered small outcrops of dolomitic siltstone concretions also occurs across the north part of the site area marking the top of the Prairie Canyon Member. Three lithologic facies were selected for mapping (Plate 1) to show the variation of this member in the site area. The lower and thickest unit is a tan, burrowed sandstone. A thin, distinctive rusty brown, burrowed sandstone unit occurs just below the uppermost dolomitic siltstone concretions. A band of discontinuous, large, resistant, dolomitic siltstone concretions is present approximately 50 ft below the top band of concretions. Each of these facies is described in the following subsections, and they are similar in many characteristics to those described by Hampson and others (1999) in this part of the outcrop belt of the Prairie Canyon.

3.2.1 Tan, burrowed sandstone

This facies is exposed in the proposed disposal cell area on a subtle, north-trending ridge approximately along the section line between Sections 26 and 27 (Plate 1). Here, the light gray to tan sandstone is fine to very fine grained, calcareous, burrowed, and is exposed in lenticular to slabby beds about 1 inch thick.

This fine- to very fine-grained, burrowed sandstone subcrops under approximately the northern 60 percent of the proposed disposal cell area. This estimated subcrop of the base of the Prairie Canyon Member shown in Plate 1 is based on scattered outcrops of the tan and gray sandstone in the proposed disposal cell area and along strike just to the east in a low ridge near test pit 0156. Also, several geotechnical boreholes (0085 and 0087) noted the presence of sandstone bedrock at their total depths.

North of the proposed disposal cell and stratigraphically higher, the sandstone crops out in scattered locations – the largest is an area over 500 ft long along the west side of a low ridge extending south-southeast from the area of the 3 ponds (Plate 1). In this outcrop area, the slabby sandstone is tan, fine grained, calcareous, slightly friable, bioturbated, with abundant sole marks and burrows. Other outcrops of this sandstone occur along strike to the west (south of corehole 0201) and east (east and north of corehole 0210). These scattered northern outcrops occur mainly on the south side of a band of low mounds formed (capped) by resistant, large, dolomitic siltstone concretions.

Core from the several holes through the Prairie Canyon Member show that most of the rock is medium gray (N5) silty claystone to clayey siltstone, and usually only 10 to 30% of the rock is very light gray (N8), very fine-grained sandstone. The sandstone is bioturbated, wavy bedded, and contains traces of framboidal pyrite, fine carbonaceous (plant fragment?) material, and pelecypod and cephalopod imprints. The percentage of sandstone (up to 30%) shown in the core is more of a true account of the stratigraphy of this member, rather than reliance on the surface outcrops, which tend to be of the more resistant sandstone. Coreholes in the mapped area that penetrated part of the Prairie Canyon Member sandstones are 0201 (penetrated nearly all of the Prairie Canyon Member), 0204, 0206, 0208, and 0210. Lithologic logs from coreholes 0201, 0208, and 0210 contain the most detailed description of the lithology. Below a

depth of about 80 ft into this bedrock, no natural fractures were noted and no evidence was seen of water movement (interior of broken core was dry).

3.2.2 Rusty brown, burrowed sandstone

This thin, distinctive facies crops out in scattered locations along an east-trending belt across the north part of the mapped area (Plate 1). The unit is only about 3 ft thick and typically occurs just below the large dolomitic siltstone concretions that form the northernmost line of low mounds. It consists of dense, resistant, rusty brown, very fine- to fine-grained sandstone that contains large burrows up to 1.5 inches in diameter, and abundant trace fossils and casts. This facies contains the most intense and diverse bioturbation. The unit was not seen in all of the northernmost dolomitic siltstone concretion mounds, possibly because of cover or poor outcrops.

3.2.3 Dolomitic siltstone concretion

This facies, the best exposed in the mapped area, occurs in two east-trending bands of low, scattered mounds up to 15 ft high in the north part of the mapped area just north of the proposed disposal cell. Each mound is capped by one or more large concretions of dolomitic siltstone. The lower band, represented by several widely scattered mounds, is stratigraphically about 50 ft below the upper band. The dolomitic concretion-capped mound just west of corehole 0210 represents this lower band (Plate 1).

The upper band contains more numerous mounds in the mapped area and consists of 10 to 15 scattered mounds. The top of these mounds represents the top of the Prairie Canyon Member in the mapped area, as shown in Plate 1. This contact of the top of the Prairie Canyon and base of the upper Blue Gate Member marks a delta-front abandonment and marine-flooding surface followed by deposition of marine shales of the upper Blue Gate (Cole and others 1997).

Concretions are hard, dense, brittle, up to 5 ft thick, and are composed of dolomitic siltstone; some contain calcite crystals and masses. Dolomitic siltstone on fresh surfaces is medium gray (N5) and weathered surfaces are grayish orange (10YR 7/4). Bedding is wavy, flaser (flame or streak)-shaped, and interrupted in places by burrowing. The concretion-capped mounds (Figure 6) vary in diameter from 20 or 30 ft to the large mound about 200 ft in exposed diameter just southwest of corehole 0201. The top of the resistant concretion mounds forms a north-dipping cuesta-like surface where the dip of the Mancos Shale could be measured in several places (Plate 1) at approximately 5 to 6 degrees. Vertical joints, some coated with limonite, form in the brittle dolomitic siltstone. These joints were measured in several locations (Plate 1). The principal joint direction is approximately N10E and subsidiary directions are N50W and N85W.

3.3 Upper Blue Gate Member

The only outcrop of the upper part of the Blue Gate Member in the mapped area is north of the 3 ponds area along a steep, west-facing slope above a small drainage. Cropping out on the slope is soft, gray brown, silty shale and some interbeds of slabby, thin, tan brown, very fine-grained, burrowed sandstone. Sandstone litter and sheet wash cover most outcrops north of the mounds, which mark the top of the Prairie Canyon Member, until the steep slopes of the Upper Blue Gate Member are reached at the base of the Book Cliffs.

3.4 Structural Features and Weathered Bedrock

No faults or evidence of faults (slickensides on fracture surfaces) were found in the deep coreholes. Lithologic logs, geophysical logs, and surface outcrops verify that the dip of Mancos Shale bedrock in most of the mapped area is approximately 5 to 6 degrees to the north. This is shown in cross sections B-B' and C-C' (Plate 2). Evidence that the northward dip may be slightly less in the western part of the mapped area is from the slightly wider subcrop belt of the Prairie Canyon Member shown in Plate 1 and the cross section A-A' (Plate 2).

Figure 6. View northeast of a low mound formed by the uppermost band of dolomitic siltstone concretions at the top of the Prairie Canyon Member of Mancos Shale.

Weathered bedrock characteristics were noted during lithologic logging of the deep coreholes. At depths of more than 40 to 45 ft, bedrock was usually competent without bedding plane fractures and had a fresh appearance. No natural fractures were noted in the core from depths greater than 80 to 100 ft.

Horizontal bedding plane fractures occur mainly in the top 20 to 30 ft of weathered bedrock; the numerous fractures rapidly decrease in frequency in the first 10 to 20 ft of depth (Figure 7). Typical colors of weathered and altered rock are yellowish gray (5Y 7/2), pale yellowish brown (10YR 6/2), and light olive gray (5Y 5/2). Limonitic alteration typically has a dark yellowish orange (10YR 6/6) color.

Higher-angle, non-bedding plane, fractures are abundant in the first 20 to 30 ft of bedrock. These fractures are typically coated or filled with white crystalline gypsum (and possibly some calcite), as shown in Figure 8. These shallow fractures and, particularly, the deeper fractures may be coated (stained) with limonite, indicating movement of small amounts of ground water (Figure 9). Only a few fractures extend below a depth of 50 ft, and those do not extend much deeper. Two deeper, limonite-stained fractures occur at 68 and 73 ft depths in corehole 0203, indicating some minor ground water movement in the past.

Conclusions

Interpretation and characterization of the surficial and bedrock geology of the mapped area in and around the proposed disposal cell area found no features that would adversely affect the geologic suitability of the disposal site. The following features and characteristics of the surficial and bedrock geology of the site area favor its suitability for a disposal cell.

- Approximately 2,400 ft of Mancos Shale, represented mainly by open-marine mudstone, is present beneath the center of the proposed disposal cell.
- No evidence for faults was noted in the surface or in bedrock units.
- No evidence of saturation in the bedrock was seen; core was dry when broken open.
- Natural fractures were mostly in the top 20 to 30 ft of bedrock and below that the rock is largely competent; fractures are rare below depths of 50 ft and not noted below 80 to 100 ft depths.
- Surficial deposits have been emplaced in a stable geologic environment mainly by a slow accumulation of material transported during infrequent heavy rainfall episodes from the base and sides of the Book Cliffs along active sheet wash paths.

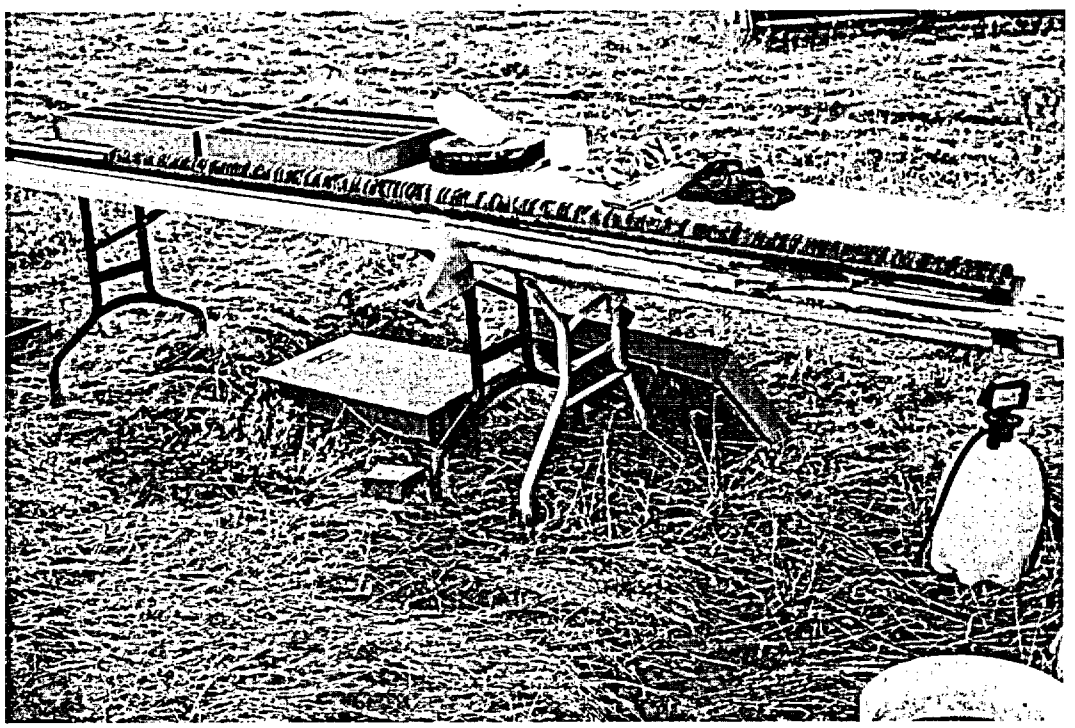

Figure 7. Core from hole 0210, from 26 (left) to 36 ft (right), showing progression in depth from highly weathered to slightly weathered bedrock.

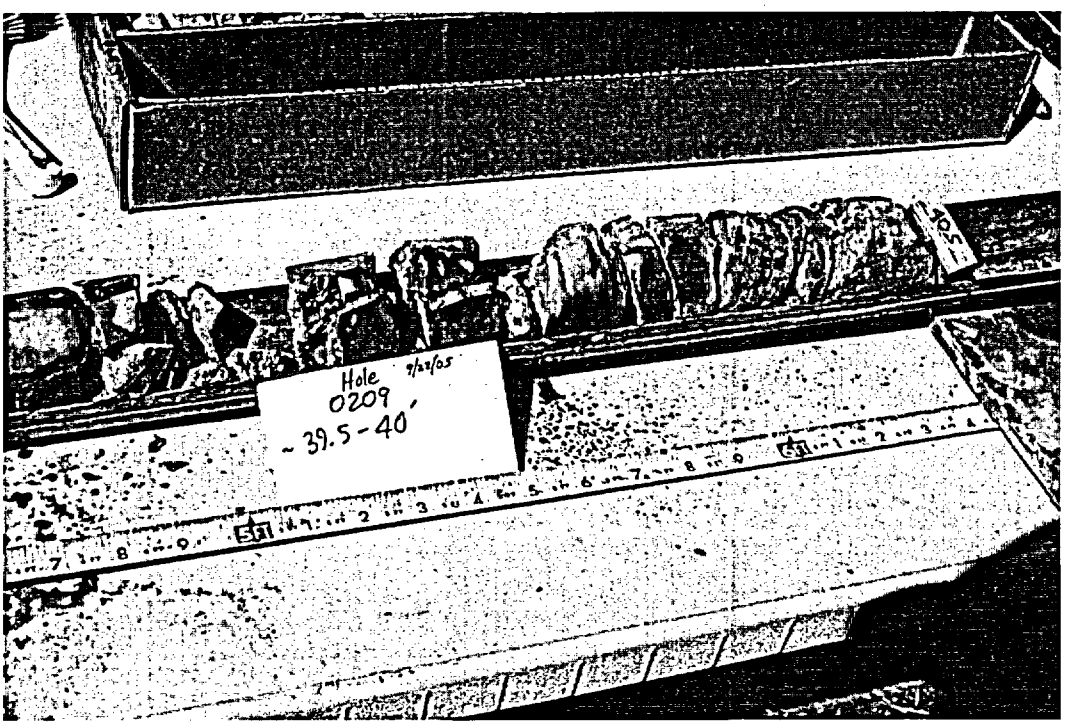

Figure 8. Gypsum (white) filling a vertical fracture at 39.5 to 40.0 ft depth in weathered lower Blue Gate Member bedrock at corehole 0209.

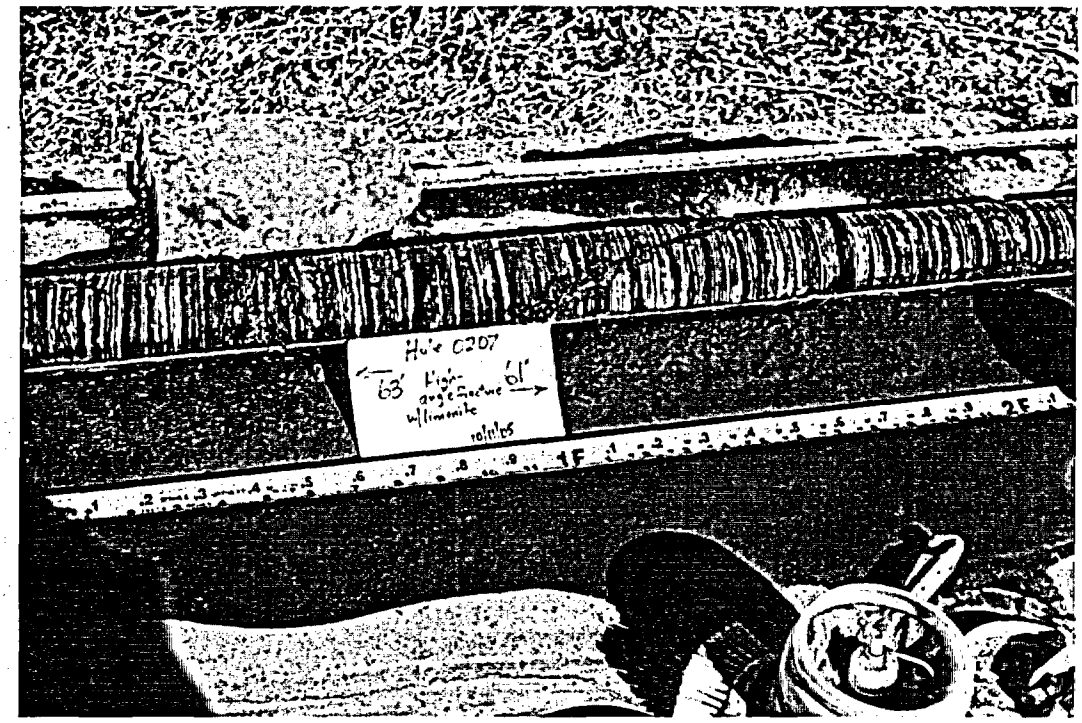

Figure 9. Limonite (orange) coating high-angle fracture at about 62 ft depth in slightly weathered lower Blue Gate Member bedrock at corehole 0207.

Computer Source:

Not applicable.

References:

Cole, R.D., Young, R.G., and Willis, G.C., 1997. *The Prairie Canyon Member, a New Unit of the Upper Cretaceous Mancos Shale, West-Central Colorado and East-Central Utah*: Utah Geological Survey Miscellaneous Publication 97-4, 23 p.

Doelling, H.H., 1997. *Interim Geologic Map of the Valley City Quadrangle, Grand County, Utah*: Utah Geological Survey Open-File Report 351, 55 p., scale 1:24,000.

Doelling, H.H., 2001. *Geologic Map of the Moab and Eastern Part of the San Rafael Desert 30' x 60' Quadrangles, Grand and Emery Counties, Utah, and Mesa County, Colorado:* Utah Geological Survey Map 180, scale 1:100,000.

Fisher, D.J., Erdmann, C.E., and Reeside, J.B., Jr., 1960. *Cretaceous and Tertiary Formations of the Book Cliffs, Carbon, Emery, and Grand Counties, Utah, and Garfield and Mesa Counties, Colorado*: U.S. Geological Survey Professional Paper, 332, 80 p.

Franczyk, K.J., Pitman, J.K., and Nichols, D.J., 1990. *Sedimentology, Mineralogy, Palynology, and Depositional History of Some Uppermost Cretaceous and Lowermost Tertiary Rocks along the Utah Book and Roan Cliffs east of the Green River*: U.S. Geological Survey Bulletin 1787-N, 27 p.

Hampson, G.J., Howell, J.A., and Flint, S.S., 1999. *A Sedimentological and Sequence Stratigraphic Re-Interpretation of the Upper Cretaceous Prairie Canyon Member ("Mancos B") and Associated Strata, Book Cliffs Area, Utah, U.S.A.*: Journal of Sedimentary Research, vol. 69, no. 2, p. 414-433.

Kellogg, H.E., 1977. *Geology and Petroleum of the Mancos B Formation, Douglas Creek Arch Area, Colorado and Utah*, in Veal, H.K., editor, Exploration Frontiers of the Central and Southern Rockies: Rocky Mountain Association of Geologists, p. 167-179.

Willis, G.C., 1994. *Geologic Map of the Harley Dome Quadrangle, Grand County, Utah*: Utah Geological Survey Map 157, 18 p., scale 1:24,000.

THIS PAGE IS AN OVERSIZED DRAWING OR FIGURE,

THAT CAN BE VIEWED AT THE RECORD TITLED:

PLATE 1,

"GEOLOGIC MAP OF BEDROCK OUTCROPS AND SURFICIAL DEPOSITS, CRESCENT JUNCTION, UT, PROPOSED REPOSITORY SITE"

WITHIN THIS PACKAGE

D-01

THIS PAGE IS AN OVERSIZED DRAWING OR FIGURE,

THAT CAN BE VIEWED AT THE RECORD TITLED: PLATE 2, "GEOLOGIC CROSS SECTIONS"

WITHIN THIS PACKAGE

D-02

THIS PAGE IS AN OVERSIZED DRAWING OR FIGURE,

THAT CAN BE VIEWED AT THE RECORD TITLED:

PLATE 3,

"BEDROCK CONTOUR MAP"

WITHIN THIS PACKAGE

D-03

Appendix C

U.S. Department of Energy—Grand Junction, Colorado

Calculation Cover Sheet

Calc. No.: MOA-02-08-2005-1-06-00 **Discipline:** Geology and Geophysical Properties **No. of Sheets:** 5

Project: Moab Project

Site: Crescent Junction Disposal Site

Feature: Site and Regional Geomorphology – Results of Literature Research

Sources of Data:

Published reports and maps – see list of references at end of calculation set.

Sources of Formulae and References:

See list of references at end of calculation set.

Preliminary Calc. ☐ **Final Calc.** ☑ **Supersedes Calc. No.**

Author: Mark Kautsky — Name — 30 Aug '05 — Date

Checked by: [signature] — Name — 30 Aug 05 — Date

Joseph L. Reed — Name — 30 Aug 05 — Date

J. Berwick — Name — 8/14/06 — Date

Approved by: Kenneth L. Kopp — Name — 8-30-05 — Date

Name — Date

Problem Statement:

Determination of the suitability of the Crescent Junction disposal site as the repository for the Moab uranium mill tailings material, and development of the site and regional geomorphology sections of the Remedial Action Plan (RAP) require a thorough review of available literature that applies to the Crescent Junction site. The compiled list of references is presented at the end of this calculation set and relevant information is summarized below.

This is Calculation Set No. 6 as defined in the Moab Project Task Order ST05-203 Modification P, to be completed by 31 August 2005. This information will be incorporated into the RAP for the Moab site.

Method of Solution:

Literature sources were identified using a combination of published reports and maps that were developed during the Crescent Junction site-selection process, on-line (internet-based) resources, and relevant literature citations from the other UMTRCA sites.

Assumptions:

It is assumed that the literature sources are reliable and representative of the current understanding of the geomorphology of the region.

Calculation:

None required.

Discussion:

A general summary of geomorphologic conditions based on the literature research is provided in this calculation set. This summary is preliminary and will be expanded as a result of future, detailed geomorphologic studies. Additional information will be presented in the RAP.

Crescent Flat, the physiographic location for the Crescent Junction disposal site, is on a broad, nearly level, plain at the base of the Book Cliffs. The elevation of Crescent Flat ranges from approximately 4,900 feet above mean seal level (ft amsl) at the southwest corner of the withdrawn area to approximately 5,120 ft amsl at the northeast corner of the withdrawn area. Crescent Flat is bounded to the north by the steep slopes of the Book Cliffs whose elevation rises to approximately 5,900 ft amsl.

Drainage features across most of Crescent Flat consist of relatively subtle depressions that comprise Kendall Wash. The name Kendall Wash is a designation that appears on the 1:250,000-scale Moab topographic sheet but is absent from the later-published 1:24,000 scale topographic quadrangle map. For the purpose of this investigation, the name Kendall Wash will be reinstated to describe the watercourse that collects surface water from Crescent Flat. Kendall Wash has two forks across Crescent Flat: the "West Branch" and the "East Branch", which are informal designations created specifically for this study (Figure 1). These two forks collect surface water from most of the withdrawn area. Kendall Wash enters Thompson Wash approximately 3.5 miles south of Crescent Junction. Thompson Wash and Crescent Wash converge approximately 7.1 miles south of Crescent Junction and form Tenmile Canyon, which is a tributary to the Green River. The confluence of Tenmile Canyon with the Green River is approximately 23 miles southeast of Crescent Junction. The subtle drainages observed over the surface of Crescent Flat are an indication that depositional, rather than erosional, processes are dominant over the landscape.

The western margin of the withdrawn area coincides with Crescent Wash, which is a 22 square mile drainage feature that emerges from Crescent Canyon in the Book Cliffs. Crescent Canyon heads approximately 10 miles north of Crescent Flat. Crescent Wash is an intermittent channel that forms an erosional cut that is entrenched some 15 ft below the surface of Crescent Flat. Based on the depth of the cut, the steep canyon walls and high relief within Crescent Canyon, and the size of the detritus within the channel, Crescent Wash appears capable of considerable erosion when it flows. The narrow and steep

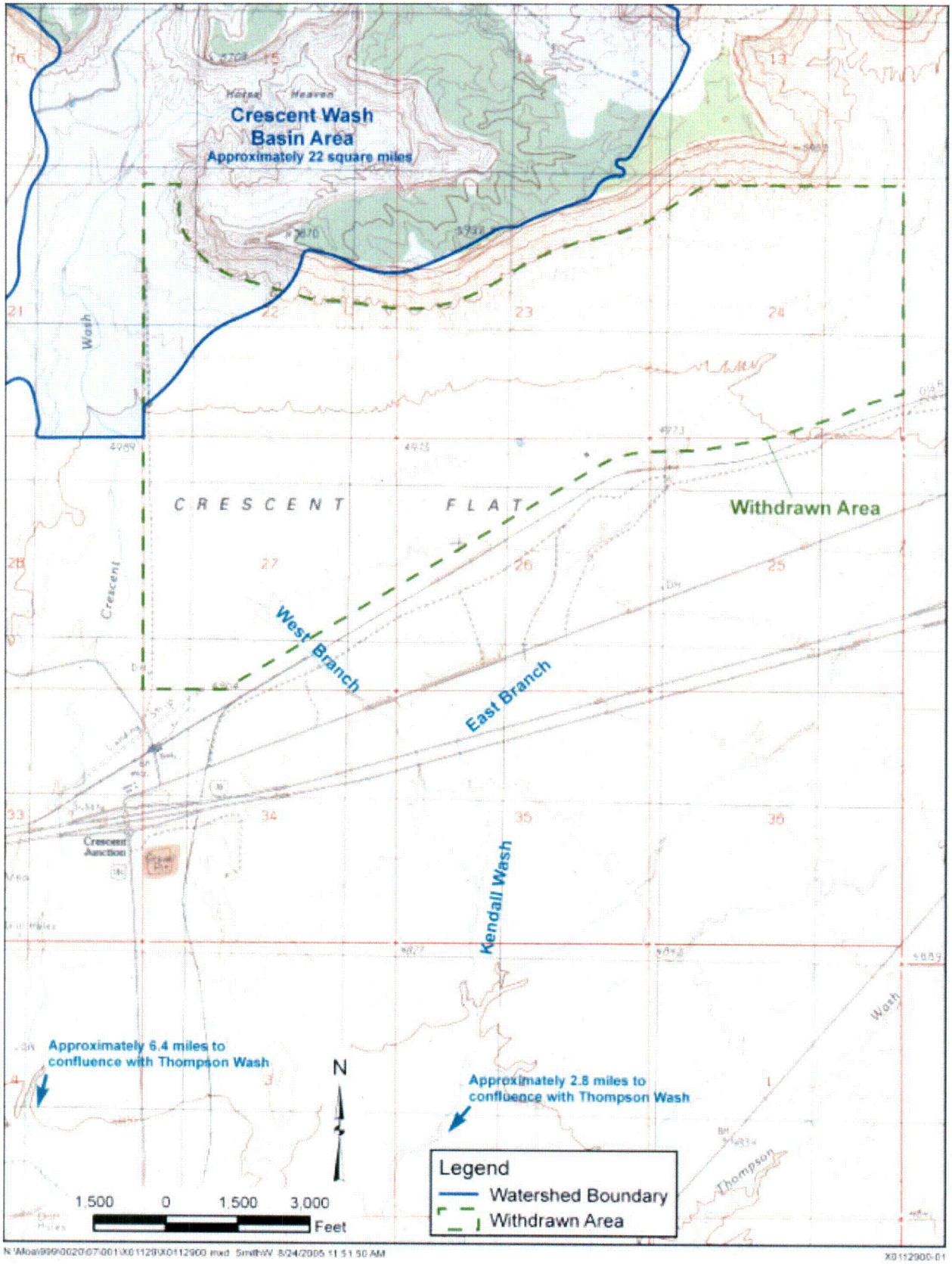

Figure 1. Topographic Map of Crescent Junction Vicinity Showing the Locations of Surface Water Features

aspect of Crescent Canyon is prime location for flash floods. Crescent Wash is therefore considered a significant fluvial-geomorphic feature with regard to the proposed repository at the Crescent Junction disposal site.

The soil profile at Crescent Flat is rather poorly developed. Over much of the site, the bedrock is covered over by "alluvial mud" of Quaternary age (Doelling 2001). This unconsolidated gray material, less than 20 ft thick, fills swales in the Mancos Shale and contains rock fragments from the underlying parent material, detrital material shed from the Book Cliffs, and occasional remnants of lag gravels that formed on earlier pediment surfaces. The alluvial mud mantles the bedrock to varying degrees. Aerial photographs and field reconnaissance have shown lineaments that form where relatively resistant ledges of suspected siltstone bedrock occur in the shallow subsurface. Detrital materials within the mud are distributed somewhat randomly at the land surface over the entire breadth of Crescent Flat. Large rock fragments, primarily sandstone, are more abundant near the base of the Book Cliffs where rock falls are an important hillslope process.

The Mancos Shale is exposed along the face of the Book Cliffs. The calcareous shale beds strike approximately N60E and dip to the northwest at less than 10 degrees. The exposed shale supports little to no vegetation; consequently, the surface is vulnerable to erosional forces, such as rill and gully erosion by running water and attendant rock falls, which were described earlier. Erosion of the exposed face of the Book Cliffs forms contrasting slopes that are carved in calcareous shale and sandstone strata. The slope angles of the Book Cliffs are controlled by a combination of geologic structure and the strength of the rock mass of the bedrock material. Running water that enters Crescent Flat at the base of the Book Cliffs rapidly looses kinetic energy and signs of sheet flow and sediment deposition become more evident. As mentioned above, Crescent Flat exhibits only incipient fluvial channeling.

Conclusion and Recommendations:

Based on preliminary evaluation of the results of the literature research effort, the Crescent Junction site appears to be suitable for disposal of the Moab uranium mill tailings and contaminated material. Additional information will be collected and reported in the RAP.

Computer Source:

Not applicable.

References:

Aerographics, Inc., 2005. *Crescent Junction Photography* – one set of 12 >> 10"x10" color contact prints of the high-altitude flight. Transmittal No. 13224 for S.M. Stoller Corporation. August 1, 2005.

Aerographics, Inc., 2005. *Crescent Junction Photography* – two sets of 10 >> 10"x10" color contact prints of the low-sun angle flight. Transmittal No. 13227 for S.M. Stoller Corporation. August 2, 2005.

Cole, R.D., Young, R.G., and Willis, G.C., 1997. *The Prairie Canyon Member, a New Unit of the Upper Cretaceous Mancos Shale, West-Central Colorado and East-Central Utah*: Utah Geological Survey Miscellaneous Publication 97-4, 23 p.

Doelling, H.H., 2001. *Geologic Map of the Moab and Eastern Part of the San Rafael Desert 30' x 60' Quadrangles, Grand and Emery Counties, Utah, and Mesa County, Colorado:* Utah Geological Survey Map 180, scale 1:100,000.

Friedman, J.D., and Simpson, S.L., 1980. *Lineaments and Geologic Structure of the Northern Paradox Basin, Colorado and Utah*: U.S. Geological Survey Miscellaneous Field Studies Map MF-1221, scale 1:250,000.

Hampson, G.J., Howell, J.A., and Flint, S.S., 1999. *A Sedimentological and Sequence Stratigraphic Re-Interpretation of the Upper Cretaceous Prairie Canyon Member ("Mancos B") and Associated Strata, Book Cliffs Area, Utah, U.S.A.*: Journal of Sedimentary Research, vol. 69, no. 2, p. 414-433.

Harty, K.M., 1993. *Landslide Map of the Moab 30' x 60' Quadrangle, Utah*: Utah Geological Survey Open-File Report 276, scale 1:100,000.

Koons, E.D., 1955. *Cliff Retreat in the Southwestern United States*: American Journal of Science, vol. 253, p. 44-52.

Leopold, L.B., Wolman, M.G., and Miller, J.P., 1964. *Fluvial Processes in Geomorphology*, W.H. Freeman and Company, San Francisco, 522 p.

Mulvey, W.E., 1992. *Soil and Rock Causing Engineering Geologic Problems in Utah*: Utah Geological Survey Special Study 80, 23 p., scale 1:500,000.

Oviatt, C.G., 1988. *Evidence for Quaternary Deformation in the Salt Valley Anticline, Southeastern Utah*, in Salt Deformation in the Paradox Region: Utah Geological and Mineral Survey Bulletin 122, p. 61-76.

Schumm, S.A., 1966. *Talus Weathering and Scarp Recession in the Colorado Plateaus*: Zeitschrift für Geomorphologic, vol. 10, p. 11-36.

Schumm, S.A., 1980. *Geomorphic Thresholds: the Concept and its Applications*: Institute of British Geographers Transactions, vol. 4, p. 485-515

Thomas Dunne and Leopold, L.B., 1978. *Water in Environmental Planning*, W.H. Freeman and Company, San Francisco, 818 p.

U.S. Department of Agriculture, Soil Conservation Service, 1989. *1989 Soil Survey of Grand County, Utah, Central Part*.

Appendix D

U.S. Department of Energy—Grand Junction, Colorado

Calculation Cover Sheet

Calc. No.: MOA-02-08-2005-1-08-00 Discipline: Geologic and Geophysical Properties No. of Sheets: 18 LE 8-21-06

Project: Moab Project

Site: Crescent Junction Disposal Site

Feature: Site and Regional Geomorphology – Results of Site Investigations

Sources of Data:

Refer to calculation.

Sources of Formulae and References:

References cited in this calculation set are listed in Calc. No. MOA-02-08-2005-1-06-00 (Site and Regional Geomorphology – Results of Literature Research).

Preliminary Calc. ☐ Final Calc. ☑ Supersedes Calc. No.

Author: Mark Kautsky for CSG 8-30-05 (Name / Date)

Checked by: [signature] 30 Aug 05 (Name / Date)

Approved by: [signature] 8-30-05 (Name / Date)

Mark Kautsky 30 Aug '05 (Name / Date)

Joseph L. Reed 30 Aug 05 (Name / Date)

Joel Benwell 8/14/06 (Name / Date)

Problem Statement:

Preliminary site selection performed jointly by the U.S. Department of Energy (DOE) and the Contractor has identified a 450–acre location in the Crescent Flat area just northeast of Crescent Junction, Utah, as a possible site for final disposal of the Moab uranium mill tailings. Based on the preliminary site-selection process, the suitability of the Crescent Junction disposal site is being evaluated from several technical aspects, including geomorphic, geologic, seismic, and geotechnical. The objective of this calculation set is to identify geomorphic processes that affect the site.

This is Calculation Set No. 5 as defined in the Moab Project Task Order ST05–203 Modification P, to be completed by 31 August 2005. Findings from this calculation will be incorporated into the Remedial Action Plan (RAP) for the Moab site.

Method of Solution:

Geomorphic characteristics of the withdrawn area for the Crescent Junction disposal site are described in this calculation set. Field reconnaissance of geomorphic features of the site was conducted from July 18 to 20, 2005. In addition to ground traverses across the site, a traverse across the top of the Book Cliffs was made on July 19, 2005 to view the site from the north. Low-sun angle (LSA) aerial photographs (from early-day and late-day sun angles) and high-altitude aerial photographs of the site area flown on July 8, 2005, by AeroGraphics, Inc. (2005a and 2005b), were also used to discern geomorphic features. Specific conclusions drawn from interpretation of LSA results will be presented in the RAP. Test pits were excavated at two locations within the proposed footprint of the tailings repository. Significant site geomorphic features together with two test–pit locations are shown in Figure 1. Test pit logs will be presented in the RAP.

Assumptions:

Not applicable.

Calculation:

None required.

Discussion:

The dynamic equilibrium that exists in topographically diverse areas may be explained as a balance that exists between degradational (erosional) and aggradational (depositional) processes. The degradational processes act on or near the sources of sediment, while the aggradational processes occur at or near sediment sinks. The landforms observed at the Crescent Flat area are discussed in terms of these two competing processes.

Degradational Processes

- **Crescent Wash**

  The basin area of Crescent Wash is approximately 22 square miles. Much of the area is composed of narrow canyons and steep slopes that gain up to 1,000 feet (ft) in elevation, but more commonly, the canyons comprise several hundred feet in vertical relief. Steep slopes within the canyon create high fluvial gradients capable of transporting significant quantities and size of sediment. Boulders derived from the canyon walls have been observed up to 4 ft in diameter in Crescent Wash (Figure 2). Runoff events within Crescent Wash were not observed first-hand during this site investigation. Results of geologic mapping (Doelling 2001) have shown that the eastward lateral extent of Crescent Wash alluvial deposits is contained within the subtle ridges of Mancos Shale bedrock that exist in the southwest corner of Section 27. Test pit 0151, constructed in the north-central part of Section 27, only showed minor fluvial channels, apparently not related to Crescent Wash. Material in the minor

channel was locally derived detritus composed of shale and sandstone. Fluvial channeling was not observed in test pit 0153.

- **Kendall Wash Tributaries**

  Drainages originating at Crescent Flat coalesced into a feature that was formerly designated as Kendall Wash (1:250,000 scale Moab topographic sheet); however, this designation is not shown on the 1:24,000 scale topographic quadrangle maps. For this investigation, the northernmost tributaries of Kendall Wash are referred to as the "West Branch" and "East Branch". West Branch (Figure 3) drains to the southeast through the southeast quarter of Section 27. The West Branch collects surface drainage from Sections 27 and 22 and is incised up to approximately 10 ft deep at its intersection with old U.S. Highway 50. The West Branch is east of the subtle Mancos Shale ridge that divides the West Branch from alluvial deposits of Crescent Wash. No evidence exists that the West Branch cuts into the surface of the Mancos Shale. The head-ward migration rate of the West Branch was not determined quantitatively as part of this calculation set.

  The East Branch drains in a southwest direction through Sections 24 and 26, and collects surface drainage from Sections 23, 24, 25, and 26. Because its drainage area is larger than that of the West Branch, the East Branch is incised considerably deeper into Crescent Flat. North of the intersection of the East Branch with U.S. Highway 50, currently the Interstate 70 frontage road, the East Branch is incised approximately 15 ft into the surface of Crescent Wash (Figure 4).

  Part of the surface water entering both the West Branch and the East Branch descends through rills and gullies along the face of the Book Cliffs and spreads out as sheet flow. Sediment deposition occurs at the base of the Book Cliffs where the water velocity is slower. Holocene to Late-Pleistocene alluvial mud that covers the Mancos Shale in Crescent Flat is probably derived from the sheet flow action. Only minor incised channels exist in the northern reaches of Crescent Flat. The absence of active fluvial down-cutting along Crescent Flat, and the Holocene to Late-Pleistocene stability of Crescent Flat are favorable attributes of the site with regard to its proposed use.

Aggradational Processes

Alluvial mud is an expression of sheet wash deposition that accumulated as a consequence of erosion of the Book Cliffs face. The rill and gully erosion on the face of the Book Cliffs demonstrates that they are a source of sediment material. Present evidence of the sheet wash process is shown in Figure 3. The discolored areas of Crescent Flat with drab gray soils from the face of the Book Cliffs are slightly braided with the long axis oriented parallel to the flow direction. The most prominent sheet wash feature trends to the south-southeast from near the three ponds between Sections 22 and 23 (Figure 5).

Bedrock Geomorphology

Low cuesta–like ridges and mounds that appear as an easterly trend lie along the northern margin of Crescent Flat. The linear feature east of the three ponds is shown in Figure 5. A ground photo of the cuesta–like feature is shown in Figure 6. The linear feature also exists west of the three ponds. More resistant, calcareous siltstone beds in the Prairie Canyon Member of the Mancos Shale form the cuesta-like features.

Low hills scattered over Crescent Flat, particularly in the southwest quarter of Section 27 and the northeast corner of Section 34, are an expression of the former pediment–mantling material that capped the Mancos Shale. Figure 6 from just west of the site shows where the pediment mantling material is in place. The subtle mounds signifying the remnants of these features are scattered over Crescent Flat.

Rock–falls are another active erosional process observed at the base of the Book Cliffs. Figure 7 shows how some of the boulders attain large proportions. These rock falls occur episodically in response to the freezing action of water that seeps into cracks in the sandstone along the rim of the Book Cliffs. Although, the northward rate of advance of the escarpment along the face of the Book Cliffs was not estimated as part of this investigation, it is probably very long in comparison to the performance life of the proposed

tailings repository. Additional information will be presented in the RAP. Because of limited precipitation, these boulders will likely take many years to disaggregate.

A large erosional feature exists north of the face of the Book Cliffs in an area known as Horse Heaven. This area is in the southern half of Section 15, the northern half of Section 22, and the eastern half of Section 14 (Figure 1). Landslide material mapped in this location by Doelling (2001) is reported to be Holocene to Pleistocene. This deposit demonstrates that mass-wasting processes are common along the north-facing canyon walls where slopes are exposed for longer periods to freezing and thawing water. Southward advance of the scarp in Horse Heaven appears to have intersected the cliff band of the Book Cliffs because dislocated bedding and phreatophytic vegetation are visible along the top of the cliff face near elevation-monument 5,870 (Figure 1) and above the vehicle in Figure 2. Because the age of the landslide deposits in Horse Heaven is long in comparison to the design life of the proposed repository, the mass wasting in Horse Heaven is not likely to impact the long-term stability of the proposed disposal cell.

Conclusion and Recommendations:

Land-forming processes at the Crescent Flat site include: (1) the rock falls from the top of the Book Cliffs; (2) formation of rills and gullies on the face of the Book Cliffs; (3) a veneer of alluvial mud deposited atop weathered Mancos Shale; (4) low cuesta-like ridges and mounds that appear as an easterly trend along the northern margin of Crescent Flat; (5) incised channel formation in Crescent Wash along the eastern boundary of the withdrawn area; and (6) incipient incised-channel formation in the West Branch and East Branch of Kendall Wash. These fluvial-geomorphologic features pose little risk to the proposed uranium mill tailings repository. Additional discussion will be provided in the RAP. However, water-carrying capacity of the West and East Branches of Kendall Wash will need to be considered carefully to maintain their long-term, post-construction stability. All information from field investigations will be compiled and assessed before the final geomorphic analysis will be completed. This information will be provided in the RAP.

Computer Source:

Not applicable.

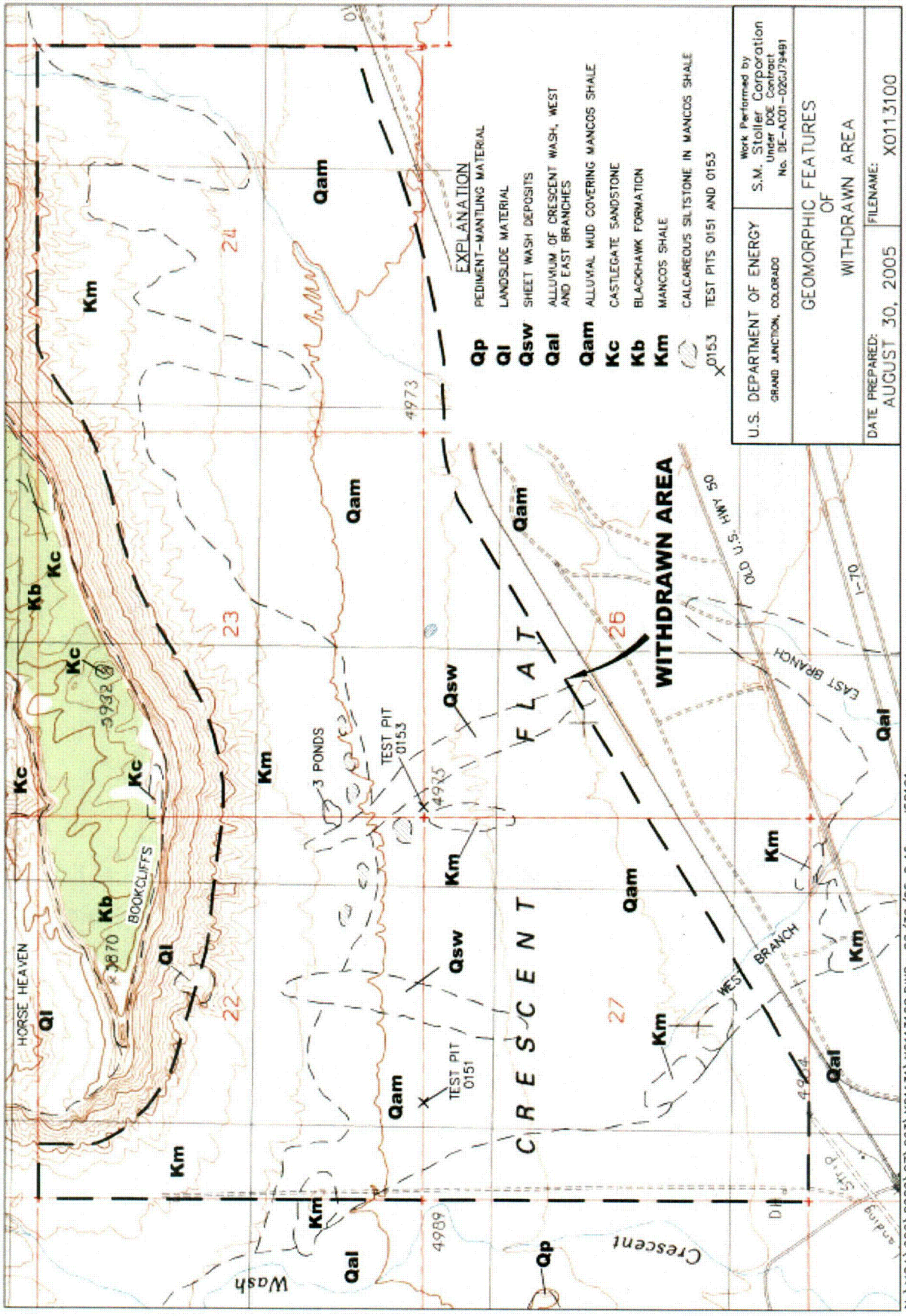

Figure 1. Geomorphic Features of the Withdrawn Area of Crescent Junction, Utah, Disposal Site

C-05

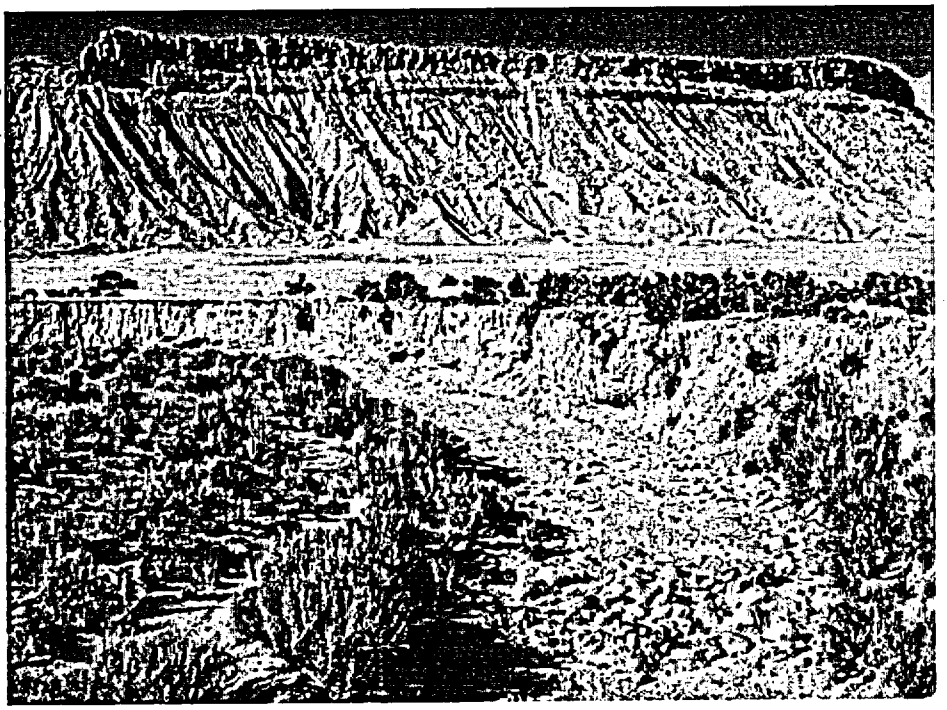

Figure 2. View north–northeast of incised meander bend in Crescent Wash just southwest of corner of Sections 21, 22, 27, 28. Incision is about 12 ft deep and does not contact Mancos Shale bedrock. Diameter of boulders in bed of wash is up to 4 ft.

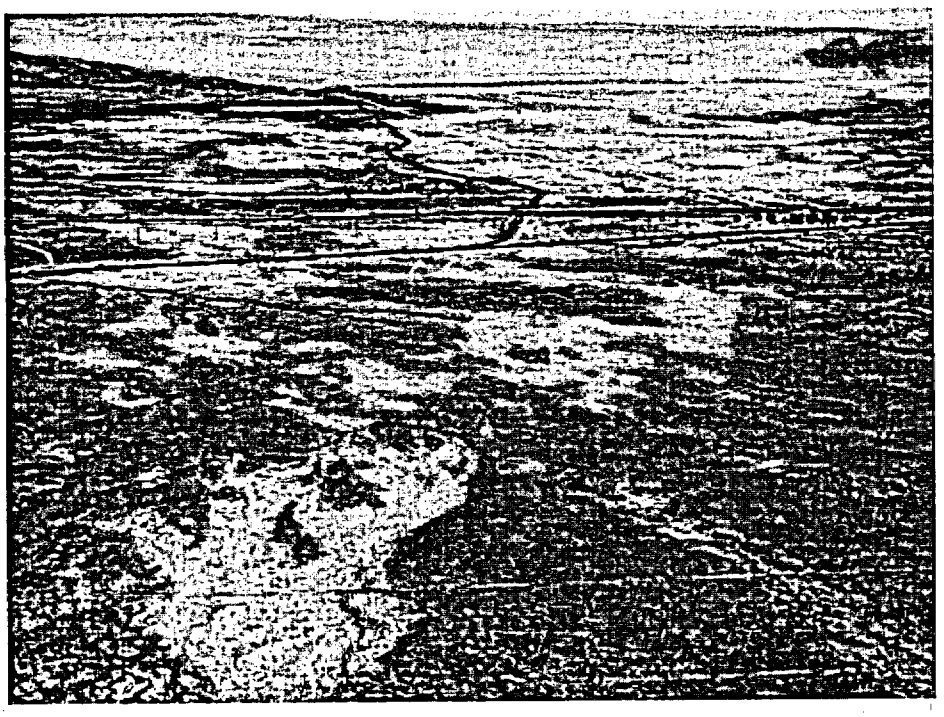

Figure 3. View southwest from top of Book Cliffs of West Branch, an incised drainage in the SE ¼ Section 27 that drains southeastward. Drab–gray discoloration in the foreground is interpreted as sediment deposition due to sheet flow.

Figure 4. View northeast of East Branch in SE¼ NE¼ Section 26. Incision at this location is about 15 feet deep and does not contact Mancos Shale bedrock; however, several hundred feet downstream of this location, the East Branch cuts several feet into weathered Mancos Shale.

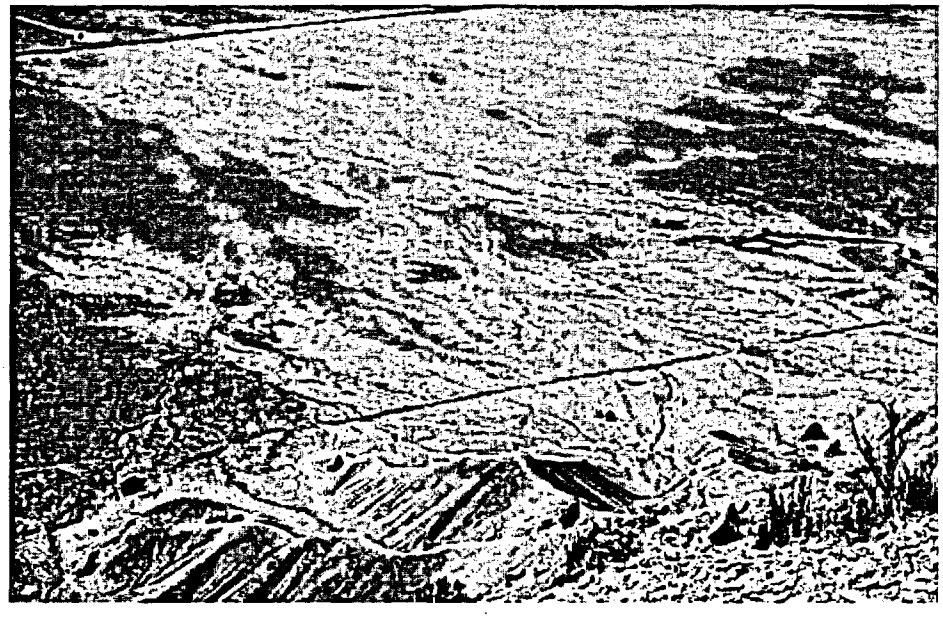

Figure 5. View south-southwest from top of Book Cliffs toward linear feature that extends eastward from the three ponds. Linear feature marks where calcareous siltstone beds of the Prairie Canyon Member of the Mancos Shale crop out. Also note the drab–gray discoloration that is interpreted as evidence of sediment deposition due to sheet flow.

Figure 6. View east–northeast of resistant calcareous siltstone bed(s?) cropping out in a low cuesta–like hill. This hill and a similar one about 50 yards to the east are along the linear feature seen from the top of the Book Cliffs.

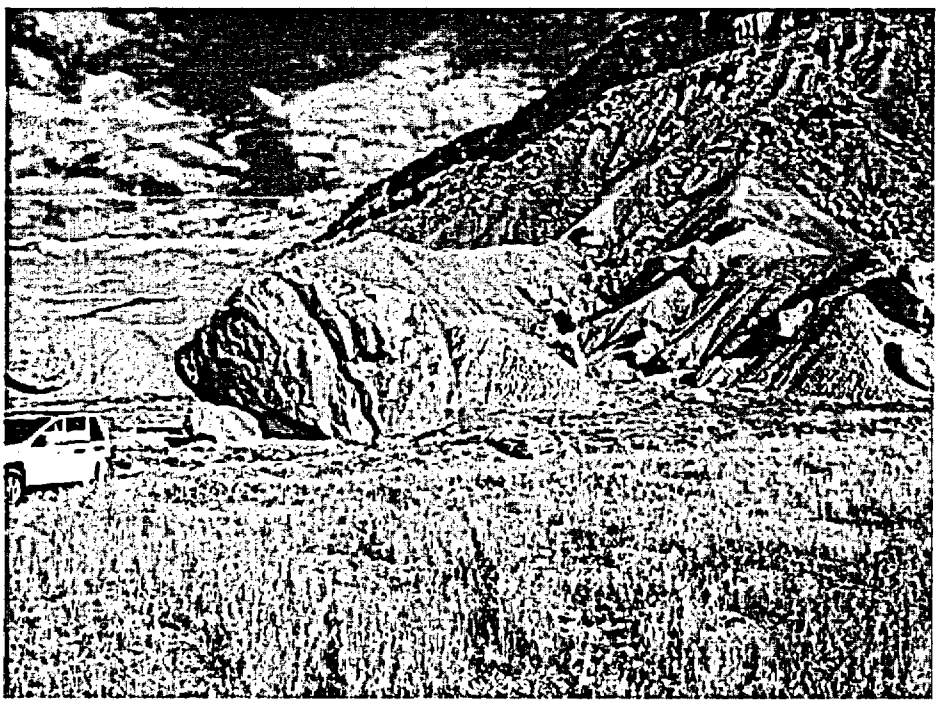

Figure 7. View northwest of large sandstone boulder from the Blackhawk Formation adjacent to road in NE¼ SW¼ Section 23. Boulders have fallen down as part of recession of the Book Cliffs escarpment.

Appendix E

U.S. Department of Energy—Grand Junction, Colorado

Calculation Cover Sheet

Calc. No.: MOA-02-08-2005-07-01-00 RE KE & LR Discipline: Geologic and Geophysical Properties No. of Sheets: 20

Project: Moab Project

Site: Crescent Junction Disposal Site

Feature:
Site and Regional Seismicity – Results of Literature Research

Sources of Data:

Published reports and maps – see list of references at end of calculation set.

Sources of Formulae and References:

See list of references at end of calculation set.

Preliminary Calc. ☐ Final Calc. ☑ Supersedes Calc. No. MOA-02-08-2005-07-00

Author: Tadg Dwight for Roslyn Stern 8/7/06
Name Date

Checked by: Ann Smith 8/7/06
Name Date

Name Date 8-7-06

Approved by: John Ellis 8/9/06
Name Date

Name Date 8/14/06

Name Date 8-11-06

Name Date 15/8/06

Problem Statement:

Determination of the suitability of the Crescent Junction disposal site as the repository for the Moab Uranium Mill tailings material, and development of the site and regional seismotectonic sections of the Remedial Action Plan (RAP) requires a thorough review of available literature that applies to the Crescent Junction Site. The compiled list of references is presented at the end of this calculation set, and relevant information is summarized below.

This calculation will be incorporated into Attachment 2 (Geology) of the Remedial Action Plan (RAP) and Site Design for Stabilization of Moab Title I Uranium Mill Tailings at the Crescent Junction, Utah, Disposal Site, and summarized in the appropriate sections of the Remedial Action Selection (RAS) report for the Moab Site.

Method of Solution:

This literature review is part of the seismotectonic calculation set to develop seismic design parameters for the disposal site. Specifically, the calculation set includes a review of the pertinent literature, development of an estimate of the Maximum Credible Earthquake (MCE), and determination of the resulting design vibratory ground motion at the site (peak horizontal ground acceleration). The objective of this literature review is to identify the appropriate previous studies and published data pertaining to seismicity in the area. This review will be used to support the calculation of the MCE and peak horizontal ground accelerations to be calculated specifically for the Crescent Junction Site.

Two studies for other Uranium Mill Tailings Remedial Action (UMTRA) sites in particular were referred to for this seismotectonic calculation set because of their similar project type and close proximity to the Crescent Junction Site. Specifically, the seismotectonic studies from the RAP for the Green River, Utah, UMTRA Site (DOE 1991a), and the Grand Junction, Colorado, UMTRA Site (DOE 1991b), were principal resources for this review. The Green River, Utah, Site is a 380,000 cubic yard (yd^3) uranium disposal site located approximately 20 miles west of the Crescent Junction Site, while the Grand Junction, Colorado, Site is a 5.3 million yd^3 uranium disposal site located approximately 80 miles east of the Crescent Junction Site. Although the Green River Site is closer to the Crescent Junction Site than the Grand Junction Site, the seismotectonic investigation for the Green River Site was not as extensive as the investigation for Grand Junction. Therefore, the use of the Green River RAP as a reference is limited.

Assumptions:

It is assumed that the literature sources are reliable and representative of the current understanding of the seismotectonics of the region.

Calculation:

None required.

Criteria and Definitions:

The following are the standards and definitions that are applied to the evaluation of the seismicity of the Crescent Junction Site as specified in the *Technical Approach Document* (TAD) (DOE 1989).

Design life. As specified by the U.S. Environmental Protection Agency (EPA) *Code of Federal Regulations* Promulgated Standards for Remedial Actions at Inactive Uranium Processing Sites (40 CFR 192), the controls implemented at UMTRA Project Sites are to be effective for up to 1,000 years, to the extent reasonably achievable and, in any case, for at least 200 years. For the purpose of the seismic hazard evaluation, a 1,000-year design life is adopted.

Design earthquake. For UMTRA Project Sites, the magnitude(s) of the earthquake(s) that produces the largest on-site peak horizontal acceleration (PHA) and that produces the most severe affects upon the site is the design earthquake. This earthquake could be either a floating earthquake or an earthquake

whose magnitude is derived from a relationship between fault length and maximum magnitude. The latter case is applied for a verified or assumed capable fault of known rupture length.

Floating earthquake (FE). An FE is an earthquake within a specific seismotectonic province that is not associated with a known tectonic structure. Before assigning the FE magnitude, the earthquake history and tectonic character of the province are analyzed.

Capable fault. A capable fault is a fault that has exhibited one or more of the following characteristics:

- Movement at or near the ground surface at least once within the past 35,000 years, or movement of a recurring nature within the past 500,000 years.
- Macroseismicity (magnitude 3.5 or greater) determined with instruments of sufficient precision to demonstrate a direct relationship with the fault.
- A structural relationship to a capable fault such that movement on one fault could be reasonably expected to cause movement on the other.

Acceleration. Acceleration is the mean of the peaks of the two orthogonal horizontal components of an accelerogram record, or PHA. The accelerations are determined from the corrected peak horizontal ground acceleration attenuation relationship based on distance and magnitude as developed by Campbell and Bozorgnia (2003). This relationship is an update to the Campbell (1981) relationship referenced in the TAD (DOE 1989). The mean-plus-one standard deviation (84th percentile) value is adopted. This value is considered a non-amplified PHA.

Surface acceleration. Surface acceleration is the site acceleration adjusted for the site soil attenuation or amplification effects.

Duration of strong earthquake ground motion. Duration is defined, after Krinitzsky and Chang (1977), as the bracketed time interval in which the acceleration is greater than 0.05 g. The methodology of Krinitzsky and Chang (1977) is applied in estimating the duration of strong ground motion at a particular site.

Magnitude and intensity. Magnitude is the base-10 logarithm of amplitude of the largest deflection observed on a torsion seismograph 100 kilometers (km) from the epicenter (Richter 1958). This local magnitude value may not be the same as the body-wave and surface-wave magnitudes derived from measurements at teleseismic distances. Unless specified otherwise, Richter magnitude values for values less than 6.5 are used in UMTRA Project seismic hazard evaluations.

Intensity is the index of the effects of any earthquake on the human population and structures. The most commonly applied scale is the 1931 Modified Mercalli (MM) Intensity Scale, which will be used in this study.

Because pre-instrumental earthquake records are reported in intensity and more recent instrumental records are in magnitude, there may be a need to relate these values. The relationship developed by Gutenburg and Richter (1956) is used:

$$M = 1 + 2/3\ Io$$

Where M = magnitude in the Richter scale and Io = Modified Mercalli intensity in the epicentral area.

Maximum earthquake. The term Maximum Earthquake (ME) was defined by Krinitzsy and Chang (1977) as the largest earthquake that is reasonably expected on a given structure or within a given area. No recurrence interval is specified for such an event.

Local regional study area. The regional study area is selected by calculating the distance at which the largest magnitude earthquake possible for a region, as determined by Algermissen, et al. (1982), produces the minimum accepted on-site design acceleration (0.10 g). All further characterization work is then limited to this region. Using this definition, the maximum earthquake for the region as determined by Algermissen, et al. (1982) is magnitude 6.1. Using Campbell (1981) attenuation relations for constrained,

84th -percentile values, distances within 29 km of the site are considered within the local regional study area.

Expanded regional study area. Although UMTRA defines the study area as discussed above, the U.S. Nuclear Regulatory Commission (NRC) for Title 10, Part 100, Appendix A, requires an investigation within 200 miles of the site. For purposes of this seismotectonic evaluation, capable faults, historical earthquakes, and floating earthquakes associated with neighboring tectonic provinces that lie within 200 miles of the site and are capable of producing a minimum on-site acceleration of 0.10 g or greater will be evaluated in the expanded regional study area.

Discussion:

Seismotectonic Setting

The Crescent Junction Site is located in the northern portion of the Colorado Plateau tectonic province (Figure 1). The Colorado Plateau is a broad, roughly circular region of relative structural stability within a more structurally active region of disturbed mountain systems. Broad basins and uplifts, monoclines, and belts of anticlines and synclines are characteristic of the plateau (Kelley 1979). These basins and uplifts are generally considered to be inactive under the present seismotectonic regime (DOE 1991b). All three of the referenced UMTRA Sites are located within the northern portion of the Colorado Plateau physiographic and tectonic province.

The Colorado Plateau is surrounded by the provinces of the Wyoming Basin and Middle Rocky Mountains to the north, the Basin and Range province to the west and south, the Intermountain Seismic Belt (ISB) to the west, and the Rio Grande Rift and the Southern Rocky Mountains to the east (Keller, et al. 1979; Kelley and Clinton 1960; Kelley 1979; Allenby 1979; Kirkham and Rogers 1981). The boundaries of the provinces vary between authors; the Southern Rocky Mountains are divided into the Eastern and Western Mountain Province by Kirkham and Rogers (1981).

Within the Colorado Plateau, the Crescent Junction Site lies in the northwestern part of the Paradox Basin (in the Paradox Fold and Fault Belt), approximately 8 miles south of the Uinta Basin sub-province. The Book Cliffs, less than 1 mile north of the Crescent Junction Site, are the erosional escarpment on the south flank of the Uinta Basin. As shown in Figure 2, additional sub-provinces in the area include the San Rafael Swell to the west; Henry Basin, White Canyon Slope, Monument Upwarp, Blanding Basin, the Four Corners Platform to the south; the San Juan Dome to the east; and the Uncompahgre Uplift to the northeast (Kelley 1955).

The Paradox Basin is characterized by complex systems of northwest-trending normal faults and landslide and slump features. Typical salt anticlinal collapse features extend to within approximately 2 miles of the site. These features have been active during Quaternary time and may be active today. However, since they result from very gradual processes of salt dissolution and flow, they are not likely capable of generating large earthquakes. Kirkham and Rogers (1981) estimate the maximum earthquakes possible on these features to be about magnitude 5 (DOE 1991b; Kelley and Clinton 1960).

- **Intermountain Seismic Belt (ISB)**

  The ISB (Smith and Sbar 1974; DOE 1991a) is a zone of pronounced earthquake activity extending north from Arizona and terminating in northwestern Montana. It is described by Ryall, et al. (1966) as being surpassed in seismic activity in the United States only by the California and Nevada seismic zones. The ISB is coincident with the boundary between the Basin and Range province and the Colorado Plateau/Middle Rocky Mountains. The largest historical event in the ISB was the 1959 Hebgen Lake earthquake of Richter magnitude 7.7 +/– 0.2. More than 15 events with magnitudes greater than 6 have been reported since the mid 1800s. The site lies approximately 50 miles east of the highly active ISB.

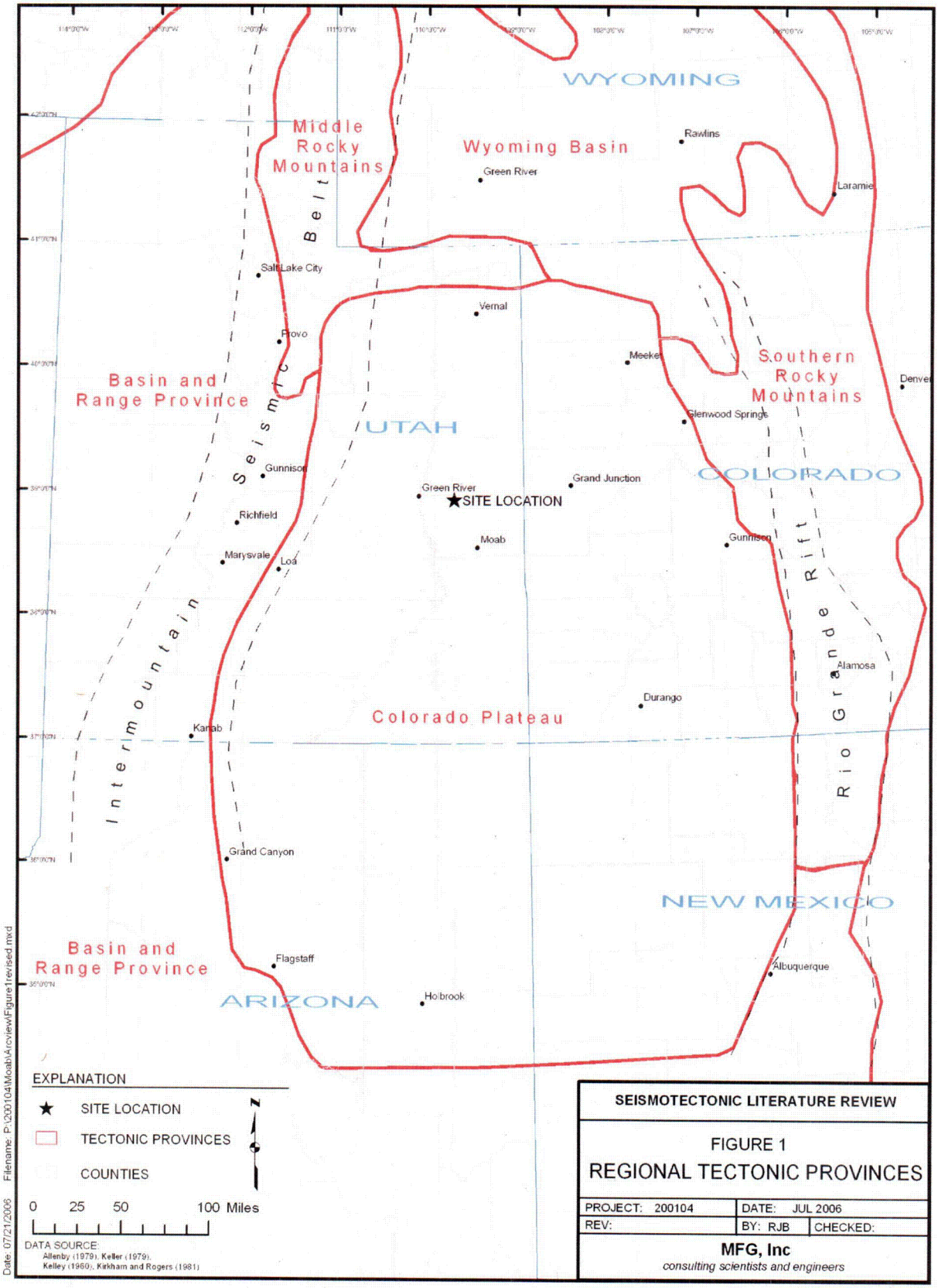

Figure 1. Regional Tectonic Provinces

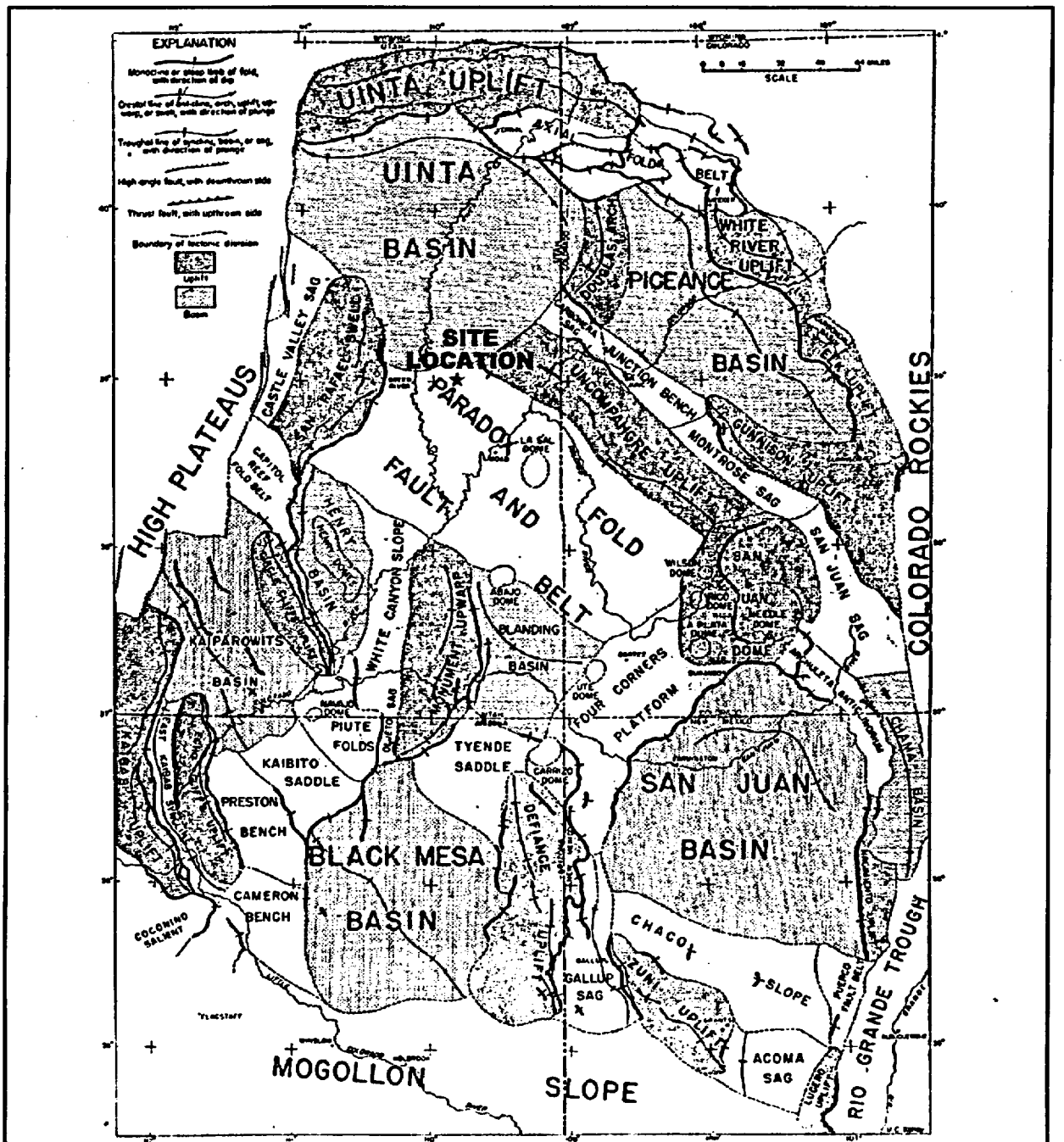

Figure 2. Tectonic Sub-Provinces of the Colorado Plateau

- **Rio Grande Rift**

  The Rio Grande Rift (Kirkham and Rogers 1981, DOE 1991a) is a north-south-trending extensional graben feature that extends from Chihuahua, Mexico, to northern Colorado. The rift was initiated in Neogene time and has experienced continued activity through the Quaternary. The rift is characterized by Neogene basin-fill sedimentary rocks; a bimodal suite of mafic and silicic igneous rocks; and abundant features suggesting recently active faults; such as, fault scarps in young alluvium, abrupt mountain fronts that exhibit faceted spurs, and deep, narrow linear valleys. A high percentage of all the potentially capable faults in Colorado and New Mexico lie within this province. Well-defined evidence of repeated Late Quaternary movement is abundant on several faults in the southern portion of the province, whereas such evidence is obscure in the northern portion. The closest approach of the Rio Grande Rift to the site area is approximately 270 km (170 miles).

- **Wyoming Basin**

  The Wyoming Basin (DOE 1991a) consists of a series of broad structural and topographic basins that merge with and resemble the adjoining part of the Colorado Plateau (Hunt 1967). These basins are partly filled with Tertiary deposits and are separated by low anticlinal uplifts of older rocks. The earthquake history of the Wyoming Basin is apparently similar to the widely distributed, low- to moderate-magnitude pattern of the stable interior portion of the Colorado Plateau. Witkind (1975) identified numerous suspected active faults in the Wyoming Basin along the Colorado-Wyoming border between 107 and 108 degrees west longitude, which may represent a continuation of structures associated with the Rio Grande Rift in Colorado. However, these faults are not known to have been associated with seismic activity.

- **Southern Rocky Mountains/Mountain Provinces**

  The Mountain Provinces are divided into the Eastern and Western Mountain Provinces by Kirkham and Rogers (1981). The Eastern Mountain Province includes the Front and Medicine Bow Ranges, the Middle and South Parks, and the east flanks of the Mosquito and Sangre de Cristo Ranges. Most of the faults in this province have Laramide, late Paleozoic, or even Precambrian ancestry. Several of the faults show considerable Neogene movement. A few of these faults have moved during the Quaternary. The distribution, orientation, and character of Neogene movement on these faults suggest rejuvenation is related to the extensional stresses responsible for rifting. The Western Mountain Province includes the San Juan Mountains, the Elk and West Elk Mountains, the west flank of the Sawatch Range, the White River uplift, and the Gunnison uplift. Neogene faults are relatively scarce in this province. Many of the faults that are present are not truly tectonic features, but rather are the results of evaporate flowage or caldera collapse. Despite an apparent absence of major Neogene tectonic faults, numerous earthquakes have been felt and/or instrumentally located in the province. The site is located approximately 200 km (130 miles) from the nearest portion of the Southern Rocky Mountain province.

Quaternary Faults

Quaternary faults and folds were evaluated using the USGS Quaternary Fault and Fold database (USGS 2002) and the Quaternary Fault and Fold database from the Utah Geological Survey (Black, et al. 2003). An initial search for critical Quaternary faults was conducted using the minimum fault lengths given in NRC document 10 CFR part 100, Appendix A, as shown in Table 1. In addition to faults included in the Quaternary Fault and Fold database, faults of undetermined age that are shown on geologic maps in the area (Williams 1964, Gualtieri 1988, Witkind 1995, Williams and Hackman 1971), were considered if the PHA associated with these structures (if considered Quaternary) is greater than 0.1 g. Quaternary faults that are within the expanded regional study area are presented in Figure 3, and in Appendix A. Faults that are within 40 miles of the site are shown on Figure 3 and are described below. Faults that are included in the Quaternary Fault and Fold database retain the original four-digit numbering system of the database. Faults from other sources are labeled with a single-digit number.

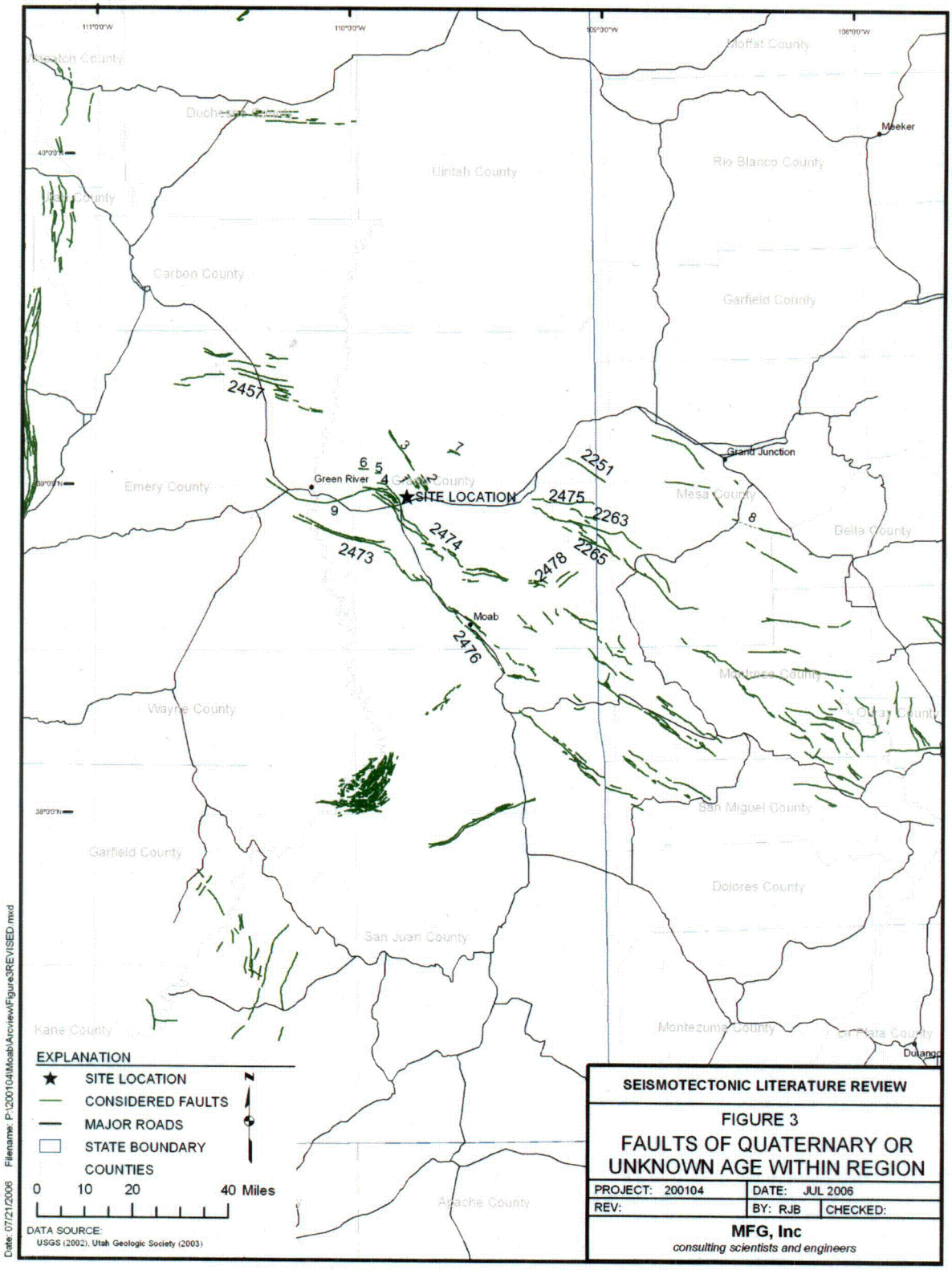

Figure 3. Faults of Quaternary or Unknown Age Within Region

C-07

Table 1. Minimum Length of Fault to be Considered in Establishing MCE

Distance from Site		Minimum Length	
Miles	Kilometers	Miles	Kilometers
0 to 20	0 to 32	1	1.6
Greater than 20 to 50	Greater than 32 to 80	5	8
Greater than 50 to 100	Greater than 80 to 161	10	16
Greater than 100 to 150	Greater than 160 to 240	20	32
Greater than 150 to 200	Greater than 240 to 320	40	64

- **Salt Valley and Cache Valley Faults (2474)**

  As described in Black, et al. (2003), the faults are within a northwest-trending zone of folding, faulting, and warping related to dissolution and collapse of the Salt Valley anticline in eastern Utah, north of Moab. Collapse of the Salt Valley anticline appears to largely post-date late Pliocene deposition of exotic fluvial gravels (likely derived from a since-eroded source in the Book Cliffs) on the rim and floor of the Salt Valley and the formation of an erosion surface on the flank of the anticline. Small depositional basins within the Salt Valley containing Bishop ash (approximately 740 thousand years ago [ka]) and Lava Creek B ash (670 ka) were localized by salt dissolution and collapse and/or salt flow during early and middle Quaternary time and record syn and post-depositional folding and faulting. Faults are parallel and appear related to the major older structures of the anticline. At the lower end of the valley, slightly tilted and relatively undeformed middle- to late-Quaternary basin fill deposits unconformably overlie older, more deformed units. Structural relations exposed at other localities in the valley suggest that Quaternary sediments have been deformed and localized by movement within salt diapirs of the Paradox Formation. Playas and mudflats in the upper Salt Valley indicate active deformation (due to salt flow or dissolution) and damming of surface runoff. A stream that crosses the south end of the Salt Valley anticline at a high angle is entrenched and bordered by probable late-Holocene terraces north of the anticline. The stream is braided and unentrenched in the short reach within Salt Valley, suggesting that the core of the anticline is presently subsiding and causing stream aggradation. In Cache Valley, a Quaternary erosion surface that apparently postdates collapse-related deformation is displaced by a major bedrock fault and may have been tilted. East of Cache Valley, Colorado River terraces are tilted upstream on the upstream side of the Cache Valley anticline, indicating that salt flowed into the collapsed structure during Quaternary time. The timing of the most recent paleoevent is Quaternary (less than 1.6 million years ago [Ma]). The slip rate is unknown, but is likely to be less than 0.2 millimeters per year (mm/yr). The length of the fault is 58 km (Black, et al. 2003).

  Reports by Woodward-Clyde (1984, 1996), based on map and seismic reflection data, found no evidence of Quaternary tectonic deformation of these structures. Surface faults occurred as a result of dissolution and collapse of the salt anticline during the Cenozoic era. Surface faults are not interpreted to extend below the top of salt, limiting the rupture depth to approximately 2 km, and are not structurally related to underlying pre-salt faults. Due to the shallow nature of the faults, large shear stresses are not sustained and potential rupture areas will be limited in extent such that significant earthquakes cannot be generated.

  In 1979, a seismic monitoring program was initiated to assess the seismicity of the Paradox Basin at the microearthquake level. The report by Woodward-Clyde (1984) indicated that from 1979 through 1984, only two events were detected in the Salt Valley area (local magnitude [M_L] of 1.2 and 2.1). They concluded that the seismicity associated with the study area is generally diffusely distributed and of low level and small magnitude, consistent with the longer historical record of the interior of the Colorado Plateau. From these data, it is assumed that there is no seismicity associated with the Salt and Cache Valley faults, and the faults are not considered capable.

- **Tenmile Graben (2473)**

  The Tenmile graben, which is approximately 35 km in length, is a narrow zone of faulting displacing Cretaceous and Jurassic bedrock along Salt Wash southeast of Green River. The graben is on the northwestern edge of an area typified by northwest-trending, elongated oval valleys that are collapsed or depressed anticlines. The graben is probably related to salt dissolution, but was included in the Quaternary Fault and Fold database as a Class B fault to indicate the possibility of a tectonic component (Black, et al. 2003). Inclusion in the Quaternary database was based on a possible structural association with the Moab fault (Hecker 1993). The youngest rocks offset by this fault are the upper members of the Cretaceous Mancos Shale (Doelling 1993). No Tertiary rocks are preserved along the Tenmile graben. Quaternary alluvium and eolian sediments do not appear offset by any of the faults (Doelling 2001).

  Woodward-Clyde Consultants (1996) evaluated the potential seismic hazards for the uranium mill tailings site in Moab, Utah. Microearthquake studies in the region from 1979 to 1987 show no evidence for earthquakes associated with the Tenmile graben. Structural incongruities between the Moab faults and the Tenmile graben suggest that if fault ruptures did occur, they would most likely be arrested at the incongruity. A kinematic incongruity between Tenmile graben and Moab faults is indicated by a change in strike of 35 degrees, an opposite sense of total net displacement, and differences in structural style between these faults.

  They concluded that the Tenmile graben may be structurally related to the Moab fault in that both may have formed during Tertiary extension, but the fault is not expected to rupture with the Moab fault, nor is there any definitive evidence that the Tenmile graben is a capable structure. They found no evidence for Quaternary deformation of the Tenmile graben and did not consider the graben as a capable fault for seismic-hazard assessment purposes. From these data, it is assumed that there is no seismicity associated with the Tenmile graben, and the structure is not considered capable.

- **Moab Fault and Spanish Valley Faults (2476)**

  The Moab fault and Spanish Valley faults are approximately 68 km in length and consist of a northwest-trending zone of faulting and warping from collapse of the Moab Valley anticline from salt dissolution. The faults are related to salt dissolution, but were included in the Quaternary Fault and Fold database as Class B faults to indicate the possibility of a tectonic component (Black, et al., 2003). Inclusion of the Moab and Spanish Valley faults in the Quaternary database was based on indirect geomorphic and stratigraphic evidence, primarily for Quaternary salt-dissolution collapse that may or may not be associated with faulting (Woodward Clyde 1996).

  Collapse of the Moab Valley anticline appears to largely post-date deposition of early and middle Pleistocene alluvium on and near the rim of the valley (Harden, et al. 1985). A well-preserved relic canyon on the rim of Moab Canyon, whose headwaters were apparently removed by collapse of the anticline, probably formed during late Tertiary to early Quaternary time (Oviatt 1988). Distribution of middle Pleistocene through Holocene alluvial deposits suggests differential subsidence in Spanish Valley (due to tectonism or salt dissolution/migration). Marshes at the lower end of Spanish Valley may be evidence of Holocene subsidence. Woodward-Clyde Consultants (1996) indicates that the youngest rocks or structures demonstrably displaced by the Moab fault are Cretaceous or Tertiary in age, and did not consider the faults as capable faults for seismic-hazard assessment purposes. Timing of the most recent paleoevent is Quaternary (less than 1.6 Ma). The slip rate is unknown, but is likely less than 0.2 mm/yr (Black, et al. 2003).

  Based on detailed mapping, structural evidence, and geophysical data, Olig, et al. (1996) determined that the faults within the Moab and Spanish Valley are most likely related to salt-dissolution. They concluded that the primary movement on the Moab fault is tectonic and occurred during a period of Tertiary extension. Everywhere that Quaternary sediments have been mapped in relation to the Moab fault, they bury the fault and do not appear to be offset by it. In addition, most, if not all, of the slip on the Moab fault is pre-Quaternary, and that the Moab fault is a shallow structure that probably soles into the Moab salt-cored anticline within a 2-km depth along much of its length. Therefore, it would most likely not be capable of producing significant earthquakes.

A seismographic network operating in the Paradox Basin from 1979 to 1987 revealed no microearthquakes that could definitely be associated with the Moab fault. A few earthquakes occurred in the vicinity of the fault, but they appear to be part of the broad pattern of scattered seismicity characteristic of the Colorado Plateau interior. Additionally, no earthquakes from 1987 through 1994 have been recorded by the University of Utah Seismographic Stations, which locate events in the vicinity of the Moab fault (Woodward Clyde 1996). From these data, it is assumed that there is no seismicity associated with the Moab fault, and the structure is not considered capable.

- **Price River Area Faults (2457)**

  The Price River Area faults are generally east-west striking faults along the Price River west of the Book Cliffs. The faults are in a long, sinuous area along the base of the Book Cliffs termed the Mancos Shale Lowlands and characterized by sloping pediments, rugged badlands, and narrow flat-bottomed alluvial valleys in Cretaceous rock. Some faults within the zone displace pre Wisconsin-age pediments less than 2 meters. Structural relations indicate that the fault zone forms the crest of a broad, collapsed anticline. The fault zone is similar in trend, pattern, and length to faults along the crest of the Moab Valley anticline (2476), although it is not as strongly developed. The faults are inferred to be related to a salt anticline at the northern margin of the Paradox basin but were included in the Quaternary fault and Fold database as Class B faults to indicate the possibility of a tectonic component (Black, et al. 2003). Early- to middle-Pleistocene pediments north of the fault zone steepen sharply at the base of the Book Cliffs, and may be warped due to elastic rebound of the Mancos Shale during erosional unloading and/or monoclinal folding. The ancestral course of Whitmore Canyon (near Sunnyside) also appears to be warped. Timing of most recent paleoevent is Quaternary (less than 1.6 Ma). The slip rate is unknown, but is likely less than 0.2 mm/yr. The fault length is 51 km (Black, et al. 2003). For the purposes of this report, the Price River Area faults are considered capable faults.

- **Little Dolores River Fault (2251)**

  The Little Dolores River fault extends from Utah into Colorado on the northeast flank of the Uncompahgre uplift. Evidence for Quaternary movement on this fault was cited in Witkind (1976) based on personal communication with Fred Cater. Based on the timing of abandonment of Unaweep Canyon, Cater (1966) indicated uplift of the Uncompahgre Plateau began in the mid-Pliocene and continued into the Pleistocene, resulting in as much as 640 meters of differential uplift. Despite the lack of evidence of faulted Quaternary deposits along the Little Dolores River fault, it has been classified as a Quaternary fault (Howard, et al. 1978; Kirkham and Rogers 1981; Colman 1985), and no references have been published that refute this age assignment. The timing of the most recent paleoevent is Quaternary (less than 1.6 Ma). Despite a lack of evidence for offset in Quaternary deposits, faults associated with the Uncompahgre uplift are often considered to have experienced Quaternary movement. The slip-rate category is unknown, but likely less than 0.2 mm/yr. The length of fault is 16 km (Black, et al. 2003). For purposes of this report, the Little Dolores River fault is considered a capable fault.

- **Sand Flat Graben Faults (2475)**

  The Sand Flat graben faults include the northern graben-bounding fault (Dry Gulch fault) and subsidiary within the Sand Flat graben. The southern graben-bounding fault is included in the discussion of the Ryan Creek fault zone (2263). The faults are west- to northwest-trending within the Sand Flat graben along the southwestern margin of the Uncompahgre uplift northeast of the Paradox Basin. The Uncompahgre uplift is a northwest-trending, east-tilted fault block. The Uinta Basin borders the northwest end of the uplift. Faults are part of a regional zone of northwest-to-west-trending normal faults along the Utah–Colorado border, within a monoclinal flexure that forms the southwest margin of the Uncompahgre uplift. Different movement histories and cumulative Quaternary displacements have been inferred for the fault zone based on studies of Unaweep Canyon and related drainage changes, but most studies suggest that differential uplift has continued into the early or late Pleistocene. Diversion of drainage (ancestral Colorado River from Unaweep Canyon), which followed impoundment and formation of a lake, occurred about 775 ka (Perry and Annis, 1990). The timing of the most recent paleoevent is Quaternary (less than 1.6 Ma). The slip rate is unknown, but is likely less than 0.2 mm/yr. The fault length is 23 km. For purposes of this report, the Sand Flat graben faults are considered capable faults.

- **Ryan Creek Fault Zone (2263)**

  The Ryan Creek fault zone trends east-west along the southwestern margin of the Uncompahgre uplift. Approximately half of the fault length is in Utah. The fault extends east into Colorado from the flank of Haystack Peaks parallel to Ryan Gulch, and then bends southeast toward Unaweep Canyon. Individual faults in the fault zone form the southern margin of the Sand Flat graben in Utah and the northeast margin of the Ute Creek graben in Colorado. The Ryan Creek fault zone lies on the southwestern margin of the Uncompahgre uplift along the Utah-Colorado border. Evidence for Quaternary movement on this fault zone is cited in Witkind (1976) based on personal communication with Fred Cater. Cater (1966) indicated uplift of the Uncompahgre Plateau began in the mid-Pliocene and continued into the Pleistocene, resulting in as much as 640 meters of differential uplift. Despite the lack of evidence of faulted Quaternary deposits along the Ryan Creek fault zone, it has been classified as a Quaternary fault (Howard, et al. 1978; Kirkham and Rogers 1981; Colman 1985), and no references have been published that refute this age assignment. Timing of the most recent paleoevent is Quaternary (less than 1.6 Ma). A small earthquake (M_L 2.9) and several aftershocks in 1985 may have occurred on the Ryan Creek fault zone (Ely, et al. 1986). The slip-rate is unknown, but is likely less than 0.2 mm/yr. The fault length is 39 km (Black, et al. 2003). For purposes of this report, the Ryan Creek fault is considered a capable fault.

- **Granite Creek Fault Zone (2265)**

  The Granite Creek fault zone is a northwest-trending fault zone, which extends from Utah into Colorado north of Steamboat Mesa on the southwest flank of the Uncompahgre uplift. Williams (1964) mapped Quaternary deposits as both concealing and abutting the fault. Cater (1966) indicated uplift of the Uncompahgre Plateau began in the mid-Pliocene and continued into the Pleistocene, resulting in as much as 640 meters of differential uplift. Despite the lack of evidence of faulted Quaternary deposits along the Granite Creek fault zone, it has been classified as a Quaternary fault (Kirkham and Rogers 1981; Colman 1985), and no references have been published that refute this age assignment. The Granite Creek fault zone consists of high-angle normal faults that are mostly down-to-the-northeast. The fault lies in a tectonically weakened area above the ancestral Uncompahgre fault zone (Stone 1977).

  The possibility of Granite Creek and Ryan Creek fault systems being connected was investigated. However, the two fault systems appear to be separate based on mapping by Doelling (2001) and their depiction in a cross section by Ely, et al. (1986). In addition, MCE calculations are based on total length of fault trace from farthest reaches of the fault. Because the Granite Creek and Ryan Creek faults are roughly parallel and overlapping, the total fault trace would not increase if they are considered collectively. Several faults of similar strike parallel the Granite Creek fault to the northeast. The Granite Creek faults are mostly down to the northeast. Granite Creek faults were named by Heyman (1983), but Doelling (2001) does not show that name for the faults on his map. Both Granite Creek and Ryan Creek faults may merge at depth with the major uplift-bounding (Uncompahgre) reverse fault.

  Offset of Quaternary deposits is inconclusive since Williams (1964) showed Quaternary deposits as abutting against the fault and concealing the fault. However, faults associated with the Uncompahgre uplift are often considered to have experienced Quaternary movement. Based on the timing of abandonment of Unaweep Canyon, Cater (1966) indicated uplift of the Uncompahgre Plateau began in the mid-Pliocene and continued into the Pleistocene, resulting in as much as 640 meters of differential uplift. The slip-rate category is unknown, but is likely less than 0.2 mm/yr. The fault length is 23 km. For purposes of this report, the Granite Creek fault zone is considered a capable fault.

- **Fisher Valley Faults (2478)**

  The Fisher Valley faults are a result of late Quaternary folding and warping in Fisher Valley from salt dissolution and collapse. Fisher Valley is on the crest of a long anticlinal structure that includes Salt and Cache Valleys in Utah, and Sinbad and Roc Creek Valleys in Colorado. The valley formed from collapse of the anticline (Onion Creek diapir) due to salt dissolution. The faults border and define Fisher Valley. Formation of the valley by collapse of the anticline beheaded streams whose broad, shallow channels are preserved on the valley rim. Upper Cenozoic deposits, by far the thickest

sequence in the Paradox basin (greater than 125 meters thick), have ages between greater than 2.5 Ma (based on paleomagnetic analysis) and approximately 250 ka (based on secondary carbonate accumulation rates), and record episodic deformation from movements of the Onion Creek salt diapir and basin subsidence (resulting from salt flowage into the diapir and/or salt dissolution and collapse). The timing of the most recent paleoevent is Quaternary (less than 1.6 Ma), based on tephrochronology, soil development, and stream dissection rate. Young basin fill deposits demonstrating recent movement are absent, but evidence for rapid incision (3 mm/y based on 14C dates), and steep, unstable slopes where Onion Creek cuts through the cap rock, suggest that the diapir may be presently active. The slip rate is unknown, but is likely less than 0.2 mm/yr. The fault length is 16 km (Black, et al. 2003). For purposes of this report, the Fisher Valley faults are considered capable faults.

- **Unnamed Faults in the Westwater and Hatch Mesa Quadrangles (1 through 7)**

  The unnamed faults in the Westwater 30-ft x 60-ft quadrangle map are of undocumented age. Faults 1, 2, and 3 are associated with the Thompson anticline. Walton (1956) earlier suggested that the Thompson anticline is on trend with the Onion Creek–Sinbad Valley salt structures and had a similar origin. The pattern of keystone collapse faulting in the Thompson Anticline is characteristic of salt structures. Mobil-American Petrofina Elba Flats unit 1-30 penetrated 178 ft of salt a short distance east of the Sego Canyon quadrangle, showing that salt does extend beneath the Thompson anticline.

  Mapping by Willis (1986) of the Sego Canyon quadrangle describes the faults as subparallel, high-angle, normal faults that trend N 20 °W. Offsets range to nearly 90 ft. Evidence suggests that fault movements in the Sego Canyon quadrangle occurred well after deposition of units and may coincide with uplift of the Colorado Plateau. The movement appears brittle, with jagged, broken sandstone blocks and small splintery branching faults extending from the major ones. Drainage patterns also support late movement on the faults. Late movement and the graben arrangement of the faults support the idea that salt dissolution may be responsible for their presence.

  The faults are described by Gualtieri (1988) as "high-angle normal faults and are the result of subsidence following the exsolution of salt." Thus, the faults may have initiated due to salt movement, similar to other salt-related features of the Paradox Fold and Fault Belt. There is currently a lack of evidence suggesting Quaternary displacement.

  Craig Goodknight of S.M. Stoller and Greg Smith, a consultant, conducted a preliminary field investigation of several of the unnamed faults on November 22, 2005. Unnamed faults 1 and 2 were investigated for evidence of Quaternary displacement. These faults, associated with the Thompson Anticline (Willis 1986; Doelling 2001), showed no evidence of Quaternary movement (no Quaternary deposits were displaced by the faults). Farther to the north, unnamed fault 3 was not investigated, but it is of similar strike and also occurs along the Thompson Anticline. It was concluded that no recent movement has occurred along these faults associated with the Thompson Anticline, and that they reflect slow, incipient subsidence related to dissolution of deep salt deposits along the northeast edge of the Paradox Basin. Based on these data, unnamed faults 1, 2, and 3 are not considered capable faults.

  Also as part of the field investigation, several faults in the northern part of the system of Salt and Cache Valley faults were checked for evidence of Quaternary movement. These west-northwest-striking faults are east and west of Floy Wash in the Hatch Mesa 7.5-minute quadrangle (Chitwood 1994; Doelling 2001). Associated with the Salt Valley Anticline, these faults showed no evidence of Quaternary movement (no displacement of Quaternary deposits by the faults). Just to the north of these faults in the Westwater 30-ft x 60-ft quadrangle, unnamed faults 4, 5, and 6 were not investigated, but are of similar strike, and appear to be related to the Salt Valley Anticline. It was similarly concluded that no Quaternary movement has occurred on these faults associated with the Salt Valley Anticline, and that they are also related to dissolution of deep salt deposits in the northern Paradox Basin. Based on these data, unnamed faults 4, 5, and 6 are not considered capable faults.

  Unnamed fault 7 is not related to either the Salt Valley or Thompson anticlines. In mapping of the Sego Canyon quadrangle, Willis (1986) calls this feature the Bull Canyon fault. He describes it as an east-west-trending fault that crosses the Cisco anticlinal axis. Wells drilled on the Cisco Anticline

encountered Precambrian rocks without passing through Paradox Basin salt-bearing rocks. Overall outcrop patterns suggest that the folding may have occurred between the Late Cretaceous and early Eocene, similar to other structures in the region that have been attributed to Laramide disturbances. Walton (1956) suggests that the Cisco Anticline is directly related to faulting along the steep western flank of the Uncompahgre uplift and is a drape fold over that structure. Additional field investigations into the origin of the fault have not been conducted for this report. For the purposes of this report, unnamed fault 7 will be considered a capable fault.

- **Cactus Park-Bridgeport Fault**

  Seismotectonic stability investigations performed for the uranium mill tailings site at Grand Junction, Colorado (DOE 1991b), concluded Fault 8 is the design fault for the Grand Junction Site. Although Fault 8 does not meet the minimum requirements as shown in Table 1 for the Crescent Junction site, it is included here for completeness. The fault is referred to as Fault 8 (Fault 71 of Kirkham and Rogers, 1981) in the DOE (1991b) report, and as "unnamed fault near Bridgeport" in the Qaternary Fault and Fold Database (USGS 2002). It is described as being the eastern extension of the East Creek monocline. Observation by photos, aerial reconnaissance, and in the field, showed no evidence of Quaternary activity on this fault. However, based on regional seismicity trends and geologic and geomorphic evidence, the Uncompahgre Uplift may be experiencing regional tectonic movement at the present time. Due to the association of Fault 8 with an active regional structure, the fault was considered capable. The fault was estimated to have a length of 11.0 km, with the closest approach to the Grand Junction site of 9.0 km. The MCE associated with this fault was estimated to have a compressional body wave magnitude (m_b) of 6.8 (based on fault length/magnitude relationship of Bonilla, et al 1984). The resulting nonamplified PHA at the Grand Junction Site was estimated to be 0.42 g, based on acceleration/attenuation relationships developed by Campbell (1981) (DOE 1991b).

  Fault 8 appears to be the southern portion of the Cactus Park-Bridgeport fault, as shown in recent mapping of Laramide structures along the northern Uncompahgre Plateau (Livaccari and Hodge 2005). This recent mapping shows the Cactus Park and Bridgeport fault as connected, with a surface trace approximately 14 miles in length. This west-northwest-striking left lateral strike slip fault is as close as about 8 km to the Cheney Site. Evidence from mapping indicates the fault may have had reactivated Quaternary movement (Livaccari and Hodge 2005). For the purposes of this report, the Cactus Park-Bridgeport fault is considered a capable fault.

- **Little Grand Wash Fault**

  The Little Grand Wash fault is an arcuate normal fault/graben system extending over a total length of approximately 47 km. It extends from the northwestern corner of the Salt Valley graben to the east flank of the San Rafael Swell. Over most of its length it separates the Jurassic Morrison Formation from the Cretaceous Mancos Shale with stratigraphic offsets of several thousand feet. It has not been identified as a suspected Quaternary fault in the Quaternary Fault and Fold Database (Black, et al. 2003).

  Because of its length and proximity to the Green River Site, this fault was considered to be the most critical fault in the seismotectonic study performed for the Green River Site (DOE 1991a). The fault is clearly marked in the field by prominent bedrock scarps, lithologic changes, and extensive linear travertine deposits such as are presently forming at Crystal Geyser on the Green River approximately 3 km south of the Green River Site. However, detailed examination of the fault trace did not reveal any evidence of Late Quaternary movement. The fault trace, when viewed in detail, is highly dissected and is crossed by numerous washes. Alluvium in these washes shows no evidence of tectonic disturbance. Talus and colluvial slopes that mantle the fault trace in many places are not deformed. Fault scarps are formed only where rocks of the hanging and footwalls are of contrasting degrees of resistance to erosion. Near Crystal Geyser the contrast of the relatively durable Morrison Formation with the nonresistant Mancos Shale has produced steep cliffs that mark the fault trace. Where shale of similar composition lies on both sides of the fault, scarps are indistinct or absent (DOE 1991a).

  The evidence from the Green River investigation indicates that the Little Grand Wash fault is of Laramide age and is not capable under the present seismotectonic regime. The prominent bedrock

scarps that mark the fault trace have been produced by erosion during Late Tertiary to Holocene time. Gradual creep, produced by salt solution at depth, may be presently occurring, but no conclusive evidence for it was seen (DOE 1991a). Based on these data, the Little Grand Wash fault is not considered a capable fault.

Historical Earthquakes

Instrumentally and historically recorded earthquakes within a study area of 200 miles around the site were documented using the National Earthquake Information Center (NEIC) website (NEIC 2005). Databases searched included USGS/NEIC Preliminary Determinations of Epicenters (PDE) monthly, weekly (PDE-W), and daily (PDE-Q) listings; Significant U.S. Earthquakes (USHIS); and Eastern, Central, and Mountain States of the United States (SRA). The earthquakes are shown graphically in Figure *4* and also in table form in Appendix B.

Maximum Credible Earthquakes

A study by Kirkham and Rogers (1981) estimated the MCEs of tectonic provinces within the state of Colorado. In addition, the RAP for the Grand Junction/Cheney disposal site (DOE 1991b) estimated maximum earthquakes associated with regional tectonic provinces. Table 2 summarizes these estimates for the provinces within this study region.

Table 2. Estimate of Maximum Credible Earthquakes Associated with Tectonic Provinces

Tectonic Province	Maximum Credible Earthquake (MCE)	
	Kirkham and Rogers (1981)	DOE (1991b)
Rio Grande Rift	6 – 7.5	6.5 – 7.5
Eastern Mountain	6 – 6.75	
Western Mountain	6 – 6.5	
Colorado Plateau	5.5 – 6.5	6.5
Paradox Basin		4 – 5
Intermountain Seismic Belt		7.0 – 7.9
Wyoming Basin		5.7 – 6.5

Peak Ground Accelerations

A contour map for PHA in rock (with a 90 percent probability of not being exceeded in 50 years) is presented for the contiguous United States by Algermissen, et al. (1990), showing the site to have a PHA of 0.025 g. Contour maps developed for the National Seismic Hazard Mapping Project (Frankel, et al. 2002a and 2002b) show the peak acceleration to be 0.045 g with a 10 percent probability of exceedance in 50 years, and 0.12 g with a 2 percent probability of exceedance in 50 years.

Halling, et al. (2002) developed peak acceleration maps for the State of Utah. In this study, the MCEs for all known or suspected Quaternary faults in the state were calculated using relationships developed by Wells and Coppersmith (1994). Ground motion was attenuated across the state using three different attenuation relationships. Contours of peak horizontal bedrock accelerations were developed. The peak ground acceleration for the Crescent Junction Site was estimated to be approximately 0.5 g.

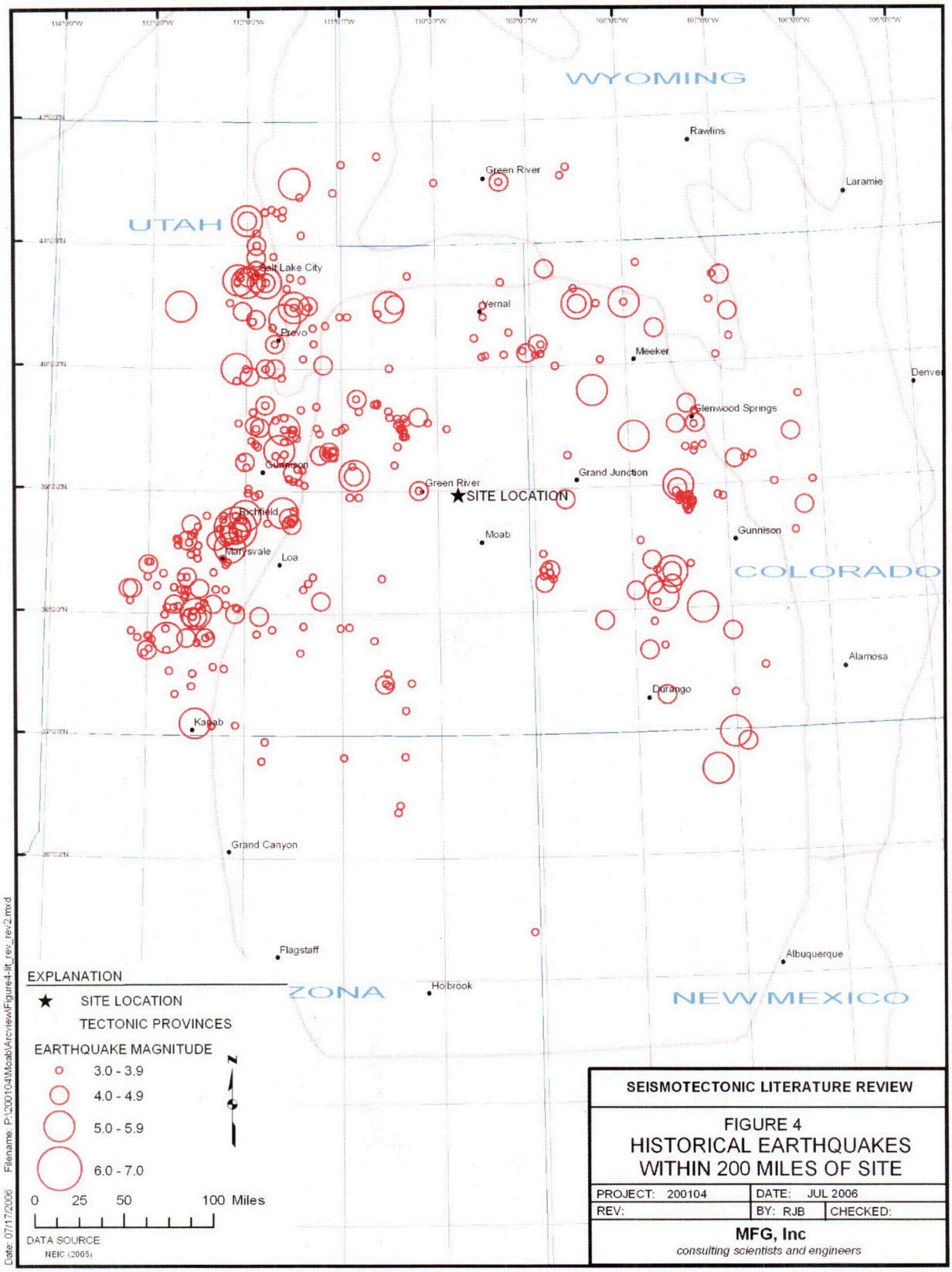

Figure 4. Historical Earthquakes Within 200 Miles of Site Location

These ground accelerations were predominately influenced by predicted ground motion from the Tenmile graben fault.

For comparison purposes only, the peak ground accelerations determined for the UMTRA sites at Green River and Grand Junction/Cheney Disposal Site were investigated. The seismotectonic stability study performed for the Green River Disposal Site recommended the design acceleration based on a floating earthquake of magnitude (ML) 6.2 occurring 15 km (9.5 miles) from the site, resulting in a peak ground acceleration of 0.21 g.

Seismotectonic stability studies done for the Grand Junction mill tailings/Cheney Disposal Site identified a fault (Fault 8) with a length of 11.0 km at a distance of 9.0 km from the site. Although no evidence of Quaternary displacement was proven, it was considered to be capable on the basis of its apparent association with a possibly active regional structure, the Uncompahgre Uplift. This fault was adopted as the design fault for the Cheney Disposal Site, resulting in a recommended design acceleration of 0.42 g.

Conclusion and Recommendations:

A thorough review of available literature that applies to the Crescent Junction Site is required to determine the suitability of the Crescent Junction Disposal Site as the repository for the Moab uranium mill tailings material and to develop the site and regional seismotectonic sections of the RAP.

The results of this review indicate that there are nine Quaternary fault systems within 40 miles of the site that have been numbered using the identification system in the USGS database. The closest fault systems to the Crescent Junction Site are the Salt Valley and Cache Valley faults (2474). However, these faults appear related to dissolution and collapse of the Salt Valley anticline in eastern Utah, north of Moab. An additional nine faults have been identified that warrant consideration in the development of the seismicity of the Crescent Junction Site. Further analysis of the faults and historical earthquake events will be performed in additional calculation sets to determine the MCE and associated ground accelerations.

Computer Source:

Not applicable.

References:

Algermissen, S. T., D. M. Perkins, P. C. Thenhause, S. L. Hanson, and B. L. Bender, 1982. *Probabilistic Estimates of Maximum Acceleration and Velocity in Rock in the Contiguous United States*, U.S. Geological Survey Open-File Report 82-1033, U.S. Department of the Interior, Washington, D.C.

———, 1990. *Probabilistic Earthquake Acceleration and Velocity Maps for the United States and Puerto Rico*, U.S. Geological Survey Miscellaneous Field Studies Map MF-2120.

Allenby, R. J., 1979. Letter section: Implications of Very Long Baseline Interferometry Measurements on North American Intra-Plate Crustal Deformation, Tectonophysics, vol. 60, p. T27–T35.

Black, B. D., S. Hecker, M. D. Hylland, G. E. Christenson, and G. N. McDonald, 2003. *Quaternary Fault and Fold Database and Map of Utah*, Utah Geological Survey Map 193DM.

Campbell, K. W., 1981. *Near-source Attenuation of Peak Horizontal Acceleration*, Bulletin of the Seismological Society of America, Vol. 71, No. 6, pp. 2039–2070, December.

Campbell, K. W., and Y. Bozorgnia, 2003. *Updated Near-Source Ground-Motion (Attenuation) Relations for the Horizontal and Vertical Components of Peak Ground Acceleration and Acceleration Response Spectra,* Bulletin of the Seismological Society of America, Vol. 93, No. 1, pp. 314–331, February.

Cater, F. W., Jr., 1966. *Age of the Uncompahgre Uplift and Unaweep Canyon, West-Central Colorado*, U.S. Geological Survey Professional Paper 550-C, p. C86–C92.

Chitwood, J. P., 1994. *Provisional geologic map of the Hatch Mesa quadrangle, Grand County, Utah*, Utah Geological Survey, Map 152, scale 1:24,000.

Colman, S. M., 1985. *Map Showing Tectonic Features of Late Cenozoic Origin in Colorado*, U.S. Geological Survey Miscellaneous Geologic Investigations Map I-1566, scale 1:1,000,000.

Doelling, H. H., 2001. *Geologic map of the Moab and eastern part of the San Rafael Desert 30' x 60' quadrangles, Grand and Emery Counties, Utah, and Mesa County, Colorado*, Utah Geological Survey, Map 180, scale 1:100,000.

Ely, R. W., I. G. Wong, and P. Chang, 1986. *Neotectonics of the Uncompahgre Uplift, Eastern Utah and Western Colorado*, in Rogers, W.P. and R.M. Kirkham, editors, Contributions to Colorado seismicity and tectonics – a 1986 Update, Colorado Geological Survey Special Publication, p. 75–92.

Frankel, A., C. Mueller, T. Barnhard, D. Perkins, E. Leyendecker, N. Dickman, S. Hanson, and M. Hopper, 2002. *Seismic-Hazard Maps for the Conterminous United States, Map A – Horizontal Peak Acceleration With 10% Probability of Exceedance in 50 years*, U.S. Geological Survey Open-File Report 97-131-A.

———, 2002. *Seismic-Hazard Maps for the Conterminous United States, Map C – Horizontal Peak Acceleration With 2% Probability of Exceedance in 50 Years*, U.S. Geological Survey Open-File Report 97-131-C.

Gaultieri, J. L, 1988. Geologic map of the Westwater 30' x 60' Quadrangle, Grand and Uintah Counties, Utah, and Garfield and Mesa Counties, Colorado: U.S. Geological Survey Miscellaneous Investigations Series Map I-1765, scale: 1:100,000.

Gutenburg, B., and C. F. Richter, 1956. *Earthquake Magnitude, Intensity, Energy, and Acceleration*: Bulletin of the Seismological Society of America, vol. 46, no. 1, pp. 105-145.

Halling, M. W., J.R. Keaton, L.R. Anderson, and W. Kohler, 2002. *Deterministic Maximum Peak Bedrock Acceleration Maps for Utah*, Utah Geological Survey Miscellaneous Publication 02-11, July.

Harden, D. R., N. E. Biggar, and M. L. Gillam, 1985. *Quaternary Deposits and Soils in and Around Spanish Valley, Utah*, in Weide, D. L., editor, Soils and Quaternary Geology of the Southwestern United States, Geological Society of America Special Paper 203, p. 43–64.

Hecker, S., 1993. *Quaternary Tectonics of Utah with Emphasis on Earthquake-Hazard Characterization*, Utah Geological Survey Bulletin 127, 15 p.

Heyman, O.G., 1983. *Distribution and Structural Geometry of Faults and Folds Along the Northwestern Uncompahgre Uplift, Western Colorado and Eastern Utah*, in Averett, W. R., editor, Northern Paradox Basin – Uncompahgre Uplift, Grand Junction Geological Society, p. 45–57.

Howard, K., J. Aaron, E. Brabb, M. Brock, H. Gower, S. Hunt, D. Milton, W. Muehlberger, J. Nakata, G. Plafker, D. Prowell, R. Wallace, and I. Witkind, 1978. *Preliminary Map of Young Faults in the United States as a Guide to Possible Fault Activity*, U.S. Geological Survey Miscellaneous Field Studies Map MF-916, 2 sheets, scale 1:5,000,000.

Hunt, C. B., 1967. *Physiography of the United States*: W.H. Freemand and Company, San Francisco, California.

Jones, R. W., 1959. *Origin of Salt Anticlines of Paradox Basin*, American Association of Petroleum Geologists Bulletin, vol. 43, no. 8, p. 1869–1895.

Keller, G., L. Braile, and P. Morgan, 1979. *Crustal Structure, Geophysical Models and Contemporary Tectonism of the Colorado Plateau*, Tectonophysics, vol. 61, p. 131–147.

Kelley, V. C. 1955. *Regional Tectonics of the Colorado Plateau and Relationship to the Origin and Distribution of Uranium*, University of New Mexico Publications in Geology, No. 5.

Kelley, V. C., and N. Clinton, 1960. *Fracture Systems and Tectonic Elements of the Colorado Plateau*, University of New Mexico Publications in Geology No. 6.

Kelley, V. C., 1979. *Tectonics of the Colorado Plateau and New Interpretation of Its Eastern Boundary*, Tectonophysics, vol. 61, p. 97–102.

Kirkham, R. M. and W. P. Rogers, 1981. *Earthquake Potential in Colorado, a Preliminary Evaluation*, Colorado Geological Survey Bulletin 43.

Krinitzsky, E. L., and F. K. Chang (1977). *State-of-the-Art for Assessing Earthquake Hazards in the United States, Report 7: Specifying Peak Motions for Design Earthquakes*, U.S. Army Engineer Waterways Experiment Station, Miscellaneous Paper S-74-1, Vicksburg, Mississippi.

Livaccari, R., and J. Hodge, 2005. *Laramide and Quaternary-age faulting along the northern Uncompahgre Plateau, Western Colorado*, Geological Society of America, Abstracts with programs, Rocky Mountain Section, v. 37, no. 6, p. 34.

National Earthquake Information Center (NEIC), 2005. *Circular Area Search of Historical Earthquakes*: http://neic.usgs.gov/neis/epic/

Olig, S. S., C. H. Fenton, J. McCleary, and I. G. Wong, 1996. *The Earthquake Potential of the Moab Fault and Its Relation to Salt Tectonics in the Paradox Basin, Utah*, in Huffman, A. C., Jr., W. R. Lund, and L. H. Godwin, editors, *Geology and Resources of the Paradox Basin*, Utah Geological Association Guidebook 25, p. 251–264.

Oviatt, C. G., 1988. *Evidence for Quaternary Deformation in the Salt Valley Anticline, Southeastern Utah*: in Doelling H. H., C. G.Oviatt, and P. W. Huntoon, editors, *Salt Deformation in the Paradox Region*, Utah Geological and Mineral Survey Bulletin 122, p. 63–76.

Perry, T., and D. Annis, 1990. *Pleistocene History of the Gunnison River in Unaweep Canyon, Colorado, and Implications for Colorado Plateau Uplift* [abs.], Geological Society of America Abstracts with Programs, vol. 22, no. 3, p. 75.

Richter, C.F. (1958). *Elementary Seismology*, W. H. Freeman and Company, San Francisco, California.

Ryall, A., D. Slemmons, and L. Gedney, 1966. *Seismicity, Tectonism, and Surface Faulting in the Western United States During Historic Time*, Seismological Society of America Bulletin, vol. 56, p. 1105–1135.

Shoemaker, E. M., J. E. Case, and D. P. Elston, 1958. *Salt Anticlines of the Paradox Basin*, in Sanborn, A. R., editor, *Guidebook to the Geology of the Paradox Basin, Ninth Annual Field Conference*, Intermountain Association of Petroleum Geologists, p. 39–59.

Smith, R., and M. Sbar, 1974. *Contemporary Tectonics and Seismicity of the Western United States with Emphasis on the Intermountain Seismic Belt*, Geological Society of America Bulletin, vol. 85, p. 1205–1218.

Stone, D. S., 1977. *Tectonic History of the Uncompahgre Uplift*, in Veal, H. K., editor, *Exploration frontiers of the central and southern Rockies*, Rocky Mountain Association of Geologists, 1977 Field Conference Guidebook, p. 23–30.

U.S. Department of Energy (DOE), 1989. *Technical Approach Document, Revision II, AL 050425.0002, United States Department of Energy, Uranium Mill Tailings Remedial Action Project*, December.

———, 1991a. *Remedial Action Plan and Final Design for Stabilization of the Inactive Uranium Mill Tailings at Green River, Utah.*

———, 1991b. *Remedial Action Plan and Site Design for Stabilization of the Inactive Uranium Mill Tailings Site at Grand Junction, Colorado.*

U.S. Geological Survey (USGS), 2002. *Quaternary Fault and Fold Database,* http://Qfaults.cr.usgs.gov/

Walton, P. T., 1956. *Structure of the North Salt Valley-Cisco Area, Grand County, Utah* in Peterson, J. A., ed., *Geology and Economic Deposits of East-central Utah,* Intermountain Association of Petroleum Geologists Guidebook, 7th Annual Field Conference, p. 186–189.

Wells, D. L., and K. J. Coppersmith, (1994). *New Empirical Relationships among Magnitude, Rupture Length, Rupture Area, and Surface Displacement,* Bulletin of the Seismological Society of America, vol. 84, p. 974–1002.

Williams, P. L., compiler, 1964. *Geology, Structure, and Uranium Deposits of the Moab Quadrangle, Colorado and Utah,* U.S. Geological Survey Miscellaneous Geologic Investigations Map I-360, scale 1:250,000.

Williams, P. L., and R. J. Hackman, 1971. *Geology of the Salina Quadrangle, Utah,* U.S. Geological Survey Miscellaneous Geologic Investigations Map I-591, scale 1:250,000.

Willis, G. C., 1986. Provisional Geologic Map of the Sego Canyon Quadrangle, Grand County, Utah, Utah Geological and Mineral Survey Map 89, scale 1:24,000.

Witkind, I., 1975. *Preliminary Map Showing Known and Suspected Active Faults in Wyoming,* U.S. Geological Survey Open-File Report 75-249.

———, 1976. *Preliminary Map Showing Known and Suspected Active Faults in Colorado,* U.S. Geological Survey Open-File Report 76-154, 42 sheets, scale 1:500,000.

Woodward-Clyde Consultants, 1984. *Geologic characterization report for the Paradox Basin study region, Utah study areas, Volume VI, Salt Valley,* Walnut Creek, California, unpublished consultant's report for Battelle Memorial Institute, Office of Nuclear Waste Isolation, ONWI-290, 190 p., scale 1:62,500.

Woodward-Clyde Consultants, 1996. *Evaluation and Potential Seismic and Salt Dissolution Hazards at the Atlas Uranium Mill Tailings Site, Moab, Utah,* Oakland, California, unpublished Consultant's report for Smith Environmental Technologies and Atlas Corporation, SK9407.

Appendix A

Quaternary and Undated Faults Within Expanded Study Region

SITE AND REGIONAL SEISMICITY - RESULTS OF LITERATURE REVIEW
APPENDIX A:
QUATERNARY AND UNDATED FAULTS WITHIN EXPANDED SITE REGION

Name	Number	Age of Most Recent Prehistoric Deformation (ya)	Slip-rate (mm/yr)	Fault Length (km)	Fault Type	Distance from site (miles)[1]
Salt and Cache Valleys faults (Class B)	2474	Class B	<0.2	57.9	N	1.8
unnamed fault in Westwater Quad, R19E, T21S (no. 1)	1			8.0		2.4
unnamed fault in Westwater Quad, R20E, T21S (no. 2)	2			6.4		3.1
unnamed fault in Westwater Quad, R18E, T21S (no. 4)	4			2.9		4.9
unnamed fault in Westwater Quad, R19E, T19S (no. 3)	3			15.7		5.3
Little Grand fault	9			47.0	N	6.5
unnamed fault in Westwater Quad, R18E, T20S (no. 5)	5			1.9		7.0
unnamed fault in Westwater Quad, R17E, T20S (no. 6)	6			3.3		9.6
Ten Mile graben faults (Class B)	2473	Class B	<0.2	34.6	N	10.5
unnamed fault in Westwater Quad, R21E, T0S (no. 7)	7			4.4		12.4
Moab fault and Spanish Valley faults (Class B)	2476	Class B	<0.2	72.4	N	12.5
Price River area faults (Class B)	2457	<1,600,000	<0.2	50.9	N	24.8
Sand Flat graben faults	2475	<1,600,000	<0.2	23.1	N	26.4
Ryan Creek fault zone	2263	<1,600,000	<0.2	39.5	N	26.6
Fisher Valley faults (Class B)	2478	Class B	<0.2	15.9		31.0
Granite Creek fault zone	2265	<1,600,000	<0.2	22.7	N	33.4
Castle Valley faults (Class B)	2477	Class B	<0.2	12.4		34.2
Little Doloras River fault	2251	<1,600,000	<0.2	15.7	R	34.5
unnamed fault in Salina Quad, R13E, T24S				19.6		36.0
Sinbad Valley graben (Class B)	2285	<1,600,000	<0.2	31.8		39.3
Lockhart fault (Class B)	2510	Class B	<0.2	15.7		40.8
Unnamed fault of Lost Horse Basin	2264	<1,600,000	<0.2	8.1		40.8
unnamed fault in Salina Quad, R11E, T22S				22.7		41.6
unnamed fault in Salina Quad, R11E, T21S				14.0		42.1
unnamed fault in Price Quad, R12E, T19S				13.7		42.4
unnamed fault in Salina Quad, R12E, T24S				10.1		42.6
unnamed fault in Salina Quad, R12E, T23S				9.0		43.5
unnamed fault in Salina Quad, R16E, T28S				9.0		43.9
unnamed fault in Salina Quad, R11E, T23S				25.8		44.7
unnamed fault in Salina Quad, R11E, T24S				9.8		47.0
Unnamed fault near Pine Mountain	2267	<1,600,000	<0.2	30.7		47.2
unnamed fault in Price Quad, R16E, T13S				9.5		48.6
Paradox Valley graben (Class B)	2286	<1,600,000	<0.2	56.4	N	49.6
Lisbon Valley fault zone (Class B)	2511	<1,600,000	<0.2	37.5		50.9
Redlands fault complex	2252	<1,600,000	<0.2	21.1	N,R	53.1
Needles fault zone (Class B)	2507	Class B	<0.2	28.5		53.9
Shay graben faults (Class B)	2513	Class B	<0.2	39.5		68.1
Cactus Park-Bridgeport fault	8			22.5		70.0
Big Gypsum Valley graben (Class B)	2288	Class B	<0.2	33.1		70.9
Southern Joes Valley fault zone	2456	<750,000	<0.2	47.2		77.2
Unnamed faults of Pinto Mesa	2277	<1,600,000	<0.2	19.7		78.4
Unnamed faults south of Love Mesa	2271	<1,600,000	<0.2	17.6		78.8
Joes Valley fault zone, east fault	2455	<15,000	0.2-1	56.6		79.0
Duchesne-Pleasant Valley fault system (Class B)	2414	<1,600,000	<0.2	45.3	N	79.1
Monitor Creek fault	2268	<1,600,000	<0.2	30.1		79.1
Joes Valley fault zone, west fault	2453	<15,000	0.2-1	57.2		81.1
Joes Valley fault zone, intragraben faults	2454	<15,000	<0.2	34.0		82.9

Name	Number	Age of Most Recent Prehistoric Deformation (ya)	Slip-rate (mm/yr)	Fault Length (km)	Fault Type	Distance from site (miles)[1]
Pleasant Valley fault zone, unnamed faults	2425	<1,600,000	<0.2	31.0	N	86.1
Pleasant Valley fault zone, graben	2426	<750,000	<0.2	17.6		88.3
Roubideau Creek fault	2270	<15,000	<0.2	20.5		88.7
Bright Angel fault system (Class B)	2514	<1,600,000	<0.2	102.3		89.6
Snow Lake graben	2452	<15,000	<0.2	25.4		89.7
Wasatch monocline (Class B)	2450	<1,600,000	<0.2	103.5	?	90.3
White Mountain area faults	2451	<1,600,000	<0.2	16.4		90.5
Unnamed fault at Red Canyon	2279	<1,600,000	<0.2	24.2		90.9
Gooseberry graben faults	2424	<750,000	<0.2	22.6		93.1
Unnamed faults near San Miguel Canyon (Class B)	2284	Class B	<0.2	32.1		94.5
Thousand Lake fault	2506	<750,000	<0.2	48.3		97.2
Unnamed fault at Hanks Creek	2281	<1,600,000	<0.2	17.5		99.0
Gunnison fault	2445	<15,000	<0.2	42.0	N	104.3
Aquarius and Awapa Plateaus faults	2505	<1,600,000	<0.2	35.7		108.6
Red Rocks fault	2291	<1,600,000	<0.2	38.3		111.8
Valley Mountains monocline (Class B)	2449	<1,600,000	<0.2	38.6		112.9
Paunsaugunt fault	2504	<1,600,000	<0.2	44.1		118.0
Wasatch fault zone, Nephi section	2351h	<15,000	1-5	43.1		119.9
Wasatch fault zone, Provo section	2351g	<15,000	1-5	58.8		122.2
Sevier fault	2355	<1,600,000	<0.2	41.3	N	126.4
East Tintic Mountains (west side) faults	2420	<750,000	<0.2	33.1		129.6
Sevier Valley-Marysvale-Circleville area faults	2500	<750,000	<0.2	34.9		133.7
Bear River fault zone	730	<15,000	0.2-1	33.2		140.4
Hogsback fault, southern section	732b	<130,000	1-5	38.3		144.3
Cannibal fault	2337	<130,000	<0.2	49.3		148.9
Sevier/Toroweap fault zone, Sevier section	997a	<130,000	0.2-1	88.7		155.4
West Kaibab fault system	994	<1,600,000	<0.2	82.9	N	187.7
Frontal fault	2302	<130,000	0.2-1	75.0	N,R	190.1
Central Kaibab fault system	993	<1,600,000	<0.2	71.5	N	192.3
Sevier/Toroweap fault zone, northern Toroweap section	997b	<130,000	<0.2	80.9		198.5
Almy fault zone	742	<1,600,000	<0.2	10.7		
Andrus Canyon fault	1013	<1,600,000	<0.2	5.6		
Annabella graben faults	2472	<15,000	<0.2	12.5		
Antelope Range fault	2517	<750,000	<0.2	24.5		
Arrowhead fault zone	953	<130,000	<0.2	5.2		
Aubrey fault zone	995	<130,000	<0.2	53.1		
Babbitt Lake fault zone	954	<750,000	<0.2	7.6		
Bald Mountain fault	2390	<1,600,000	<0.2	2.3		
Bangs Canyon fault	2256	<1,600,000	<0.2	6.3		
Basalt Mountain fault (Class B)	2299	Class B	<0.2	7.0		
Bear Lake (west side) fault (Class B)	2531	<1,600,000	<0.2	5.5		
Bear River Range faults	2410	<1,600,000	<0.2	62.9	N, D	
Beaver Basin faults, eastern margin faults	2492a	<15,000	<0.2	34.2		
Beaver Basin faults, intrabasin faults	2492b	<15,000	<0.2	38.9		
Beaver Ridge faults	2464	<130,000	<0.2	14.2		
Big Pass faults	2366	<1,600,000	<0.2	17.3		
Black Mesa fault zone	2006	<1,600,000	<0.2	18.5		
Black Mountains faults	2487	<750,000	<0.2	25.9		
Black Point/Doney Mountain fault zone	957	<750,000	<0.2	23.8	N	
Black Rock area faults	2461	<130,000	<0.2	8.2		
Blue Springs Hills faults	2363	<750,000	<0.2	2.5		
Bright Angel fault zone	991	<1,600,000	<0.2	66.0	N	

Name	Number	Age of Most Recent Prehistoric Deformation (ya)	Slip-rate (mm/yr)	Fault Length (km)	Fault Type	Distance from site (miles)[1]
Broadmouth Canyon faults	2377	<130,000	<0.2	3.4		
Buckskin Valley faults (Class B)	2499	Class B	<0.2	3.5		
Busted Boiler fault	2274	<130,000	<0.2	18.0		
Cactus Park fault	2258	<1,600,000	<0.2	1.9		
Calabacillas fault	2035	<750,000	<0.2	31.3		
Cameron graben and faults	988	<750,000	<0.2	10.8		
Campbell Francis fault zone	959	<750,000	<0.2	10.1		
Canones fault (Class B)	2003	<1,600,000	<0.2	29.4		
Cataract Creek fault zone	990	<1,600,000	<0.2	51.1	N	
Cattle Creek anticline (Class B)	2293	Class B	<0.2	8.6		
Cedar City-Parowan monocline (and faults)	2530	<15,000	<0.2	24.8		
Cedar Ranch fault zone	961	<750,000	<0.2	10.2		
Cedar Valley (north end) faults	2529	<130,000	<0.2	15.5		
Cedar Valley (south side) fault	2408	<750,000	<0.2	2.8		
Cedar Valley (west side) faults	2527	<750,000	<0.2	12.8		
Cedar Wash fault zone	962	<750,000	<0.2	11.6		
Chicken Springs faults	780	<15,000	<0.2	13.7		
Cimmarron fault, Blue Mesa section	2290c	<1,600,000	<0.2	22.5		
Cimmarron fault, Bostwick Park section (Class B)	2290a	Class B	<0.2	11.2		
Cimmarron fault, Poverty Mesa section (Class B)	2290b	Class B	<0.2	24.1		
Citadel Ruins fault zone	963	<1,600,000	<0.2	4.5		
Clear Lake fault zone (Class B)	2436	<15,000	<0.2	35.5		
Clover fault zone	2396	<130,000	<0.2	4.0		
County Dump fault	2038	<1,600,000	<0.2	35.3		
Cove Fort fault zone (Class B)	2491	Class B	<0.2	22.2		
Crater Bench faults	2433	<15,000	<0.2	15.9		
Crawford Mountains (west side) fault	2346	<130,000	<0.2	25.3		
Cricket Mountains (north end) faults	2434	<750,000	<0.2	2.8		
Cricket Mountains (west side) fault	2460	<15,000	<0.2	41.0		
Cross Hollow Hills faults	2524	<1,600,000	<0.2	5.3		
Curlew Valley faults	3504	<15,000	<0.2	20.0		
Dayton fault (Class B)	2370	Class B	<0.2	16.3		
Deadman Wash faults	964	<1,600,000	<0.2	1.8		
Deep Creek Range (east side) faults	2416	<750,000	<0.2	20.7		
Deep Creek Range (northwest side) fault zone	2403	<130,000	<0.2	10.7		
Deseret faults	2435	<750,000	<0.2	7.1		
Diamond Gulch faults	2393	<1,600,000	<0.2	20.2		
Doloras fault zone (Class B)	2289	Class B	<0.2	15.2		
Dolphin Island fracture zone	2367	<750,000	<0.2	19.2		
Double Knobs fault	966	<1,600,000	<0.2	6.0		
Double Top fault zone	965	<1,600,000	<0.2	6.1		
Drum Mountains fault zone	2432	<15,000	<0.2	51.5	N	
Dry Wash fault and syncline	2496	<130,000	<0.2	18.6		
Duncomb Hollow fault	743	<1,600,000	<0.2	2.4		
Dutchman Draw fault	1003	<130,000	<0.2	16.3	N	
East Cache fault zone, central section	2352b	<15,000	0.2-1	16.5		
East Cache fault zone, northern section	2352a	<750,000	<0.2	25.7		
East Cache fault zone, southern section	2352c	<130,000	<0.2	22.1		
East Canyon (east side) fault (Class B)	2350	<1,600,000	<0.2	28.9		
East Canyon fault, Northern East Canyon section (Class B)	2354a	Class B	<0.2	22.5		
East Canyon fault, Southern East Canyon section	2354b	<750,000	<0.2	8.4		
East Dayton-oxford fault	3509	<130,000	<0.2	23.2	N	

Name	Number	Age of Most Recent Prehistoric Deformation (ya)	Slip-rate (mm/yr)	Fault Length (km)	Fault Type	Distance from site (miles)[1]
East Great Salt Lake fault zone, Antelope Island section	2369c	<15,000	0.2-1	35.1		
East Great Salt Lake fault zone, Fremont Island section	2369b	<15,000	0.2-1	30.1		
East Great Salt Lake fault zone, Promontory section	2369a	<15,000	0.2-1	49.2	N	
East Kamas fault	2391	<1,600,000	<0.2	14.6		
East Lakeside Mountains fault zone	2368	<1,600,000	<0.2	36.0		
East Pocatello valley faults	3507	<15,000	<0.2	6.8		
Eastern Bear Lake fault, central section	2364b	<15,000	<0.2	23.8		
Eastern Bear Lake fault, southern section	2364c	<15,000	0.2-1	34.8		
Eastern Bear Valley fault (Class B)	734	Class B	<0.2	47.2		
Eastern Pilot Range fault	2371	<1,600,000	<0.2	10.6		
East-Side Chase Gulch fault	2317	<130,000	<0.2	30.7		
Ebert Tank fault zone	967	<750,000	<0.2	3.1		
Eleven Mile fault	2318	<130,000	<0.2	4.7		
Elk Mountain fault	736	<1,600,000	<0.2	7.8		
Ellison Gulch scarp (Class B)	2304	Class B	<0.2	1.2		
Elsinore fault (fold)	2470	<1,600,000	<0.2	28.1		
Embudo fault, Hernandez section	2007b	<1,600,000	<0.2	31.6		
Embudo fault, Pilar section	2007a	<130,000	<0.2	38.7		
Eminence fault zone	992	<1,600,000	<0.2	36.0		
Enoch graben faults	2528	<15,000	<0.2	17.2		
Enterprise faults	2516	<750,000	<0.2	8.4		
Escalante Desert (east side) faults	2526	<15,000	<0.2	6.4		
Escalante Desert faults (Class B)	2488	Class B	<0.2	6.6		
Escalante Desert faults near Zane	2518	<130,000	<0.2	3.9		
Faults in Raft River Valley	3503	<750,000	<0.2	35.2		
Faults near Garcia	2323	<130,000	<0.2	3.4		
Faults near Monte Vista	2315	<1,600,000	<0.2	16.2		
Faults near of Cochiti Pueblo	2142	<1,600,000	<0.2	32.2		
Faults north of Placitas	2043	<750,000	<0.2	10.5		
Faults of Cove Creek Dome	2462	<1,600,000	<0.2	18.8		
Faults of the northern Basaltic Hills	2322	<1,600,000	<0.2	12.6		
Faults on north flank of Phil Pico Mountains	744	<130,000	<0.2	4.4		
Fish Springs fault	2417	<15,000	<0.2	29.7		
Foote Range fault	2429	<750,000	<0.2	3.1		
Fremont Wash faults	2495	<750,000	<0.2	7.2		
Frog Valley fault	2389	<1,600,000	<0.2	4.6		
Gallina fault	2001	<1,600,000	<0.2	39.3		
Glade Park fault	2254	<1,600,000	<0.2	9.4	R	
Goose Creek Mountains faults (Class B)	2356	Class B	<0.2	4.0		
Grand Hogback monocline (Class B)	2331	Class B	<0.2	22.0		
Grand Wash fault zone	1005	<130,000	<0.2	34.9	N	
Gray Mountain faults	1018	<1,600,000	<0.2	23.6		
Greenhorn Mountain fault (Class B)	2297	Class B	<0.2	21.5		
Grouse Creek and Dove Creek Mountains faults	2357	<750,000	<0.2	47.7		
Guaje Mountain fault	2027	<15,000	<0.2	10.7		
Gunlock fault (Class B)	2515	Class B	<0.2	7.5		
Gyp Pocket graben and faults	1001	<130,000	<0.2	11.8	N	
Hansel Mountains (east side) faults	2359	<750,000	<0.2	14.7		
Hansel Valley (valley floor) faults	2360	<750,000	<0.2	19.5		
Hansel Valley fault	2358	<150	<0.2	13.0		
Hidden Tank fault zone	970	<750,000	<0.2	10.2		
Hogsback fault, northern section	732a	<750,000	0.2-1	22.4		

Name	Number	Age of Most Recent Prehistoric Deformation (ya)	Slip-rate (mm/yr)	Fault Length (km)	Fault Type	Distance from site (miles)[1]
House Range (west side) fault	2430	<15,000	<0.2	45.5	N	
Hurricane fault zone, Anderson Junction section	998c	<15,000	0.2-1	42.2		
Hurricane fault zone, Ash Creek section	998b	<15,000	<0.2	32.0		
Hurricane fault zone, Cedar City section	998a	<15,000	<0.2	13.2		
Hurricane fault zone, Shivwitz section	998d	<130,000	<0.2	56.5	N	
Hurricane fault zone, southern section	998f	<1,600,000	<0.2	66.6	N	
Hurricane fault zone, Whitmore Canyon section	998e	<15,000	<0.2	28.5		
Hyrum fault	2374	<1,600,000	<0.2	3.1		
James Peak fault	2378	<130,000	<0.2	6.3		
Japanese and Cal Valleys faults	2447	<750,000	<0.2	30.1		
Jemez-San Ysidro fault, Jemez section	2029a	<1,600,000	<0.2	24.1		
Jemez-San Ysidro fault, San Ysidro section	2029b	<1,600,000	<0.2	30.1		
Johns Valley fault (Class B)	2539	Class B	<0.2	2.1		
Joseph Flats area faults and syncline (Class B)	2468	Class B	<0.2	3.2		
Juab Valley (west side) faults (Class B)	2423	<750,000	<0.2	13.2		
Judd Mountain fault	1597	<1,600,000	<0.2	20.4		
Killarney faults	2336	<1,600,000	<0.2	5.6		
Kolob Terrace faults	2525	<750,000	<0.2	12.1		
Koosharem fault	2503	<1,600,000	<0.2	2.2		
La Bajada fault	2032	<1,600,000	<0.2	40.3		
La Canada del Amagre fault zone	2005	<1,600,000	<0.2	17.2		
Ladder Creek fault	2255	<1,600,000	<0.2	6.2		
Lakeside Mountains (west side) fault (Class B)	2384	Class B	<0.2	4.7		
Large Whiskers fault zone	972	<1,600,000	<0.2	11.6		
Las Tablas fault	2020	<1,600,000	<0.2	14.8		
Lee Dam faults	973	<1,600,000	<0.2	7.6		
Leupp faults	1017	<750,000	<0.2	32.2		
Lime Mountain fault	2415	<1,600,000	<0.2	10.6		
Little Diamond Creek fault	2411	<750,000	<0.2	20.0		
Little Rough Range faults	2458	<750,000	<0.2	3.2		
Little Valley faults	2439	<15,000	<0.2	19.2		
Littlefield Mesa faults	1008	<750,000	<0.2	21.2		
Lobato Mesa fault zone	2004	<1,600,000	<0.2	21.3		
Lockwood Canyon fault zone	974	<1,600,000	<0.2	20.8		
Log Hill Mesa graben	2275	<130,000	<0.2	9.5		
Long Ridge (northwest side) fault	2422	<1,600,000	<0.2	20.8		
Long Ridge (west side) faults	2421	<750,000	<0.2	15.2		
Lookout Pass fault	2404	<1,600,000	<0.2	3.9		
Los Cordovas faults	2022	<1,600,000	<0.2	12.2		
Lucky Boy fault	2314	<1,600,000	<0.2	11.1		
Main Street fault zone	1002	<130,000	<0.2	87.3	N	
Malpais Tank faults	975	<750,000	<0.2	4.6		
Mantua area faults	2373	<750,000	<0.2	21.1		
Maple Grove faults	2443	<15,000	<0.2	12.8		
Markagunt Plateau faults (Class B)	2535	<750,000	<0.2	56.4		
Martin Ranch fault	731	<15,000	0.2-1	3.7		
Maverick Butte faults	976	<750,000	<0.2	3.7		
Meadow-Hatton area faults	2466	<15,000	<0.2	4.0		
Mesa Butte North fault zone	987	<1,600,000	<0.2	22.6		
Mesita fault	2015	<130,000	<0.2	27.9		
Mesquite fault	1007	<130,000	<0.2	36.2		
Michelbach Tank faults	978	<750,000	<0.2	13.4		

Name	Number	Age of Most Recent Prehistoric Deformation (ya)	Slip-rate (mm/yr)	Fault Length (km)	Fault Type	Distance from site (miles)[1]
Mineral Hot Springs fault	2320	<130,000	<0.2	7.8		
Mineral Mountains (northeast side) fault (Class B)	2490	Class B	<0.2	14.2		
Mineral Mountains (west side) faults	2489	<15,000	<0.2	36.6		
Morgan fault, central section	2353b	<15,000	<0.2	4.9		
Morgan fault, northern section	2353a	<750,000	<0.2	7.9		
Morgan fault, southern section	2353c	<750,000	<0.2	2.3		
Mosquito fault	2303	<130,000	<0.2	51.5		
Mountain Home Range (west side) faults	2480	<1,600,000	<0.2	26.4		
Nacimiento fault, northern section	2002a	<1,600,000	<0.2	35.9		
Nacimiento fault, southern section	2002b	<1,600,000	<0.2	45.2		
Nambe fault	2024	<1,600,000	<0.2	47.8		
North Bridger Creek fault	737	<1,600,000	<0.2	4.2		
North Hills faults	2522	<750,000	<0.2	5.0		
North of Wah Wah Mountains faults	2459	<750,000	<0.2	12.5		
North Promontory fault	2361	<15,000	<0.2	25.8		
North Promontory Mountains fault	2362	<1,600,000	<0.2	6.3		
Northern Boundary fault system	2309	<750,000	<0.2	49.0		
Northern Sangre de Cristo fault, Blanca section	2321c	<15,000	<0.2	6.7		
Northern Sangre de Cristo fault, Crestone section	2321a	<15,000	<0.2	79.1	N	
Northern Sangre de Cristo fault, San Luis section	2321d	<15,000	<0.2	59.1	N	
Northern Sangre de Cristo fault, Zapata section	2321b	<15,000	<0.2	25.8		
Ogden Valley North Fork fault	2376	<750,000	<0.2	26.1		
Ogden Valley northeastern margin fault	2379	<1,600,000	<0.2	12.8		
Ogden Valley southwestern margin faults	2375	<750,000	<0.2	17.8		
Oquirrh fault zone	2398	<15,000	<0.2	21.1		
Overton Arm faults	1119	<130,000	<0.2	50.9		
Pajarito fault	2008	<130,000	<0.2	49.4		
Paragonah fault	2534	<130,000	0.2-1	27.2		
Parleys Park faults (Class B)	2388	Class B	<0.2	3.4		
Parowan Valley faults	2533	<15,000	<0.2	16.3		
Pavant faults	2438	<15,000	<0.2	30.1		
Pavant Range fault	2442	<15,000	<0.2	14.2		
Pearl Harbor fault zone	981	<1,600,000	<0.2	15.3		
Picuris-Pecos fault	2023	<1,600,000	<0.2	98.2	N	
Pilot Range faults	1599	<1,600,000	<0.2	40.2		
Pine Ridge faults (Class B)	2512	Class B	<0.2	5.5		
Pine Valley (south end) faults	2482	<1,600,000	<0.2	10.7		
Pine Valley faults	2481	<750,000	<0.2	3.7		
Pleasant Valley fault zone, Dry Valley graben	2427	<750,000	<0.2	12.4		
Pojoaque fault zone	2010	<1,600,000	<0.2	46.5		
Porcupine Mountain faults	2380	<130,000	<0.2	34.6	N	
Pot Creek faults	2394	<1,600,000	<0.2	13.4		
Puddle Valley fault zone	2383	<15,000	<0.2	6.5		
Puye fault	2009	<130,000	<0.2	16.7		
Raft River Mountains fault	2448	<750,000	<0.2	1.5		
Red Canyon fault scarps	2471	<15,000	<0.2	9.4		
Red Hills fault	2532	<130,000	<0.2	13.8		
Red House faults	983	<750,000	<0.2	3.4		
Red River fault zone	2019	<1,600,000	<0.2	10.0		
Rendija Canyon fault	2026	<130,000	<0.2	11.1		
Ridgway fault	2276	<1,600,000	<0.2	23.8		
Rimmy Jim fault zone	984	<1,600,000	<0.2	8.2		

Name	Number	Age of Most Recent Prehistoric Deformation (ya)	Slip-rate (mm/yr)	Fault Length (km)	Fault Type	Distance from site (miles)[1]
Rock Creek fault	729	<15,000	0.2-1	40.5	N	
Round Valley faults	2400	<750,000	<0.2	12.8	N	
Ryckman Creek fault	740	<1,600,000	<0.2	5.3		
Sage Valley fault	2444	<1,600,000	<0.2	10.5		
Saint John Station fault zone	2397	<130,000	<0.2	5.2		
Saleratus Creek fault	2365	<750,000	<0.2	37.6		
San Felipe fault, Algodones section	2030b	<1,600,000	<0.2	15.9		
San Felipe fault, Santa Ana section	2030a	<1,600,000	<0.2	43.8		
San Francisco fault	2031	<1,600,000	<0.2	25.7		
San Francisco Mountains (west side) fault	2486	<750,000	<0.2	41.4		
Sand Hill fault zone	2039	<1,600,000	<0.2	35.6		
Sawatch fault, northern section	2308a	<130,000	<0.2	34.0		
Sawatch fault, southern section	2308b	<15,000	<0.2	41.1		
Sawyer Canyon fault	2028	<130,000	<0.2	8.4		
Scipio fault zone	2441	<15,000	<0.2	12.5		
Scipio Valley faults	2440	<15,000	<0.2	7.3		
Sevier Valley fault	2502	<1,600,000	<0.2	7.4		
Sevier Valley faults and folds (Class B)	2537	<130,000	<0.2	23.6		
Sevier Valley faults north of Panguitch	2536	<130,000	<0.2	6.2		
Sevier/Toroweap fault zone, central Toroweap section	997c	<15,000	<0.2	60.4	N	
Sevier/Toroweap fault zone, southern Toroweap section	997d	<750,000	<0.2	18.8		
Shadow Mountain grabens	989	<750,000	<0.2	10.4		
Sheeprock fault zone	2405	<130,000	<0.2	11.7		
Sheeprock Mountains fault	2419	<1,600,000	<0.2	6.7		
Silver Island Mountains (southeast side) fault	2382	<15,000	<0.2	1.8		
Silver Island Mountains (west side) fault	2381	<1,600,000	<0.2	6.4		
Simpson Mountains faults	2418	<750,000	<0.2	10.8		
Sinagua faults	986	<130,000	<0.2	4.9		
Sinbad Valley graben (Class B)	2385	<1,600,000	<0.2	9.9		
Skull Valley (mid-valley) faults	2387	<15,000	<0.2	54.8	N	
Snake Valley fault	1246	<15,000	<0.2	41.1		
Snake Valley faults	2428	<15,000	<0.2	45.3	N	
South Granite Mountains fault system, Seminoe Mountains section (Class B)	779e	Class B	<0.2	35.0		
Southern Oquirrh Mountains fault zone	2399	<130,000	<0.2	24.1		
Southern Sangre de Cristo fault zone, San Pedro section	2017a	<130,000	<0.2	24.4		
Southern Sangre de Cristo fault, Cañon section	2017e	<15,000	<0.2	15.2		
Southern Sangre de Cristo fault, Hondo section	2017d	<15,000	<0.2	22.2		
Southern Sangre de Cristo fault, Questa section	2017c	<15,000	<0.2	17.8		
Southern Sangre de Cristo fault, Urraca section	2017b	<15,000	<0.2	21.9		
Southern Snake Range fault zone	1433	<130,000	<0.2	27.5	N	
SP fault zone	958	<130,000	<0.2	12.5		
Spring Creek fault	738	<1,600,000	<0.2	2.3		
Spry area faults	2498	<750,000	<0.2	5.1		
Stansbury fault zone	2395	<15,000	<0.2	49.8	N	
Stinking Springs fault	2413	<130,000	0.2-1	10.0		
Strawberry fault	2412	<15,000	<0.2	31.9		
Strong fault	2021	<1,600,000	<0.2	8.1		
Sublette Flat fault	733	<750,000	<0.2	36.0		
Sugarville area faults	2437	<15,000	<0.2	4.3		
Sunshine faults	1000	<130,000	<0.2	29.2	N	
Sunshine Trail graben and faults	999	<130,000	<0.2	17.0	N	

Name	Number	Age of Most Recent Prehistoric Deformation (ya)	Slip-rate (mm/yr)	Fault Length (km)	Fault Type	Distance from site (miles)[1]
Sunshine Valley faults	2016	<130,000	<0.2	14.1		
Swasey Mountain (east side) faults	2431	<750,000	<0.2	3.8		
Tabernacle faults	2465	<15,000	<0.2	7.9		
The Pinnacle fault	739	<1,600,000	<0.2	2.3		
Tijeras-Cañoncito fault system, Galisteo section	2033a	<1,600,000	<0.2	37.1		
Topliff Hill fault zone	2407	<130,000	<0.2	19.9		
Towanta Flat graben (Class B)	2401	<750,000	<0.2	5.2		
Tushar Mountains (east side) fault	2501	<1,600,000	<0.2	18.5		
Uinkaret Volcanic field faults	1012	<1,600,000	<0.2	18.5		
Unnamed fault along Grand Hogback monocline (Class B)	2292	Class B	<0.2	2.4		
Unnamed fault at Big Dominquez Creek	2260	<1,600,000	<0.2	3.9		
Unnamed fault at Little Dominquez Creek	2261	<1,600,000	<0.2	14.2		
Unnamed fault at northwest end of Paradox Valley (Class B)	2287	Class B	<0.2	5.1		
Unnamed fault east of Whitewater	2257	<1,600,000	<0.2	1.9		
Unnamed fault near Bridgeport	2259	<1,600,000	<0.2	11.0		
Unnamed fault near Escalante	2262	<1,600,000	<0.2	1.6		
Unnamed fault near Johnson Spring	2282	<1,600,000	<0.2	7.1		
Unnamed fault near Wolf Hill	2266	<1,600,000	<0.2	15.2		
Unnamed fault north of Horsefly Creek	2280	<1,600,000	<0.2	8.1		
Unnamed fault of Missouri Peak	2312	<130,000	<0.2	5.9		
Unnamed fault south of Shavano Peak	2311	<1,600,000	<0.2	5.8		
Unnamed fault southeast of China Mountain	1598	<1,600,000	<0.2	2.9		
Unnamed fault west of Buena Vista	2310	<1,600,000	<0.2	2.7		
Unnamed fault west of White Rock Mountains	1437	<1,600,000	<0.2	27.7		
Unnamed fault zone in Ferber Hills	1721	<1,600,000	<0.2	37.3		
Unnamed faults along the Grand Hogback monocline near Fourmile Creek (Class B)	2294	Class B	<0.2	2.5		
Unnamed faults along the Grand Hogback monocline near Freeman Creek (Class B)	2295	Class B	<0.2	5.7		
Unnamed faults at Clay Creek	2283	<1,600,000	<0.2	9.2		
Unnamed faults east of Atkinson Masa	2269	<1,600,000	<0.2	41.1	N	
Unnamed faults east of Roubideau Creek (Class B)	2272	Class B	<0.2	11.7		
Unnamed faults in Williams Fork Valley	2300	<750,000	<0.2	18.4		
Unnamed faults near Burns (Class B)	2296	Class B	<0.2	13.3		
Unnamed faults near Cottonwood Creek	2278	<1,600,000	<0.2	10.8		
Unnamed faults near Loma Barbon	2045	<1,600,000	<0.2	1.2		
Unnamed faults near Picuda Peak	2041	<1,600,000	<0.2	10.6		
Unnamed faults near Twin Lakes Reservoir	2307	<1,600,000	<0.2	14.0		
Unnamed faults northwest of Leadville	2306	<1,600,000	<0.2	18.8		
Unnamed faults of Jemez Mountains, caldera margin section (Class B)	2143c	<750,000	<0.2	20.3		
Unnamed faults of Jemez Mountains, Intracaldera section (Class B)	2143d	<1,600,000	<0.2	11.3	N	
Unnamed faults of Jemez Mountains, Toledo caldera section (Class B)	2143b	<1,600,000	<0.2	10.9		
Unnamed faults of Jemez Mountains, Valles caldera section (Class B)	2143a	<1,600,000	<0.2	16.7		
Unnamed faults of Red Hill (Class B)	2298	Class B	<0.2	6.1		
Unnamed faults on southeast side of Kern Mountains	1256	<1,600,000	<0.2	11.4	N	
Unnamed faults south of Leadville	2305	<1,600,000	<0.2	12.8		
Unnamed faults southeast of Montrose (Class B)	2273	Class B	<0.2	9.2		
Unnamed syncline northeast of Carbondale (Class B)	2333	Class B	<0.2	1.5		

Name	Number	Age of Most Recent Prehistoric Deformation (ya)	Slip-rate (mm/yr)	Fault Length (km)	Fault Type	Distance from site (miles)[1]
Unnamed syncline northwest of Carbondale (Class B)	2334	Class B	<0.2	1.9		
Unnamed syncline southwest of Carbondale (Class B)	2332	Class B	<0.2	3.0		
Unnamed syncline west of Carbondale (Class B)	2335	Class B	<0.2	0.6		
Utah Lake faults	2409	<15,000	<0.2	30.8		
Vernon Hills fault zone	2406	<130,000	<0.2	3.7		
Villa Grove fault zone	2319	<15,000	<0.2	19.0		
Volcano Mountain faults	2520	<750,000	<0.2	2.9		
Wah Wah Mountains (south end near Lund) fault	2485	<130,000	<0.2	40.2		
Wah Wah Mountains faults	2483	<1,600,000	<0.2	53.6		
Wah Wah Valley (west side) faults (Class B)	2484	Class B	<0.2	2.1		
Wasatch fault zone, Brigham City section	2351d	<15,000	0.2-1	37.3		
Wasatch fault zone, City section	2351a	<130,000	<0.2	39.6		
Wasatch fault zone, Clarkston Mountain section	2351b	<130,000	<0.2	10.4		
Wasatch fault zone, Collinston section	2351c	<15,000	<0.2	29.7		
Wasatch fault zone, Fayette section	2351j	<15,000	<0.2	15.6		
Wasatch fault zone, Levan section	2351i	<15,000	<0.2	30.1		
Wasatch fault zone, Salt Lake City section	2351f	<15,000	1-5	42.5		
Wasatch fault zone, Weber section	2351e	<15,000	1-5	56.2		
Washington fault zone, Mokaac section	1004b	<130,000	<0.2	11.2	N	
Washington fault zone, northern section	1004a	<15,000	<0.2	36.2	N	
Washington fault zone, Sullivan Draw section	1004c	<130,000	<0.2	34.5	N	
West Cache fault zone, Clarkston fault	2521a	<15,000	0.2-1	13.0		
West Cache fault zone, Junction Hills fault	2521b	<15,000	<0.2	24.3		
West Cache fault zone, Wellsville fault	2521c	<15,000	<0.2	19.9		
West Pocatello Valley faults	3506	<1,600,000	<0.2	7.7		
West Valley fault zone, Granger fault	2386b	<15,000	0.2-1	16.0	N	
West Valley fault zone, Taylorsville fault	2386a	<15,000	<0.2	15.1	N	
Western Bear Lake fault	622	<15,000	<0.2	58.2		
Western Bear Valley faults	735	<1,600,000	<0.2	12.4		
Western Boundary fault	2313	<1,600,000	<0.2	20.1		
West-Side Chase Gulch fault	2316	<130,000	<0.2	2.7		
Wheeler fault zone and graben	1006	<750,000	<0.2	45.3		
White Sage Flat faults	2467	<130,000	<0.2	11.8		
Whitney Canyon fault	741	<15,000	<0.2	5.5		
Williams Fork Mountains fault	2301	<15,000	0.2-1	37.7		
Woodruff fault	3508	<1,600,000	<0.2	12.5		
Yampal graben	996	<1,600,000	<0.2	6.9		
Zia fault	2046	<750,000	<0.2	32.4		

Class B=Geologic evidence demonstrates the existence of Quaternary deformation, but either (1) the fault might not extend deeply enough to be a potential source of significant earthquakes, or (2) the currently available geologic evidence is too strong to confidently assign the feature to Class C but not strong enough to assign it to Class A.
Fault Type: N=normal, R=reverse, D=Dextral
[1]Distance from site only measured for those faults meeting the minimum length requirements as given in NRC 10 CFR part 100, Appendix A. Other faults have minimal impact on site.

Appendix B

NEIC: Earthquake Search Results

SITE AND REGIONAL SEISMICITY - RESULTS OF LITERATURE REVIEW
APPENDIX B:
NEIC: Earthquake Search Results

UNITED STATES GEOLOGICAL SURVEY

EARTHQUAKE DATA BASE

FILE CREATED: Tue Jul 26 09:46:31 2005
Circle Search Earthquakes= 598
Circle Center Point Latitude: 38.970N Longitude: 109.790W
Radius: 320.000 km
Catalog Used: PDE
Data Selection: Historical & Preliminary Data
Catalog Used: PDE
Data Selection: Preliminary Data Only
Catalog Used: SRA
Data Selection: Eastern, Central and Mountain States of U.S. (SRA)
Catalog Used: USHIS
Data Selection: Significant U.S. Earthquakes (USHIS)

This file includes all earthquakes in PDE, SRA, and USHIS databases within 200 miles (320 km) of site with magnitudes greater than or equal to 3.0 and intensities greater than or equal to 4.0.
Data has been declustered to remove aftershocks and foreshocks

CATALOG SOURCE	DATE			ORIGIN	COORDINATES		DEPTH	MAGNITUDES				INFORMATION (see below for explanation of symbols)																RADIAL DIST (km)	Converted Magnitude
	YEAR	MO	DA	TIME	LAT	LONG	km	mb	Ms	Other Value	Other Scale	INT	EFF	MAP	FPS	MO	DEP	IDE	PFD	FLG	D	T	S	V	N	W	G		
	Largest magnitude earthquake possible for region 016 as determined by Algermissen et al. (1982)																											29	6.1
	at furthest distance from site such that PHA from event is 0.1 g or greater																												
SRA	1850	2	22	22	40.7	-111.8						4	.	.	.	.	.	.	.	.	.	.	.	.	.	.	.	257	3.7
SRA	1853	12	1	1845	40	-111.8						5	.	.	.	.	.	.	.	.	.	.	.	.	.	.	.	207	4.3
SRA	1859	8	28		37.7	-112.8						4	.	.	.	.	.	.	.	.	.	.	.	.	.	.	.	298	3.7
SRA	1871	10			40.5	-108.5						6	.	.	.	.	.	.	.	.	.	.	.	.	.	.	.	202	5.0
SRA	1873	7	31	315	38.3	-112.6						5	.	.	.	.	.	.	.	.	.	.	.	.	.	.	.	255	4.3
SRA	1873	12	27	3	41	-111.9						4	.	.	.	.	.	.	.	.	.	.	.	.	.	.	.	288	3.7
SRA	1874	6	18	6	40.7	-111.8						4	.	.	.	.	.	.	.	.	.	.	.	.	.	.	.	257	3.7
SRA	1876	3	22		39.5	-111.6						6	.	.	.	.	.	.	.	.	.	.	.	.	.	.	.	166	5.0
SRA	1877	1	1		38.8	-112.1						4	.	.	.	.	.	.	.	.	.	.	.	.	.	.	.	201	3.7
SRA	1878	8	14		38.6	-112.6						5	.	.	.	.	.	.	.	.	.	.	.	.	.	.	.	247	4.3
SRA	1880	9	17	627	40.7	-111.8						5	.	.	.	.	.	.	.	.	.	.	.	.	.	.	.	257	4.3
SRA	1882	2	11	830	37.3	-107						4	.	.	.	.	.	.	.	.	.	.	.	.	.	.	.	306	3.7
SRA	1883	9	28	11	39.9	-112.1						4	.	.	.	.	.	.	.	.	.	.	.	.	.	.	.	223	3.7
SRA	1885	10	26	610	38.3	-113						4	.	.	.	.	.	.	.	.	.	.	.	.	.	.	.	289	3.7
SRA	1885	12	17	1	38.2	-112.3						4	.	.	.	.	.	.	.	.	.	.	.	.	.	.	.	234	3.7
SRA	1887	12	5	1530	37.1	-112.5						6	.	.	.	.	.	.	.	.	.	.	.	.	.	.	.	315	5.0
SRA	1889	1	15	22	39.5	-107.3						5	.	.	.	.	.	.	.	.	.	.	.	.	.	.	.	222	4.3
SRA	1889	12	7	11	39.3	-111.6						4	.	.	.	.	.	.	.	.	.	.	.	.	.	.	.	160	3.7
SRA	1891	12		21	40.5	-108						6	.	.	.	.	.	.	.	.	.	.	.	.	.	.	.	228	5.0
SRA	1894	1	1	10	37.9	-107.8						4	.	.	.	.	.	.	.	.	.	.	.	.	.	.	.	210	3.7
SRA	1894	2	5	330	38.8	-112.4						4	.	.	.	.	.	.	.	.	.	.	.	.	.	.	.	227	3.7
SRA	1894	7	18	2250	41.2	-112						6	.	.	.	.	.	.	.	.	.	.	.	.	.	.	.	311	5.0
SRA	1895	3	22	20	40.5	-107.1						4	.	.	.	.	.	.	.	.	.	.	.	.	.	.	.	286	3.7
SRA	1895	7	27	2225	39.5	-111.5						4	.	.	.	.	.	.	.	.	.	.	.	.	.	.	.	158	3.7
SRA	1896	9	12	130	39.7	-111.8						4	.	.	.	.	.	.	.	.	.	.	.	.	.	.	.	191	3.7
SRA	1897	8	3	7	38.2	-107.8						5	.	.	.	.	.	.	.	.	.	.	.	.	.	.	.	193	4.3
SRA	1899	11	10	9	38.3	-112.6						4	.	.	.	.	.	.	.	.	.	.	.	.	.	.	.	255	3.7
SRA	1899	12	13	1350	40.7	-111.8						4	.	.	.	.	.	.	.	.	.	.	.	.	.	.	.	257	3.7
SRA	1899			230	40.5	-108						4	.	.	.	.	.	.	.	.	.	.	.	.	.	.	.	228	3.7
SRA	1900	5	0	0	36.9	-106.9						5	.	.	.	.	.	.	.	.	.	.	.	.	.	.	.		4.3
SRA	1900	8	1	745	40	-112.1						7	.	.	.	.	.	.	.	.	.	.	.	.	.	.	.	229	5.7
SRA	1901	8	11	18	40.2	-111.7						4	.	.	.	.	.	.	.	.	.	.	.	.	.	.	.	213	3.7
SRA	1901	11	14	432	38.7	-112.1						9	.	.	.	.	.	.	.	.	.	.	.	.	.	.	.	202	7.0
SRA	1901	11	15	10	38.8	-106.2						5	.	.	.	.	.	.	.	.	.	.	.	.	.	.	.	311	4.3
SRA	1902	7	31	7	38.3	-112.6						4	.	.	.	.	.	.	.	.	.	.	.	.	.	.	.	255	3.7

CATALOG SOURCE	DATE			ORIGIN	COORDINATES		DEPTH	MAGNITUDES				INFORMATION (see below for explanation of symbols)																RADIAL DIST (km)	Converted Magnitude
										Other																			
	YEAR	MO	DA	TIME	LAT	LONG	km	mb	Ms	Value	Scale	INT	EFF	MAP	FPS	MO	DEP	IDE	PFD	FLG	D	T	S	V	N	W	G		
SRA	1903	7	23	834	41.1	-111.9						4																297	3.7
SRA	1906	4			40.5	-108.3						4																212	3.7
SRA	1906	5	24	2110	41.2	-112						5																311	4.3
SRA	1908	4	15		38.4	-113						5																286	4.3
SRA	1910	1	10	13	38.7	-112.1						6																202	5.0
SRA	1910	5	22	1428	40.7	-111.8						7																257	5.7
SRA	1910	7	26	130	41.5	-109.3						5																283	4.3
SRA	1913	10	20	10	37.8	-112.4						4																262	3.7
SRA	1913	11	11	2155	38.1	-107.7						6																206	5.0
SRA	1914	4	8	1606	41	-111.9						5																288	4.3
SRA	1914	5	13	1715	41.2	-112						7																311	5.7
SRA	1915	7	15	22	40.4	-111.6						6																221	5.0
SRA	1915	8	11	1020	40.5	-112.7						6																301	5.0
SRA	1916	2	5	625	40	-111.8						5																207	4.3
SRA	1919	5	7	2330	39.5	-111.6						4																166	3.7
SRA	1920	12	29	250	39.5	-107.5						5																206	4.3
SRA	1921	2	4	826	38.6	-106.3						4																305	3.7
SRA	1921	9	29	1412	38.7	-112.1				5.2	UK	8																202	5.2
SRA	1923	5	14	1210	38.2	-113.2						5																309	4.3
SRA	1926	12	19	330	40	-112						4																221	3.7
SRA	1928	4	30	1550	37.8	-107						5																276	4.3
SRA	1930	7	28	935	41.5	-109.3						4																283	3.7
SRA	1932	11	11	10	40.5	-111.5						4																224	3.7
SRA	1933	1	20	1305	37.8	-112.8						6																293	5.0
SRA	1934	4	7	216	41.5	-111.5				5.5	ML	3																316	5.5
SRA	1935	7	9	1059	40.7	-111.8						4																257	3.7
SRA	1935	10	6	3	37.9	-111.4						4																183	3.7
SRA	1937	2	18	630	37.8	-112.6						5																277	4.3
SRA	1938	6	30	1337	40.7	-111.8						5																257	4.3
SRA	1940	11	23	13	39.3	-111.6						4																160	3.7
SRA	1941	8	29	1134	37.3	-107.7						5																260	4.3
SRA	1942	3	28	141030	38.5	-112.5						4																241	3.7
SRA	1942	6	4	2304	39.6	-111.6						4																171	3.7
SRA	1942	7	23	1940	40.5	-108.5						5																202	4.3
SRA	1943	1	16	115018	37.7	-113						5																313	4.3
SRA	1943	2	22	1420	40.7	-112						6																269	5.0
SRA	1943	3	12	1345	39.4	-111.6						4																163	3.7
SRA	1943	8	14	540	38.2	-111.4						4																164	3.7
SRA	1943	11	3	1030	38.6	-112.3						5																221	4.3
SRA	1944	9	9	41220	39	-107.5						6																198	5.0
SRA	1944	10	5	1405	39.2	-106.8						4																259	3.7
SRA	1945	3	28	1040	39.7	-111.8						4																191	3.7
SRA	1945	4	29	1708	37.7	-107.7						4																230	3.7
SRA	1945	11	18	10741	38.8	-112						6																192	5.0
SRA	1946	1	31	2245	39.6	-107.3						4																225	3.7
SRA	1946	10	25	1653	40.7	-112.1						4																275	3.7
SRA	1947	3	28	1102	40.7	-111.9						5																263	4.3
SRA	1948	11	4	1318	39.3	-111.6						4																160	3.7
SRA	1949	3	7	650	40.7	-111.8						6																257	5.0
SRA	1950	1	18	15551	40.5	-110.5				5.3	UK	5																180	5.3
SRA	1950	5	5	735	38.2	-112.2						4																226	3.7
SRA	1950	5	8	2235	40	-111.7						5																200	4.3
SRA	1951	1	23	1333	39.7	-111.8						4																191	3.7
SRA	1951	8	12	26	40.2	-111.7						5																213	4.3
SRA	1952	7	22	1	40	-111.8						4																207	3.7
SRA	1952	9	28	20	40.4	-111.9						5																240	4.3
SRA	1953	4	18	515	38.6	-112.1						4																204	3.7
SRA	1953	5	24	25429	40.5	-111.5						5																224	4.3
SRA	1953	7	30	545	39	-110.2						5																35	4.3
SRA	1953	8	16	16	40.8	-112						4																277	3.7
SRA	1953	10	22	3	37.8	-112.4						5																262	4.3
SRA	1954	2	21	202051	40	-108.75						4																145	3.7

CATALOG SOURCE	DATE			ORIGIN	COORDINATES		DEPTH	MAGNITUDES				INFORMATION (see below for explanation of symbols)																	RADIAL DIST (km)	Converted Magnitude
										Other		INT	EFF	MAP	FPS	MO	DEP	IDE	PFD	FLG	D	T	S	V	N	W	G		
	YEAR	MO	DA	TIME	LAT	LONG	km	mb	Ms	Value	Scale																			
SRA	1954	3	31	14	39	-110.2						4																	35	3.7
SRA	1955	2	2	1923	40.8	-111.9						5																	271	4.3
SRA	1955	2	10	1730	40.4	-106.9						5																	294	4.3
SRA	1955	3	27	1213	38.3	-111.3						4																	150	3.7
SRA	1955	5	12	2257	40.9	-111.9						5																	279	4.3
SRA	1955	8	3	63942	38	-107.3						6																	242	5.0
SRA	1956	2	12	3	40.5	-109.5						4																	171	3.7
SRA	1956	10	3	202140	41.5	-110						4																	281	3.7
SRA	1957	7	18	152420	40	-110.5						4																	129	3.7
SRA	1958	2	13	2252	40.5	-111.5						6																	224	5.0
SRA	1958	11	28	133039	39.7	-111.8						5																	191	4.3
SRA	1958	12	11	930	39.5	-111						4																	119	3.7
SRA	1959	2	27	221952	38	-112.5						6																	259	5.0
SRA	1959	9	17	620	38.4	-112.2						4																	218	3.7
SRA	1960	10	11	80530.5	38.3	-107.6	49			5.5	mb	6																	204	5.5
SRA	1960	10	17	16	39.2	-106.9						5																	251	4.3
SRA	1961	4	16	50239.3	39.33	-111.65						6																	165	5.0
SRA	1961	5	6	161220.7	39.6	-110.2	25					5																	78	4.3
SRA	1961	11	27	5545.7	39	-106.1	33					4																	319	3.7
SRA	1962	1	13	1333	38.4	-107.8				4.4	ML	4																	184	4.4
SRA	1962	2	5	144551.1	38.2	-107.6	25			4.7	ML	5																	208	4.7
SRA	1962	6	5	222945	38	-112.1	33			4.5	ML																		228	4.5
SRA	1962	8	19	173241.4	38.05	-112.09	7			3.2	ML																		224	3.2
SRA	1962	9	5	160427.8	40.72	-112.09	7	5.1		5.2	ML	6																	276	5.2
SRA	1962	9	7	165023.8	39.2	-110.89	7			3.1	ML																		98	3.1
SRA	1962	12	11	102813.5	39.36	-110.42	7			3.4	ML																		69	3.4
SRA	1963	4	15	221824.6	39.59	-110.35	7	4.2		3.4	ML														N					3.4
SRA	1963	4	24	133303.3	39.44	-110.33	7	4.6		3.3	ML														N					3.3
SRA	1963	6	19	83844.9	38.02	-112.53	7	4.2		3.7	ML																		261	3.7
SRA	1963	7	7	192039.6	39.53	-111.91	7	4.9		4.4	ML	6																	193	4.4
SRA	1963	7	9	202525.8	40.03	-111.19	7	4.1		4	ML		F																168	4.0
SRA	1963	9	30	91739.3	38.1	-111.22	7	4.5		4.3	ML																		157	4.3
SRA	1963	11	13	61730.1	38.3	-112.66	7	3.8		3.2	ML																		260	3.2
SRA	1963	12	24	145108.8	39.56	-110.32	7	4.1		3	ML														N					3
SRA	1964	1	17	1503.5	38.19	-112.62	7			3.3	ML																		261	3.3
SRA	1964	8	5	151756.2	38.95	-110.92	7			3	ML																		97	3.0
SRA	1964	8	24	15100.6	38.77	-112.23	7			3.1	ML																		212	3.1
SRA	1964	9	6	190333.8	39.18	-111.46	7			3.1	ML																		146	3.1
SRA	1965	1	14	123010.8	39.44	-110.35	7	4.5		3.3	ML														N					3.3
SRA	1965	5	30	173104.1	39.4	-106.3	33	4.3																					305	4.3
SRA	1965	6	27	192408.7	39.51	-110.38	7	4		3.1	ML	3																		
SRA	1965	6	29	74628.7	39.5	-110.39	7	4.3		3.2	ML																			
SRA	1965	7	13	180315.4	37.71	-112.98	7			3	ML																		311	3.0
SRA	1965	7	18	35551.4	39.5	-109.9	33	3.1																					59	3.1
SRA	1965	7	20	144924.9	38.03	-112.44	7			3	ML																		253	3.0
SRA	1965	9	10	214744.6	39.43	-111.47	7			3	ML																		153	3.0
USHIS	1966	1	23	15638	36.98	-107.02	3	5.1		4.99	Mw	7	F																	5.0
SRA	1966	4	23	202053.3	39.1	-111.55	7	4.4		3.5	ML																		153	3.5
SRA	1966	5	20	134047.9	37.98	-111.85	7	4.3		4.1	ML																		210	4.1
SRA	1966	7	6	54708.4	40.09	-108.95	7	4.1		3.7	ML																			3.7
SRA	1966	7	30	32531	39.44	-110.36	7	4.1		3.1	ML																			
SRA	1966	9	4	95234.5	38.3	-107.6	33	4.2																					204	4.2
SRA	1966	10	21	71348.9	38.2	-113.16	7			4.2	ML																		305	4.2
SRA	1966	11	1	74028	40.2	-106.9	33	4		3.9	ML																		283	3.9
SRA	1966	11	11	164534.6	39.6	-110.5	15	3.2																	N					
SRA	1966	12	19	205233.3	39	-106.5	5	4.6		3.3	ML	3																	284	3.3
SRA	1967	1	12	35206.2	38.98	-107.51	33	4.4																					197	4.4
SRA	1967	1	16	92245.9	37.67	-107.86	33	4.1																					221	4.1
SRA	1967	1	18	61200.6	40.05	-107.05	33	3.8																					264	3.8
SRA	1967	2	5	100716.6	39.55	-110.1	33	3																					69	3.0
SRA	1967	2	15	32803.5	40.11	-109.05	7	4.5		4	ML	5																	141	4.0
SRA	1967	4	4	225339.5	38.32	-107.75	33	4.5		3	ML																		191	3.0

CATALOG SOURCE	DATE			ORIGIN	COORDINATES		DEPTH	MAGNITUDES				INFORMATION (see below for explanation of symbols)																	RADIAL DIST (km)	Converted Magnitude
										Other																					
	YEAR	MO	DA	TIME	LAT	LONG	km	mb	Ms	Value	Scale	INT	EFF	MAP	FPS	MO	DEP	IDE	PFD	FLG	D	T	S	V	N	W	G			
SRA	1967	7	22	215127.4	38.8	-112.22	7	4.2		3.6	ML																		211	3.6
SRA	1967	9	24	50028.6	40.71	-112.1	7	3.7		3	ML	5																	276	3.0
SRA	1967	10	4	102012.8	38.54	-112.16	7	5.2		5.2	ML	7																	211	5.2
SRA	1967	10	25	24134.6	39.47	-110.35	0	4		3.2	ML																		73	3.2
SRA	1967	10	25	55308.8	39.46	-110.34	2	4		3.1	ML																			
SRA	1967	12	7	133322.5	41.29	-111.74	7	4.3		3.7	ML	3																	306	3.7
SRA	1967	12	10	193000.1	36.68	-107.21	0	5.1																	N					5.1
SRA	1968	1	16	94252.1	39.27	-112.04	7	4		3.9	ML																		197	3.9
SRA	1968	2	20	63426.4	41.72	-110.61	7	3.7		3.2	ML																		313	3.2
SRA	1968	6	2	185923.2	39.21	-110.45	7	3.8		3.3	ML																		62	3.3
SRA	1968	6	23	201613	39.31	-107.41	33	3.8																					209	3.8
SRA	1968	9	24	21049.6	38.04	-112.08	7	4		3.6	ML																		224	3.6
SRA	1968	11	17	143338.2	39.52	-110.97	7	4.6		3.5	ML																		118	3.5
SRA	1969	4	10	83705.5	38.66	-112.07	7			3.6	ML																		200	3.6
SRA	1969	5	23	52451.6	39.02	-111.97	7	4		3.3	ML																		188	3.3
SRA	1969	9	10	210000.1	39.41	-107.95	0	5.3				5													N					5.3
SRA	1970	2	3	55935.6	37.92	-108.31	33	4																					173	4.0
SRA	1970	2	21	61348	39.49	-110.35	7	4.1		3.1	ML																		75	3.1
SRA	1970	4	14	104054.1	39.65	-110.82	7	4.2		3	ML																		116	3.0
SRA	1970	4	18	104211	37.87	-111.72	7	4.4		3.7	ML																			3.7
SRA	1970	4	21	85352.4	40.1	-108.9	4	4.3		3.9	ML	5																	146	3.9
SRA	1970	5	23	225523.2	38.06	-112.47	7	4.6		3.9	ML																		254	3.9
SRA	1970	10	25	74821.9	39.17	-111.41	7			3.1	ML																		141	3.1
SRA	1971	1	7	203952.1	39.49	-107.31	33	4.3		3.8	ML	5																	221	3.8
SRA	1971	3	18	90859.9	40.7	-106.97	10	4.4				5																	308	4.4
SRA	1971	4	22	230102.8	39.41	-111.94	7			3.1	ML	3																	191	3.1
SRA	1971	6	23	60835.9	38.61	-112.71	7	4.6		3.1	ML																		256	3.1
SRA	1971	7	10	172236.8	40.24	-109.6	7	3.8		3.7	ML																		141	3.7
SRA	1971	11	10	141023	37.8	-113.1	7	4.5		3.7	ML		F																316	3.7
SRA	1971	11	12	93044.6	38.91	-108.68	5			4	ML	3																	96	4.0
SRA	1971	12	15	125814.5	36.791	-111.824	5			3	ML																		300	3.0
SRA	1972	1	3	102038.9	38.65	-112.17	7	4.6		4.4	ML	6																	209	4.4
SRA	1972	6	2	31548.2	38.67	-112.07	7	4.6		4	ML	5																	200	4.0
SRA	1972	10	1	194229.5	40.51	-111.35	7	4.7		4.3	ML	6																	216	4.3
SRA	1972	10	16	214931.2	40.42	-111.02	7	4.1		3.4	ML	4																		3.4
SRA	1972	11	16	21745.2	37.53	-112.77	7			3.6	ML	3																	305	3.6
PDE	1973	2	9	173837	36.43	-110.425	5			3.2	ML						4		P										287	3.2
SRA	1973	2	18	93139.6	38.1	-113.18	7			3.3	ML																		310	3.3
SRA	1973	5	17	16	39.793	-108.366	0	5.4	4.1	5.7	UK						3		P						E					5.7
PDE	1973	7	16	63642.8	39.149	-111.508	10	4.2									1		P										149	4.2
PDE	1974	3	31	115847.1	40.703	-107.053	5			3.5	ML	2	F				4		P										303	3.5
PDE	1974	4	29	73551.8	37.814	-112.983	5	4.4		3.2	ML	3	F				4		P										306	3.2
PDE	1974	11	4	90228	38.341	-112.325	17	4.3		3.9	ML	3	F				4		P										231	3.9
PDE	1975	1	30	144840.3	39.27	-108.646	5	4.4		3.7	ML		F				4		P										104	3.7
PDE	1975	9	10	63942.5	38.483	-112.563	5			3.3	ML		F				4		P										247	3.3
PDE	1975	10	6	155046.9	39.072	-111.447	5	4.2		3.2	ML	2	F				4		P										143	3.2
SRA	1976	4	19	233545.5	35.39	-109.1	5			3.5	ML	5													?					3.5
SRA	1976	7	30	221900.2	40.75	-110.3	7			3.1	MD																		202	3.1
SRA	1976	8	13	103021.1	38.42	-112.18	7			3.1	MD																		216	3.1
PDE	1976	8	19	132953.3	39.272	-111.08	2			3.3	ML						4		P										116	3.3
PDE	1976	10	6	111504.1	39.081	-111.505	2			3	ML						4		P										148	3.0
SRA	1976	11	26	222629.4	39.51	-111.26	7			3.1	ML																		140	3.1
PDE	1977	2	9	4216.4	39.306	-111.154	7			3.4	ML		F				4		P										123	3.4
SRA	1977	6	3	13722	39.65	-110.51	7			3.2	MD																		97	3.2
PDE	1977	9	24	111648.4	39.309	-107.311	5	4		3	ML						4		P										217	3.0
SRA	1977	9	30	101920	40.47	-110.47	6	5		4.5	ML	6																		4.5
SRA	1977	11	29	213123.4	36.82	-110.99	7			3	MD																		260	3.0
SRA	1978	2	24	194948.8	38.33	-112.84	2			3.5	ML																		274	3.5
PDE	1978	3	9	63051.8	40.761	-112.081	9			3.3	ML	6	D				4		P										279	3.3
PDE	1978	5	29	164518	39.275	-107.322	5			3	ML						4		P										216	3.0
PDE	1978	9	23	82006.6	39.319	-111.093	2			3	ML						4		P										119	3.0
PDE	1978	12	9	145948.3	38.658	-112.527	4			3.3	ML						4		P										240	3.3

CATALOG SOURCE	DATE			ORIGIN	COORDINATES		DEPTH	MAGNITUDES				INFORMATION (see below for explanation of symbols)																	RADIAL DIST (km)	Converted Magnitude
										Other		I N T	E F F	M A P	F P S	M O	D E P	I D E	P F D	F L G	D	T	S	V	N	W	G		
	YEAR	MO	DA	TIME	LAT	LONG	km	mb	Ms	Value	Scale																			
PDE	1979	1	20	65908.4	40.818	-107.861	5			3.3	ML	.	.	.	.	.	4	.	P	.	.	.	.	.	.	.	.	.	263	3.3
PDE	1979	2	24	124338.2	41.653	-110.998	5			3.5	ML	.	.	.	.	.	4	.	P	.	.	.	.	.	.	.	.	.	314	3.5
PDE	1979	3	19	145929.7	40.177	-108.895	2			3.3	ML	4	F	.	.	.	4	.	P	.	.	.	.	.	.	.	.	.	154	3.3
PDE	1979	4	30	20710.3	37.883	-111.016	7			3.8	ML	4	F	.	.	.	4	.	P	.	.	.	.	.	.	.	.	.	161	3.8
PDE	1979	10	6	101235.2	39.286	-111.687	7			3.2	ML	.	F	.	.	.	4	.	P	.	.	.	.	.	.	.	.	.	167	3.2
SRA	1979	10	23	41719.9	37.89	-110.93	7			3.5	ML	.	F	.	.	.	.	.	.	.	.	.	.	.	.	.	.	.	155	3.5
PDE	1980	5	24	100336.3	39.937	-111.966	5	5		4.2	ML	5	F	.	.	.	4	.	P	.	.	.	.	.	.	.	.	.	215	4.2
PDE	1981	2	20	91301.4	40.334	-111.723	7	4.7		3.9	ML	5	F	.	.	.	4	.	P	.	.	.	.	.	.	.	.	.	224	3.9
PDE	1981	5	14	51104.1	39.481	-111.06	1	4.5		3.5	ML	5	F	.	.	.	4	.	P	.	.	.	.	.	.	.	.	.	123	3.5
SRA	1981	5	29	30902.2	36.83	-110.37	1			3	MD	.	.	.	.	.	.	.	.	.	.	.	.	.	.	.	.	.	242	3.0
SRA	1981	8	8	62016.9	38.05	-112.8	1			3.3	MD	.	.	.	.	.	.	.	.	.	.	.	.	.	.	.	.	.	281	3.3
PDE	1981	9	10	75509.32	37.511	-110.542	7			3.1	ML	.	.	.	.	.	4	.	P	.	.	.	.	.	.	.	.	.	174	3.1
PDE	1981	9	21	80133.93	39.578	-110.44	7			3.2	ML	3	F	.	.	.	3	.	P	.	.	.	.	.	.	.	.	.	87	3.2
SRA	1981	9	22	50359.4	39.59	-110.39	8			3	ML	.	F																	
PDE	1982	2	12	104413.7	37.405	-112.545	7			3.6	ML	.	.	.	.	.	4	.	P	.	.	.	.	.	.	.	.	.	297	3.6
PDE	1982	5	24	121327	38.706	-112.041	8	4.7		4	ML	6	D	.	.	.	4	.	P	.	.	.	.	.	.	.	.	.	197	4.0
SRA	1983	1	27	233711.8	37.778	-110.674	7			3.3	MD	.	.	.	.	.	.	.	.	.	.	.	.	.	.	.	.	.	153	3.3
SRA	1983	3	22	111235.1	39.546	-110.422	2			3.1	MD	.	F																	
PDE	1983	5	3	124338.1	38.288	-110.592	7			3	ML	.	.	.	.	.	3	.	P	.	.	.	.	.	.	.	.	.	102	3.0
PDE	1983	8	14	190830.7	38.359	-107.402	5			3.4	ML	2	F	.	.	.	4	.	P	.	.	.	.	.	.	.	.	.	218	3.4
SRA	1983	8	29	125311.5	41.083	-111.427	10			3	ML	.	F	.	.	.	.	.	.	.	.	.	.	.	.	.	.	.	272	3.0
PDE	1983	9	24	165745.8	40.789	-108.837	5			4.1	ML	3	F	.	.	.	4	.	P	.	.	.	.	.	.	.	.	.	217	4.1
PDE	1983	10	8	115754.2	40.746	-111.993	4	4.5		4.3	ML	6	D	.	.	.	3	.	P	.	.	.	.	.	.	.	.	.	272	4.3
PDE	1983	12	9	85841.34	38.583	-112.582	7	4.3		3.6	ML	3	F	.	.	.	4	.	P	.	.	.	.	.	.	.	.	.	246	3.6
SRA	1984	3	1	181300.9	41.539	-108.638	2			3.2	MD	.	.	.	.	.	.	.	.	.	.	.	.	.	.	.	.	.	301	3.2
PDE	1984	3	21	111930.3	39.331	-111.096	1			3.5	ML	.	F	.	.	.	4	.	P	.	.	.	.	.	.	.	.	.	119	3.5
PDE	1984	5	14	101417.3	39.322	-107.228	5			3.2	ML	4	F	.	.	.	4	.	P	.	.	.	.	.	.	.	.	.	224	3.2
PDE	1984	8	16	141921.8	39.383	-111.904	9			3.7	ML	4	F	.	.	.	4	.	P	.	.	.	.	.	.	.	.	.	188	3.7
SRA	1984	9	14	190426.3	41.61	-108.582	2			3.2	MD	.	.	.	.	.	.	.	.	.	.	.	.	.	.	.	.	.	310	3.2
SRA	1985	6	27	103629.5	39.558	-110.396	1			3	MD	.	.	.	.	.	.	.	.	.	.	.	.	.	.	.	.	.	83	3.0
SRA	1985	10	7	203340.1	40.407	-109.498	21			3	MD	.	.	.	.	.	.	.	.	.	.	.	.	.	.	.	.	.	161	3.0
PDE	1986	3	24	224023.5	39.236	-112.009	0	4.7		4.4	ML	5	F	.	.	.	4	.	P	.	.	.	.	.	.	.	.	.	194	4.4
PDE	1986	5	14	150257.4	37.429	-110.561	5			3.2	ML	.	.	.	.	.	4	.	P	.	.	.	.	.	.	.	.	.	183	3.2
PDE	1986	6	5	80541.8	41.267	-111.686	7			3.6	ML	.	F	.	.	.	4	.	P	.	.	.	.	.	.	.	.	.	301	3.6
PDE	1986	8	22	132633.4	37.42	-110.574	5			4	ML	5	F	.	.	.	4	.	P	.	.	.	.	.	.	.	.	.	185	4.0
PDE	1986	8	26	20602.61	38.9	-107.041	5			3.1	ML	3	F	.	.	.	4	.	P	.	.	.	.	.	.	.	.	.	238	3.1
PDE	1986	9	3	62050.98	38.912	-107.09	5			3.5	ML	5	F	.	.	.	4	.	P	.	.	.	.	.	.	.	.	.	234	3.5
PDE	1986	10	5	154733.5	38.64	-112.559	1			3.3	ML	3	F	.	.	.	4	.	P	.	.	.	.	.	.	.	.	.	243	3.3
SRA	1986	11	7	13153.7	37.43	-110.297	1			3	MD	.	.	.	.	.	.	.	.	.	.	.	.	.	.	.	.	.	176	3.0
PDE	1987	3	5	30250.49	40.442	-110.616	1	4		3.7	ML	4	F	.	.	.	4	.	P	.	.	.	.	.	.	.	.	.	178	3.7
PDE	1987	3	11	153103	39.25	-111.636	1			3	ML	.	F	.	.	.	4	.	P	.	.	.	.	.	.	.	.	.	162	3.0
PDE	1987	4	4	62434.82	37.675	-113.027	5			3	ML	5	F	.	.	.	4	.	P	.	.	.	.	.	.	.	.	.	317	3.0
PDE	1987	6	26	123627.5	38.738	-111.77	5			3.5	ML	.	.	.	.	.	4	.	P	.	.	.	.	.	.	.	.	.	173	3.5
PDE	1987	9	2	50020.55	38.559	-112.695	1			3.4	ML	.	.	.	.	.	4	.	P	.	.	.	.	.	.	.	.	.	256	3.4
PDE	1987	10	19	71709.71	39.664	-111.427	0			3.8	ML	4	F	.	.	.	3	.	P	.	.	.	.	.	.	.	.	.	160	3.8
PDE	1987	12	16	174307.6	39.291	-111.229	5			4	ML	.	.	.	.	.	4	.	P	.	.	.	.	.	.	.	.	.	129	4.0
PDE	1988	1	15	73329.2	37.515	-106.684	5			3.1	ML	.	F	.	.	.	4	.	P	.	.	.	.	.	.	.	.	.	316	3.1
PDE	1988	2	14	183240.5	40.626	-108.532	5			3.3	ML	4	F	.	.	.	4	.	P	.	.	.	.	.	.	.	.	.	213	3.3
PDE	1988	7	10	204559.4	41.225	-111.629	7			3.6	ML	.	.	.	.	.	4	.	P	.	.	.	.	.	.	.	.	.	295	3.6
PDE	1988	7	11	114656	39.192	-111.988	1			3.1	ML	4	F	.	.	.	4	.	P	.	.	.	.	.	.	.	.	.	191	3.1
PDE	1988	7	15	3809.59	36.374	-110.448	5			3.3	ML	.	.	.	.	.	4	.	P	.	.	.	.	.	.	.	.	.	293	3.3
PDE	1988	8	14	200303.9	39.128	-110.869	9	5.5		5.3	ML	6	D	U	.	.	4	.	P	.	.	.	.	.	.	.	.	S	95	5.3
PDE	1988	9	21	175825.9	39.308	-111.165	9			3.1	MD	.	.	.	.	.	4	.	P	.	.	.	.	.	.	.	.	.	124	3.1
PDE	1988	11	6	153058.8	40.722	-111.418	11			3.3	ML	5	F	.	.	.	4	.	P	.	.	.	.	.	.	.	.	.	239	3.3
PDE	1989	1	30	40622.78	38.824	-111.614	24	5	4.8	5.4	ML	6	D	U	.	M	4	.	P	.	.	.	.	.	.	.	.	.	158	5.4
PDE	1989	4	9	112419.4	40.419	-110.942	9			3.2	ML	2	F	.	.	.	4	.	P	.	.	.	.	.	.	.	.	.	188	3.2
PDE	1989	5	13	210148.8	38.473	-108.924	7			3.1	MD	.	.	.	.	.	4	.	P	.	.	.	.	.	.	.	.	.	93	3.1
PDE	1989	8	9	152833.4	38.188	-112.589	2			3.3	MD	.	F	.	.	.	4	.	P	.	.	.	.	.	.	.	.	.	258	3.3
PDE	1989	11	19	32113.61	38.055	-107.767	5			3	ML	.	F	.	.	.	4	.	P	.	.	.	.	.	.	.	.	.	203	3.0
PDE	1990	2	5	102325.2	39.504	-111.517	10			3.1	ML	3	F	.	.	.	4	.	P	.	.	.	.	.	.	.	.	.	160	3.1
PDE	1990	4	7	153754.9	40.082	-109.519	3			3.5	ML	.	.	.	.	.	4	.	P	.	.	.	.	.	.	.	.	.	125	3.5
PDE	1990	6	25	171533.5	38.952	-110.828	11			3	MD	.	.	.	.	.	4	.	P	.	.	.	.	.	.	.	.	.	89	3.0

CATALOG SOURCE	DATE			ORIGIN	COORDINATES		DEPTH	MAGNITUDES				INFORMATION (see below for explanation of symbols)																RADIAL DIST (km)	Converted Magnitude
										Other		INT	EFF	MAP	FPS	MO	DEP	IDE	PFD	FLG	D	T	S	V	N	W	G		
	YEAR	MO	DA	TIME	LAT	LONG	km	mb	Ms	Value	Scale																		
PDE	1990	9	1	181229.4	39.299	-111.135	7			3.3	MD	.	.	.	.	.	4	.	P	.	.	.	.	.	.	.	.	121	3.3
PDE	1990	9	12	213857.6	39.701	-106.206	5			3	ML	5	F	.	.	.	4	.	P	.	.	.	.	.	.	.	.	319	3.0
PDE	1990	10	23	84912.5	38.733	-111.525	1			3.2	MD	.	.	.	.	.	4	.	P	.	.	.	.	.	.	.	.	152	3.2
PDE	1991	1	26	214938	37.681	-111.429	9			3.3	ML	3	F	.	.	.	3	.	P	.	.	.	.	.	.	.	.	202	3.3
PDE	1991	2	21	112345.6	38.96	-111.901	1	3.4		3.4	ML	4	F	.	.	.	4	.	P	.	.	.	.	.	.	.	.	182	3.4
PDE	1991	3	2	84137.49	40.091	-109.483	1	3		3.3	ML	.	.	.	.	.	4	.	P	.	.	.	.	.	.	.	.	127	3.3
PDE	1991	3	22	145959.2	37.817	-112.997	3	3.2		3.1	ML	.	F	.	.	.	4	.	P	.	.	.	.	.	.	.	.	307	3.1
PDE	1991	4	20	125651.1	38.049	-112.728	2	4		3.8	ML	4	F	.	.	.	4	.	P	.	.	.	.	.	.	.	.	275	3.8
PDE	1991	5	23	73840.57	39.298	-111.149	12	3.5		3.6	ML	3	F	.	.	.	3	.	P	.	.	.	.	.	.	.	.	122	3.6
PDE	1991	6	25	210213.6	37.209	-110.358	1			3	MD	.	.	.	.	.	4	.	P	.	.	.	.	.	.	.	.	201	3.0
PDE	1991	8	21	134706.3	39.364	-111.878	3			3	ML	.	.	.	.	.	4	.	P	.	.	.	.	.	.	.	.	185	3.0
PDE	1991	11	8	131505.3	40.1	-109.286	2	3.4		3.8	ML	3	F	.	.	.	4	.	P	.	.	.	.	.	.	.	.	132	3.8
PDE	1991	12	21	202635.7	37.567	-112.322	7	3.6		3.8	ML	3	F	.	.	.	4	.	P	.	.	.	.	.	.	.	.	270	3.8
PDE	1992	3	16	144249.5	40.465	-112.043	12	4.4		4.2	ML	5	F	.	.	.	4	.	P	.	.	.	.	.	.	.	.	254	4.2
PDE	1992	5	15	213624	38.563	-107.914	5					4	F	.	.	.	4	.	P	.	.	.	.	.	.	.	.		3.7
PDE	1992	6	24	73120.21	38.783	-111.554	0	4.4		4.4	ML	.	F	.	.	.	4	.	P	.	.	.	.	.	.	.	.	154	4.4
PDE	1992	7	5	181729	35.982	-112.219	5	4					F	.	.	.	4	.	P	.	.	.	.	.	.	.	.		4.0
PDE	1992	9	10	62012.6	39.702	-110.632	0			3.4	MD	.	.	.	.	.	4	.	P	.	.	.	.	.	.	.	.	108	3.4
PDE	1992	9	24	143541	37.974	-112.533	3			3.1	MD	.	.	.	.	.	4	.	P	.	.	.	.	.	.	.	.	263	3.1
PDE	1993	1	21	90120.4	39.712	-110.622	1	3.4				.													C				3.4
PDE	1993	2	25	112714.4	39.69	-111.263	8			3.1	MD	.	.	.	.	.	4	.	P	.	.	.	.	.	.	.	.	150	3.1
PDE	1993	3	15	104849.9	39.552	-112.075	5			3.3	ML	.	.	.	.	.	4	.	P	.	.	.	.	.	.	.	.	207	3.3
PDE	1993	5	13	161326.1	40.126	-109.087	5			3	ML	.	.	.	.	.	4	.	P	.	.	.	.	.	.	.	.	141	3.0
PDE	1993	5	27	62153.98	37.084	-112.089	10	3.3		3.5	ML	3	F	.	.	.	3	.	P	.	.	.	.	.	.	.	.	290	3.5
PDE	1993	6	16	72224.2	38.06	-112.688	5			3.5	MD	.	.	.	.	.	4	.	P	.	.	.	.	.	.	.	.	272	3.5
PDE	1993	7	8	40352.25	39.227	-106.715	5			3.1	ML	.	F	.	.	.	4	.	P	.	.	.	.	.	.	.	.	267	3.1
PDE	1993	7	20	35703.06	38.767	-112.056	2			3.6	MD	5	F	.	.	.	4	.	P	.	.	.	.	.	.	.	.	197	3.6
PDE	1993	9	27	112100.9	39.333	-111.159	1			3.3	MD	.	.	.	.	.	4	.	P	.	.	.	.	.	.	.	.	124	3.3
PDE	1993	10	5	22409.85	38.135	-112.622	5			3.1	ML	.	.	.	.	.	3	.	P	.	.	.	.	.	.	.	.	263	3.1
PDE	1993	10	21	220716.3	38.979	-111.861	5			3.5	MD	4	F	.	.	.	4	.	P	.	.	.	.	.	.	.	.	179	3.5
PDE	1993	11	6	73003.44	37.876	-112.812	5			3	ML	.	.	.	.	.	4	.	P	.	.	.	.	.	.	.	.	290	3.0
PDE	1994	5	6	224246	40.078	-111.402	1			3.2	MD	.	.	.	.	.	3	.	P	.	.	.	.	.	.	.	.	185	3.2
PDE	1994	6	3	42529.08	38.449	-112.229	5			3.3	ML	.	.	.	.	.	4	.	P	.	.	.	.	.	.	.	.	219	3.3
PDE	1994	9	6	34837.63	38.078	-112.327	5	3.9		4.3	ML	4	F	.	.	.	4	.	P	.	.	.	.	.	.	.	.	242	4.3
PDE	1994	9	10	63341.76	39.468	-111.52	5			3.7	ML	4	F	.	.	.	4	.	P	.	.	.	.	.	.	.	.	159	3.7
PDE	1994	9	13	60123.01	38.151	-107.976	10	4.4		4.6	ML	6	D	.	.	.	4	.	P	.	.	.	.	.	.	.	.	182	4.6
PDE	1994	11	3	114010.1	40.04	-108.269	5			3.4	ML	.	.	.	.	.	4	.	P	.	.	.	.	.	.	.	.	176	3.4
PDE	1994	11	17	111101.2	38.216	-112.728	5			3.6	MD	.	F	.	.	.	4	.	P	.	.	.	.	.	.	.	.	269	3.6
PDE	1994	11	19	180144.6	37.786	-112.954	5			3.1	ML	4	F	.	.	.	4	.	P	.	.	.	.	.	.	.	.	305	3.1
PDE	1994	11	23	163049	39.5	-111.52	5			3.3	ML	3	F	.	.	.	4	.	P	.	.	.	.	.	.	.	.	160	3.3
PDE	1995	3	20	124616.4	40.179	-108.925	5	4.2		4.1	ML	5	F	.	.	.	4	.	P	.	.	.	.	.	.	.	.	153	4.1
PDE	1995	4	27	195558.1	38.088	-112.419	5			3.7	MD	.	.	.	.	.	4	.	P	.	.	.	.	.	.	.	.	249	3.7
PDE	1995	7	6	2223.31	39.926	-111.629	10			3.3	ML	.	.	.	.	.	4	.	P	.	.	.	.	.	.	.	.	190	3.3
PDE	1995	7	21	172146.9	38.226	-112.904	5			3.6	ML	.	.	.	.	.	4	.	P	.	.	.	.	.	.	.	.	283	3.6
PDE	1995	10	8	62502.61	40.909	-111.716	5			3.2	ML	.	F	.	.	.	4	.	P	.	.	.	.	.	.	.	.	270	3.2
PDE	1995	11	3	70941.84	37.993	-112.826	1			3.1	MD	.	.	.	.	.	4	.	P	.	.	.	.	.	.	.	.	286	3.1
PDE	1995	12	3	230542.6	38.195	-112.657	0			3.1	MD	.	.	.	.	.	4	.	P	.	.	.	.	.	.	.	.	264	3.1
PDE	1995	12	6	42528.23	40.737	-111.54	10	3.4		3.5	ML	5	F	.	.	.	4	.	P	.	.	.	.	.	.	.	.	246	3.5
PDE	1995	12	31	121107.9	38.988	-111.974	1			3.1	MD	.	.	.	.	.	4	.	P	.	.	.	.	.	.	.	.	189	3.1
PDE	1996	1	6	125558.6	39.12	-110.878	0	4.3		4.2	MD	5	F	.	.	.	4	.	P	.	.	.	.	.	.	.	.	95	4.2
PDE	1996	2	2	21114.62	39.467	-111.23	1			3.2	ML	.	.	.	.	.	4	.	P	.	.	.	.	.	.	.	.	135	3.2
PDE	1996	12	6	135314.4	39.706	-110.658	3			3.4	ML	.	.	.	.	.	3	.	P	.	.	.	.	.	.	.	.	110	3.4
PDE	1996	12	28	113502.8	37.855	-113.166	5			3.2	ML	.	.	.	.	.	3	.	P	.	.	.	.	.	.	.	.	319	3.2
PDE	1997	4	14	93048.42	39.048	-111.389	5			3.1	MD	.	.	.	.	.	3	.	P	.	.	.	.	.	.	.	.	138	3.1
PDE	1997	8	13	142401.4	38.006	-112.592	5			3.7	ML	.	.	.	.	.	3	.	P	.	.	.	.	.	.	.	.	266	3.7
PDE	1997	9	17	3900.1	40.535	-112.179	1			3	ML	.	.	.	.	.	3	.	P	.	.	.	.	.	.	.	.	268	3.0
PDE	1997	10	20	70220.73	37.834	-111.879	10			3.1	ML	.	.	.	.	.	3	.	P	.	.	.	.	.	.	.	.	221	3.1
PDE	1998	1	2	72829.08	38.206	-112.467	5			4.5	ML	.	F	.	.	.	3	.	P	.	.	.	.	.	.	.	.	248	4.5
PDE	1998	1	5	22046.04	40.202	-111.291	5			3	ML	.	.	.	.	.	3	.	P	.	.	.	.	.	.	.	.	187	3.0
PDE	1998	1	30	215315.2	37.968	-112.547	5	4		4	ML	.	F	.	.	.	3	.	P	.	.	.	.	.	.	.	.	264	4.0
PDE	1998	2	5	51956.62	39.751	-110.846	1	3.6		3.7	ML	.	F	.	.	.	3	.	P	.	.	.	.	.	.	.	.	125	3.7
PDE	1998	3	29	121242	38.25	-111.35	3	3		3.2	ML	.	F	.	.	.	3	.	P	.	.	.	.	.	.	.	.	157	3.2

CATALOG SOURCE	DATE			ORIGIN	COORDINATES		DEPTH	MAGNITUDES				INFORMATION (see below for explanation of symbols)																	RADIAL DIST (km)	Converted Magnitude
										Other		INT	EFF	MAP	FPS	MO	DEP	IDE	PFD	FLG	D	T	S	V	N	W	G		
	YEAR	MO	DA	TIME	LAT	LONG	km	mb	Ms	Value	Scale																			
PDE	1998	4	10	200716	38.419	-113	5			3.9	ML		F				3		P										285	3.9
PDE	1998	6	18	110040	37.97	-112.49	2	4		4.2	ML		F				3		P										260	4.2
PDE	1999	1	8	152415.2	38.762	-111.554	0	3.5		3.8	ML						3		P										154	3.8
PDE	1999	1	14	103651	38.42	-112.98	5			3.2	ML		F				3		P										284	3.2
PDE	1999	1	26	214928	38.71	-112.49	1			3.2	ML						3		P										236	3.2
PDE	1999	1	30	90547	37.55	-112.21	1	3.2		3	ML						3		P										263	3.0
PDE	1999	2	23	32041	37.08	-112.33	10			3.1	ML						3		P										305	3.1
PDE	1999	3	9	123909	37.82	-112.36	0	3.4		3.5	ML						3		P										258	3.5
PDE	1999	4	19	144232	38.72	-112.14	0			3.5	ML		F				3		P										205	3.5
PDE	1999	4	25	52207	37.76	-112.49	2			3.1	ML						3		P										271	3.1
PDE	1999	6	3	153534.3	38.293	-108.921	4			3.6	ML		F				3		P										106	3.6
PDE	1999	6	30	152732.6	40.65	-111.576	11	3.5		3.7	ML		F				3		P										241	3.7
PDE	1999	7	6	220545.2	38.319	-108.859	5			3.5	ML		F				3		P										108	3.5
PDE	1999	7	19	102638	40.33	-111.3	1			3.2	ML						3		P										198	3.2
PDE	1999	8	4	183312	38.59	-112.18	0			3.3	ML		F				3		P										211	3.3
PDE	1999	10	11	224315	38.76	-112.02	2			3.9	ML		F				3		P										194	3.9
PDE	1999	10	22	175115.6	38.077	-112.727	5			4.2	ML		F				3		P										274	4.2
PDE	1999	12	22	80331	38.75	-111.53	2	4.1		3.9	ML						3		P										152	3.9
PDE	2000	3	7	21604	39.75	-110.84	1	4.3		4.2	ML		F				3		P									S	125	4.2
PDE	2000	3	15	121427.5	38.367	-108.867	5			3.3	ML						3		P										104	3.3
PDE	2000	5	26	32404.59	38.074	-112.192	0	3		3.6	ML						3		P										231	3.6
PDE	2000	5	27	215818.8	38.341	-108.859	5			4.3	ML		F				3		P										106	4.3
PDE	2000	6	20	175546	40.69	-109.31	1			3	ML						3		P										195	3.0
PDE	2000	8	3	133412	39.58	-111.69	5			3.2	ML						3		P										177	3.2
PDE	2000	11	11	211753	40.28	-109.23	5			3.7	ML						3		P										153	3.7
PDE	2000	12	10	193901	40.5	-111.35	13			3	ML						3		P										216	3.0
PDE	2001	2	23	214350	38.73	-112.56	0			4.1	ML		F				3		P										241	4.1
PDE	2001	5	24	24040	40.382	-111.938	0	2.9		3.3	ML		F				3		P										241	3.3
PDE	2001	7	8	135551	40.741	-112.069	13			3.4	ML	3	F				3		P										276	3.4
PDE	2001	7	19	201534	38.731	-111.521	3	4.5		4.3	ML		F				3		P										152	4.3
PDE	2001	8	9	223854.5	39.66	-107.378	5			4	ML	4	F				3		P										221	4.0
PDE	2001	11	5	83423.02	38.851	-107.384	1			3.4	ML		F				3		P										209	3.4
PDE	2001	11	19	213625.1	38.557	-112.483	1			3.6	ML						3		P										238	3.6
PDE	2002	1	8	172606	37.34	-112.71	8			3.2	ML						3		P										313	3.2
PDE	2002	1	31	181745.5	40.287	-107.693	5			4.3	ML	3	F				3		P										231	4.3
PDE	2002	3	30	213843.9	38.853	-107.386	1			3.1	ML														C					3.1
PDE	2002	6	3	32523.98	38.907	-107.418	1			3.3	ML														C					3.3
PDE	2002	6	6	122910	38.34	-108.93	1			3.2	ML						3		P										102	3.2
PDE	2002	6	14	74546	41.39	-111.44	7			3.1	ML						3		P										303	3.1
PDE	2002	6	20	221704.8	38.908	-107.416	1			3.6	ML														C					3.6
PDE	2002	8	12	13140	38.15	-112.61	0			3.4	ML						3		P										261	3.4
PDE	2002	8	24	153719.7	38.92	-107.481	1			3.2	ML														C					3.2
PDE	2002	9	10	161811.4	38.789	-107.412	1			3.3	ML														C					3.3
PDE	2002	9	26	103210	37.41	-110.53	3			3	ML						3		P										184	3.0
PDE	2002	11	8	125522	38.84	-111.5	5			3.2	ML						3		P										148	3.2
PDE	2002	11	26	54616.37	38.904	-107.448	1			3.1	ML														C					3.1
PDE	2003	1	3	50212	41.271	-111.815	12	3.4		3.7	ML	4	F				3		P										308	3.7
PDE	2003	2	11	90042	38.697	-112.259	0			3.3	ML	3	F				3		P										216	3.3
PDE	2003	4	17	10419	39.516	-111.857	0	4.7		4.4	ML	5	F				1		P										188	4.4
PDE	2003	7	8	22033	36.95	-111.79	6			3.3	ML						3		P										284	3.3
PDE	2003	7	12	15440	41.283	-111.622	9			3.7	ML	3	F				3		P										300	3.7
PDE	2003	8	8	61105.19	38.907	-107.458	1			3.4	ML														C					3.4
PDE	2003	11	17	231852	40.35	-111.17	12			3	ML						3		P											3.0
PDE	2003	11	29	223308	38.45	-112.49	1			3.1	ML						3		P										241	3.1
PDE	2003	12	27	3924	39.644	-111.929	1			3.8	ML	3	F				3		P										199	3.8
PDE	2004	4	15	45359.34	38.87	-107.35	1			3.1	ML														C					3.1
PDE-W	2004	9	19	60943.8	38.853	-107.358	1			3.5	ML						3		P										211	3.5
PDE	2004	10	11	5841.02	38.825	-107.425	1			3.3	ML														C					3.3
PDE-W	2004	11	7	65459	38.236	-108.915	0			4.1	ML	4	F				3		P										111	4.1
PDE	2004	11	13	182830.4	38.875	-107.497	1			3.2	ML														C					3.2
PDE-W	2005	3	14	53327	39.509	-111.895	1			3	ML						3		P										191	3.0
PDE	2005	4	30	45704.76	38.918	-107.393	1			3.1	ML														C					3.1

CATALOG SOURCE	DATE			ORIGIN	COORDINATES		DEPTH	MAGNITUDES				INFORMATION (see below for explanation of symbols)																	RADIAL DIST (km)	Converted Magnitude
										Other		I NT	E FF	M AP	F PS	MO	D EP	I DE	P FD	F LG	D	T	S	V	N	W	G		
	YEAR	MO	DA	TIME	LAT	LONG	km	mb	Ms	Value	Scale																			
PDE-W	2005	5	2	172955.8	38.795	-107.393	1			3.2	ML	.													C					3.2
PDE-W	2005	5	13	142604.3	38.835	-107.372	1			3.3	ML	.													C					3.3
PDE-W	2005	5	18	192146	41.425	-111.09	1			3.3	ML	.	.	.		.	3	.	P	.	.	.	.	.	.	.	.		294	3.3
PDE-W	2005	5	30	14921.14	38.889	-107.474	1			3.3	ML	.													C					3.3
PDE-W	2005	6	8	84600.4	38.953	-107.527	1			3.5	ML	.													C					3.5
PDE-Q	2005	6	24	130133	37.511	-112.534	6			3.6	ML	3	F	.		.	3	.	P	.	.	.	.	.	.	.	.		289	3.6
PDE-Q	2005	7	20	70615	38.601	-112.691	1			3.5	ML	.	.	.		.	3	.	P	.	.	.	.	.	.	.	.		255	3.5
PDE-W	2005	7	25	115128.3	38.831	-107.415	1			3.1	ML	.													C					3.1

INFORMATION

INFORMATION (IEFM DTSVNWG on Screen Search): Dots are used in place of blanks to aid in the distinction between the columns. Read the sub-headers vertically.

Intensity (sub-header INT):
Maximum intensity on the Modified Mercalli Intensity Scale of 1931 (Wood and Neumann, 1931) or any similar 12-point intensity scale. It may also be an MMI value approximated from other intensity scales such as Ross-Forel or Japan Meteorological Agency. Possible intensity values are 1 - 9; X = 10; E = 11; T = 12.

Cultural Effects (sub-header EFF):
The most severe effect is listed (C = Casualities; D = Damage; F = Felt; H = Heard). Note that casualties includes human deaths or injuries. Domestic animal casualties are considered to be damage.

Isoseismal Map (sub-header MAP): (Expanded Format only)
Indicates the publication where an isoseismal map for this event has been published.
U = United States Earthquakes.
E = Earthquake Notes. (Now Seismological Research Letters)
P = Preliminary Determination of Epicenters.
W = Wellington (New Zealand Seismology Reports, Wellington, N.Z.).
N = Nature Magazine.
S = Bulletin of the Seismological Society of America.

Fault Plane Solution (sub-header FPS):
Coded as an "F" to indicate the availability of a fault plane solution in the publication, "Preliminary Determination of Epicenters, Monthly Listing".

Moment Tensor Solution (sub-header MO):
Coded as an "G" to indicate the availability of a moment tensor solution in the publication "Preliminary Determination of Epicenters, Monthly Listing" (Sipkin, 1982; Dziewonski, 1980; and Hanks and others, 1979).

ISC Alternate Depth Indicator (sub-header DEP):
A "D" in this column indicates that a pP depth is given, but the pP depth is not the adopted depth in the hypocenter solution.

International Data Exchange (sub-header IDE):
An "X" in this column identifies the event as a "IDE" earthquake.

Preferred Solution (sub-header PFD):
A "P" in this column designates a preferred solution. Earthquake hypocenters which are located within a seismic network, such as Pasadena or Berkeley, or seismic catalogs which have undergone critical review during their compilation will be designated as a preferred solution.

Flag (sub-header FLG): Currently not used.

PHENOMENA

Diastrophism: (sub-header D)
F = Faulting.
U = Uplift.
S = Subsidence.
3 = Uplift and Subsidence.
4 = Uplift and Faulting.
5 = Faulting and Subsidence.
6 = Faulting with Uplift and Subsidence.
7 = Uplift or Subsidence.
8 = Faulting and Uplift or Subsidence.

Tsunami: (sub-header T)
T = Tsunami generated.
Q = Questionable Tsunami.

Seiche: (sub-header S)
S = Seiche.
Q = Questionable Seiche.

Volcanism: (sub-header V)
V = Earthquake associated with volcanism.

Non-Tectonic: (sub-header N)
E = Explosion.
I = Collapse.
C = Coal bump or Rockburst in a coal mine.
R = Rockburst.
M = Meteoritic.
N = Either known to be or likely to be of non-tectonic origin.
? = Classified as an earthquake, but a non-tectonic origin cannot be ruled out.
V = Reservoir induced earthquake.

Guided Waves in Atmospheric And/Or Ocean: (sub-header W)
T = T-wave.
A = Acoustic wave.
G = Gravity wave.
B = Both A and G.
M = T-wave plus and A or G.

Miscellaneous Phenomena: (sub-header G)
L = Liquefaction.
G = Geyser.
S = Landslides and/or Avalanches.
B = Sandblows.
C = Ground cracks not known to be an expression of faulting.
V = Lights or other visual phenomena seen.
O = Olfactory (Unusual odors noted).
M = More than one of these phenomena observed.

Appendix F

U.S. Department of Energy—Grand Junction, Colorado

Calculation Cover Sheet

MW 8-23-06

Calc. No.: MOA-02-09-2005-01-09-01 Discipline: Geologic and Geophysical Properties No. of Sheets: 20

Project: Moab Project

Site: Crescent Junction Disposal Site

Feature:
Site and Regional Seismicity – Results of Maximum Credible Earthquake Estimation and Peak Horizontal Acceleration

Sources of Data:

See list of references at end of calculation set.

Sources of Formulae and References:

See list of references at end of calculation set.

MW 8-23-06

Preliminary Calc. ☐ Final Calc. ☑ Supersedes Calc. No. MOA-02-09-2005-01-09-00

Author: Tobey Wyatt 8/23/06 (Name / Date)

Checked by: [signature] 8-23-06 (Name / Date)

Approved by: For Roslyn Stern John E Elmer 8/26/06 (Name / Date)

[signature] 8-23-06 (Name / Date)

[signature] 8-24-06 (Name / Date)

[signature] 8-23-06 (Name / Date)

Problem Statement:

Determination of the suitability of the Crescent Junction Disposal Site as the repository for the Moab uranium mill tailings material, and development of the site and regional seismotectonic sections of the Remedial Action Plan (RAP) requires an estimation of the Maximum Credible Earthquake (MCE) and the attenuation of the peak horizontal acceleration (PHA) associated with this MCE to the site.

Method of Solution:

The estimation of MCE and the associated PHA are part of the seismotectonic calculation set to develop seismic design parameters for the disposal site. Following procedures outlined in the UMTRA–DOE Technical Approach Document (TAD) (DOE 1989), the calculation set includes an estimation of the floating earthquake (FE) associated with the Colorado Plateau province applied 15 kilometers (km) from the site, the MCE associated with all pertinent outlying provinces, and the MCE associated with all known or suspected Quaternary faults within the study region. For each of these identified earthquake events, the on-site PHA is assessed, and the design PHA is established.

Assumptions:

It is assumed that the literature sources are reliable and representative of the current understanding of the seismotectonic characteristics of the region.

Calculation:

MCE estimations are calculated using the formulas developed by Wells and Coppersmith (1994) as follows:

$$M_w = 5.08 + 1.16 \times \log(SRL) \quad \text{(Eq. 1)}$$

$$M_w = 4.07 + 0.98 \times \log(RA) \quad \text{(Eq. 2)}$$

where M_w is Moment Magnitude, SRL is surface rupture length (km), and RA is rupture area (km^2).

The coefficients in these equations are based on regression data developed for all slip types.

Attenuation to the site is calculated using the corrected peak ground acceleration, mean-plus-one standard deviation (84^{th} percentile) relationship developed by Campbell and Bozorgnia (2003) as follows:

$$\ln Y = c_1 + f_1(M_w) + c_4 * \ln\sqrt{f_2(M_w, r_{seis}, S)} + f_3(F) + f_4(S) + f_5(HW, F, M_w, r_{seis}) + \varepsilon \quad \text{(Eq. 3)}$$

where:

Y = peak horizontal ground acceleration,

c_1, c_4 = coefficients corresponding to corrected PHA regression analysis,

M_w =moment magnitude,

R_{seis} = closest distance from site to seismogenic rupture (km), where depth to seismogenic rupture is a minimum of 3 km (Campbell 1997),

S = local site condition factors (consistent with firm rock sites for Crescent Junction),

F = faulting mechanism factors (consistent with normal faulting for Crescent Junction),

HW = hanging-wall effect factor for faults with surface projection within 5 km of site and fault dip less than or equal to 70 degrees, and

ε = random error term equivalent to zero for mean and standard deviation equal to σ_{lny}, defined as a function of magnitude.

The Campbell and Bozorgnia (2003) relationship is an updated attenuation relationship to the Campbell (1981) relationship referenced in the TAD (DOE 1989).

Criteria and Definitions:

The following are the standards and definitions that are applied to the evaluation of the seismicity of the Crescent Junction Site as specified in the TAD (DOE 1989, p. 133).

Design life. As specified by the U.S. Environmental Protection Agency (EPA) Promulgated Standards for Remedial Actions at Inactive Uranium Processing Sites (40 CFR 192), the controls implemented at UMTRA Project Sites are to be effective for up to 1,000 years, to the extent reasonably achievable and, in any case, for at least 200 years. For the purpose of the seismic hazard evaluation, a 1,000-year design life is adopted.

Design earthquake. For UMTRA Project Sites, the magnitude(s) of the earthquake(s) that produces the largest on-site PHA and that produces the most severe effects upon the site is the design earthquake. This earthquake could be either a floating earthquake or an earthquake whose magnitude is derived from a relationship between fault length and maximum magnitude. The latter case is applied for a verified or assumed capable fault of known rupture length.

Floating earthquake. An FE is an earthquake within a specific seismotectonic province that is not associated with a known tectonic structure. Before assigning the FE magnitude, the earthquake history and tectonic character of the province are analyzed.

Capable fault. A capable fault is a fault that has exhibited one or more of the following characteristics:

- Movement at or near the ground surface at least once within the past 35,000 years, or movement of a recurring nature within the past 500,000 years.
- Macroseismicity (magnitude 3.5 or greater) determined with instruments of sufficient precision to demonstrate a direct relationship with the fault.
- A structural relationship to a capable fault such that movement on one fault could be reasonably expected to cause movement on the other.

Acceleration. Acceleration, or PHA, is the mean of the peaks of the two orthogonal horizontal components of an accelerogram record. The accelerations are determined from the corrected peak horizontal ground acceleration attenuation relationship based on distance and magnitude as developed by Campbell and Bozorgnia (2003). The mean-plus-one standard deviation (84th percentile) value is adopted. This relationship is an update to the Campbell (1981) relationship referenced in the TAD (DOE 1989).

Surface acceleration. Surface acceleration is the site acceleration adjusted for the site soil attenuation or amplification effects.

Magnitude and intensity. Magnitude is the base-10 logarithm of amplitude of the largest deflection observed on a torsion seismograph 100 km from the epicenter (Richter 1958). This local magnitude value may not be the same as the body-wave and surface-wave magnitudes derived from measurements at teleseismic distances. Unless specified otherwise, Richter magnitudes for values less than 6.5 are used in UMTRA Project seismic hazard evaluations. Intensity is the index of the effects of any earthquake on the human population and structures. The most commonly applied scale is the 1931 Modified Mercalli (MM) Intensity Scale, which will be used in this study.

Maximum earthquake. The term "Maximum Earthquake" (ME) was defined by Krinitzsy and Chang (1977) as the largest earthquake that is reasonably expected on a given structure or within a given area. No recurrence interval is specified for such an event.

Local regional study area. The regional study area is selected by calculating the distance at which the largest magnitude earthquake possible for a region, as determined by Algermissen et al. (1982), produces the minimum accepted on-site design acceleration (0.10g). All further characterization work is

then limited to this region. Using this definition, the ME for the region as determined by Algermissen et al. (1982) is magnitude 6.1. Using Campbell and Bozorgnia (2003) attenuation relations for corrected peak ground accelerations, 84th-percentile values, distances within 30 km of the site are considered within the local regional study area.

Expanded regional study area. Although UMTRA defines the study area as discussed above, the U.S. Nuclear Regulatory Commission (NRC), per *Code of Federal Regulations* Title 10, Part 100 (10 CFR 100), Appendix A, requires an investigation within 200 miles of the site. For purposes of this seismotectonic evaluation, capable faults, historical earthquakes, and floating earthquakes associated with neighboring tectonic provinces that lie within 200 miles of the site and are capable of producing a minimum on-site acceleration of 0.10 g or greater will be evaluated in the expanded regional study area.

Discussion:

Floating Earthquake

The purpose of the FE evaluation is to estimate a "background" level of seismicity within a tectonic province. The FE evaluation allows for potential low to moderate earthquakes not associated with tectonic structures to contribute to the seismic hazard of the site. Because these events are not associated with a known structure, the location of these events is assumed to occur randomly. The maximum magnitude for these background events within the Intermountain U.S. ranges between local magnitude (M_L) 6.0 and 6.5 (Woodward-Clyde 1996). Larger earthquakes would be expected to leave a detectable surface expression, especially in arid to semiarid climates, with slow erosion rates and limited vegetation. In seismically less active areas such as the Colorado Plateau, the maximum magnitude associated with an FE event is assumed to be 6.2, consistent with that used in the Green River RAP (DOE 1991a, pg. 26), Grand Junction RAP (DOE 1991b, pg. 71), and the seismic evaluation performed for the tailings site in Moab (Woodward-Clyde 1996, pg. 4–19).

Historical earthquake data for the area within a 200-mile radius of the Crescent Junction Site were obtained for the initial phase of this study. The complete data file was included in Appendix B of the *Site and Regional Seismicity – Results of Literature Research* calculation set (Calculation No. MOA-02-08-2005-07-01, Attachment 2, Appendix E [DOE 2006a]). To assess the FE magnitude and recurrence interval associated with the Colorado Plateau, a second historical earthquake search was conducted to limit events to those occurring within the boundaries of the Colorado Plateau (NEIC 2005). A rectangular search was conducted initially, with the latitudes constrained to between 34.5 and 40.75 degrees north, and the longitude between 106.5 and 112.5 degrees west. After the initial search, events with epicenters lying outside the boundaries of the Colorado Plateau (as shown in Figure 1) were deleted. For consistency, moment magnitude (M_w) was used where possible. Consistent with Campbell (1981) attenuation equations, M_w was considered approximately equal to surface wave magnitudes (M_s) for events greater than 6.0, and approximately equal to local magnitude (M_L) for events smaller than 6.0. Modified Mercalli Intensity (MMI) values were converted to Richter scale using the following equation:

$$M = 1 + \frac{2}{3} * I_o \qquad \text{(Eq. 4)}$$

where M = magnitude on the Richter scale, and I_o is the MMI in the epicentral area.

Magnitudes were used in this order of preference: M_w, M_s if >6.0, M_L if ≤ 6.0, other reported magnitudes, and MMI values converted to magnitude.

Events were filtered to include only events with magnitudes equal or greater than 3.0. Events that are thought to be non-tectonic in origin or induced by non-natural causes are not considered further in the evaluation. One cluster of such events is described by Smith and Sbar (1974) to include a swarm of events at approximately latitude 39.5 N and longitude 110.5 W located along the Book Cliffs in the coal-mining district of eastern Utah. These earthquakes, the largest having a compressional body wave magnitude (M_b) of 4.5, are thought to be indirectly triggered by subsurface coal mining in an area of high regional stress. Other clusters of events include those associated with fluid injection at the Rangely oil field along the border between northeastern Utah and northwestern Colorado, and a series of events associated with the Paradox Valley desalinization project that included deep water injections beginning in

1995 (Colorado Geological Survey 2002). In addition, the earthquake data was declustered to remove aftershocks and foreshocks. The events considered in the evaluation of the Colorado Plateau FE are shown in Appendix A.

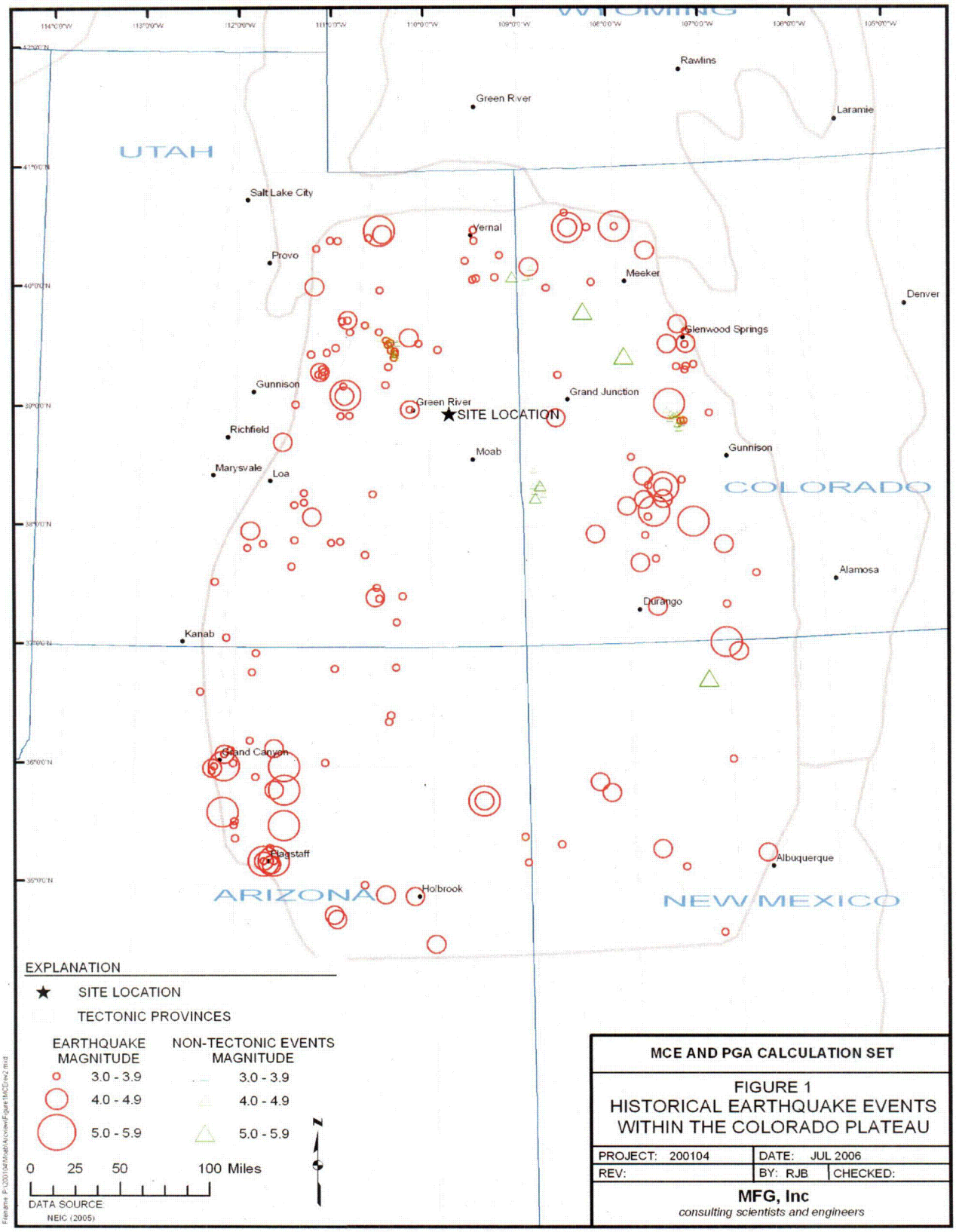

Figure 1. Historical Earthquake Events within the Colorado Plateau

C-09

As shown in Figure 1, there is more activity on the borders of the Colorado Plateau than within the interior portions. This increased activity is associated with the transitional area of crustal thinning (30 to 35 km along the perimeter area) associated with extension. The interior of the Plateau has a crustal thickness of approximately 45 km (Keller et al. 1979). For the FE evaluation, a conservative recurrence of events was evaluated for the entire Colorado Plateau; the interior and perimeter portions were not evaluated separately.

The regional study area is located in an area with a relatively quiet recorded earthquake history. The first recorded earthquake in the state of Utah was estimated to have an MMI of IV, and occurred near Salt Lake City in 1850 (Arabasz et al. 1979). The earliest recorded earthquake event in Colorado had an MMI of VI, and occurred near Pueblo in 1870 (Kirkham and Rogers 1981). Since this time, only approximately 15 events have been recorded within the Colorado Plateau with an intensity greater than VI or a magnitude greater than 5. Most of these early events were recorded in populated areas. This short recorded history can be misleading when attempting to predict future events, especially in sparsely populated areas such as the Colorado Plateau, and should be used with caution (Kirkham and Rogers 1981).

The historical completeness record was estimated by examining the data set of events and the frequency of recorded occurrence as grouped by magnitude. By examining the frequency distribution with time, the completeness record can be estimated, as shown in Figures 2, 3, and 4. For this report, it is estimated that the historical record is complete since approximately 1890 for events with a magnitude 5.0 or greater, approximately 1960 for events with a magnitude of 4.0 or greater, and approximately 1970 for events with a magnitude of 3.0 or greater. This is in general agreement with the completeness record assumed for the Cheney disposal cell in Grand Junction, Colorado (DOE 1991, p. 68).

A log-frequency versus magnitude plot was generated for the Colorado Plateau, and a straight line fit to the data. The estimated recurrence interval for the Colorado Plateau was estimated to be represented by the equation

$$M = 4.35 - 0.82 * \log(\frac{1}{y}) \qquad \text{(Eq. 5)}$$

where y is the recurrence interval.

The graphical representation is shown in Figure 5. The frequency-magnitude data can also be normalized with area to be of the form

$$M = 4.35 - 0.82 * \log\frac{A_p}{y * a}, \qquad \text{(Eq. 5)}$$

where:

Ap= area of the Colorado Plateau Province (approximately 117,000 square miles or 303,000 square km),
y = recurrence interval, and
a = area of interest.

When normalized to 1 square km, the recurrence interval is represented by

$$M = -0.14 - 0.82 * \log(\frac{1}{y}). \qquad \text{(Eq. 6)}$$

Limiting the FE event to magnitude 6.2, and assuming this event occurs at a radial distance of 15 km (9 miles) from the site, results in a PHA of 0.22 g (using Campbell and Bozorgnia 2003 corrected peak horizontal ground acceleration, 84th percentile relationship). It should be noted that the largest historical event within the Colorado Plateau had a magnitude of 5.7 (1912 Lockett Tanks, Arizona earthquake, reported MMI of 7). The use of a magnitude 6.2 for evaluation of the FE is based on extrapolation of the log-frequency plot, limited, as discussed previously, to a practical maximum event that could result in an undetected tectonic structure. Based on Equation 5, above, the recurrence interval of a magnitude-6.2 event occurring within 15 km of the site is 77,000 years. The probability of this event being exceeded within the assumed design life of 1,000 years is 1 percent.

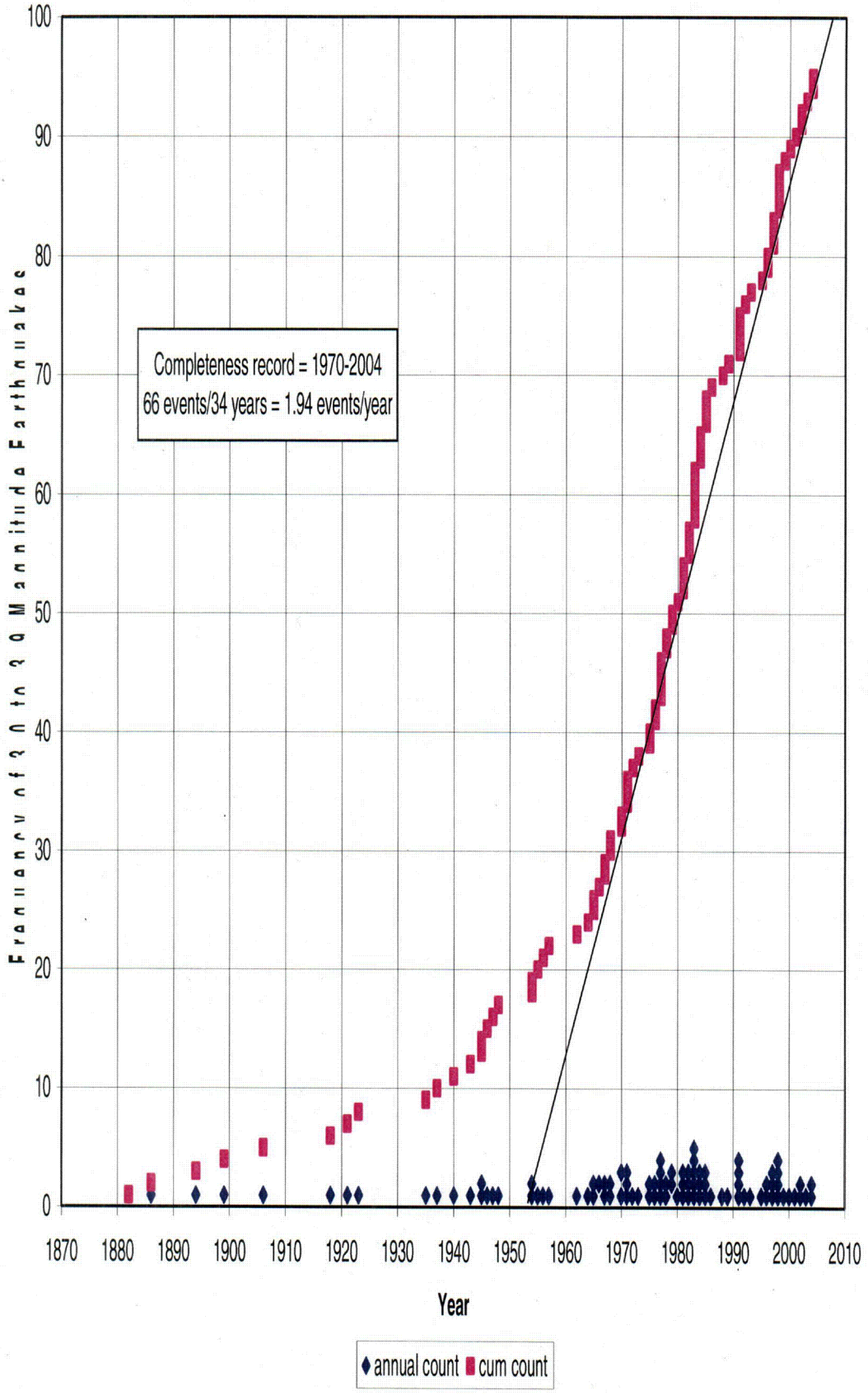

Figure 2. Magnitude 3.0 to 3.9 Earthquake Frequency—Colorado Plateau

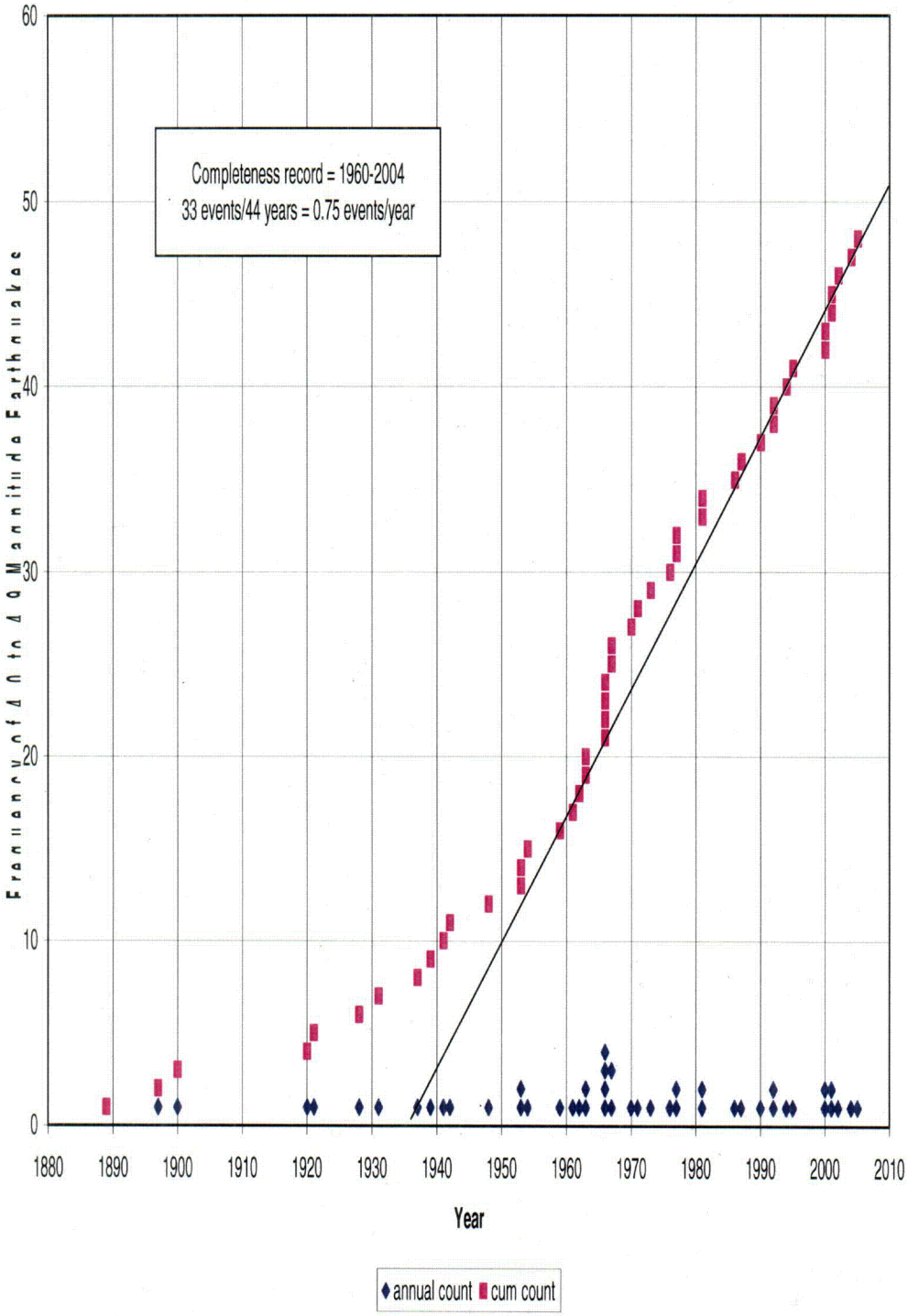

Figure 3. Magnitude 4.0 to 4.9 Earthquake Frequency—Colorado Plateau

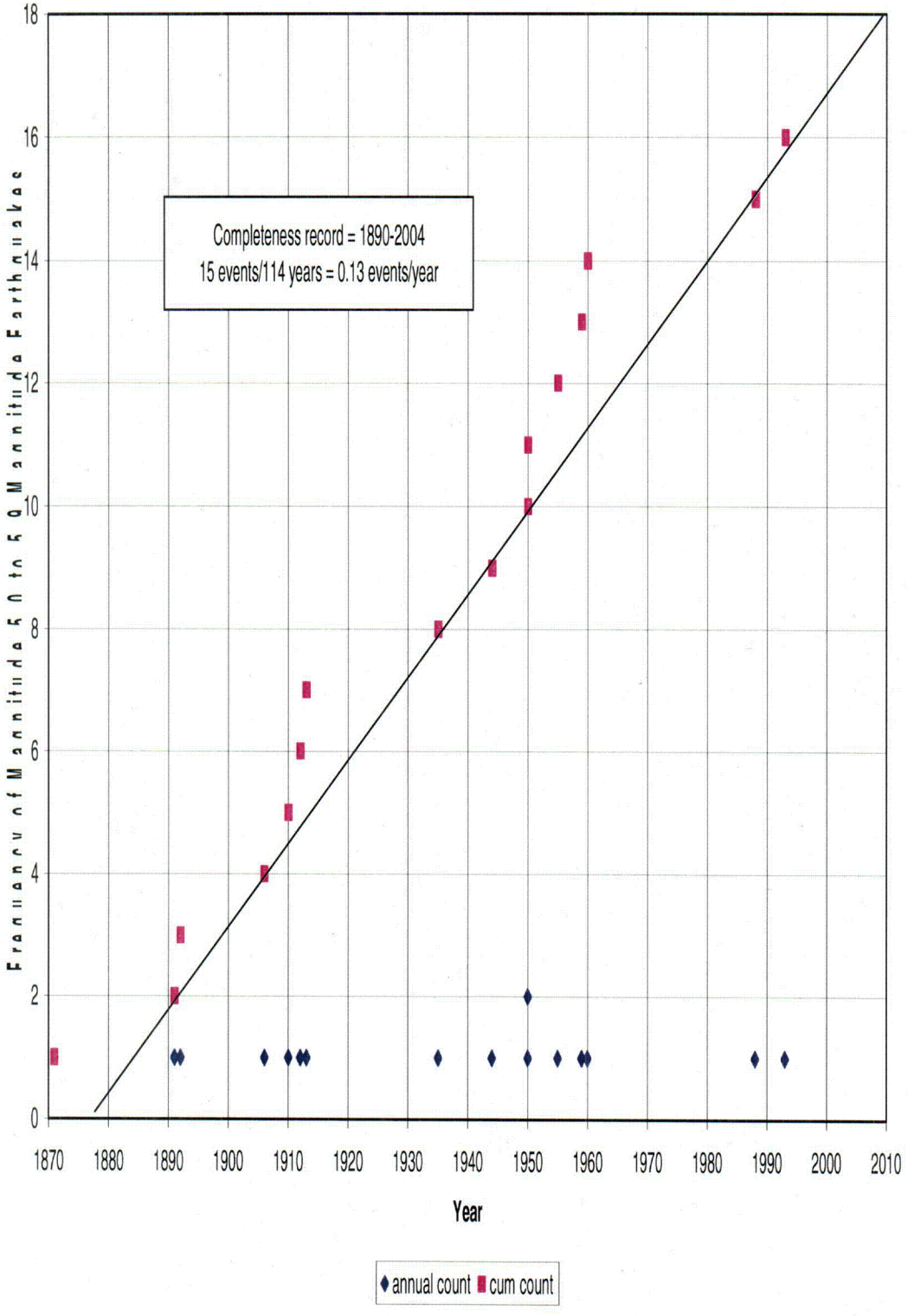

Figure 4. Magnitude 5.0 to 5.9 Earthquake Frequency—Colorado Plateau

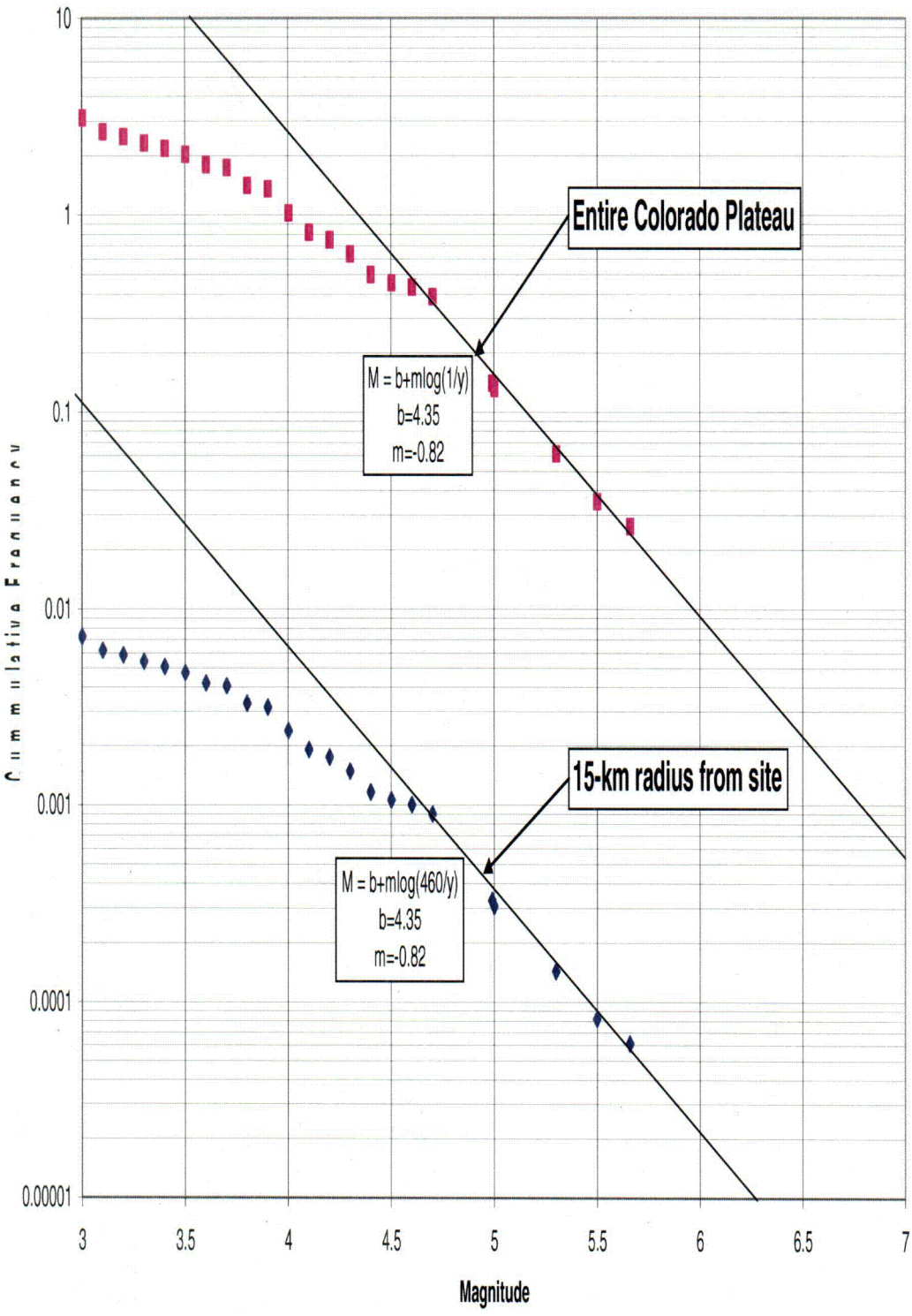

Figure 5. Magnitude Versus Earthquake Frequency—Colorado Plateau

MCE Associated with Outlying Tectonic Provinces

The MCE values for remote seismotectonic provinces, such as the Intermountain Seismic Belt, Rio Grande Rift, Wyoming Basin, and Southern Rocky Mountains, were taken from published studies (Kirkham and Rogers 1981, DOE 1991). The MCE from each event is attenuated to the site assuming that the event occurs at the point within the outlying province that is closest to the site. The PHA calculated for each event is shown in Table 1.

Table 1. PHA Associated with MCE Event in Outlying Tectonic Provinces

Tectonic Province	MCE	Closest Point to Site (miles)	PHA (g)
Rio Grande Rift	7.5	180	0.02
Intermountain Seismic Zone	7.9	65	0.08
Eastern Mountain	6.75	200	0.01
Western Mountain	6.5	140	0.02
Wyoming Basin	6.5	140	0.02

As shown in the above table, the greatest PHA associated with an outlying province is a 7.9-magnitude event occurring within the Intermountain Seismic Zone, resulting in a PHA of 0.08 g.

MCE associated with known or suspected Quaternary faults

Quaternary faults were identified using the USGS and Utah Geological Survey Quaternary Fault and Fold databases (Black et al. 2003, USGS 2002). An initial search for critical Quaternary faults was conducted using the minimum fault lengths given in NRC document 10 CFR 100, Appendix A, as shown in Table 2. The complete list of faults meeting these minimum length requirements is included in the *Site and Regional Geology–Results of Literature Research* calculation (Calculation No. MOA-02-08-2005-1-05-00, [DOE 2005]) in Appendix A of this Attachment.

Table 2. Minimum Length of Fault to Be Considered in Establishing MCE

Distance from Site		Minimum Length	
Miles	Kilometers	Miles	Kilometers
0 to 20	0 to 32	1	1.6
Greater than 20 to 50	Greater than 32 to 80	5	8
Greater than 50 to 100	Greater than 80 to 161	10	16
Greater than 100 to 150	Greater than 160 to 240	20	32
Greater than 150 to 200	Greater than 240 to 320	40	64

In addition to faults included in the Quaternary Fault and Fold database, faults of undetermined age that are shown on geologic maps in the area (Williams 1964, Gaultieri 1988, Witkind 1995, Williams and Hackman 1971), were considered if the PHA associated with these structures (if considered Quaternary) is greater than 0.1 g. The faults considered in this study are shown in Figure 6. In addition, a tabular form of the data is shown in the current calculation set as Appendix B. Figure 7 shows the considered faults overlain by historical earthquakes in the area. No historical earthquake events (above magnitude 3.0) are associated with any of the considered faults that could impact the site.

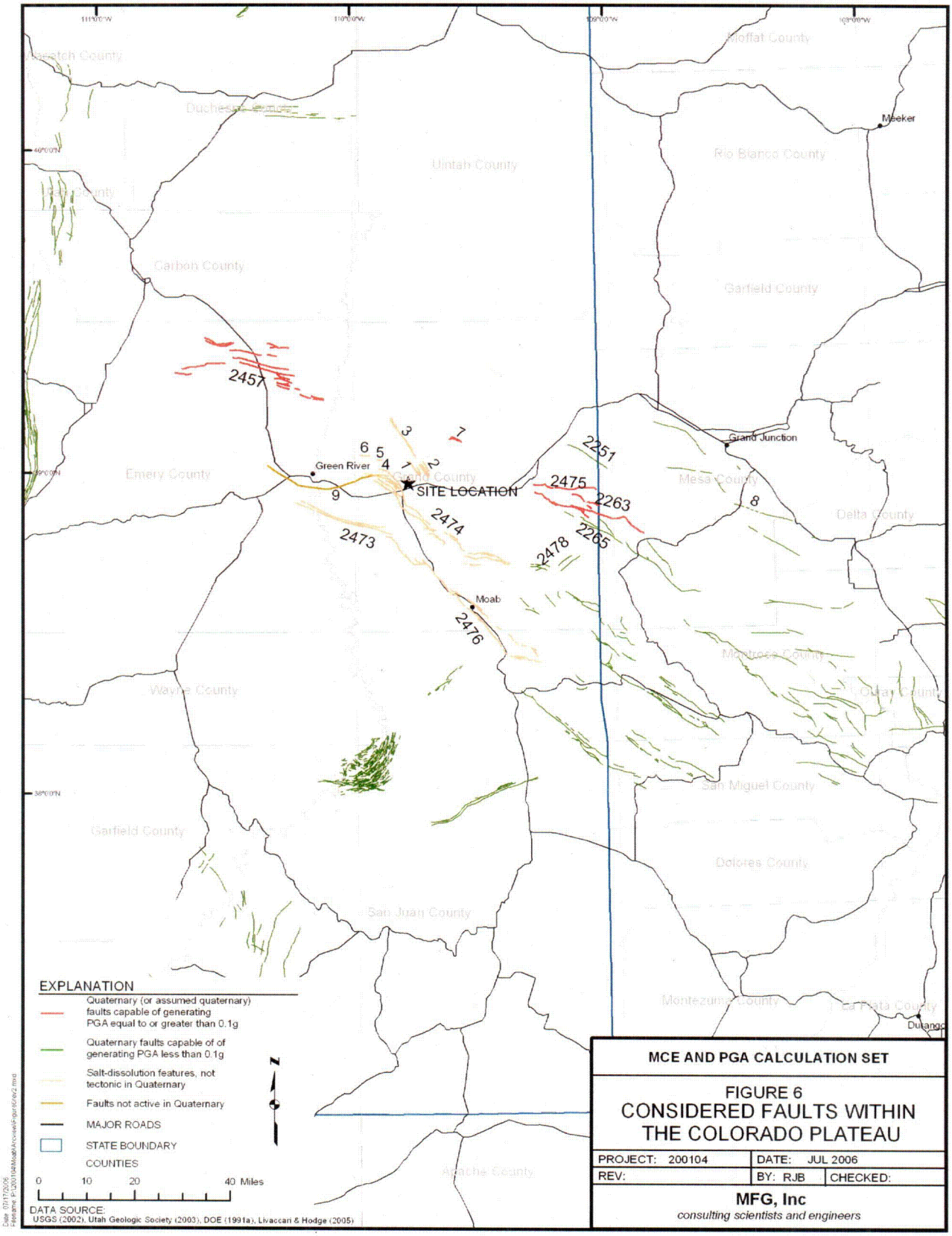

Figure 6. Considered Faults within the Colorado Plateau

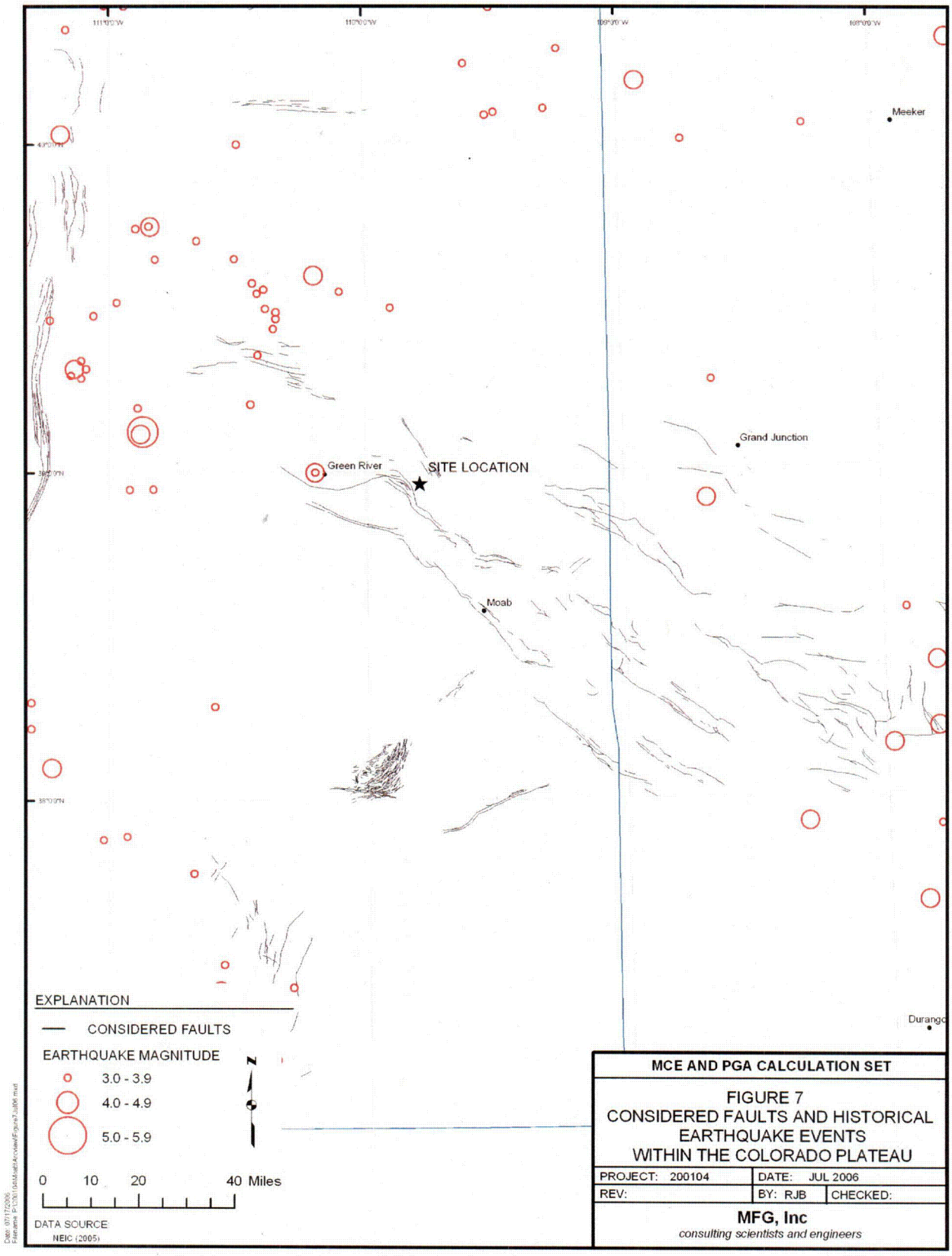

Figure 7. Considered Faults and Historical Earthquake Events within the Colorado Plateau

The MCE associated with each fault was calculated using Wells and Coppersmith (1994) relationships. PHA was calculated using Campbell and Bozorgnia (2003) attenuation equations. Using these relationships, 14 faults were initially identified as potentially capable of producing site PHA of 0.10 g or greater, and are summarized in Table 3.

As discussed in the *Site and Regional Seismicity – Results of Literature Research* calculation set (MOA-02-08-2005-07-01-00, Attachment 2, Appendix E [DOE 2006a]), the Salt and Cache Valley faults, Tenmile graben, and the Moab and Spanish Valley faults are all associated with the salt structures within the Paradox Basin. Reports by Olig et al. (1996), Woodward-Clyde (1996), and Woodward-Clyde (1984) found no evidence of Quaternary tectonic deformation of these structures. Based on detailed mapping, structural evidence, and geophysical data, Olig et al (1996) determined that the faults within the Moab and Spanish Valley areas are most likely related to salt dissolution. They concluded that the primary movement on the Moab fault is tectonic and occurred during a period of Tertiary extension. They also concluded that most, if not all, of the slip on the Moab fault is pre-Quaternary, and that the Moab fault is a shallow structure that probably soles into the Moab salt-cored anticline within 2-km depth along much of its length. Therefore, it is not likely to be capable of producing significant earthquakes.

In addition, geomorphic expression of the fault indicates very low rates of activity. The report also indicates that the earthquake potential of the other salt structures within the Paradox Basin may also be similarly low. From these discussions, the MCE associated with these structures was calculated using Wells and Coppersmith (1994) relationships based on rupture area, assuming that the rupture depth is 2 km.

Of the faults listed in Table 3, only the Salt and Cache Valley faults, Little Grand Wash fault, and faults No. 2, 3, and 4 would generate PHA values greater than those estimated by the FE (0.22 g). As discussed in the literature review, these five faults have been determined to not be capable faults. Of the faults whose capability is still undetermined or proven capable, the Price River Area faults have the potential of creating the largest PHA at the site, at 0.13 g.

Conclusion and Recommendations:

Of the faults that are suspected of being active in the Quaternary, none are expected to have an impact on the site greater than that calculated for an FE event occurring 15 km from the site. Therefore, the design PHA is estimated to be 0.22 g. Features such as the Salt and Cache Valley faults, Tenmile graben, Moab fault, Little Grand fault, and the faults associated with the Thompson Anticline have been investigated and determined to not be seismogenic.

Amplification

Amplification of horizontal accelerations due to specific site conditions must be considered. Geotechnical investigations at the site (Calculation No. MOA-02-02-2006-1-11-00, Attachment 5, Appendix B [DOE 2006b]) indicate alluvial and eolian soils overlying the withdrawal area range in depth from approximately 2 to 23 feet (ft). In the proposed area of the disposal cell, refusal (standard penetration tests [SPT] greater than 50 blows per 6 inches) was typically encountered between 5 and 15 ft below ground surface. Correlations between SPT and shear wave velocities (Sykora 1987) estimate the range of shear wave velocities at a blow count of 100 blows per ft to be between approximately 600 and 1850 ft per second (fps).

The TAD (DOE 1989) states in section 5.4.4 that for shallow soil sites with less than 30 ft of overburden above bedrock, the site surface acceleration is considered to be the same as the acceleration derived from the seismic study. In Campbell and Bozorgnia (2003) attenuation relations, the PHA equations account for local site conditions of the upper 30 meters of rock or soil. As defined in their paper, the site is categorized as a firm rock site, based on underlying geologic unit consisting of pre-Tertiary sedimentary rock (Late Cretaceous Mancos Shale). This category assignment is supported by the SPT data, which place the less-weathered Mancos Shale as a BC soil class as defined by the National Earthquake Hazard Reduction Program.

Table 3. Preliminary MCE Associated with Quaternary Faults and Faults of Unknown Age

Fault Name	Fault Number[a]	Length (km)	Depth of Rupture (km)	Rupture Area (km^2)	Distance From Site (mi)	MCE (M_w)[b]	PHA (g) Campbell and Bozorgnia (2003)	Comments
Salt and Cache Valley faults	2474	57.9	<2	115.8	1.8	6.09	0.67	Fault determined to not be active in Quaternary based on field evidence and lack of microearthquake activity (Wong et al. 1996, Woodward-Clyde 1984). Not potential design fault.
Tenmile graben faults	2473	34.6	<2	69.2	10.5	5.87	0.16	Fault likely not active in Quaternary (Woodward-Clyde 1996). Shallow structure not likely capable of large events (Olig et al. 1996). Not potential design fault.
Moab fault and Spanish Valley faults	2476	72.4	<2	114.8	12.5	6.19	0.16	Fault likely not active in Quaternary (Olig et al. 1996). Shallow structure likely not capable of large events (Olig et al. 1996). Not potential design fault.
Price River area faults	2457	50.9			24.8	7.06	0.13	Potential design fault.
Ryan Creek fault zone	2263	39.5			26.6	6.93	0.11	Potential design fault.
Sand Flat graben faults	2475	23.1			26.4	6.66	0.10	Potential design fault.
Unnamed fault in Westwater Quad, R19E, T21S	1	8.0			2.4	6.13	0.60	Associated with Thompson Anticline. Subsidence features. Not potential design fault.
Unnamed parallel faults in Westwater Quad, R20E, T21S	2	6.4			3.1	6.02	0.49	Associated with Thompson Anticline. Subsidence features. Not potential design fault.

Table 3 (continued). Preliminary MCE Associated with Quaternary Faults and Faults of Unknown Age

Fault Name	Fault Number[a]	Length (km)	Depth of Rupture (km)	Rupture Area (km^2)	Distance From Site (mi)	MCE (M_w)[b]	PHA (g) Campbell and Bozorgnia (2003)	Comments
Unnamed fault in Westwater Quad, R19E, T19S	3	15.7			5.3	6.47	0.42	Associated with Thompson Anticline. Subsidence features. Not potential design fault.
Unnamed fault in Westwater Quad, R18E, T21S	4	2.9			4.9	5.62	0.29	Associated with Salt Valley Anticline. No evidence of Quaternary faulting. Not potential design fault.
Unnamed fault in Westwater Quad, R18E, T20S	5	1.9			7.0	5.40	0.19	Associated with Salt Valley Anticline. No evidence of Quaternary faulting. Not potential design fault.
Unnamed fault in Westwater Quad, R17E, T20S	6	3.3			9.6	5.68	0.16	Associated with Salt Valley Anticline. No evidence of Quaternary faulting. Not potential design fault.
Unnamed fault in Westwater Quad, R21E, T20S	7	4.4			12.4	5.83	0.13	No evidence of Quaternary faulting. Potential design fault.
Cactus Park-Bridgeport fault	8	22.5			70	6.65	0.02	Design fault for Grand Junction Site (1991b). Potential design fault.
Little Grand fault	9	47.0			6.5	7.02	0.47	Fault determined not to be active in Quaternary based on field evidence (DOE 1991a). Not potential design fault.

[a]Fault number identical to UGS Quaternary Fault and Fold Database if fault is included in database, otherwise assigned number 1 – 7 unique to this report.
[b]MCE based on rupture area, where data available, otherwise based on rupture length.

A geophysical investigation at the Crescent Junction Site was done specifically to access rippability of the Mancos Shale during construction of the disposal cell (Calculation No. MOA-02-03-2006-4-07-00, Attachment 5, Appendix G [DOE 2006c). As such, the investigation consisted of determining the seismic velocities of the weathered and unweathered shale deposits using compression wave data. Shear wave velocities and shear modulus are typically the parameters used to evaluate the stiffness of the foundational materials to evaluate whether amplification of ground motions would be expected. However, on a qualitative basis, the seismic velocity data is discussed here as further evidence the site is founded on firm rock. The investigation summarized the three main geologic layers. The upper layer (alluvium and eolian deposits) ranged in depths from 4.5 to 18 ft, with seismic velocities ranging from approximately 1,160 to 1,330 fps, typical for unsaturated alluvial overburden soils. The base of the second layer (weathered Mancos Shale) was interpreted to vary between approximately 24 and 60 ft, with seismic velocities ranging from about 4,060 to 5,220 fps. Velocities for the unweathered Mancos Shale ranged from about 9,000 to 10,000 fps. The apparent discrepancy between the depth to unweathered Mancos Shale from the borehole data (5 to 15 ft) versus the geophysical data (24 to 60 ft) is due to differences between definitions of weathered shale. From a geologic standpoint, the shale contains fractures to a significant depth. The grading from weathered to unweathered is gradual and somewhat arbitrary. However, as indicated by SPT data, at a depth of 15 ft, the shale is sufficiently stiff to classify as a firm rock.

Based on the above data, the PHA of 0.22 g should be used in slope stability and liquefaction analyses. Amplification of site accelerations due to soil conditions is not warranted.

Comparison to Other Sites

As discussed in the *Site and Regional Seismicity – Results of Literature Search* calculation (MOA-02-08-2005-07-01, Attachment 2, Appendix E [DOE 2006a]), several other studies have estimated PHAs for nearby sites. Specifically, the study done by Utah Geological Survey, and the Green River, Grand Junction, and Moab Sites are addressed here.

Halling et al. (2002) developed peak acceleration maps for the state of Utah. A statewide map was published in the document that shows peak horizontal ground acceleration for the Crescent Junction Site to be approximately 0.5 g. These ground accelerations were entirely influenced by predicted ground motion from the Tenmile graben fault. Substantial studies have been done (Woodward-Clyde 1996, Olig et al. 1996) that indicate this structure is not capable. It is unclear why the Tenmile graben was included in this map while similar salt-related features, such as Salt and Cache Valley faults, Moab fault, and Fisher Valley faults, were not included. Documentation regarding these faults reads "A number of faults identified in Hecker's (1993) report were cited as having questionable seismogenic potential. The majority of these faults are located in eastern Utah, where the faults are attributed to salt diapers or salt dissolution and flow instead of actual tectonic faulting. These faults were not included in the peak bedrock acceleration calculations" (Halling et al. 2002).

In addition, several conservative assumptions resulted in the ground accelerations at the Crescent Junction Site as calculated by Halling et al. (0.5 g) to be substantially higher than those values calculated in this study (0.16 g). First, PHAs generated for the map were estimated using relationships developed by Abrahamson and Silva (1997). Comparisons done by Halling et al. show that of the three attenuation relations considered (Abrahamson and Silva 1997, Campbell 1997, and Spudich et al. 1996), the Abrahamson and Silva relationship is the most conservative of the three for the magnitude and distance considered for the Tenmile graben. The Campbell relationship yielded a middle value between the three and is thought to be appropriate for this study. In addition, Halling et al. conservatively modeled the Tenmile graben to dip at 60 degrees on both sides of the fault, to a depth of 15 km. The effect of this assumption is to decrease the distance from the site to the fault rupture plane from 17.1 km to 14.6 km. However, because the graben scarps define the extent of the rupture plane, it seems reasonable to define the distance from the site to the rupture plane as the distance from the site to the nearest surface expression of the structure. These two main differences account for the variability in site acceleration determined by the two studies.

For comparison purposes only, the peak ground accelerations determined for the UMTRA Project Sites at Green River and Grand Junction/Cheney Disposal Site were investigated. The seismotectonic stability study performed for the Green River Disposal Site recommended the design acceleration based on a floating earthquake of 6.2 M_L occurring 15 km (9.5 miles) from the site, resulting in a peak ground acceleration of 0.21 g. This recommendation is essentially the same as the recommendation for this study.

Seismotectonic stability studies done for the Grand Junction mill tailings/Cheney Disposal Site identified a fault (Fault 8) with a length of 11.0 km at a distance of 9.0 km from the site. Although no evidence of Quaternary displacement was proven, it was considered to be capable on the basis of its apparent association with a possibly active regional structure, the Uncompahgre Uplift. This fault was adopted as the design fault for the Cheney Disposal Site, resulting in a recommended design acceleration of 0.42 g. The capability of this fault and other faults related to the Uncompahgre Uplift have negligible impact on the Crescent Junction Site due to the distance of these faults to the Crescent Junction Site.

Woodward-Clyde (1996) performed a probabilistic seismic hazard analysis for the uranium mill tailings site in Moab, Utah. In their study, seismic sources included 11 faults, an area of seismicity along the Colorado River, and the random seismic events within the Colorado Plateau. At a return period of 10,000 years, they estimated a mean PHA of 0.18 g. The dominant contributor to the PHA is the random event, or FE, within the Colorado Plateau.

Computer Source:

- Not applicable.

References:

Abrahamson, N. A., and W. J. Silva, 1997. "Empirical Response Spectral Attenuation Relationships for Shallow Crustal Earthquakes," Seismological Research Letters 8: 94-127.

Algermissen, S. T., D. M. Perkins, P.C. Thenhaus, S. L. Benson, and S.L Bender, 1982. *Probabilistic Estimates of Maximum Acceleration and Velocity in Rock in the Contiguous United States,* Open-File Report 82-1033, U.S. Geological Survey.

Arabasz, W. J., R. B. Smith, and W. D. Richins, 1979. Earthquake Studies in Utah, 1850 to 1978, University of Utah Seismograph Stations, Department of Geology and Geophysics, University of Utah, Special Publication 5527, Salt Lake City, Utah.

Black, B., S. Hecker, M. Hylland, G. Christenson, and G. McDonald, 2003. *Quaternary Fault and Fold Database and Map of Utah*, Utah Geological Survey Map 193DM.

Campbell, K. W., 1981. *Near-source Attenuation of Peak Horizontal Acceleration,* Bulletin of the Seismological Society of America, Vol. 71, No. 6, pp. 2039–2070, December.

———,1997. *Empirical near-source attenuation relationships for horizontal and vertical components of peak ground acceleration, peak ground velocity, and pseudo-absolute acceleration response spectra,* Seismological Research Letters. 68, 154–179.

Campbell, K. W., and Y. Bozorgnia, 2003. *Updated Near-Source Ground-Motion (Attenuation) Relations for the Horizontal and Vertical Components of Peak Ground Acceleration and Acceleration Response Spectra,* Bulletin of the Seismological Society of America, Vol. 93, No. 1, pp. 314–331, February.

Colorado Geological Survey, 2002. *Earthquakes Caused by Humans in Colorado,* RockTalk, Vol. 5, No. 2, April.

DOE (U.S. Department of Energy), 1989. Technical Approach Document, Revision II, AL 050425.0002, United States Department of Energy, Uranium Mill Tailings Remedial Action Project, December.

———, 1991a. *Remedial Action Plan and Final Design for Stabilization of the Inactive Uranium Mill Tailings at Green River, Utah.*

———, 1991b. *Remedial Action Plan and Site Design for Stabilization of the Inactive Uranium Mill Tailings Site at Grand Junction, Colorado.*

———, 2005. *Remedial Action Plan and Site Design for Stabilization of Moab Title I Uranium Mill Tailings at the Crescent Junction, Utah, Disposal Site*, Attachment 2, Appendix A, Calculation No. MOA-02-08-2005-1-05-00, *Site and Regional Geology–Results of Literature Research*, Prepared for DOE by S.M. Stoller, Grand Junction, Colorado, August.

———, 2006a. *Remedial Action Plan and Site Design for Stabilization of Moab Title I Uranium Mill Tailings at the Crescent Junction, Utah, Disposal Site*, Attachment 2, Appendix E, Calculation No. MOA-02-08-2005-07-01 *Site and Regional Seismicity – Results of Literature Research*, Prepared for DOE by S.M. Stoller, Grand Junction, Colorado, August.

———, 2006b. *Remedial Action Plan and Site Design for Stabilization of Moab Title I Uranium Mill Tailings at the Crescent Junction, Utah, Disposal Site*, Attachment 5, Appendix B, Calculation No. MOA-02-02-2006-1-11-00, *Borehole Logs*, Prepared for DOE by S.M. Stoller, Grand Junction, Colorado, March.

———, 2006c. *Remedial Action Plan and Site Design for Stabilization of Moab Title I Uranium Mill Tailings at the Crescent Junction, Utah, Disposal Site*, Attachment 5, Appendix G, Calculation No. MOA-02-03-2006-4-07-00, *Seismic Rippability Investigation*, Prepared for DOE by S.M. Stoller, Grand Junction, Colorado, May.

Gaultieri, J. L, 1988. Geologic map of the Westwater 30' x 60' Quadrangle, Grand and Uintah Counties, Utah, and Garfield and Mesa Counties, Colorado, U.S. Geological Survey Miscellaneous Investigations Series Map I-1765, scale: 1:100,000.

Keller, G., L. Braile, and P. Morgan, 1979. *Crustal Structure, Geophysical Models and Contemporary Tectonism of the Colorado Plateau*, Tectonophysics, vol. 61, p. 131–147.

Kirkham, R., and W. Rogers, 1981. *Earthquake Potential in Colorado, a Preliminary Evaluation*, Colorado Geological Survey Bulletin 43.

Krinitzsky, E. L., and F. K. Chang, 1977. *State-of-the-art for Assessing Earthquake Hazards in the United States, Report 7, Specifying Peak Motions for Design Earthquakes*, U.S. Army Engineer Waterways Experiment Station, Miscellaneous Paper S-74-1, Vicksburg, Mississippi.

NEIC (National Earthquake Information Center), 2005. *Circular and Rectangular Searches of Historical Earthquakes*, http://neic.usgs.gov/neis/epic/.

NRC (U.S. Nuclear Regulatory Commission). *Code of Federal Regulations*, Title 10, Part 100 (10 CFR 100), Appendix A.

Olig, S. S., C. H. Fenton, J. McCleary, and I. G. Wong, 1996. The Earthquake Potential of the Moab Fault and Its Relation to Salt Tectonics in the Paradox Basin, Utah, *in* Huffman, A.C., Jr., Lund, W.R., and Godwin, L.H., editors, Geology and Resources of the Paradox Basin, Utah Geological Association Guidebook 25, p. 251–264.

Richter, C. F., 1958. *Elementary Seismology*, W.H. Freeman and Company, San Francisco, California.

Smith, R. and M. Sbar, 1974. *Contemporary Tectonics and Seismicity of the Western United States with Emphasis on the Intermountain Seismic Belt*, Geological Society of America Bulletin, vol. 85, p. 1205–1218.

Spudich, P., J. Fletcher, M. Hellweg, J. Boatwright, C. Sullivan, W. Joyner, T. Hanks, D. Boore, A. McGarr, L. Baker, and A. Lindh, 1997. *SEA96, A new predictive relationship for earthquake ground motions in extensional tectonic regimes,* Seismological Research Letters, vol. 68, p. 190–198.

Sykora, D. W., 1987. *Examination of Existing Shear Wave Velocity and Shear Modulus Correlations in Soils*, U.S. Army Engineer Waterway Experiment Station, Miscellaneous Paper GL-87-22, Vicksburg, Mississippi.

USGS (U.S. Geological Survey) 2002. *Quaternary Fault and Fold Database*, http: //Qfaults.cr.usgs.gov/.

Wells, D. L., and K. J. Coppersmith, 1994. *New Empirical Relationships among Magnitude, Rupture Length, Rupture Width, Rupture Area, and Surface Displacement*, Bulletin of the Seismological Society of America, Vol. 84, No. 4, pp. 974–1002, August.

Williams, P., compiler, 1964. *Geology, Structure, and Uranium Deposits of the Moab Quadrangle, Colorado and Utah*, U.S. Geological Survey Miscellaneous Geologic Investigations Map I-360, scale 1:250,000.

Williams, P., and R. Hackman, 1971. *Geology of the Salina Quadrangle, Utah*, U.S. Geological Survey Miscellaneous Geologic Investigations Map I-591, scale 1:250,000.

Willis, G. C., 1986. *Provisional geologic map of the Sego Canyon quadrangle, Grand County, Utah,* Utah Geological Survey, Map 89, scale 1:24,000.

Witkind, I., 1995. Geologic Map of the Price 1 x 2 quadrangle, Utah, scale 1:250,000, USGS.

Wong, I. G., S. S Olig, and J. D. J. Bott, 1996. *Earthquake potential and seismic hazards in the Paradox Basin, southeastern Utah*, in Huffman, A. C., Jr., W. R. Lund, and L. H. Godwin, editors, *Geology and Resources of the Paradox Basin*, Utah Geological Association Guidebook 25, p. 241–250.

Woodward-Clyde Consultants, 1984. Geologic characterization report for the Paradox Basin study region, Utah study areas, Volume VI, Salt Valley, Walnut Creek, California, unpublished consultant's report for Battelle Memorial Institute, Office of Nuclear Waste Isolation, ONWI-290, 190 p., scale 1:62,500.

Woodward-Clyde Consultants, 1996. *Evaluation and Potential Seismic and Salt Dissolution Hazards at the Atlas Uranium Mill Tailings Site, Moab, Utah*, Oakland, California, unpublished Consultant's report for Smith Environmental Technologies and Atlas Corporation, SK9407.

Appendix A

National Earthquake Information Center (NEIC): Earthquake Search Results

Site and Regional Seismicity - Results of MCE and PHA
APPENDIX A
NEIC: Earthquake Search Results

UNITED STATES GEOLOGICAL SURVEY

EARTHQUAKE DATA BASE

FILE CREATED: Mon Aug 15 14:28:55 2005
Geographic Grid Search Earthquakes= 549
Latitude: 40.750N - 34.500N
Longitude: 106.500W - 112.500W
Catalog Used: PDE
Data Selection: Historical & Preliminary Data

FILE CREATED: Mon Aug 15 14:31:32 2005
Geographic Grid Search Earthquakes= 991
Latitude: 40.750N - 34.500N
Longitude: 106.500W - 112.500W
Catalog Used: SRA
Data Selection: Eastern, Central and Mountain States of U.S. (SRA)

FILE CREATED: Mon Aug 15 14:30:22 2005
Geographic Grid Search Earthquakes= 64
Latitude: 40.750N - 34.500N
Longitude: 106.500W - 112.500W
Catalog Used: USHIS
Data Selection: Significant U.S. Earthquakes (USHIS)

The above searches have been filtered to include only events occuring within the Colorado Plateau
Only events with magnitudes 3.0 or greater or intensities of 4 or greater are considered further.
Data has been declustered to remove aftershocks and foreshocks.
BOLD EVENTS ARE EVENTS CONSIDERED NON-TECTONIC IN ORIGIN AND ARE NOT INCLUDED IN RECURRENCE CALCULATIONS

	Date			ORIGIN	COORDINATES		DEPTH	MAGNITUDES				INFORMATION (see below for explanation of symbols)																Converted Magnitude	Comments
										Other																			
CATALOG SOURCE	YEAR	MO	DA	TIME	LAT	LONG	km	mb	Ms	Value	Scale	INT	EFF	MAP	FPS	MO	DEP	IDE	PFD	FLG	D	T	S	V	N	W	G		
SRA	1871	10	0	0	40.5	-108.5						6																5.0	
SRA	1882	2	11	830	37.3	-107						4																3.7	
SRA	1889	1	15	22	39.5	-107.3						5																4.3	
SRA	1891	12	0	21	40.5	-108						6																5.0	
SRA	1892	2	2	830	35.2	-111.6						6																5.0	
SRA	1894	1	1	10	37.9	-107.8						4																3.7	
SRA	1897	8	3	7	38.2	-107.8						5																4.3	
SRA	1899	0	0	230	40.5	-108						4																3.7	
SRA	1900	5	0	0	36.9	-106.9						5																4.3	
SRA	1906	1	25	213230	35.2	-111.7						7																5.7	
SRA	1906	4	0	0	40.5	-108.3						4																3.7	
SRA	1910	9	24	405	35.8	-111.5						7																5.7	
SRA	1912	8	18	2112	36	-111.5						7																5.7	
SRA	1913	11	11	2155	38.1	-107.7						6																5.0	
SRA	1918	4	28	1258	35.2	-111.6						4																3.7	
SRA	1920	12	29	250	39.5	-107.5						5																4.3	
SRA	1921	4	6	2107	34.9	-110.2						5																4.3	
SRA	1921	7	31	355	36	-107						4																3.7	
SRA	1923	9	28	0	35.2	-111.7						4																3.7	
SRA	1928	4	30	1550	37.8	-107						5																4.3	
SRA	1931	4	17	1238	34.5	-110						5																4.3	
SRA	1935	1	10	810	36	-112.1						6																5.0	
SRA	1935	10	8	3	37.9	-111.4						4																3.7	
SRA	1937	4	8	12	35.7	-109.5						5																4.3	
SRA	1937	12	17	2330	35.2	-111.7						4																3.7	
SRA	1939	3	9	1330	36.1	-112.1						5																4.3	
SRA	1940	10	16	1325	35.2	-111.7						4																3.7	
SRA	1941	8	29	1134	37.3	-107.7						5																4.3	
SRA	1942	7	23	1940	40.5	-108.5						5																4.3	
SRA	1943	8	14	540	38.2	-111.4						4																3.7	
SRA	1944	9	9	41220	39	-107.5						6																5.0	
SRA	1945	4	29	1708	37.7	-107.7						4																3.7	
SRA	1945	7	0	1155	36.1	-112.1						4																3.7	
SRA	1946	1	31	2245	39.6	-107.3						4																3.7	
SRA	1947	10	27	41540	35.5	-112						4																3.7	
SRA	1948	8	8	2320	36.1	-112.1						5																4.3	
SRA	1948	12	3	1845	35	-110.7						4																3.7	
SRA	1950	1	17	51	35.7	-109.5						6																5.0	
SRA	1950	1	18	15551	40.5	-110.5				5.3	UK	5																5.3	
SRA	1953	7	30	545	39	-110.2						5																4.3	
SRA	1953	10	8	201946	34.75	-111						5																4.3	
SRA	1954	2	21	202051	40	-108.75						4																3.7	
SRA	1954	3	31	14	39	-110.2						4																3.7	
SRA	1954	11	3	2039	35.2	-106.7						5																4.3	
SRA	1955	3	27	1213	38.3	-111.3						4																3.7	
SRA	1955	8	3	63942	38	-107.3						6																5.0	

CATALOG SOURCE	Date YEAR	MO	DA	ORIGIN TIME	COORDINATES LAT	LONG	DEPTH km	MAGNITUDES mb	Ms	Other Value	Other Scale	INFORMATION (see below for explanation of symbols) I NT	E FF	MAP	FPS	MO	DEP	IDE	PFD	FLG	D	T	S	V	N	W	G	Converted Magnitude	Comments
SRA	1956	2	12	3	40.5	-109.5						4																3.7	
SRA	1957	7	18	152420	40	-110.5						4																3.7	
SRA	1959	2	11	1401	35.2	-111.7						5																4.3	
SRA	1959	10	13	815	35.5	-111.5		5		5	ML	5																5.0	
SRA	1960	10	11	80530	38.3	-107.6	49			5.5	mb	6																5.5	
SRA	1961	5	6	161220	39.6	-110.2	25					5																4.3	
SRA	1962	1	13	1333	38.4	-107.8				4.4	ML	4																4.4	
SRA	1962	2	5	144551	38.2	-107.6	25			4.7	ML	5																4.7	
SRA	1962	9	7	165023.8	39.2	-110.89	7			3.1	ML																	3.1	
SRA	1962	12	11	102813	39.36	-110.42	7			3.4	ML																	3.4	
SRA	1963	4	15	221824.6	39.59	-110.35	7	4.2		3.4	ML														N			3.4	Related to coal mining (Smith and Sbar)
SRA	1963	4	24	133303.3	39.44	-110.33	7	4.6		3.3	ML														N			3.3	Related to coal mining (Smith and Sbar)
SRA	1963	7	9	202525	40.03	-111.19	7	4.1		4	ML		F															4.0	
SRA	1963	9	30	91739	38.1	-111.22	7	4.5		4.3	ML																	4.3	
SRA	1963	12	24	145108.8	39.56	-110.32	7	4.1		3	ML														N			3.0	Related to coal mining (Smith and Sbar)
SRA	1964	8	5	151756	38.95	-110.92	7			3	ML																	3.0	
SRA	1965	1	14	123010.8	39.44	-110.35	7	4.5		3.3	ML														N			3.3	Related to coal mining (Smith and Sbar)
SRA	1965	6	7	142801	36	-112.2	33			3.5	mb																	3.5	
SRA	1965	6	27	192408.7	39.51	-110.38	7	4		3.1	ML																	3.1	Related to coal mining (Smith and Sbar)
SRA	1965	6	29	74628	39.5	-110.39	7	4.3		3.2	ML																	3.2	Related to coal mining (Smith and Sbar)
SRA	1965	7	18	35551.4	39.5	-109.9	33	3.1																				3.1	
USHIS	1966	1	23	15638	36.98	-107.02	3	5.1		4.99	Mw	7	F															5.0	
SRA	1966	5	20	134047	37.98	-111.85	7	4.3		4.1	ML																	4.1	
SRA	1966	7	6	54708	40.1	-109	7	4.1		3.7	ML																	3.7	Rangley Oil Field gas oil and gas withdrawl
SRA	1966	7	30	32531	39.44	-110.36	7	4.1		3.1	ML																	3.1	Related to coal mining (Smith and Sbar)
SRA	1966	9	4	95234	38.3	-107.6	33	4.2																				4.2	
SRA	1966	10	3	160350	35.8	-111.6	34	4.4																				4.4	
SRA	1966	11	11	184534.6	39.6	-110.5	15	3.2																	N			3.2	Non-tectonic
SRA	1967	1	16	92245	37.67	-107.86	33	4.1																				4.1	
SRA	1967	2	5	100718.6	39.55	-110.1	33	3																				3.0	
SRA	1967	2	15	32803	40.1	-109.1	7	4.5		4	ML	5																4.0	Rangley Oil Field gas oil and gas withdrawl
SRA	1967	4	4	225339	38.32	-107.75	33	4.5		3	ML																	3.0	
SRA	1967	9	4	232746	36.15	-111.6	33			4.2	ML																	4.2	
SRA	1967	10	25	24134	39.47	-110.35	0	4		3.2	ML																	3.2	Related to coal mining (Smith and Sbar)
SRA	1967	12	10	193000.1	36.68	-107.21	0	5.1																	N			5.1	Non-tectonic
SRA	1968	6	2	185923.2	39.21	-110.45	7	3.8		3.3	ML																	3.3	
SRA	1968	6	23	201613	39.31	-107.41	33	3.8																				3.8	
SRA	1968	11	17	143338	39.52	-110.97	7	4.6		3.5	ML																	3.5	
SRA	1969	9	10	210000.1	39.41	-107.95	0	5.3				5													N			5.3	Non-tectonic
SRA	1970	2	3	55935	37.92	-108.31	33	4																				4.0	
SRA	1970	2	21	61348	39.49	-110.35	7	4.1		3.1	ML																	3.1	Related to coal mining (Smith and Sbar)
SRA	1970	4	18	104211	37.87	-111.72	7	4.4		3.7	ML																	3.7	
SRA	1970	4	14	104054.1	39.65	-110.82	7	4.2		3	ML																	3.0	
SRA	1970	4	21	85352	40.1	-108.9	4	4.3		3.9	ML	5																3.9	Rangley Oil Field gas oil and gas withdrawl
SRA	1971	1	7	203952	39.49	-107.31	33	4.3		3.8	ML	5																3.8	
SRA	1971	7	10	172236	40.24	-109.6	7	3.8		3.7	ML																	3.7	
SRA	1971	11	12	93044	38.91	-108.68	5			4	ML	3																4.0	
SRA	1971	12	15	125814	36.791	-111.824	5			3	ML																	3.0	
SRA	1972	4	20	132816	35.311	-111.64	5	3.7				4																3.7	
SRA	1972	10	16	214931.2	40.42	-111.02	7	4.1		3.4	ML	4																3.4	
SRA	1973	2	9	173837	36.43	-110.425	5			3.2	ML																	3.2	
PDE	1973	5	17	16	39.793	-108.366	0	5.4	4.1	5.7	UK						3		P						E			5.7	Explosion
SRA	1973	12	24	22014	35.26	-107.74	18	4.4		4.1	ML	6																4.1	
SRA	1975	1	30	144840	39.27	-108.65	5	4.4		3.7	ML	5																3.7	
SRA	1975	3	7	31613	34.55	-107.16				3	ML																	3.0	
SRA	1976	1	5	62332	35.84	-108.34	25	5		4.6	ML	6																4.6	
SRA	1976	2	28	205358	35.91	-111.788	5			3	ML																	3.0	
SRA	1976	4	19	233545	35.39	-109.1	5			3.5	ML	5													?			3.5	Classified as an earthquake, but a non-tectonic origin cannot be ruled out
SRA	1977	2	9	4216	39.29	-111.11	7			3.2	ML	6																3.2	

CATALOG SOURCE	Date YEAR	MO	DA	ORIGIN TIME	COORDINATES LAT	LONG	DEPTH km	MAGNITUDES mb	Ms	Other Value	Other Scale	INFORMATION (see below for explanation of symbols) INT	EFF	MAP	FPS	MO	DEP	IDE	PFD	FLG	D	T	S	V	N	W	G	Converted Magnitude	Comments
USHIS	1977	3	5	30055	35.748	-108.222	44	4.6		4.2	ML	6	F															4.2	
SRA	1977	6	3	13722	39.65	-110.51	7			3.2	MD																	3.2	
SRA	1977	9	24	111648	39.31	-107.31	5	4		3	ML																	3.0	
SRA	1977	9	30	101920	40.47	-110.47	6	5		4.5	ML	6																4.5	
SRA	1977	11	29	213123	36.82	-110.99	7			3	MD																	3.0	
SRA	1978	5	29	164518	39.26	-107.32	5			3	ML																	3.0	
SRA	1978	9	23	82006	39.32	-111.09	2			3	ML																	3.0	
SRA	1979	3	19	145929	40.2	-108.9	2			3.1	ML	4																3.1	Rangley Oil Field gas oil and gas withdrawl
SRA	1979	4	30	20710	37.88	-111.02	7			3.8	ML	3																3.8	
SRA	1979	10	23	41719	37.89	-110.93	7			3.5	ML		F															3.5	
SRA	1980	6	1	84027	35.391	-111.986	5			3.6	ML	2																3.6	
PDE	1981	5	14	51104.1	39.481	-111.06	1	4.5		3.5	ML	5	F				4		P									3.5	
SRA	1981	5	29	30902	36.83	-110.37	1			3	MD																	3.0	
SRA	1981	9	10	75509	37.5	-110.56	2			3.1	MD																	3.1	
PDE	1981	9	21	80133	39.578	-110.44	7			3.5	ML	3	F				3		P									3.5	Related to coal mining (Smith and Sbar)
SRA	1981	12	8	90920	35.17	-111.62						5																	
SRA	1982	4	17	60012	38.22	-111.3	9			3	ML																	3.0	
SRA	1982	11	3	175411	35.32	-108.74	5			3	ML																	3.0	
SRA	1982	11	19	205734	36.03	-112.01	5			3	ML		F															3.0	
SRA	1983	1	27	233711	37.778	-110.674	7			3.3	MD																	3.3	
SRA	1983	3	22	111235	39.546	-110.422	2			3.1	MD		F															3.1	Related to coal mining (Smith and Sbar)
PDE	1983	5	3	124338	38.288	-110.592	7			3.2	ML						3		P									3.2	
SRA	1983	6	14	190830	38.359	-107.402	5			3.4	ML	2																3.4	
SRA	1983	8	31	81008	36.135	-112.037	5			3.3	ML		F															3.3	
SRA	1984	3	21	111930	39.344	-111.109	0			3.5	ML		F															3.5	
SRA	1984	5	14	101417	39.322	-107.228	5			3.2	ML	4																3.2	
SRA	1984	7	18	142931	36.216	-111.844	5			3	ML																	3.0	
SRA	1985	4	14	214800	35.174	-109.071	5			3.3	ML	3																3.3	
SRA	1985	6	27	103629	39.558	-110.396	1			3	MD																	3.0	Related to coal mining (Smith and Sbar)
SRA	1985	10	7	203340	40.407	-109.498	21			3	MD																	3.0	
SRA	1986	8	22	132633	37.42	-110.574	5			4	ML	5																4.0	
SRA	1986	9	3	62050	38.912	-107.09	5			3.5	ML	5																3.5	
SRA	1986	11	7	13153.7	37.43	-110.297	1			3	MD																	3.0	
PDE	1987	3	5	30250.49	40.442	-110.616	1	4		3.7	ML	4	F				4		P									3.7	
PDE	1988	1	15	73329.2	37.515	-106.684	5			3.1	ML		F				4		P									3.1	
PDE	1988	2	14	183240	40.626	-108.532	5					4	F				4		P									3.7	
PDE	1988	7	15	3809.59	36.374	-110.448	5			3.3	ML						4		P									3.3	
USHIS	1988	8	14	200303	39.128	-110.869	10	5.5		5.3	ML	6	F															5.3	
PDE	1989	2	3	180821	39.744	-110.897	0					4	F				4		P									3.7	
PDE	1989	4	9	112419.39	40.419	-110.942	9			3.2	ML	2	F				4		P									3.2	
PDE	1989	5	13	210148.82	38.473	-108.924	7			3.1	MD						4		P									3.1	Paradox Valley salt-water injection
PDE	1989	11	19	32113.61	38.055	-107.767	5			3	ML		F				4		P									3.0	
PDE	1990	4	7	153754.86	40.082	-109.519	3			3.5	ML						4		P									3.5	
PDE	1990	6	25	171533.54	38.952	-110.828	11			3	MD						4		P									3.0	
PDE	1990	10	21	43119	38.908	-108.355	10					5	F				4		P									4.3	
PDE	1991	1	26	214938	37.681	-111.429	9			3.5	ML	3	F				3		P									3.5	
PDE	1991	3	2	84137.49	40.091	-109.483	1	3		3.3	ML						4		P									3.3	
PDE	1991	4	26	130820	36.627	-112.345	10	3.3				4	F				4		P									3.3	
PDE	1991	6	25	210213.63	37.209	-110.358	1			3	MD						4		P									3.0	
PDE	1991	5	23	73840	39.298	-111.149	12	3.5		3.6	ML	3	F				3		P									3.6	
PDE	1991	11	8	131505	40.1	-109.286	2	3.4				3	F				4		P									3.4	
PDE	1992	5	15	213624	38.563	-107.914	5					4	F				4		P									3.7	
PDE	1992	7	5	181729	35.982	-112.219	5	4					F				4		P									4.0	
PDE	1992	7	5	122223	39.318	-111.134	5	4				3	F				1		P									4.0	
PDE	1993	1	21	90120.4	39.712	-110.622	1	3.4						D			4		P						C			3.4	Coal bump or Rockburst in a coal mine
PDE	1993	4	29	82100	35.611	-112.112	10	5.5	5	5.3	Mw	5	D	U		M	3		P									5.3	
PDE	1993	5	27	62153	37.064	-112.089	10	3.3		3.5	MD	3	F				3		P									3.5	
PDE	1994	9	13	60123	38.151	-107.976	10	4.4				6	D				4		P									4.4	
PDE	1994	11	3	114010.14	40.04	-108.269	5			3.4	ML						4		P									3.4	
PDE	1995	3	20	124616	40.179	-108.925	5	4.2				5	F				4		P									4.2	
PDE	1995	4	17	82346	35.964	-112.223	5	3.7				5	D				4		P									3.7	
PDE	1996	1	6	125558.62	39.12	-110.878	0	4.3		4.2	MD	5	F				4		P									4.2	
PDE	1996	2	2	21114	39.467	-111.23	1			3.2	ML						4		P									3.2	
PDE	1996	12	6	135314	39.706	-110.658	3			3.4	ML						3		P									3.4	
PDE	1997	3	31	73448	35.534	-111.993	5			3.7	ML		F				3		P									3.7	
PDE	1997	4	14	93048	39.048	-111.389	5			3.1	MD						3		P									3.1	
PDE	1997	10	20	70220	37.834	-111.879	10			3.1	ML						3		P									3.1	
PDE	1998	1	6	83646	34.916	-110.495	5			3.9	ML		D				3		P									3.9	
PDE	1998	2	5	51956	39.751	-110.846	1	3.6		3.7	ML		F				3		P									3.7	
PDE	1998	4	10	65216	38.3	-108.8	5			3	ML		F				3		P									3.0	Paradox Valley salt-water injection
PDE	1998	10	18	71310	36.033	-111.091	5			3.4	ML		F				3		P									3.4	

CATALOG SOURCE	Date YEAR	MO	DA	ORIGIN TIME	COORDINATES LAT	LONG	DEPTH km	MAGNITUDES mb	Ms	Other Value	Scale	INFORMATION (see below for explanation of symbols) INT	EFF	MAP	FPS	MO	DEP	IDE	PFD	FLG	D	T	S	V	N	W	G	Converted Magnitude	Comments
PDE	1999	1	30	90547	37.55	-112.21	1	3.2		3	ML						3		P									3.0	
PDE	1999	6	3	153534	38.3	-108.9	4			3.6	ML		F				3		P									3.6	Paradox Valley salt-water injection
PDE	1999	7	6	220545.19	38.319	-108.859	5			3.5	ML		F				3		P									3.5	Paradox Valley salt-water injection
PDE	2000	3	7	21604	39.75	-110.84	1	4.3		4.2	ML		F				3		P								S	4.2	
PDE	2000	3	15	121427.5	38.367	-108.867	5			3.3	ML																	3.3	Paradox Valley salt-water injection
PDE	2000	5	27	215818	38.3	-108.9	5			4.3	ML		F				3		P									4.3	Paradox Valley salt-water injection
PDE	2000	11	11	211753	40.28	-109.23	5			3.7	ML						3		P									3.7	
PDE	2001	7	19	201534	38.731	-111.521	3	4.5		4.3	ML		F				3		P									4.3	
PDE	2001	8	9	223854	39.66	-107.378	5			4	ML	4	F				3		P									4.0	
PDE	2001	11	5	83423	38.851	-107.384	1			3.4	ML		F				3		P									3.4	
PDE	2002	1	31	181745	40.287	-107.693	5			4.3	ML	3	F				3		P									4.3	
PDE	2002	3	30	213843.9	38.853	-107.386	1			3.1	ML		F				3		P						C			3.1	Coal bump or Rockburst in a coal mine
PDE	2002	6	3	32523.98	38.907	-107.418	1			3.3	ML		F				3		P						C			3.3	Coal bump or Rockburst in a coal mine
PDE	2002	6	6	122910	38.3	-108.9	1			3.2	ML						3		P									3.2	Paradox Valley salt-water injection
PDE	2002	6	20	221704.8	38.908	-107.416	1			3.6	ML		F				3		P						C			3.6	Coal bump or Rockburst in a coal mine
PDE	2002	8	24	153719.7	38.92	-107.481	1			3.2	ML		F				3		P						C			3.2	Coal bump or Rockburst in a coal mine
PDE	2002	9	10	161811.4	38.789	-107.412	1			3.3	ML		F				3		P						C			3.3	Coal bump or Rockburst in a coal mine
PDE	2002	9	26	103210	37.41	-110.53	3			3	ML						3		P									3.0	
PDE	2002	11	26	54616.37	38.904	-107.448	1			3.1	ML						3		P						C			3.1	Coal bump or Rockburst in a coal mine
PDE	2003	7	8	22033	36.95	-111.79	6			3.3	ML						3		P									3.3	
PDE	2003	8	8	61105.19	38.907	-107.458	1			3.4	ML						3		P						C			3.4	Coal bump or Rockburst in a coal mine
PDE	2003	11	17	231852	40.35	-111.17	12			3	ML																	3.0	
PDE	2004	4	15	45359.34	38.87	-107.35	1			3.1	ML						3		P						C			3.1	Coal bump or Rockburst in a coal mine
PDE-W	2004	9	19	60943	38.853	-107.358	1			3.5	ML						3		P									3.5	
PDE	2004	10	11	5841.02	38.825	-107.425	1			3.3	ML						3		P						C			3.3	Coal bump or Rockburst in a coal mine
PDE-W	2004	11	7	65459	38.2	-108.9	0			4.1	ML	4	F				3		P									4.1	Paradox Valley salt-water injection
PDE	2004	11	13	182830.4	38.875	-107.497	1			3.2	ML		F				3		P						C			3.2	Coal bump or Rockburst in a coal mine
PDE-W	2004	11	24	101638	35.105	-107.51	5			3	ML						3		P									3.0	
PDE-W	2005	3	2	111257	34.715	-110.97	5	5.1		4.6	ML	3	F				1		P									4.6	
PDE	2005	4	30	45704.76	38.918	-107.393	1			3.1	ML						3		P						C			3.1	Coal bump or Rockburst in a coal mine
PDE-W	2005	5	2	172955.8	38.795	-107.393	1			3.2	ML		F				3		P						C			3.2	Coal bump or Rockburst in a coal mine
PDE-W	2005	6	13	142604.3	38.835	-107.372	1			3.3	ML		F				3		P						C			3.3	Coal bump or Rockburst in a coal mine
PDE-W	2005	5	30	14921.14	38.889	-107.474	1			3.3	ML						3		P						C			3.3	Coal bump or Rockburst in a coal mine
PDE-W	2005	6	8	84600.4	38.953	-107.527	1			3.5	ML						3		P						C			3.5	Coal bump or Rockburst in a coal mine
PDE-W	2005	7	25	115128.3	38.831	-107.415	1			3.1	ML						3		P						C			3.1	Coal bump or Rockburst in a coal mine

INFORMATION

INFORMATION (IEFM DTSVNWG on Screen Search): Dots are used in place of blanks to aid in the distinction between the columns. Read the sub-headers vertically.

Intensity (sub-header INT):
Maximum intensity on the Modified Mercalli Intensity Scale of 1931 (Wood and Neumann, 1931) or any similar 12-point intensity scale. It may also be an MMI value approximated from other intensity scales such as Ross-Forel or Japan Meteorological Agency. Possible intensity values are 1 - 9; X = 10; E = 11; T = 12.

Cultural Effects (sub-header EFF):
The most severe effect is listed (C = Casualities; D = Damage; F = Felt; H = Heard).
Note that casualties includes human deaths or injuries. Domestic animal casualties are considered to be damage.

Isoseismal Map (sub-header MAP): (Expanded Format only)
Indicates the publication where an isoseismal map for this event has been published.
U = United States Earthquakes.
E = Earthquake Notes. (Now Seismological Research Letters)
P = Preliminary Determination of Epicenters.
W = Wellington (New Zealand Seismology Reports, Wellington, N.Z.).
N = Nature Magazine.
S = Bulletin of the Seismological Society of America.

Fault Plane Solution (sub-header FPS):
Coded as an "F" to indicate the availability of a fault plane solution in the publication, "Preliminary Determination of Epicenters, Monthly Listing".

Moment Tensor Solution (sub-header MO):
Coded as an "G" to indicate the availability of a moment tensor solution in the publication "Preliminary Determination of Epicenters, Monthly Listing" (Sipkin, 1982; Dziewonski, 1980; and Hanks and others, 1979).

ISC Alternate Depth Indicator (sub-header DEP):
A "D" in this column indicates that a pP depth is given, but the pP depth is not the adopted depth in the hypocenter solution.

International Data Exchange (sub-header IDE):
An "X" in this column identifies the event as a "IDE" earthquake.

Preferred Solution (sub-header PFD):
A "P" in this column designates a preferred solution. Earthquake hypocenters which are located within a seismic network, such as Pasadena or Berkeley, or seismic catalogs which have undergone critical review during their compilation will be designated as a preferred solution.

Flag (sub-header FLG): Currently not used.

PHENOMENA

Diastrophism: (sub-header D)
F = Faulting.
U = Uplift.
S = Subsidence.
3 = Uplift and Subsidence.
4 = Uplift and Faulting.
5 = Faulting and Subsidence.
6 = Faulting with Uplift and Subsidence.
7 = Uplift or Subsidence.
8 = Faulting and Uplift or Subsidence.

Tsunami: (sub-header T)
T = Tsunami generated.
Q = Questionable Tsunami.

Seiche: (sub-header S)
S = Seiche.
Q = Questionable Seiche.

Volcanism: (sub-header V)
V = Earthquake associated with volcanism.

Non-Tectonic: (sub-header N)
E = Explosion.
I = Collapse.
C = Coal bump or Rockburst in a coal mine.
R = Rockburst.
M = Meteoritic.
N = Either known to be or likely to be of non-tectonic origin.
? = Classified as an earthquake, but a non-tectonic origin cannot be ruled out.
V = Reservoir induced earthquake.

Guided Waves in Atmospheric And/Or Ocean: (sub-header W)
T = T-wave.
A = Acoustic wave.
G = Gravity wave.
B = Both A and G.
M = T-wave plus and A or G.

Miscellaneous Phenomena: (sub-header G)
L = Liquefaction.
G = Geyser.
S = Landslides and/or Avalanches.
B = Sandblows.
C = Ground cracks not known to be an expression of faulting.
V = Lights or other visual phenomena seen.
O = Olfactory (Unusual odors noted).
M = More than one of these phenomena observed.

Appendix B

Quaternary and Undated Faults within Expanded Site Region

SITE AND REGIONAL SEISMICITY - RESULTS OF MCE AND PHA
APPENDIX B:
QUATERNARY AND UNDATED FAULTS WITHIN EXPANDED SITE REGION

Name	Number	Age of Most Recent Prehistoric Deformation (ya)	Slip-rate (mm/yr)	Fault Length (km)	Fault Type	Distance from site (miles)[1]	Distance from site (km)	Depth to seismo-genic rupture (km)	r_{seis} (km)	MCE (Based on fault length, all slip types, Wells and Coppersmith, 1994)	Rupture depth (km)	Rupture area (km^2)	MCE (based on fracture area, Wells and Coppersmith, 1994)	PGA (Campbell-Bozorgnia 2003) corrected, plus 1SD (based on Mw)
Salt and Cache Valleys faults (Class B)	2474	Class B	<0.2	57.9	N	1.8	2.9	3	4.2	7.12	2.00	115.80	6.09	0.67
unnamed fault in Westwater Quad, R19E, T21S (no. 1)	1			8.0		2.4	3.8	3	4.8	6.13				0.60
unnamed fault in Westwater Quad, R20E, T21S (no. 2)	2			6.4		3.1	5.1	3	5.9	6.02				0.49
Little Grand fault	9			47.0	N	6.5	10.5	3	10.9	7.02				0.47
unnamed fault in Westwater Quad, R19E, T19S (no. 3)	3			15.7		5.3	8.5	3	9.0	6.47				0.42
unnamed fault in Westwater Quad, R18E, T21S (no. 4)	4			2.9		4.9	7.9	3	8.4	5.62				0.29
unnamed fault in Westwater Quad, R18E, T20S (no. 5)	5			1.9		7.0	11.3	3	11.7	5.40				0.19
Ten Mile graben faults (Class B)[2]	2473	Class B	<0.2	34.6	N	10.5	16.8	3	17.1	6.87	2.00	69.20	5.87	0.16
Ten Mile graben faults (Class B)[3]	2473	Class B	<0.2	34.6	N	10.5	16.8	3	17.1	6.87	2.00	69.20	5.87	0.31
Ten Mile graben faults (Class B)[5]	2473	Class B	<0.2	34.6	N	10.5	16.8	3	14.6	7.15	2.00	69.20	5.87	0.45
Moab fault and Spanish Valley faults (Class B)	2476	Class B	<0.2	72.4	N	12.5	20.1	3	20.3	7.24	2.00	144.80	6.19	0.16
unnamed fault in Westwater Quad, R17E, T20S (no. 6)	6			3.3		9.6	15.5	3	15.7	5.68				0.16
Price River area faults (Class B)	2457	<1,600,000	<0.2	50.9	N	24.8	39.9	3	40.0	7.06				0.13
unnamed fault in Westwater Quad, R21E, T0S (no. 7)	7			4.4		12.4	19.9	3	20.1	5.83				0.13
Ryan Creek fault zone	2263	<1,600,000	<0.2	39.5	N	26.6	42.8	3	42.9	6.93				0.11
Sand Flat graben faults	2475	<1,600,000	<0.2	23.1	N	26.4	42.5	3	42.6	6.66				0.10
Granite Creek fault zone	2265	<1,600,000	<0.2	22.7	N	33.4	53.8	3	53.8	6.65				0.08
Fisher Valley faults (Class B)	2478	Class B	<0.2	15.9		31.0	49.8	3	49.9	6.47				0.07
Sinbad Valley graben (Class B)	2285	<1,600,000	<0.2	31.8		39.3	63.2	3	63.3	6.82				0.07
unnamed fault in Salina Quad, R13E, T24S				19.6		36.0	57.9	3	57.9	6.58				0.07
Paradox Valley graben (Class B)	2286	<1,600,000	<0.2	56.4	N	49.6	79.9	3	79.9	7.11				0.07
Little Dolores River fault	2251	<1,600,000	<0.2	15.7	R	34.5	55.5	3	55.6	6.47				0.07
Castle Valley faults (Class B)	2477	Class B	<0.2	12.4		34.2	54.9	3	55.0	6.35				0.06
unnamed fault in Salina Quad, R11E, T22S				22.7		41.6	66.9	3	67.0	6.65				0.06
unnamed fault in Salina Quad, R11E, T23S				25.8		44.7	72.0	3	72.0	6.72				0.06
Unnamed fault near Pine Mountain	2267	<1,600,000	<0.2	30.7		47.2	75.9	3	75.9	6.81				0.06
Lisbon Valley fault zone (Class B)	2511	<1,600,000	<0.2	37.5		50.9	81.9	3	82.0	6.91				0.06
Lockhart fault (Class B)	2510	Class B	<0.2	15.7		40.8	65.6	3	65.7	6.47				0.06
unnamed fault in Salina Quad, R11E, T21S				14.0		42.1	67.7	3	67.8	6.41				0.05
unnamed fault in Price Quad, R12E, T19S				13.7		42.4	68.2	3	68.3	6.40				0.05
Needles fault zone (Class B)	2507	Class B	<0.2	28.5		53.9	86.6	3	86.7	6.77				0.05
unnamed fault in Salina Quad, R12E, T24S				10.1		42.6	68.6	3	68.7	6.25				0.05
Redlands fault complex	2252	<1,600,000	<0.2	21.1	N,R	53.1	85.4	3	85.4	6.62				0.05
Unnamed fault of Lost Horse Basin	2264	<1,600,000	<0.2	8.1		40.8	65.6	3	65.7	6.13				0.05
unnamed fault in Salina Quad, R12E, T23S				9.0		43.5	70.0	3	70.1	6.19				0.04
Bright Angel fault system (Class B)	2514	<1,600,000	<0.2	102.3		89.6	144.1	3	144.1	7.41				0.04
unnamed fault in Salina Quad, R16E, T28S				9.0		43.9	70.6	3	70.6	6.19				0.04
Wasatch monocline (Class B)	2450	<1,600,000	<0.2	103.5	?	90.3	145.3	3	145.3	7.42				0.04

Name	Number	Age of Most Recent Prehistoric Deformation (ya)	Slip-rate (mm/yr)	Fault Length (km)	Fault Type	Distance from site (miles)[1]	Distance from site (km)	Depth to seismo-genic rupture (km)	r_{seis} (km)	MCE (Based on fault length, all slip types, Wells and Coppersmith, 1994)	Rupture depth (km)	Rupture area (km^2)	MCE (based on fracture area, Wells and Coppersmith, 1994)	PGA (Campbell-Bozorgnia 2003) corrected, plus 1SD (based on Mw)
Shay graben faults (Class B)	2513	Class B	<0.2	39.5		68.1	109.5	3	109.6	6.93				0.04
unnamed fault in Salina Quad, R11E, T24S				9.8		47.0	75.7	3	75.7	6.23				0.04
Joes Valley fault zone, east fault	2455	<15,000	0.2-1	56.6		79.0	127.0	3	127.1	7.11				0.04
Joes Valley fault zone, west fault	2453	<15,000	0.2-1	57.2		81.1	130.4	3	130.4	7.12				0.04
unnamed fault in Price Quad, R16E, T13S				9.5		48.6	78.2	3	78.2	6.22				0.04
Southern Joes Valley fault zone	2456	<750,000	<0.2	47.2		77.2	124.2	3	124.3	7.02				0.04
Big Gypsum Valley graben (Class B)	2288	Class B	<0.2	33.1		70.9	114.0	3	114.0	6.84				0.04
Duchesne-Pleasant Valley fault system (Class B)	2414	<1,600,000	<0.2	45.3	N	79.1	127.2	3	127.3	7.00				0.04
Monitor Creek fault	2268	<1,600,000	<0.2	30.1		79.1	127.3	3	127.3	6.80				0.03
Joes Valley fault zone, intragraben faults	2454	<15,000	<0.2	34.0		82.9	133.3	3	133.4	6.86				0.03
Thousand Lake fault	2506	<750,000	<0.2	48.3		97.2	156.4	3	156.5	7.03				0.03
Pleasant Valley fault zone, unnamed faults	2425	<1,600,000	<0.2	31.0	N	86.1	138.5	3	138.5	6.81				0.03
Unnamed faults of Pinto Mesa	2277	<1,600,000	<0.2	19.7		78.4	126.1	3	126.1	6.58				0.03
Unnamed faults south of Love Mesa	2271	<1,600,000	<0.2	17.6		78.8	126.8	3	126.8	6.52				0.03
Unnamed faults near San Miguel Canyon (Class B)	2284	Class B	<0.2	32.1		94.5	152.1	3	152.1	6.83				0.03
Snow Lake graben	2452	<15,000	<0.2	25.4		89.7	144.3	3	144.4	6.71				0.03
Gunnison fault	2445	<15,000	<0.2	42.0	N	104.3	167.8	3	167.9	6.96				0.03
Unnamed fault at Red Canyon	2279	<1,600,000	<0.2	24.2		90.9	146.3	3	146.4	6.69				0.03
Roubideau Creek fault	2270	<15,000	<0.2	20.5		88.7	142.7	3	142.7	6.60				0.03
Wasatch fault zone, Provo section	2351g	<15,000	1-5	58.8		122.2	196.6	3	196.6	7.13				0.03
Gooseberry graben faults	2424	<750,000	<0.2	22.6		93.1	149.8	3	149.8	6.65				0.03
Pleasant Valley fault zone, graben	2426	<750,000	<0.2	17.6		88.3	142.1	3	142.2	6.52				0.03
Aquarius and Awapa Plateaus faults	2505	<1,600,000	<0.2	35.7		108.6	174.8	3	174.8	6.88				0.03
Red Rocks fault	2291	<1,600,000	<0.2	38.3		111.8	179.9	3	179.9	6.92				0.02
Valley Mountains monocline (Class B)	2449	<1,600,000	<0.2	38.6		112.9	181.7	3	181.7	6.92				0.02
Paunsaugunt fault	2504	<1,600,000	<0.2	44.1		118.0	189.8	3	189.8	6.99				0.02
Wasatch fault zone, Nephi section	2351h	<15,000	1-5	43.1		119.9	192.9	3	193.0	6.98				0.02
White Mountain area faults	2451	<1,600,000	<0.2	16.4		90.5	145.6	3	145.6	6.49				0.02
Sevier/Toroweap fault zone, Sevier section	997a	<130,000	0.2-1	88.7		155.4	250.0	3	250.1	7.34				0.02
Sevier fault	2355	<1,600,000	<0.2	41.3	N	126.4	203.4	3	203.4	6.95				0.02
Unnamed fault at Hanks Creek	2281	<1,600,000	<0.2	17.5		99.0	159.2	3	159.3	6.52				0.02
Cactus Park-Bridgeport fault	8			22.5		70.0	112.6	3	112.7	6.65				0.02
East Tintic Mountains (west side) faults	2420	<750,000	<0.2	33.1		129.6	208.6	3	208.6	6.84				0.02
Sevier Valley-Marysvale-Circleville area faults	2500	<750,000	<0.2	34.9		133.7	215.2	3	215.2	6.87				0.02
Cannibal fault	2337	<130,000	<0.2	49.3		148.9	239.6	3	239.6	7.04				0.02
Hogsback fault, southern section	732b	<130,000	1-5	38.3		144.3	232.1	3	232.1	6.92				0.02
Bear River fault zone	730	<15,000	0.2-1	33.2		140.4	225.8	3	225.9	6.84				0.02
West Kaibab fault system	994	<1,600,000	<0.2	82.9	N	187.7	301.9	3	302.0	7.31				0.02
Frontal fault	2302	<130,000	0.2-1	75.0	N,R	190.1	305.8	3	305.9	7.26				0.02
Sevier/Toroweap fault zone, northern Toroweap section	997b	<130,000	<0.2	80.9		198.5	319.4	3	319.4	7.29				0.02
Central Kaibab fault system	993	<1,600,000	<0.2	71.5	N	192.3	309.5	3	309.5	7.23				0.02
Almy fault zone	742	<1,600,000	<0.2	10.7				3		6.27				

Name	Number	Age of Most Recent Prehistoric Deformation (ya)	Slip-rate (mm/yr)	Fault Length (km)	Fault Type	Distance from site (miles)[1]	Distance from site (km)	Depth to seismo-genic rupture (km)	r_{seis} (km)	MCE (Based on fault length, all slip types, Wells and Coppersmith, 1994)	Rupture depth (km)	Rupture area (km^2)	MCE (based on fracture area, Wells and Coppersmith, 1994)	PGA (Campbell-Bozorgnia 2003) corrected, plus 1SD (based on Mw)
Andrus Canyon fault	1013	<1,600,000	<0.2	5.6				3		5.95				
Annabella graben faults	2472	<15,000	<0.2	12.5				3		6.35				
Antelope Range fault	2517	<750,000	<0.2	24.5				3		6.69				
Arrowhead fault zone	953	<130,000	<0.2	5.2				3		5.91				
Aubrey fault zone	995	<130,000	<0.2	53.1				3		7.08				
Babbitt Lake fault zone	954	<750,000	<0.2	7.6				3		6.10				
Bald Mountain fault	2390	<1,600,000	<0.2	2.3				3		5.50				
Bangs Canyon fault	2256	<1,600,000	<0.2	6.3				3		6.01				
Basalt Mountain fault (Class B)	2299	Class B	<0.2	7.0				3		6.06				
Bear Lake (west side) fault (Class B)	2531	<1,600,000	<0.2	5.5				3		5.94				
Bear River Range faults	2410	<1,600,000	<0.2	62.9	N, Dextral			3		7.17				
Beaver Basin faults, eastern margin faults	2492a	<15,000	<0.2	34.2				3		6.86				
Beaver Basin faults, intrabasin faults	2492b	<15,000	<0.2	38.9				3		6.92				
Beaver Ridge faults	2464	<130,000	<0.2	14.2				3		6.42				
Big Pass faults	2366	<1,600,000	<0.2	17.3				3		6.52				
Black Mesa fault zone	2006	<1,600,000	<0.2	18.5				3		6.55				
Black Mountains faults	2487	<750,000	<0.2	25.9				3		6.72				
Black Point/Doney Mountain fault zone	957	<750,000	<0.2	23.8	N			3		6.68				
Black Rock area faults	2461	<130,000	<0.2	8.2				3		6.14				
Blue Springs Hills faults	2363	<750,000	<0.2	2.5				3		5.54				
Bright Angel fault zone	991	<1,600,000	<0.2	66.0	N			3		7.19				
Broadmouth Canyon faults	2377	<130,000	<0.2	3.4				3		5.70				
Buckskin Valley faults (Class B)	2499	Class B	<0.2	3.5				3		5.71				
Busted Boiler fault	2274	<130,000	<0.2	18.0				3		6.54				
Cactus Park fault	2258	<1,600,000	<0.2	1.9				3		5.40				
Calabacillas fault	2035	<750,000	<0.2	31.3				3		6.81				
Cameron graben and faults	988	<750,000	<0.2	10.8				3		6.28				
Campbell Francis fault zone	959	<750,000	<0.2	10.1				3		6.25				
Canones fault (Class B)	2003	<1,600,000	<0.2	29.4				3		6.78				
Cataract Creek fault zone	990	<1,600,000	<0.2	51.1	N			3		7.06				
Cattle Creek anticline (Class B)	2293	Class B	<0.2	8.6				3		6.16				
Cedar City-Parowan monocline (and faults)	2530	<15,000	<0.2	24.8				3		6.70				
Cedar Ranch fault zone	961	<750,000	<0.2	10.2				3		6.25				
Cedar Valley (north end) faults	2529	<130,000	<0.2	15.5				3		6.46				
Cedar Valley (south side) fault	2408	<750,000	<0.2	2.8				3		5.60				
Cedar Valley (west side) faults	2527	<750,000	<0.2	12.8				3		6.36				
Cedar Wash fault zone	962	<750,000	<0.2	11.6				3		6.31				
Chicken Springs faults	780	<15,000	<0.2	13.7				3		6.40				
Cimmarron fault, Blue Mesa section	2290c	<1,600,000	<0.2	22.5				3		6.65				
Cimmarron fault, Bostwick Park section (Class B)	2290a	Class B	<0.2	11.2				3		6.30				
Cimmarron fault, Poverty Mesa section (Class B)	2290b	Class B	<0.2	24.1				3		6.68				
Citadel Ruins fault zone	963	<1,600,000	<0.2	4.5				3		5.84				

Name	Number	Age of Most Recent Prehistoric Deformation (ya)	Slip-rate (mm/yr)	Fault Length (km)	Fault Type	Distance from site (miles)[1]	Distance from site (km)	Depth to seismo-genic rupture (km)	r_{seis} (km)	MCE (Based on fault length, all slip types, Wells and Coppersmith, 1994)	Rupture depth (km)	Rupture area (km^2)	MCE (based on fracture area, Wells and Coppersmith, 1994)	PGA (Campbell-Bozorgnia 2003) corrected, plus 1SD (based on Mw)
Clear Lake fault zone (Class B)	2436	<15,000	<0.2	35.5				3		6.88				
Clover fault zone	2396	<130,000	<0.2	4.0				3		5.78				
County Dump fault	2038	<1,600,000	<0.2	35.3				3		6.88				
Cove Fort fault zone (Class B)	2491	Class B	<0.2	22.2				3		6.64				
Crater Bench faults	2433	<15,000	<0.2	15.9				3		6.47				
Crawford Mountains (west side) fault	2346	<130,000	<0.2	25.3				3		6.71				
Cricket Mountains (north end) faults	2434	<750,000	<0.2	2.8				3		5.60				
Cricket Mountains (west side) fault	2460	<15,000	<0.2	41.0				3		6.95				
Cross Hollow Hills faults	2524	<1,600,000	<0.2	5.3				3		5.92				
Curlew Valley faults	3504	<15,000	<0.2	20.0				3		6.59				
Dayton fault (Class B)	2370	Class B	<0.2	16.3				3		6.49				
Deadman Wash faults	964	<1,600,000	<0.2	1.8				3		5.38				
Deep Creek Range (east side) faults	2416	<750,000	<0.2	20.7				3		6.61				
Deep Creek Range (northwest side) fault zone	2403	<130,000	<0.2	10.7				3		6.27				
Deseret faults	2435	<750,000	<0.2	7.1				3		6.07				
Diamond Gulch faults	2393	<1,600,000	<0.2	20.2				3		6.59				
Doloras fault zone (Class B)	2289	Class B	<0.2	15.2				3		6.45				
Dolphin Island fracture zone	2367	<750,000	<0.2	19.2				3		6.57				
Double Knobs fault	966	<1,600,000	<0.2	6.0				3		5.98				
Double Top fault zone	965	<1,600,000	<0.2	6.1				3		5.99				
Drum Mountains fault zone	2432	<15,000	<0.2	51.5	N			3		7.07				
Dry Wash fault and syncline	2496	<130,000	<0.2	18.6				3		6.55				
Duncomb Hollow fault	743	<1,600,000	<0.2	2.4				3		5.52				
Dutchman Draw fault	1003	<130,000	<0.2	16.3	N			3		6.49				
East Cache fault zone, central section	2352b	<15,000	0.2-1	16.5				3		6.49				
East Cache fault zone, northern section	2352a	<750,000	<0.2	25.7				3		6.72				
East Cache fault zone, southern section	2352c	<130,000	<0.2	22.1				3		6.64				
East Canyon (east side) fault (Class B)	2350	<1,600,000	<0.2	28.9				3		6.77				
East Canyon fault, Northern East Canyon section (Class B)	2354a	Class B	<0.2	22.5				3		6.65				
East Canyon fault, Southern East Canyon section	2354b	<750,000	<0.2	8.4				3		6.15				
East Dayton-oxford fault	3509	<130,000	<0.2	23.2	N			3		6.66				
East Great Salt Lake fault zone, Antelope Island section	2369c	<15,000	0.2-1	35.1				3		6.87				
East Great Salt Lake fault zone, Fremont Island section	2369b	<15,000	0.2-1	30.1				3		6.80				
East Great Salt Lake fault zone, Promontory section	2369a	<15,000	0.2-1	49.2	N			3		7.04				
East Kamas fault	2391	<1,600,000	<0.2	14.6				3		6.43				
East Lakeside Mountains fault zone	2368	<1,600,000	<0.2	36.0				3		6.89				
East Pocatello valley faults	3507	<15,000	<0.2	6.8				3		6.05				
Eastern Bear Lake fault, central section	2364b	<15,000	<0.2	23.8				3		6.68				
Eastern Bear Lake fault, southern section	2364c	<15,000	0.2-1	34.8				3		6.87				
Eastern Bear Valley fault (Class B)	734	Class B	<0.2	47.2				3		7.02				
Eastern Pilot Range fault	2371	<1,600,000	<0.2	10.6				3		6.27				
East-Side Chase Gulch fault	2317	<130,000	<0.2	30.7				3		6.81				

Name	Number	Age of Most Recent Prehistoric Deformation (ya)	Slip-rate (mm/yr)	Fault Length (km)	Fault Type	Distance from site (miles)[1]	Distance from site (km)	Depth to seismo-genic rupture (km)	r_{seis} (km)	MCE (Based on fault length, all slip types, Wells and Coppersmith, 1994)	Rupture depth (km)	Rupture area (km^2)	MCE (based on fracture area, Wells and Coppersmith, 1994)	PGA (Campbell-Bozorgnia 2003) corrected, plus 1SD (based on Mw)
Ebert Tank fault zone	967	<750,000	<0.2	3.1				3		5.65				
Eleven Mile fault	2318	<130,000	<0.2	4.7				3		5.86				
Elk Mountain fault	736	<1,600,000	<0.2	7.8				3		6.11				
Ellison Gulch scarp (Class B)	2304	Class B	<0.2	1.2				3		5.17				
Elsinore fault (fold)	2470	<1,600,000	<0.2	28.1				3		6.76				
Embudo fault, Hernandez section	2007b	<1,600,000	<0.2	31.6				3		6.82				
Embudo fault, Pilar section	2007a	<130,000	<0.2	38.7				3		6.92				
Eminence fault zone	992	<1,600,000	<0.2	36.0				3		6.89				
Enoch graben faults	2528	<15,000	<0.2	17.2				3		6.51				
Enterprise faults	2516	<750,000	<0.2	8.4				3		6.15				
Escalante Desert (east side) faults	2526	<15,000	<0.2	6.4				3		6.02				
Escalante Desert faults (Class B)	2488	Class B	<0.2	6.6				3		6.03				
Escalante Desert faults near Zane	2518	<130,000	<0.2	3.9				3		5.77				
Faults in Raft River Valley	3503	<750,000	<0.2	35.2				3		6.87				
Faults near Garcia	2323	<130,000	<0.2	3.4				3		5.70				
Faults near Monte Vista	2315	<1,600,000	<0.2	16.2				3		6.48				
Faults near of Cochiti Pueblo	2142	<1,600,000	<0.2	32.2				3		6.83				
Faults north of Placitas	2043	<750,000	<0.2	10.5				3		6.26				
Faults of Cove Creek Dome	2462	<1,600,000	<0.2	18.8				3		6.56				
Faults of the northern Basaltic Hills	2322	<1,600,000	<0.2	12.6				3		6.36				
Faults on north flank of Phil Pico Mountains	744	<130,000	<0.2	4.4				3		5.83				
Fish Springs fault	2417	<15,000	<0.2	29.7				3		6.79				
Foote Range fault	2429	<750,000	<0.2	3.1				3		5.65				
Fremont Wash faults	2495	<750,000	<0.2	7.2				3		6.07				
Frog Valley fault	2389	<1,600,000	<0.2	4.6				3		5.85				
Gallina fault	2001	<1,600,000	<0.2	39.3				3		6.93				
Glade Park fault	2254	<1,600,000	<0.2	9.4	R			3		6.21				
Goose Creek Mountains faults (Class B)	2356	Class B	<0.2	4.0				3		5.78				
Grand Hogback monocline (Class B)	2331	Class B	<0.2	22.0				3		6.64				
Grand Wash fault zone	1005	<130,000	<0.2	34.9	N			3		6.87				
Gray Mountain faults	1018	<1,600,000	<0.2	23.6				3		6.67				
Greenhorn Mountain fault (Class B)	2297	Class B	<0.2	21.5				3		6.63				
Grouse Creek and Dove Creek Mountains faults	2357	<750,000	<0.2	47.7				3		7.03				
Guaje Mountain fault	2027	<15,000	<0.2	10.7				3		6.27				
Gunlock fault (Class B)	2515	Class B	<0.2	7.5				3		6.10				
Gyp Pocket graben and faults	1001	<130,000	<0.2	11.8	N			3		6.32				
Hansel Mountains (east side) faults	2359	<750,000	<0.2	14.7				3		6.43				
Hansel Valley (valley floor) faults	2360	<750,000	<0.2	19.5				3		6.58				
Hansel Valley fault	2358	<150	<0.2	13.0				3		6.37				
Hidden Tank fault zone	970	<750,000	<0.2	10.2				3		6.25				
Hogsback fault, northern section	732a	<750,000	0.2-1	22.4				3		6.65				
House Range (west side) fault	2430	<15,000	<0.2	45.5	N			3		7.00				

Name	Number	Age of Most Recent Prehistoric Deformation (ya)	Slip-rate (mm/yr)	Fault Length (km)	Fault Type	Distance from site (miles)[1]	Distance from site (km)	Depth to seismo-genic rupture (km)	r_{seis} (km)	MCE (Based on fault length, all slip types, Wells and Coppersmith, 1994)	Rupture depth (km)	Rupture area (km^2)	MCE (based on fracture area, Wells and Coppersmith, 1994)	PGA (Campbell-Bozorgnia 2003) corrected, plus 1SD (based on Mw)
Hurricane fault zone, Anderson Junction section	998c	<15,000	0.2-1	42.2				3		6.97				
Hurricane fault zone, Ash Creek section	998b	<15,000	<0.2	32.0				3		6.83				
Hurricane fault zone, Cedar City section	998a	<15,000	<0.2	13.2				3		6.38				
Hurricane fault zone, Shivwitz section	998d	<130,000	<0.2	56.5	N			3		7.11				
Hurricane fault zone, southern section	998f	<1,600,000	<0.2	66.6	N			3		7.20				
Hurricane fault zone, Whitmore Canyon section	998e	<15,000	<0.2	28.5				3		6.77				
Hyrum fault	2374	<1,600,000	<0.2	3.1				3		5.65				
James Peak fault	2378	<130,000	<0.2	6.3				3		6.01				
Japanese and Cal Valleys faults	2447	<750,000	<0.2	30.1				3		6.80				
Jemez-San Ysidro fault, Jemez section	2029a	<1,600,000	<0.2	24.1				3		6.68				
Jemez-San Ysidro fault, San Ysidro section	2029b	<1,600,000	<0.2	30.1				3		6.80				
Johns Valley fault (Class B)	2539	Class B	<0.2	2.1				3		5.45				
Joseph Flats area faults and syncline (Class B)	2468	Class B	<0.2	3.2				3		5.67				
Juab Valley (west side) faults (Class B)	2423	<750,000	<0.2	13.2				3		6.38				
Judd Mountain fault	1597	<1,600,000	<0.2	20.4				3		6.60				
Killarney faults	2336	<1,600,000	<0.2	5.6				3		5.95				
Kolob Terrace faults	2525	<750,000	<0.2	12.1				3		6.34				
Koosharem fault	2503	<1,600,000	<0.2	2.2				3		5.48				
La Bajada fault	2032	<1,600,000	<0.2	40.3				3		6.94				
La Canada del Amagre fault zone	2005	<1,600,000	<0.2	17.2				3		6.51				
Ladder Creek fault	2255	<1,600,000	<0.2	6.2				3		6.00				
Lakeside Mountains (west side) fault (Class B)	2384	Class B	<0.2	4.7				3		5.86				
Large Whiskers fault zone	972	<1,600,000	<0.2	11.6				3		6.31				
Las Tablas fault	2020	<1,600,000	<0.2	14.8				3		6.44				
Lee Dam faults	973	<1,600,000	<0.2	7.6				3		6.10				
Leupp faults	1017	<750,000	<0.2	32.2				3		6.83				
Lime Mountain fault	2415	<1,600,000	<0.2	10.6				3		6.27				
Little Diamond Creek fault	2411	<750,000	<0.2	20.0				3		6.59				
Little Rough Range faults	2458	<750,000	<0.2	3.2				3		5.67				
Little Valley faults	2439	<15,000	<0.2	19.2				3		6.57				
Littlefield Mesa faults	1008	<750,000	<0.2	21.2				3		6.62				
Lobato Mesa fault zone	2004	<1,600,000	<0.2	21.3				3		6.62				
Lockwood Canyon fault zone	974	<1,600,000	<0.2	20.8				3		6.61				
Log Hill Mesa graben	2275	<130,000	<0.2	9.5				3		6.21				
Long Ridge (northwest side) fault	2422	<1,600,000	<0.2	20.8				3		6.61				
Long Ridge (west side) faults	2421	<750,000	<0.2	15.2				3		6.45				
Lookout Pass fault	2404	<1,600,000	<0.2	3.9				3		5.77				
Los Cordovas faults	2022	<1,600,000	<0.2	12.2				3		6.34				
Lucky Boy fault	2314	<1,600,000	<0.2	11.1				3		6.29				
Main Street fault zone	1002	<130,000	<0.2	87.3	N			3		7.33				
Malpais Tank faults	975	<750,000	<0.2	4.6				3		5.85				
Mantua area faults	2373	<750,000	<0.2	21.1				3		6.62				

Name	Number	Age of Most Recent Prehistoric Deformation (ya)	Slip-rate (mm/yr)	Fault Length (km)	Fault Type	Distance from site (miles)[1]	Distance from site (km)	Depth to seismo-genic rupture (km)	r_{seis} (km)	MCE (Based on fault length, all slip types, Wells and Coppersmith, 1994)	Rupture depth (km)	Rupture area (km^2)	MCE (based on fracture area, Wells and Coppersmith, 1994)	PGA (Campbell-Bozorgnia 2003) corrected, plus 1SD (based on Mw)
Maple Grove faults	2443	<15,000	<0.2	12.8				3		6.36				
Markagunt Plateau faults (Class B)	2535	<750,000	<0.2	56.4				3		7.11				
Martin Ranch fault	731	<15,000	0.2-1	3.7				3		5.74				
Maverick Butte faults	976	<750,000	<0.2	3.7				3		5.74				
Meadow-Hatton area faults	2466	<15,000	<0.2	4.0				3		5.78				
Mesa Butte North fault zone	987	<1,600,000	<0.2	22.6				3		6.65				
Mesita fault	2015	<130,000	<0.2	27.9				3		6.76				
Mesquite fault	1007	<130,000	<0.2	36.2				3		6.89				
Michelbach Tank faults	978	<750,000	<0.2	13.4				3		6.39				
Mineral Hot Springs fault	2320	<130,000	<0.2	7.8				3		6.11				
Mineral Mountains (northeast side) fault (Class B)	2490	Class B	<0.2	14.2				3		6.42				
Mineral Mountains (west side) faults	2489	<15,000	<0.2	36.6				3		6.89				
Morgan fault, central section	2353b	<15,000	<0.2	4.9				3		5.88				
Morgan fault, northern section	2353a	<750,000	<0.2	7.9				3		6.12				
Morgan fault, southern section	2353c	<750,000	<0.2	2.3				3		5.50				
Mosquito fault	2303	<130,000	<0.2	51.5				3		7.07				
Mountain Home Range (west side) faults	2480	<1,600,000	<0.2	26.4				3		6.73				
Nacimiento fault, northern section	2002a	<1,600,000	<0.2	35.9				3		6.88				
Nacimiento fault, southern section	2002b	<1,600,000	<0.2	45.2				3		7.00				
Nambe fault	2024	<1,600,000	<0.2	47.8				3		7.03				
North Bridger Creek fault	737	<1,600,000	<0.2	4.2				3		5.80				
North Hills faults	2522	<750,000	<0.2	5.0				3		5.89				
North of Wah Wah Mountains faults	2459	<750,000	<0.2	12.5				3		6.35				
North Promontory fault	2361	<15,000	<0.2	25.8				3		6.72				
North Promontory Mountains fault	2362	<1,600,000	<0.2	6.3				3		6.01				
Northern Boundary fault system	2309	<750,000	<0.2	49.0				3		7.04				
Northern Sangre de Cristo fault, Blanca section	2321c	<15,000	<0.2	6.7				3		6.04				
Northern Sangre de Cristo fault, Crestone section	2321a	<15,000	<0.2	79.1	N			3		7.28				
Northern Sangre de Cristo fault, San Luis section	2321d	<15,000	<0.2	59.1	N			3		7.14				
Northern Sangre de Cristo fault, Zapata section	2321b	<15,000	<0.2	25.8				3		6.72				
Ogden Valley North Fork fault	2376	<750,000	<0.2	26.1				3		6.72				
Ogden Valley northeastern margin fault	2379	<1,600,000	<0.2	12.8				3		6.36				
Ogden Valley southwestern margin faults	2375	<750,000	<0.2	17.8				3		6.53				
Oquirrh fault zone	2398	<15,000	<0.2	21.1				3		6.62				
Overton Arm faults	1119	<130,000	<0.2	50.9				3		7.06				
Pajarito fault	2008	<130,000	<0.2	49.4				3		7.04				
Paragonah fault	2534	<130,000	0.2-1	27.2				3		6.74				
Parleys Park faults (Class B)	2388	Class B	<0.2	3.4				3		5.70				
Parowan Valley faults	2533	<15,000	<0.2	16.3				3		6.49				
Pavant faults	2438	<15,000	<0.2	30.1				3		6.80				
Pavant Range fault	2442	<15,000	<0.2	14.2				3		6.42				
Pearl Harbor fault zone	981	<1,600,000	<0.2	15.3				3		6.45				

Name	Number	Age of Most Recent Prehistoric Deformation (ya)	Slip-rate (mm/yr)	Fault Length (km)	Fault Type	Distance from site (miles)[1]	Distance from site (km)	Depth to seismo-genic rupture (km)	r_{seis} (km)	MCE (Based on fault length, all slip types, Wells and Coppersmith, 1994)	Rupture depth (km)	Rupture area (km^2)	MCE (based on fracture area, Wells and Coppersmith, 1994)	PGA (Campbell-Bozorgnia 2003) corrected, plus 1SD (based on Mw)
Picuris-Pecos fault	2023	<1,600,000	<0.2	98.2	N			3		7.39				
Pilot Range faults	1599	<1,600,000	<0.2	40.2				3		6.94				
Pine Ridge faults (Class B)	2512	Class B	<0.2	5.5				3		5.94				
Pine Valley (south end) faults	2482	<1,600,000	<0.2	10.7				3		6.27				
Pine Valley faults	2481	<750,000	<0.2	3.7				3		5.74				
Pleasant Valley fault zone, Dry Valley graben	2427	<750,000	<0.2	12.4				3		6.35				
Pojoaque fault zone	2010	<1,600,000	<0.2	46.5				3		7.01				
Porcupine Mountain faults	2380	<130,000	<0.2	34.6	N			3		6.87				
Pot Creek faults	2394	<1,600,000	<0.2	13.4				3		6.39				
Puddle Valley fault zone	2383	<15,000	<0.2	6.5				3		6.02				
Puye fault	2009	<130,000	<0.2	16.7				3		6.50				
Raft River Mountains fault	2448	<750,000	<0.2	1.5				3		5.28				
Red Canyon fault scarps	2471	<15,000	<0.2	9.4				3		6.21				
Red Hills fault	2532	<130,000	<0.2	13.8				3		6.40				
Red House faults	983	<750,000	<0.2	3.4				3		5.70				
Red River fault zone	2019	<1,600,000	<0.2	10.0				3		6.24				
Rendija Canyon fault	2026	<130,000	<0.2	11.1				3		6.29				
Ridgway fault	2276	<1,600,000	<0.2	23.8				3		6.68				
Rimmy Jim fault zone	984	<1,600,000	<0.2	8.2				3		6.14				
Rock Creek fault	729	<15,000	0.2-1	40.5	N			3		6.94				
Round Valley faults	2400	<750,000	<0.2	12.8	N			3		6.36				
Ryckman Creek fault	740	<1,600,000	<0.2	5.3				3		5.92				
Sage Valley fault	2444	<1,600,000	<0.2	10.5				3		6.26				
Saint John Station fault zone	2397	<130,000	<0.2	5.2				3		5.91				
Saleratus Creek fault	2365	<750,000	<0.2	37.6				3		6.91				
San Felipe fault, Algodones section	2030b	<1,600,000	<0.2	15.9				3		6.47				
San Felipe fault, Santa Ana section	2030a	<1,600,000	<0.2	43.8				3		6.98				
San Francisco fault	2031	<1,600,000	<0.2	25.7				3		6.72				
San Francisco Mountains (west side) fault	2486	<750,000	<0.2	41.4				3		6.96				
Sand Hill fault zone	2039	<1,600,000	<0.2	35.6				3		6.88				
Sawatch fault, northern section	2308a	<130,000	<0.2	34.0				3		6.86				
Sawatch fault, southern section	2308b	<15,000	<0.2	41.1				3		6.95				
Sawyer Canyon fault	2028	<130,000	<0.2	8.4				3		6.15				
Scipio fault zone	2441	<15,000	<0.2	12.5				3		6.35				
Scipio Valley faults	2440	<15,000	<0.2	7.3				3		6.08				
Sevier Valley fault	2502	<1,600,000	<0.2	7.4				3		6.09				
Sevier Valley faults and folds (Class B)	2537	<130,000	<0.2	23.6				3		6.67				
Sevier Valley faults north of Panguitch	2536	<130,000	<0.2	6.2				3		6.00				
Sevier/Toroweap fault zone, central Toroweap section	997c	<15,000	<0.2	60.4	N			3		7.15				
Sevier/Toroweap fault zone, southern Toroweap section	997d	<750,000	<0.2	18.8				3		6.56				
Shadow Mountain grabens	989	<750,000	<0.2	10.4				3		6.26				
Sheeprock fault zone	2405	<130,000	<0.2	11.7				3		6.32				

Name	Number	Age of Most Recent Prehistoric Deformation (ya)	Slip-rate (mm/yr)	Fault Length (km)	Fault Type	Distance from site (miles)[1]	Distance from site (km)	Depth to seismo-genic rupture (km)	r_{seis} (km)	MCE (Based on fault length, all slip types, Wells and Coppersmith, 1994)	Rupture depth (km)	Rupture area (km^2)	MCE (based on fracture area, Wells and Coppersmith, 1994)	PGA (Campbell-Bozorgnia 2003) corrected, plus 1SD (based on Mw)
Sheeprock Mountains fault	2419	<1,600,000	<0.2	6.7				3		6.04				
Silver Island Mountains (southeast side) fault	2382	<15,000	<0.2	1.8				3		5.38				
Silver Island Mountains (west side) fault	2381	<1,600,000	<0.2	6.4				3		6.02				
Simpson Mountains faults	2418	<750,000	<0.2	10.8				3		6.28				
Sinagua faults	986	<130,000	<0.2	4.9				3		5.88				
Sinbad Valley graben (Class B)	2385	<1,600,000	<0.2	9.9				3		6.23				
Skull Valley (mid-valley) faults	2387	<15,000	<0.2	54.8	N			3		7.10				
Snake Valley fault	1246	<15,000	<0.2	41.1				3		6.95				
Snake Valley faults	2428	<15,000	<0.2	45.3	N			3		7.00				
South Granite Mountains fault system, Seminoe Mountains section (Class B)	779e	Class B	<0.2	35.0				3		6.87				
Southern Oquirrh Mountains fault zone	2399	<130,000	<0.2	24.1				3		6.68				
Southern Sangre de Cristo fault zone, San Pedro section	2017a	<130,000	<0.2	24.4				3		6.69				
Southern Sangre de Cristo fault, Cañon section	2017e	<15,000	<0.2	15.2				3		6.45				
Southern Sangre de Cristo fault, Hondo section	2017d	<15,000	<0.2	22.2				3		6.64				
Southern Sangre de Cristo fault, Questa section	2017c	<15,000	<0.2	17.8				3		6.53				
Southern Sangre de Cristo fault, Urraca section	2017b	<15,000	<0.2	21.9				3		6.63				
Southern Snake Range fault zone	1433	<130,000	<0.2	27.5	N			3		6.75				
SP fault zone	958	<130,000	<0.2	12.5				3		6.35				
Spring Creek fault	738	<1,600,000	<0.2	2.3				3		5.50				
Spry area faults	2498	<750,000	<0.2	5.1				3		5.90				
Stansbury fault zone	2395	<15,000	<0.2	49.8	N			3		7.05				
Stinking Springs fault	2413	<130,000	0.2-1	10.0				3		6.24				
Strawberry fault	2412	<15,000	<0.2	31.9				3		6.82				
Strong fault	2021	<1,600,000	<0.2	8.1				3		6.13				
Sublette Flat fault	733	<750,000	<0.2	36.0				3		6.89				
Sugarville area faults	2437	<15,000	<0.2	4.3				3		5.81				
Sunshine faults	1000	<130,000	<0.2	29.2	N			3		6.78				
Sunshine Trail graben and faults	999	<130,000	<0.2	17.0	N			3		6.51				
Sunshine Valley faults	2016	<130,000	<0.2	14.1				3		6.41				
Swasey Mountain (east side) faults	2431	<750,000	<0.2	3.8				3		5.75				
Tabernacle faults	2465	<15,000	<0.2	7.9				3		6.12				
The Pinnacle fault	739	<1,600,000	<0.2	2.3				3		5.50				
Tijeras-Cañoncito fault system, Galisteo section	2033a	<1,600,000	<0.2	37.1				3		6.90				
Topliff Hill fault zone	2407	<130,000	<0.2	19.9				3		6.59				
Towanta Flat graben (Class B)	2401	<750,000	<0.2	5.2				3		5.91				
Tushar Mountains (east side) fault	2501	<1,600,000	<0.2	18.5				3		6.55				
Uinkaret Volcanic field faults	1012	<1,600,000	<0.2	18.5				3		6.55				
Unnamed fault along Grand Hogback monocline (Class B)	2292	Class B	<0.2	2.4				3		5.52				
Unnamed fault at Big Dominquez Creek	2260	<1,600,000	<0.2	3.9				3		5.77				
Unnamed fault at Little Dominquez Creek	2261	<1,600,000	<0.2	14.2				3		6.42				
Unnamed fault at northwest end of Paradox Valley (Class B)	2287	Class B	<0.2	5.1				3		5.90				

Name	Number	Age of Most Recent Prehistoric Deformation (ya)	Slip-rate (mm/yr)	Fault Length (km)	Fault Type	Distance from site (miles)[1]	Distance from site (km)	Depth to seismo-genic rupture (km)	r_{seis} (km)	MCE (Based on fault length, all slip types, Wells and Coppersmith, 1994)	Rupture depth (km)	Rupture area (km^2)	MCE (based on fracture area, Wells and Coppersmith, 1994)	PGA (Campbell-Bozorgnia 2003) corrected, plus 1SD (based on Mw)
Unnamed fault east of Whitewater	2257	<1,600,000	<0.2	1.9				3		5.40				
Unnamed fault near Bridgeport	2259	<1,600,000	<0.2	11.0				3		6.29				
Unnamed fault near Escalante	2262	<1,600,000	<0.2	1.6				3		5.32				
Unnamed fault near Johnson Spring	2282	<1,600,000	<0.2	7.1				3		6.07				
Unnamed fault near Wolf Hill	2266	<1,600,000	<0.2	15.2				3		6.45				
Unnamed fault north of Horsefly Creek	2280	<1,600,000	<0.2	8.1				3		6.13				
Unnamed fault of Missouri Peak	2312	<130,000	<0.2	5.9				3		5.97				
Unnamed fault south of Shavano Peak	2311	<1,600,000	<0.2	5.8				3		5.97				
Unnamed fault southeast of China Mountain	1598	<1,600,000	<0.2	2.9				3		5.62				
Unnamed fault west of Buena Vista	2310	<1,600,000	<0.2	2.7				3		5.58				
Unnamed fault west of White Rock Mountains	1437	<1,600,000	<0.2	27.7				3		6.75				
Unnamed fault zone in Ferber Hills	1721	<1,600,000	<0.2	37.3				3		6.90				
Creek (Class B)	2294	Class B	<0.2	2.5				3		5.54				
Creek (Class B)	2295	Class B	<0.2	5.7				3		5.96				
Unnamed faults at Clay Creek	2283	<1,600,000	<0.2	9.2				3		6.20				
Unnamed faults east of Atkinson Masa	2269	<1,600,000	<0.2	41.1	N			3		6.95				
Unnamed faults east of Roubideau Creek (Class B)	2272	Class B	<0.2	11.7				3		6.32				
Unnamed faults in Williams Fork Valley	2300	<750,000	<0.2	18.4				3		6.55				
Unnamed faults near Burns (Class B)	2296	Class B	<0.2	13.3				3		6.38				
Unnamed faults near Cottonwood Creek	2278	<1,600,000	<0.2	10.8				3		6.28				
Unnamed faults near Loma Barbon	2045	<1,600,000	<0.2	1.2				3		5.17				
Unnamed faults near Picuda Peak	2041	<1,600,000	<0.2	10.6				3		6.27				
Unnamed faults near Twin Lakes Reservoir	2307	<1,600,000	<0.2	14.0				3		6.41				
Unnamed faults northwest of Leadville	2306	<1,600,000	<0.2	18.8				3		6.56				
Unnamed faults of Jemez Mountains, caldera margin section (Class B)	2143c	<750,000	<0.2	20.3				3		6.60				
Unnamed faults of Jemez Mountains, Intracaldera section (Class B)	2143d	<1,600,000	<0.2	11.3	N			3		6.30				
Unnamed faults of Jemez Mountains, Toledo caldera section (Class B)	2143b	<1,600,000	<0.2	10.9				3		6.28				
Unnamed faults of Jemez Mountains, Valles caldera section (Class B)	2143a	<1,600,000	<0.2	16.7				3		6.50				
Unnamed faults of Red Hill (Class B)	2298	Class B	<0.2	6.1				3		5.99				
Unnamed faults on southeast side of Kern Mountains	1256	<1,600,000	<0.2	11.4	N			3		6.31				
Unnamed faults south of Leadville	2305	<1,600,000	<0.2	12.8				3		6.36				
Unnamed faults southeast of Montrose (Class B)	2273	Class B	<0.2	9.2				3		6.20				
Unnamed syncline northeast of Carbondale (Class B)	2333	Class B	<0.2	1.5				3		5.28				
Unnamed syncline northwest of Carbondale (Class B)	2334	Class B	<0.2	1.9				3		5.40				
Unnamed syncline southwest of Carbondale (Class B)	2332	Class B	<0.2	3.0				3		5.63				
Unnamed syncline west of Carbondale (Class B)	2335	Class B	<0.2	0.6				3		4.82				
Utah Lake faults	2409	<15,000	<0.2	30.8				3		6.81				
Vernon Hills fault zone	2406	<130,000	<0.2	3.7				3		5.74				

Name	Number	Age of Most Recent Prehistoric Deformation (ya)	Slip-rate (mm/yr)	Fault Length (km)	Fault Type	Distance from site (miles)[1]	Distance from site (km)	Depth to seismo-genic rupture (km)	r_{seis} (km)	MCE (Based on fault length, all slip types, Wells and Coppersmith, 1994)	Rupture depth (km)	Rupture area (km^2)	MCE (based on fracture area, Wells and Coppersmith, 1994)	PGA (Campbell-Bozorgnia 2003) corrected, plus 1SD (based on Mw)
Villa Grove fault zone	2319	<15,000	<0.2	19.0				3		6.56				
Volcano Mountain faults	2520	<750,000	<0.2	2.9				3		5.62				
Wah Wah Mountains (south end near Lund) fault	2485	<130,000	<0.2	40.2				3		6.94				
Wah Wah Mountains faults	2483	<1,600,000	<0.2	53.6				3		7.09				
Wah Wah Valley (west side) faults (Class B)	2484	Class B	<0.2	2.1				3		5.45				
Wasatch fault zone, Brigham City section	2351d	<15,000	0.2-1	37.3				3		6.90				
Wasatch fault zone, City section	2351a	<130,000	<0.2	39.6				3		6.93				
Wasatch fault zone, Clarkston Mountain section	2351b	<130,000	<0.2	10.4				3		6.26				
Wasatch fault zone, Collinston section	2351c	<15,000	<0.2	29.7				3		6.79				
Wasatch fault zone, Fayette section	2351j	<15,000	<0.2	15.6				3		6.46				
Wasatch fault zone, Levan section	2351i	<15,000	<0.2	30.1				3		6.80				
Wasatch fault zone, Salt Lake City section	2351f	<15,000	1-5	42.5				3		6.97				
Wasatch fault zone, Weber section	2351e	<15,000	1-5	56.2				3		7.11				
Washington fault zone, Mokaac section	1004b	<130,000	<0.2	11.2	N			3		6.30				
Washington fault zone, northern section	1004a	<15,000	<0.2	36.2	N			3		6.89				
Washington fault zone, Sullivan Draw section	1004c	<130,000	<0.2	34.5	N			3		6.86				
West Cache fault zone, Clarkston fault	2521a	<15,000	0.2-1	13.0				3		6.37				
West Cache fault zone, Junction Hills fault	2521b	<15,000	<0.2	24.3				3		6.69				
West Cache fault zone, Wellsville fault	2521c	<15,000	<0.2	19.9				3		6.59				
West Pocatello Valley faults	3506	<1,600,000	<0.2	7.7				3		6.11				
West Valley fault zone, Granger fault	2386b	<15,000	0.2-1	16.0	N			3		6.48				
West Valley fault zone, Taylorsville fault	2386a	<15,000	<0.2	15.1	N			3		6.45				
Western Bear Lake fault	622	<15,000	<0.2	58.2				3		7.13				
Western Bear Valley faults	735	<1,600,000	<0.2	12.4				3		6.35				
Western Boundary fault	2313	<1,600,000	<0.2	20.1				3		6.59				
West-Side Chase Gulch fault	2316	<130,000	<0.2	2.7				3		5.58				
Wheeler fault zone and graben	1006	<750,000	<0.2	45.3				3		7.00				
White Sage Flat faults	2467	<130,000	<0.2	11.8				3		6.32				
Whitney Canyon fault	741	<15,000	<0.2	5.5				3		5.94				
Williams Fork Mountains fault	2301	<15,000	0.2-1	37.7				3		6.91				
Woodruff fault	3508	<1,600,000	<0.2	12.5				3		6.35				
Yampai graben	996	<1,600,000	<0.2	6.9				3		6.05				
Zia fault	2046	<750,000	<0.2	32.4				3		6.83				

Class B=Geologic evidence demonstrates the existence of Quaternary deformation, but either (1) the fault might not extend deeply enough to be a potential source of significant earthquakes, or (2) the currently available geologic evidence is too strong to confidently assign the feature to Class C but not strong enough to assign it to Class A.

Fault Type: N=normal, R=reverse, D=Dextral

r_{seis}=distance from site to fault plane

[1]Distance from site only measured for those faults meeting the minimum length requirements as given in NRC 10 CFR part 100, Appendix A. Other faults have minimal impact on site.

[2]Attenuation calculated using mean MCE value based on rupture area, distance to site based on vertical projection of fault

[3]Attenuation calculation using mean MCE value based on rupture length, distance to site based on vertical projection of fault

[4]Attenuation calculation using mean plus one standard deviation MCE value based on rupture length, distance to site based on projecting fault dip at 60 degrees to NE

Appendix G

U.S. Department of Energy—Grand Junction, Colorado

Calculation Cover Sheet

Calc. No.: MOA-02-11-2005-1-02-00 **Discipline:** Geologic and Geophysical Properties **No. of Sheets:** 6

Project: Moab UMTRA Project

Site: Crescent Junction, Utah

Feature: Photogeologic Interpretation

Sources of Data:

Aero-graphics, Inc., 2005. *Crescent Junction Photography* – one set of 12 -- 10"x10" color contact prints of the high-altitude flight. Transmittal No. 13224 for S.M. Stoller Corporation. August 1, 2005.

Aero-graphics, Inc., 2005. *Crescent Junction Photography* – two sets of 10 -- 10"x10" color contact prints of the low-sun angle flight. Transmittal No. 13330 for S.M. Stoller Corporation. October 3, 2005.

Sources of Formulae and References:

N/A.

Preliminary Calc. ☐ **Final Calc.** ☑ **Supersedes Calc. No.**

Author: Craig Goodknight (Name) 2/27/06 (Date)

Approved by: Kurt D. Kupp (Name) 3-6-06 (Date)

Checked by:

Mark Kautsky (Name) 2/28/06 (Date)

Joel Berwick (Name) 3/7/06 (Date)

Tim Wyatt (Name) 3/8/06 (Date)

R. Kapp for R. Heydenburg (Name) 3/9/06 (Date)

Problem Statement:

Preliminary site selection performed jointly by the U.S. Department of Energy (DOE) and the Contractor has identified an approximately 300-acre location in the Crescent Flat area just northeast of Crescent Junction, Utah, as a possible site for final disposal of the Moab uranium mill tailings. The 300-acre site is within a withdrawal area consisting of approximately 2,300 acres. Situated between the Union Pacific Railroad and the base of the Book Cliffs, the withdrawal area extends for about 3 miles (mi) in an east-west direction and is approximately 1 mi wide in a north-south direction (Plate 1). Based on the preliminary site-selection process, the suitability of the Crescent Junction disposal site is being evaluated from several technical aspects, including geomorphic, geologic, hydrologic, seismic, geochemical, and geotechnical. The objective of this calculation set is to interpret stereographic color aerial photographs (including High Altitude Vertical [HAV] and Low Sun-Angle [LSA] photographs) of the area to analyze structural and geomorphic conditions that may affect the site.

Findings from this calculation will be incorporated into Attachment 2 (Geology) of the Remedial Action Plan (RAP) and Site Design for Stabilization of Moab Title I Uranium Mill Tailings at the Crescent Junction, Utah, Disposal Site, and summarized in the appropriate section of the Remedial Action Selection (RAS) report for the Moab site.

Method of Solution:

Color aerial photographs of an area of approximately 25 square mi, which included the proposed disposal site, the withdrawal area, and surrounding area, were taken by Aero-graphics, Inc., in July 2005. Both HAV and LSA photographs of the area were made at a scale of 1:24,000. The HAV photographs were taken on July 8, and two sets of the LSA photographs were taken—one in the morning and one in the evening—on July 27. Both HAV and LSA aerial photographs were taken in two flight lines from west to east across the north and south parts of the site area. The photographic coverage extends approximately 2.5 mi outside of the site withdrawal area in all directions. These photographs were interpreted to provide an assessment of geologic structures and geomorphic conditions that may affect the disposal site. Standard procedures and techniques were used to perform these analyses.

Assumptions:

Not applicable.

Calculation:

None required.

Discussion:

Results of these interpretations are used to assess structural and geomorphic conditions that may affect the Crescent Junction disposal site. These results are also used to confirm and supplement other field observations associated with site geologic mapping and with fault investigation for the site and regional seismicity calculation set. These interpretations contribute toward the comprehensive evaluation of the area relative to its suitability for location of the disposal facility. Features noted from inspection of the HAV and the LSA photographs are described in the following subsections along with an explanation of their significance, if known. Also, the features are divided into two groups: those which occur on or adjacent to the withdrawal area (numbered 1 through 6), and those which occur outside the withdrawal area (a through h). Each feature was assigned a relative importance by their number and letter order. All features are shown, with their relation to the withdrawal area, in Plate 1.

High-Altitude Vertical Photographs

1. Paths of active sheet wash flow are shown in gray (the color of Mancos Shale) from the base of the Book Cliffs south to south-southeast across parts of the site withdrawal area. Water flowing in this sheet wash drains across the site to the West and East Branches of Kendall Wash. These sheet wash deposits are quite evident on the ground and are mapped as such in the geologic map of the proposed site and nearby area included in the Field and Drilling Investigation Results calculation set. The active sheet wash areas continue the process of deposition of alluvial mud, which may be up to 25 feet (ft) thick, covering the Mancos Shale bedrock over most of the site.

2. An east-trending discontinuous line of low mounds that appear as a lineament are in the SE ¼ Section 22 and SW ¼ Section 23. These mounds are up to 15 ft high and are capped by a calcareous, dolomitic concretionary layer that marks the top of the Prairie Canyon Member of the Mancos Shale in this area, as described by Cole and others (1997) and Hampson and others (1999). The straight line of these mounds follows the strike direction of the Mancos Shale in this area and indicates that the stratigraphic horizon in the Mancos Shale is not displaced by faults.

3. The incised course of the N45W-trending West Branch of Kendall Wash is well exposed in the southwest part of the withdrawal area in the south-central part of Section 27. This trend reflects the prominent bedrock joint trend in this area. No exposed bedrock has been found in the wash bottom, which has been incised to a depth of about 10 ft north of the Union Pacific Railroad. Incision of the wash appears to be actively advancing to the northwest.

4. In the west parts of Sections 22 and 15, the west end of the Book Cliffs terminates abruptly along a linear feature that trends several degrees east of north. This feature continues northward across Crescent Canyon into the west part of Section 10. Mapped from Landsat images of the northern Paradox Basin as a lineament by Friedman and Simpson (1980), this feature is also shown in Friedman and others (1994). The feature does not coincide to any faults mapped for the area by Doelling (2001) or Gualtieri (1988), but the trend is similar to a joint system measured in the withdrawal area in the SW ¼ of Section 22. It is concluded that this topographic lineament or feature is likely an expression of a prominent joint system in the area trending several degrees east of due north. This feature may have influenced the direction of Crescent Wash, just west of the withdrawal area.

5. An abandoned wash course in SE ¼ of Section 24 in the northeast part of the withdrawal area trends south and extends for nearly 0.5 mi. The north end of the abandoned wash appears to intersect the incised present course of the southwest-draining East Branch of Kendall Wash. From the photographs, it appears that the south-trending drainage was abandoned either by capture from headcutting of the present East Branch or by blockage of the drainage by railroad personnel to consolidate drainages and minimize the number of rail crossings. Field examination of this abandoned drainage found that it was naturally abandoned, many thousand years ago. No connection with the present East Branch exists at the north end of the drainage; the floor of the drainage is approximately 10 ft higher than the incised depth of the East Branch. The drainage bottom is wide and flat, and the depth of the broad drainage decreases from about 8 ft at the north end to nearly zero at the south end near the Union Pacific Railroad. Abundant sandstone boulders, 2 to 5 ft in diameter, line the top sides of the drainage and occur in a broad fan (expressed as a boulder field) at the south (filled in) end of the drainage. This large material more than a mile away from its source, the top of the Book Cliffs, is anomalous for this area. These boulders indicate that the drainage was one of the major ones draining the Book Cliffs, possibly several hundred thousand to 1 million years ago when the front of the Book Cliffs was much closer (less than 0.5 mi).

6. Several slump blocks containing sandstone of the Blackhawk Formation are along the south face of the Book Cliffs, immediately north of the site withdrawal area, in Sections 22 and 23. These slump blocks are lighter colored (tan to yellowish brown) than the typical gray Mancos Shale in the lower slope of the Book Cliffs and appear to represent erosional remnants of larger slumps that slid down from the Book Cliffs in wetter Pleistocene times. Two additional slump blocks

covering larger areas are well shown. One is north of the withdrawal area in the south part of Horse Heaven just north of the western point of the Book Cliffs (elevation point 5,870 ft). The other is northeast of the withdrawal area just north of the detached block of the Book Cliffs (elevation point 5,903 ft, which is mislabeled and should be 5,803 ft) in the south-central part of Section 13. Both of these are shown in the landslide map by Harty (1993), and the slides were likely initiated in wetter times during the Pleistocene.

a. The head of south-draining Crooked Wash, about 0.5 mi northwest of the northwest end of the withdrawal area, bends abruptly to strike N45W and forms an embayment in the Book Cliffs in the NW ¼ of Section 16. This trend extends farther to the northwest and influences topography, forming an elongated cliff face just southwest of elevation point 5,882 ft. Southeastward along this trend, at the northwest end of the withdrawal area, is the abrupt west end of the Book Cliffs in the NW ¼ of Section 22. No fault coincides with this feature from mapping by Doelling (2001) for this area. The N45W trend is a common joint orientation in the area, and it is concluded that this major joint imparts some topographic control on the shape of the front of the Book Cliffs.

b. A linear feature that trends approximately N50W appears to control the shape of the front of the Book Cliffs in the NE ¼ of Section 13 approximately 1 mi north of the northeast end of the withdrawal area. This feature appears to extend northwestward for at least 0.5 mi into the SW ¼ of Section 12 where it forms a low saddle on the ridge northwest of elevation point 6,545 ft. No fault corresponds to this feature from mapping of the Moab 30' x 60' quadrangle by Doelling (2001) and mapping of the adjacent Westwater 30' x 60' quadrangle to the north by Gualtieri (1988). Nearest fault to this feature is about 0.5 mi to the northeast and it strikes almost parallel at N40W (Doelling 2001). Prominent vertical joints that strike N40W were measured along the top of the Book Cliffs about 1.5 mi to the southwest of this feature at elevation point 5,932 ft. From the orientation of this joint system and faults of similar orientation to the northeast of this feature, it is concluded that this feature is a major joint that imparts some topographic control on the shape of the face of the Book Cliffs and drainages/ridges to the north.

c. Approximately 20 small pits are spaced about 200 ft apart in an area mainly north of old U.S. Highway 50, south of the Union Pacific Railroad, and just east of the East Branch of Kendall Wash. Field examination of the pits indicates that they are about 60 ft long, 25 ft wide, and 5 ft deep. Several 4 inch by 4 inch wooden posts were also found scattered on the ground through this area. These pits were likely dug as part of assessment work for mining claims staked for gold in the late 1970s and early 1980s. This area was part of a larger area (Floy to Cisco) sampled in a study by Marlatt (1991) for analysis of gold content in Mancos Shale. He found the gold content ranged from 30 to 100 parts per billion (ppb), which is about ten times the background level, but much too low for economic extraction.

d. Green vegetation just north of old U.S. Highway 50 occurs in washes from the area of the East Branch of Kendall Wash westward to the West Branch of Kendall Wash. This occurrence of vegetation coincides with and verifies the location of the buried (and leaking) water line from Thompson Springs to Crescent Junction.

Low Sun-Angle Photographs

The LSA photographs covering the withdrawal area show that no terraces or mantled pediment surfaces are displaced and no scarps or linear features are present that would suggest the presence of faulting.

e. Best-shown of all the structural features in the LSA photographic coverage area are the bounding normal faults of the graben that strikes N20W along the axis of the Thompson anticline. This graben structure is about 2 mi northeast of the northeast end of the withdrawal area. The southwest-bounding fault of the graben has the greater displacement (up to 90 ft) of the two faults (Willis 1986) and is well shown in the evening LSA photographs. The faults displace resistant sandstone beds of the Blackhawk Formation and Castlegate Sandstone, both of which cap the Book Cliffs. No displacement on these faults has been discerned where they contact the underlying, soft Mancos Shale on the slopes of the Book Cliffs.

f. A prominent vertical joint system that strikes N55W is well shown in sandstone of the Blackhawk Formation exposed on a point on the Book Cliffs in Horse Heaven in the east-central part of Section 15 approximately 1 mi north of the withdrawal area. No displacement occurs along this joint and it is a common joint orientation exposed elsewhere in the surrounding area.

g. An abrupt change in elevation of the terrace surface occurs just north of Interstate 70 across from the rest area about 0.5 mi west of Crescent Junction. The highest surface, at elevation point 4,995 ft near the center of Section 33, abruptly drops down 40 to 50 ft to the northwest to a lower surface. Both surfaces are covered by pediment-mantling material as mapped by Doelling (2001). It is uncertain whether the two surfaces represent two terrace (or pediment) levels or they are the same surface that has been displaced by a fault. The higher terrace surface to the south corresponds to what is mapped as Crescent Bench to the south of Interstate 70.

h. A pediment mantled by surficial (terrace?) material (mapped by Doelling 2001) that is possibly displaced is about 1.5 mi west of the west edge of the withdrawal area. This pediment is about 0.5 mi southeast of Thompson Pass in SE ¼ SW ¼ of Section 17. The faint linear feature along which displacement possibly has occurred could also be an old geophysical seismic exploration line because the linear feature extends to the east-southeast for nearly a mile toward Crooked Wash.

Conclusion and Recommendations:

Interpretation of aerial photographs for the withdrawal area supplement what is observed on the ground regarding areas of active sheet wash, the line of low mounds indicating the top of the Prairie Canyon Member of the Mancos Shale, and the headward incision of the West Branch of Kendall Wash. A south-trending (and draining) wash course that appears to drain away from the East Branch of Kendall Wash in the northeast part of the withdrawal area represents a major drainage course that was in place several hundred thousand to as much as 1 million years ago. This drainage is not related to the present East Branch, and it appears to have been naturally abandoned many thousand years ago. Known and possible fault displacements were noted in areas near but outside of the withdrawal area, but far enough away that they do not adversely affect the geologic suitability of the disposal site. Aerial photographs covering the withdrawal area showed no features that would suggest the presence of faulting. Also, no structural features outside of the withdrawal area were identified that would be of sufficient significance to be addressed further in the calculation set for Site and Regional Seismicity – Results of Maximum Credible Earthquake Estimation and Peak Horizontal Acceleration.

Computer Source:

Not applicable.

References:

Cole, R.D., Young, R.G., and Willis, G.C., 1997. "The Prairie Canyon Member, a new unit of the Upper Cretaceous Mancos Shale, west-central Colorado and east-central Utah," *Utah Geological Survey Miscellaneous Publication*, 97-4, 23 p.

Doelling, H.H., 2001. "Geologic map of the Moab and eastern part of the San Rafael Desert 30' X 60' quadrangles, Grand and Emery Counties, Utah, and Mesa County, Colorado," *Utah Geological Survey Map 180,* scale 1:100,000.

Friedman, J.D., Case, J.E., and Simpson, S.L., 1994. "Tectonic trends of the northern part of the Paradox Basin, southeastern Utah and southwestern Colorado, as derived from Landsat multispectral scanner imaging and geophysical and geologic mapping," *U.S. Geological Survey Bulletin*, 2000–C, 30 p.

Friedman, J.D., and Simpson, S.L., 1980. "Lineaments and geologic structure of the northern Paradox Basin, Colorado and Utah," *U.S. Geological Survey Miscellaneous Field Studies Map MF–1221*, scale 1:250,000.

Gualtieri, J.L., 1988. "Geologic map of the Westwater 30' X 60' quadrangle, Grand and Uintah Counties, Utah, and Garfield and Mesa Counties, Colorado," *U.S. Geological Survey Miscellaneous Investigations Series Map I–1765,* scale 1:100,000.

Hampson, G.J., Howell, J.A., and Flint, S.S., 1999. "A sedimentological and sequence stratigraphic re-interpretation of the Upper Cretaceous Prairie Canyon Member ("Mancos B") and associated strata, Book Cliffs area, Utah, U.S.A.," *Journal of Sedimentary Research,* Volume 69, No. 2, p. 414–433.

Harty, K.M., 1993. "Landslide map of the Moab 30' X 60' quadrangle, Utah," *Utah Geological Survey Open File Report 276,* scale 1:100,000.

Marlatt, Gordon, 1991. "Gold occurrence in the Cretaceous Mancos Shale, eastern Utah," *Utah Geological and Mineral Survey Contract Report,* 91–5, 21 p.

Willis, G.C., 1986. "Provisional geologic map of the Sego Canyon quadrangle, Grand County, Utah," *Utah Geological and Mineral Survey Map 89,* scale 1:24,000.

THIS PAGE IS AN OVERSIZED DRAWING OR FIGURE,

THAT CAN BE VIEWED AT THE RECORD TITLED:

PLATE 1,

"AERIAL PHOTOGRAPHY INTERPRETATION FOR CRESCENT JUNCTION WITHDRAWAL AREA AND NEARBY SURROUNDING AREA"

WITHIN THIS PACKAGE

D-04